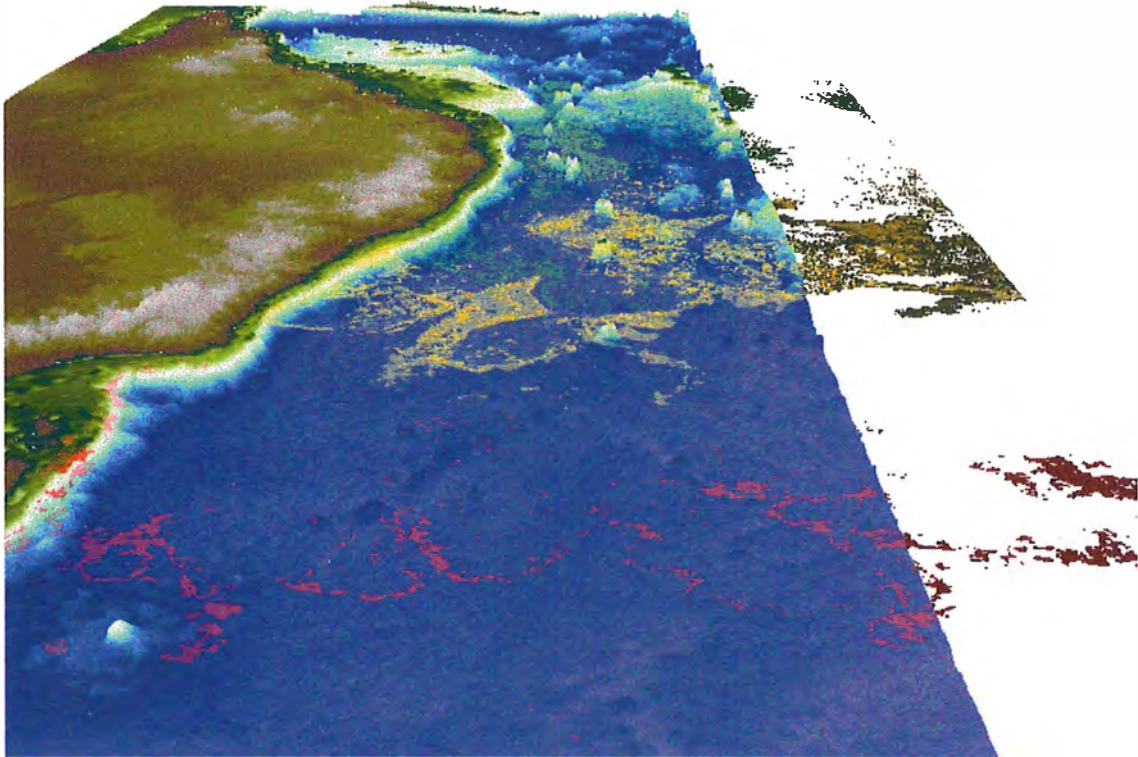


Development, Application and Evaluation of the use of Remote Sensing Data by Australian Fisheries



Editor: Vincent Lyne

Principal Authors: Vincent Lyne, John Parslow, Jock Young, Alan Pearce, Mervyn Lynch

Contributing Authors: Leslie Clementson, Ann Cowling, Randall Gray, Don McKenzie,
Roger Scott, Clive Stanley



Project No. 94/045 April 2000

© CSIRO Marine Research, Australia, 2000

GPO Box 1538
Hobart, Tasmania
Australia 7001

Intl Tel: 61-3-62325222
Intl Fax: 61-3-62325000
Website: <http://www.marine.csiro.au>

This work is copyright. Apart from any use as permitted under the *Copyright Act 1968*, no part of this work may be reproduced by any process without the written permission of the Chief, CSIRO Marine Research, Australia.

The National Library of Australia Cataloguing-in-Publication entry

Development, application and evaluation of the use of
remote sensing data by Australian fisheries.

Bibliography.
ISBN 0 643 06234 3.

1. Fisheries.
2. Remote sensing.
3. Fishery technology.

- I. Lyne, Vincent David.
- II. CSIRO. Marine Research.

639.20994

Funded by the Fisheries Research and Development Corporation, CSIRO Marine Research, Eastern Tuna & Billfish Committee, Australian Fisheries Management Authority, Curtin University.

Disclaimer: CSIRO Marine Research does not warrant that the information contained in this book is free from errors or omissions. CSIRO Marine Research shall not be in any way liable for any loss, damage or injury suffered by the user consequent upon, or incidental to, the existence of errors or omissions in the information.

**Development, application and evaluation of the use of remote sensing
data by Australian fisheries**

PRINCIPAL INVESTIGATORS:

Dr Vincent Lyne & Dr John Parslow
CSIRO Marine Research
PO Box 1538
Hobart. TAS 7001
AUSTRALIA
Ph: (03) 6232 5222
Fx: (03) 6232 5000

TABLE OF CONTENTS

2. ABSTRACT	6
3. OBJECTIVES	7
NOTES ON OBJECTIVES:.....	7
4. NON-TECHNICAL SUMMARY	8
5. BACKGROUND AND NEED.....	10
BACKGROUND	10
NEED	10
FISHERIES OCEANOGRAPHY AND REMOTE SENSING	13
REMOTE SENSING AND FISHERIES INFORMATION SYSTEMS.....	15
REMOTE SENSING SYSTEMS	15
OPERATIONAL FISHERIES INFORMATION SYSTEMS.....	18
SST AND OCEAN COLOR IN FISHERIES APPLICATIONS	19
"MAPS OF OCEAN COLOR:....."	23
REGIONAL PERSPECTIVES	24
LOCAL PERSPECTIVES.....	25
<i>Oceanography of the study area</i>	25
THE FISHERY	25
<i>Catch Distributions</i>	27
6. METHODS	34
CATCH DATA	34
SEA-SURFACE TEMPERATURE DATA.....	34
OCEAN COLOR DATA.....	35
CZCS DATA	35
OCTS DATA.....	37
SEAWIFS DATA	37
IN-SITU GROUND TRUTH DATA	38
UNDERWAY SAMPLER	39
CZCS OCEAN COLOR DATA PROCESSING.....	43
7. RESULTS	51
SST VALIDATION	51
UNDERWAY SYSTEM: INSTRUMENT PERFORMANCE.....	51
CONVERTING FLUORESCENCE TO CHLOROPHYLL.....	52
COMPARISON OF FLUORESCENCE-BASED CHLOROPHYLL AND SEAWIFS CHLOROPHYLL.....	55
EVALUATION OF SEAWIFS ACCURACY.	59
LOGBOOK RETURNS FROM PARTICIPANTS	60
CATCH PREDICTIONS	65
<i>Catch Predictions – An Objective Assessment</i>	65
<i>Catch Predictions - Case Study</i>	68
<i>Catch Predictions – Information from Ocean Color</i>	70
<i>Catch Predictions – Subjective Information from Operators</i>	72
8. FINE-SCALE RESULTS	74
9. BENEFITS AND ECONOMIC EVALUATION.....	75
10. DISCUSSION	77
11. CONCLUSIONS AND FURTHER DEVELOPMENT	79
12. REFERENCES.....	80

CREDITS

Numerous individuals contributed to the overall effort and individual credits on the work conducted on this project and report include:

Principal Investigators	<i>Vincent Lyne, John Parslow</i>
Automated Underway System Development and Installation	<i>Matt Sherlock, Don McKenzie, John Parslow, Jeff Cordell (Lesley Clementson)</i>
Field Work on Underway Vessels	<i>Jock Young, Don McKenzie, (Clive Stanley)</i>
East Coast Underway Sensor Calibration	<i>John Parslow, Lesley Clementson, Alison Turnbull</i>
Western Australia Calibration/Validation of SeaWiFS and AVHRR data	<i>Alan Pearce, Mervyn Lynch (and a number of student and other contributors)</i>
Logbook Data	<i>Rosemary Bailey, Kim Woolley</i>
Underway Vessel Catch Analysis	<i>Jock Young, Rosemary Bailey, Ann Cowling, (Clive Stanley)</i>
SeaWiFS Data Reception, Processing and algorithm development	<i>John Parslow, Chris Rathbone, (CSIRO Remote Sensing Facility)</i>
NOAA AVHRR Data	<i>CSIRO Remote Sensing Facility, Chris Rathbone, John Parslow</i>
Historical Data Analysis	<i>Vincent Lyne, (Roger Scott, Randall Gray)</i>
SST-catch movie	<i>Randall Gray, (Roger Scott)</i>
SST poster	<i>Chris Rathbone, John Parslow, (Melanie Martin)</i>
Catch/Ocean Color Prediction Algorithms	<i>Vincent Lyne, Randall Gray, Roger Scott</i>
Catch Prediction Programming	<i>Roger Scott, Randall Gray</i>
Catch Prediction Liaison	<i>Vincent Lyne, David McDonald</i>
Prediction Production	<i>Roger Scott, Vincent Lyne, Kim Woolley, Melanie Martin</i>
Project Finance Management	<i>Greg Lyden, Toni Moate, (Peter Green, Vincent Lyne)</i>
Report Production	<i>Melanie Martin, Vincent Lyne</i>
Participating Operators and Liaison Personnel	<i>Mark Ebbels, John Hine, John Gibson, Duncan Thomas, Brett, Brendon Doyle, Geoff Binns, Gary Warren, Pat Broder, (Grant Taylor, Tracey Taylor, Marlene Warren, Hans Jussiet, Jim Uttleymore)</i>

Names in parentheses () denote assistant contributors.

We especially thank the funding agencies: Fisheries Research and Development Committee, Australian Fisheries Management Authority and the East Coast Tuna Management Advisory Committee and its subsidiary RRR subgroup, for their support and patience in the long gestation period of this project. The vision and active guidance of Dr Keith Sainsbury was instrumental in initialing this complex project

2. ABSTRACT

We describe one of the largest Australian fisheries oceanography projects ever undertaken. Its specific aim was to develop, evaluate and apply remote sensing information for Australian fisheries. We show that considerable synergies are possible when working directly with tuna fisheries operators. This is evident from the development of the automated underway system for measuring temperature, salinity and fluorescence, its unexpected use in fine-scale operations, and through the implementation of the catch predictions. Despite the interest, and emphasis, in ocean color we show that regional ocean color provides little additional information for regional-scale fisheries operations but it may be of value at fine scales especially for bigeye tuna. Calibration, validation and maintenance of a quality-controlled historical remote sensing data archive, which are often expensive tasks affordable only by large government-funded agencies, is critical in providing the necessary environmental data for analyzing environmental influences on fisheries. The comprehensive and integrated set of remote sensing validations carried off Western Australia, and the underway cal/val activities off eastern Australia, highlights the fact, often taken for granted, that remote sensing data must be reliably and accurately calibrated and validated to be of use. Sea Surface Temperature (SST) algorithms were within 0.5°C of in-situ measurements, and chlorophyll estimates from SeaWiFS were within ±35% off WA, ±30% off eastern Australia, for open offshore waters; comparisons with turbid coastal waters were not as reliable. The poor quality of tropical SST images, due to cloud problems, needs to be improved before we attempt improvements of catch predictions for tropical tuna especially yellowfin tuna. The economic value of remote sensing to fisheries operations is illustrated by the majority of operators participating in the field trials subscribing to receive remote sensing products to assist their operations. Finally, the lessons of history in respect of the use of new technologies suggest that managers need to take early steps in understanding, and incorporating in their management strategies, the use of remote sensing by fisheries operators. At the start of this project in 1992 we would have said that remote sensing has the potential to revolutionize fisheries operations. At the end of this project in 1999 we can safely say that it has and will continue to do so into the future.

3. OBJECTIVES

The original objectives of the project are stated here as presented in our original application proposal and as subsequently modified to reflect the delays in the launch of the ocean color satellite SeaWiFS, and the rapidly changing operations of east coast tuna operators (changes from original are underlined)

1. To develop computational procedures for the validation, analysis and interpretation of ocean color data and to provide derived data sets suitable as input to the analysis of selected fisheries (including seasonal and interannual changes in plankton conditions affecting recruitment conditions for gemfish larvae, exploring relationship between distribution and spawning of orange roughy stocks, some Western Australian fisheries, and the east Australian longline tuna fishery (Objective 2).
2. To determine in conjunction with key industry operators of the east Australian tuna fisheries the utility of ocean color and satellite temperature data in improving the catch efficiency for long-line tuna (potential species include: yellowfin, SBT, Bigeye, Broadbill but will depend on discussions with industry operators), and to determine the economic cost-benefit of the use of satellite imagery in the operational fishery. *(Changed from original to reflect regional shift in operational fishery to longline tuna off Mooloolaba)*

Notes on objectives:

With the delay of the SeaWiFS launch from 1993 to 1997 and changes in operations of the fisheries in that time, the original objective 2 which read as follow:

"2. To determine in conjunction with key industry operators of the east Australian tuna fisheries the utility of SeaWiFS and satellite temperature data in improving the catch efficiency for yellowfin and skipjack tuna, and to determine the economic cost-benefit of the use of satellite imagery in the operational fishery."

was changed to include bigeye and broadbill, and further the area of operation for the project expanded north to include the intensifying operations off Mooloolaba. In a series of meetings with the then eastern Australia tuna management advisory committee ECTUNAMAC and its RRR research subcommittee in the latter half of 1998, the project's objectives were again extended to include an operational (i.e. near real-time) catch prediction component for yellowfin, bigeye, broadbill and skipjack tuna. These predictions were to be carried out till end-February 1999; the area of prediction had to be extended to include Tasmanian waters to track the summer migration of skipjack south so the area of operation effectively extended along the east Australian coast up to about 20°N. In June 1999, at the request of the East Coast Tuna Boat Owners Association, and with funding from the Australian Fisheries Management Authority (AFMA) and Australian Fisheries Funding Agency (AFFA), a series of predictions to assist in minimizing by-catches of southern bluefin tuna were produced till end-September 1999. These predictions showed where the likely areas of yellowfin catches were maximized and by-catches of southern bluefin minimized. Despite all these extensions, the project funding has remained the same except for the small supplemental funding provided by AFMA/AFFA specifically to assist with the SBT by-catch reduction. All of the additional cost increases due to project extensions and general cost increases over the years (e.g. salaries, travel) have been borne by CSIRO.

4. NON-TECHNICAL SUMMARY

The genesis of this project was in 1992 when we foresaw the arrival of a range of new remote sensing systems, and the opportunity to utilize an increasing archive of sea-surface temperature images, which could be of potential benefit to fisheries operations and management. We sought to develop, evaluate and apply remote sensing data to Australian fisheries with the specific application focussed on the east coast tuna fisheries. After a number of years of delays with the construction and launch of the outsourced SeaWiFS ocean color satellite by the commercial company OrbImage, the project eventually began in earnest in July 1996, a few months before SeaWiFS was eventually launched successfully. The repeated delays and huge cost increases (by a factor of 10!) in accessing SeaWiFS data led us to seek alternate ways of obtaining ground-truth data and to extend the utility of sea-surface temperature (SST) in fisheries applications. The end result of this perseverance is the development of a highly successful Automated Underway System, and a catch prediction system based on SST. A less obvious benefit of this project is the lessons it teaches us about the application of new technologies to old problems.

One undeniable conclusion of this work is that there are considerable synergies to be gained from involving industry in both data gathering and exchange of knowledge. Satellite sea-surface temperature data is indispensable in fisheries operations. Operators who are aware of this are capitalizing on the information and others involved in this project are also now utilizing the information. There is a clear need for an educational process to further the use of remote sensing information for the benefit of operators and managers. A subjective, but fair, assessment is that the most successful operators in the east coast tuna fisheries now actively use remote sensing data to assist their operations.

Being smarter about how we use existing data can offer considerable benefits as we demonstrate with our catch prediction methodology. However, such insights rely upon a long history of information on both the environment and the resource. With remote sensing data, quality control via dedicated calibration/validation activities are vital and the need for such activities must be carefully considered and budgeted for especially for the new range of multi-spectral sensors – of which SeaWiFS is one. The comprehensive and integrated set of field surveys conducted in Western Australia, on a minimal budget and with much help from enthusiastic students of Curtin University, provides an indication of the scale and complexity of field, laboratory and algorithm development required to support remote sensing applications. Even so, the achievable accuracy for current satellite sensors is within 0.5°C of in-situ measurements, and chlorophyll estimates from SeaWiFS were within $\pm 35\%$ off WA, $\pm 30\%$ off eastern Australia, for open offshore waters; comparisons with turbid coastal waters were not as reliable. At regional scales, we find that ocean color adds little additional value to information obtainable from SST for fisheries operations. Better atmospheric correction and cloud detection algorithms for the tropical ocean areas promise to add even more value to the existing open ocean SST datasets. The foundation of enhanced understanding of environmental influence on fisheries begins with good quality environmental data. The calibration/validation procedures carried out in Western Australia by Alan Pearce and Mervyn Lynch (appended report) shows how this can be achieved with a standard transect approach, and the automated underway system used on the east coast shows how broad detailed coverage is possible using fishing vessels.

It cannot be overemphasized that while satellite images are attractive in providing pretty pictures over a wide area, the utility of the numbers in the images depends on hard core calibration/validation and careful algorithm development. While there is scope for developing the catch prediction methodology, operators need to use both regional and local knowledge in their operations. The automated underway system can assist in providing local environmental and catch information while at the same time collecting valuable information for ground-truthing regional satellite data and fine-scale catch information. Progress in utilizing the new generation of satellite sensors will we expect rely increasingly upon better use of ships-of-opportunity, such as fishing vessels, as these can offer a more comprehensive data collection capacity than dedicated research ships (for some types of data). However, it is vital that a close liaison is maintained with the vessels and that robust data collection strategies are developed.

One of the ultimate tests of whether this project has been successful is in whether industry is utilizing remote sensing information for their operations. In this respect we can claim, from the uptake of SST information by operators, to have been successful with at least those operators who took part in the trials. Our negative findings with respect to regional ocean color are also an important contribution but this was for a limited test and only for large scales. Analyses of finescale results suggest that the conclusion may not hold at small scales.

Finally, we need to be conscious of history in respect of new technologies whether it be cars, computers, or as we are currently witnessing, the internet. History teaches us there are defined phases in the uptake and application of new technologies and those at the end of what is usually the final phase – management – must come to grips with the implications of the technology as early as possible, especially in respect of the impact of the technology on resources (including the environment).

The report is organized as a main report and a series of appendices. The two main sets of appendices comprise:

Alan Pearce et al: Seasonal and cross-shelf variability of physical, chemical, bio-optical and plankton properties off Perth, Western Australia: 1996-1998

This report describes a detailed set of monthly calibration transects extending 40km due west from Hillarys, Perth during which a comprehensive set of physical, chemical and biological station data were collected. This dataset provides a good foundation for calibrating temperature and ocean color maps for the Western Australian fishing industry.

Jock Young et al: A two boat study of the relationship between swordfish and tuna catch rates and fine- and broad-scale physical and environmental variables off eastern Australia.

This appendix report describes field observations on the fine-scale distribution of catches of tuna in relation to environmental features. In the main paper, a generalized linear model analysis is used to identify explanatory variables and general additive models are used to fit trends to the data. These initial analyses show that fine-scale salinity and fluorescence data is of value after accounting for large-scale variables such as area and month.

Relevant excerpts from the appendix reports are used in the main report where appropriate.

5. BACKGROUND AND NEED

In our original application in 1993, we wrote the following on the background and need:

Background

With the launch of the NASA SeaWiFS ocean color satellite scheduled for mid-1994, a number of Australian Fisheries can potentially benefit from the data to be provided. CSIRO with its international links with NASA is in a prime position to transfer this new technology to the fishing industry and researchers. The satellite can provide for the first time almost real-time data on biologically productive regions to aid targeting of tunas in the east coast fishery as well as other pelagic and demersal fisheries. The proposal outlines the work necessary if we are to be in a position to benefit from this new data.

Need

The lack of knowledge of the status of the environment and its influence on fisheries is a major concern with a number of established and emerging fisheries: the collapse of the gemfish, the recent large catches of young SBT (Southern Bluefin Tuna) off NSW, the fluctuating catches of albacore, yellowfin tuna and skipjack, and the boom and bust catches of jack mackerel off eastern Tasmania all beg the questions: what is the influence of the environment and how can this effect can be quantified and predicted? Past studies of the environmental effect have been based on point measurements from vessels, usually of surface temperature alone, in what we know is a highly dynamic ocean. These are of limited help and indeed in many cases misleading. Scientists and fishermen are increasingly relying on remotely-sensed sea surface temperature data but the biological productivity of water masses and their suitability for various fisheries is still a subject of conjecture. The advent of operational ocean color data that can provide a direct indication of biological production provides an exciting opportunity to advance the state-of-the-art in operational fisheries oceanography.

The potential application of this new tool to fisheries problems requires first of all that we develop a facility to receive, process, archive and disseminate the data. Second, we must work in conjunction with industry to properly interpret the data in terms of catch success or failure and by this means enhance the value of the data to industry. The demand for more accurate assessments of depleted stocks will increasingly require that any stock assessments or evaluations of changes in catch rate properly incorporate the effect of the environment. Satellite data and in particular SeaWiFS data have the potential to substantially advance our understanding of the role of the environment on the distribution of many commercial fish species. This project will provide both a strategic base for the development and application of ocean color data to a number of fisheries, and a detailed technical and economic evaluation of the value of the data in selected emerging fisheries.

Over the last few years, the CSIRO Fisheries remote sensing group has been preparing to receive data from the ocean color sensor SeaWiFS, to be launched by NASA in mid-1994. The value of SeaWiFS over temperature data is that it will allow monitoring of near-surface chlorophyll distributions (an indicator of primary production) every 1-2 days with a spatial resolution of approximately 1 km within the coverage area of receiving stations in Hobart and Perth. SeaWiFS in combination with satellite temperature data will allow us to much better quantify the water mass preferences of various fish stocks.

Before making this data available to researchers and the industry, two technical problems must be overcome. First, the raw satellite data must be calibrated and processed to accurately calculate the parameter of interest. To achieve this, water sample measurements over selected areas of the ocean and throughout the various seasons are required as "ground truth" to support algorithm development and testing. Second, the substantial volume of satellite data that will be received must be efficiently processed, disseminated and archived in order that it can be utilized for the various studies. The processing software must also be able to efficiently scan the archive to produce time series and spatial maps of trends so that changes in time and space at scales down to days and kilometers can be quantified. It is the resulting sequence of highly processed derived data sets that are vital for many fisheries oceanography applications. Potential fisheries applications include the Southeast Fishery (recruitment trends in redfish and gemfish, orange roughy spawning and feeding around "hills"), the Southern Bluefin Tuna Fishery and the East Coast Longline Fishery (effects of mesoscale and interannual variation on catch rates of yellowfin tuna and striped marlin), and several West Australian fisheries (effects of Leeuwin Current variation on recruitment and availability of coastal fish, shellfish and rock lobster).

Interpretation of the significance to the fisheries of temporal and spatial environmental patterns, and indeed the identification of relevant patterns, requires extensive feedback between the scientists and industry operators utilizing these interpretations. The Japanese experience suggests that an empirical approach, where scientists rely solely on information from the fishery and temperature data to identify good fishing strategies, requires some 10 to 15 years to provide useful feedback to the industry (information obtained during a visit to the Japan Fisheries Information Centre (JFIC) by Dr Vincent Lyne and Dr Tim Davis in February 1992). A major part of the uncertainty in data interpretation is the prediction of the biologically productive zones from the temperature data. The Japanese empirical scientists have identified that these productive zones often occur on particular 'sides' of a contorted oceanic front. However, with the availability of SeaWiFS data in almost real-time, we will have direct information on the distribution of biologically productive zones. This together with information from the extensive research cruises conducted by CSIRO will allow us to provide useful feedback to the industry on a much shorter timescale than the Japanese experience.

To be successful, there must be active and effective information exchange between the scientists and industry operators. Again, the JFIC experience is that it would require a full time liaison officer at each major port of call (there are 20 'prefectures' in Japan) and about 20 additional full-time staff to provide the data processing and interpretation. Clearly such resources are not available in Australia, and for our project to be feasible we must restrict the focus of our efforts to only one or two fisheries where we can be assured of good cooperation and feedback.

The example chosen for a first development of operational fisheries oceanography is the southeast coast fishery for yellowfin tuna and skipjack tuna. These fisheries were chosen as representing clear examples where the effective use of remotely-sensed data is expected to make a substantial difference to the operational fishery:

- *The yellowfin and skipjack tuna are recognized as being among the few Australian fish resources that are presently under utilized and that have the potential for supporting an expanded fishery. The skipjack tuna fishery in particular has considerable potential for growth, and is already a key species in supporting Australia's two fish canning factories.*
- *Previous economic research (Campbell and McIlgorm, FRDC Final Report 90/98, 1992) has shown that the southeast coast fisheries for yellowfin and skipjack tuna are highly profitable when the industry can find and track the available fish, but that the fishery as a whole has very limited profitability because of present difficulties in consistently locating and tracking the fish.*
- *Previous biological research has demonstrated that the spatial distribution and availability of yellowfin and skipjack tuna are related to oceanographic conditions, and so the fisheries on these species should be particularly amenable to operational improvements from improved use of remotely sensed data.*
- *Our proposed work has received an enthusiastic response from operators keen to take part in the project.*

The east coast yellowfin and skipjack tuna fisheries provide a very favorable set of circumstances for the first development of operational fisheries oceanography in Australia, and the development will be conducted in such a way as to provide maximum opportunity to quantitatively determine the economic cost-benefit of the operational use of SeaWiFS data by the fishery.

Since the project proposal in 1992 and its commencement in 1994, the project tasks were modified to account for the following key events:

1. *Foremost amongst these were the repeated delays in the launch of SeaWiFS, from 1994 through to August 1997, when SeaWiFS was successfully launched. The sensor has operated successfully since October 1997. These delays have complicated the allocation of resources within CSIRO, and significantly reduced the overall period of SeaWiFS data available to the project for analysis and testing. This necessitated extending the project deadline to December 1998 to allow two years of field activities with the underway system (discussed below) and a period of 16 months or so overlap with SeaWiFS.*
2. *The operational tuna fishery off the east coast has undergone a rapid change from a yellowfin/skip jack fishery to an actively developing fishery for yellowfin, bigeye, and broadbill with a number of operators shifting their operations to northern waters off Mooloolaba. After consultation with the industry, the emphasis of the operational fisheries component has been shifted to include this expanding effort. This necessitated alterations to our plans to accommodate these northern operators and the change in species targets. In discussions with ECTUNAMAC and its RRR research committee in the latter half of 1998, near real-time catch predictions were implemented till end-February 1999. As discussed in the Notes to objectives, further extensions of the project included the SBT by-catch reduction predictions and extensions of the operational region to include Tasmanian waters.*
3. *ORBIMAGE changed its policy on data costs after the study was originally proposed, and increased the costs for a real-time commercial license from US\$20000 to US\$200000, putting it well beyond the means of the project. We have continued the project on a NASA research license, but this license does not allow us to transmit SeaWiFS images to the fishery. To accommodate this change, resources allocated originally for acquiring a*

commercial license were used to manufacture two automated underway sampling systems, which continuously log temperature, salinity, fluorescence and GPS position. This change was in-lieu of the original proposal to use water samplers and two temperature-depth profilers. The underway systems provided valuable information from two different regions and at a range of scales of interest to fishing operations.

Fisheries Oceanography and Remote Sensing

Well before the days of satellite remote sensing, fishers and scientists have known of associations of tuna catches with large-scale patterns in water conditions. Much of the early Australian work on environmental effects on tuna fisheries off eastern Australia was initiated by Hynd (1968) who trialed the use of airborne infrared radiation mapping in assisting fisheries operations. Fishers collected information on surface hydrological conditions to “ground truth” the rapid mapping airborne surveys. This work was initiated in response to observations by fishermen that off NSW surface schools of southern bluefin tuna (SBT) aggregated in frontal regions where the surface temperature ranged from 16.7 to 20°C. Preliminary trials with the instrument successfully identified frontal areas in the preferred temperature range where SBT were subsequently caught. Frontal regions as well as movements of the major water masses were identified and this allowed insights into the chronology of SBT movement off NSW.

The mapping program showed major changes in water masses, due to upwelling and intense currents, taking place within a period of days, and that mapping at half-monthly intervals was not adequate to track such events. The mapping also showed that most catches were in the vicinity of fronts and generally in the “blue water” side of the front rather than the “dirty” or “green water” side. Thus the (subjective) role of water clarity/color was also realized early on. Hynd (1969) also observed that while fronts visible to the spotters may not always be accompanied by temperature changes, fronts separating waters of distinct color change were associated with temperature fronts. The temperature maps were estimated to increase the fishing efficiency by 15 - 20% and to reduce search costs by 20%. A similar trial in the Great Australian Bight showed that water mass conditions were very different and the surveys were not as successful in locating stocks (Humphrey, 1969).

Reflecting on over 30 years of studies on the effects of the environment on distribution and abundance of adult tunas, Blackburn (1969), in his contribution to papers dedicated to Professor Michitaka Uda (Bull. Jap. Soc. Fish. Ocean., Spec. Publ. Nov. 1969), summarized a wealth of long-term observations down to a few key concepts:

- Temperature and pelagic food supply have major direct effects; light and dissolved oxygen may have indirect effects in special situations; nutrients and plankton have indirect effects and salinity has no “certain effect”.
- Indirect effects on temperature and food supply may be associated with currents, fronts, upwelling, thermocline topography and gradient, convection and overturn, and islands and banks.
- Marine animals, which are less mobile and opportunistic than tunas (e.g. inshore and demersal species), can be expected to be affected by more ocean properties than would be needed to explain and specify tuna distributions.

Blackburn (1969) observed that while temperature was a necessary condition, in particular temperature range limits for a particular tuna species, actual occurrence also depended on a suitable food supply. Sea-surface chlorophyll was suggested as a useful property for charting the distribution of tuna food supply. Monitoring and mapping via continuous automatic underway systems aboard ships, or from airborne, or satellite, sensors were suggested but the cost of both systems were deemed to be fairly high. Blackburn foresaw the key requirements of a successful fisheries oceanography project; namely:

- Continuous data gathering and mapping of temperature and other ocean properties
- New instrument technologies for ocean observations
- Skill in inducing relationships between tuna distributions and ocean properties
- Organizing the flow of information between fishers and oceanographers (scientists)

It is appropriate at this point to remark that 30 years or more on from the time that Hynd (1968) and Blackburn (1969), perhaps independently, made their observations and reviews of tuna oceanography, the basic elements required of a successful fisheries oceanography program have not changed. The accuracy and detail of predictions and speed of access to data may have substantially increased in 3 decades but, as we describe in subsequent sections and in the Discussion (Chapter 10), the conceptual fundamentals are still the same.

Lyne et al (1997) summarized a number of other international studies on tuna fisheries oceanography as follows:

The role of environmental factors on pelagic fisheries has been the subject of considerable interest and study for much of the latter half of this century. The impact of the so-called El-Nino induced changes in upwelling off the Peruvian coast on the sardine and other associated marine resources is the best known example (see for example references in Allan et al. 1996). Massive changes in upwelling caused by coupled trans-Pacific changes in atmosphere-ocean interactions cause direct and large-scale impacts on the Peruvian fisheries. On lesser scales, the effects of upwelling on a range of pelagic fisheries (discussed below) suggests direct links between upwelling, nutrient input to the photic zone, primary production and small pelagics. It is however fair to say that the role of environmental factors on larger pelagics has not been well documented.

Yamanaka (1978), in reviewing the work of Japanese scientists summarizes two streams of research on tunas: 1) The "current system theory" in which the life cycle of tuna at various stages in its ecology are linked to special current systems, and 2) The theory that tuna aggregate in regions of upwelling and/or frontal systems with enhanced primary production. Yamanaka (1978) summarized the state of the work at that time by saying that much progress has not been made in the difficult task of studying the relationship between environmental factors and stock size. However, for fisheries operations (at that time), the frontal theory had much to offer if better facilities for the dissemination of satellite imagery were developed.

The extensive experience of Japanese longline skippers combined with the detailed historical data contained in logbooks submitted to Japanese research organizations have allowed Japanese researchers to gain valuable insights into environmental effects on local distributions.

Warashina et al (1989) summarize much of this understanding in detailing two hypotheses based on examinations of sea surface temperature, bottom topographic data and logbook data. The two hypotheses are:

1. Seamounts, plateaus and other topographic structure provide regions of aggregation when they intercept the seasonal migration of major frontal systems such as the subtropical convergence zone.
2. In areas of strong boundary current regimes such as the Agulhas Current, productive zones (in terms of primary productivity) formed from meanders or frontal systems, associated with the boundary current, provide sites of aggregation of SBT.

Australian Observers aboard longline vessels report that off South Africa abnormally cold conditions will inhibit the appearance of fish normally found in a region. Thus, whilst the presence of topographic structures or frontal systems provide sites for aggregation, a prerequisite for the appearance of SBT is water temperatures within a suitable range associated with the fish. Whilst these observations by the Japanese researchers provide valuable insights into the spatial dynamics of SBT, Warashina et al (1989) summarize the state of research, and the necessary future research, by hypothesizing that higher primary production may be associated with the dynamic meanders of boundary currents. He suggested that detailed study of this hypothesis using satellite ocean color data was required. Biological factors of size and maturity and availability of food organisms were also suggested as worthy of future research.

A number of studies of other pelagic species also highlight the role of oceanographic features in inducing aggregations. Off Chile, thermal fronts and upwellings are related to aggregation sites for albacore (Barbieri et al 1989), and small pelagic species (Castillo et al 1996). Off Vancouver Is Canada, salmon fishing effort is concentrated around topographic features and thermal boundaries (Borstad et al 1989). A number of other studies also show that good fishing areas for a range of pelagic fish, such as skipjack tuna, yellowfin tuna and albacore, are located near thermal fronts and upwellings (Laurs & Lynn, 1977, Breaker, 1983, Laurs, Fielder & Montgomery, 1984, Maul et al. 1984, Fielder, Smith & Laurs, 1985, Fielder & Bernard, 1987, Ramos et al. 1996). For skipjack tuna (Katsuwonus Pelamus), Barkley et al. (1978) use laboratory studies to infer that small skipjack tuna are able to inhabit the warm surface waters of the tropical and subtropical ocean but larger skipjack fish require cooler waters with unusually higher concentrations of dissolved oxygen.

Remote Sensing and Fisheries Information Systems

What is the role of remote sensing in a fisheries information system? And, for an end-user what are the potential benefits and requirements to use such information? In this section we review and summarize the available remotely-sensed information, the various nations that have established information systems, commercial companies providing fisheries forecasting services and we then summarize key attributes of successful operations.

Remote sensing systems

A number of government and private agencies have established fisheries information services to aid targeting operations. An effective and efficient information service relies upon many complex data sources and timely processing and dissemination of resulting products. A variety of data and remote sensing technologies are used (discussed below) and the potential list of satellites available, or soon to be available, continues to grow quickly (Table 5-1).

Table 5-1 Select list of satellite sensors providing sea-surface temperature, ocean color or radar/scatterometer images of the ocean. This table is an abridged version obtained from the Goddard Space Flight Center site at: <http://rac.gsfc.nasa.gov/sensor.html> We list only those of potential application to ocean studies.

Sensors	Country	Launch Date	Full Name	Spectral Res. (um)	Spatial Res. (m)	Swath Width (km)	Revisit Freq. (Days)	Data Communication Information
AVNIR	Jpn	August 1999	Advanced Visible and Near-Infrared Radiometer	.42-.89	16	80	4	Frequency: S-Band (Command/Telemetry), 2220.00 MHz (Return), 2044.25 MHz Forward, Ka-Band (Mission Data), 25.8505 GHz (Mx. 66 Mbps). Bit Rate: 500 bps (Command), 4096 Telemetry. Tracking Method: About and Program Tracking. Data Processing: Data Bus System. Data Recorder: HK Data Recorder x 1. Mission Data: X-Band 8.15/8.25 MHz. Direct Transmission for Local Users: 467.7 MHz (Transmission Frequency), 23.4375 (Data Rate)
GLI	Jpn		Global Imager	.38-11.95	250-1000	1600	4	
AMSR	Jpn		Advanced Microwave Scanning Radiometer	6.93-52.8 GHz	500-50000	1600	4	
VSAR	Jpn		Variable Off-Nadir SAR	L (GHz) HH, VV	10-100	70	45	
ARIES-1	Aus	2001	Australian Resource Information and Environment Satellite	Visible	10	15		Landsat-7 Communications: "S-Band (2 omni-directional antennas), 5 W, with real-time telemetry data rates of 1.2 kbits/s and 4.8 kbits/s of playback data, 2 kbits/s of command data. "X-Band (3 steerable antennas), 3.5 W; each antenna transmits data on two channels, with each channel carrying 75 Mbits/s (total of 150 Mbits/s per antenna); up to 3 separate links are supported.
ARIES-1	Aus		Australian Resource Information and Environment Satellite	.4-2.5	30	15		
ALI	US	Dec-99	Advanced Land Imager	.48-.69	10		16	Ground Stations to receive, process, and route science and housekeeping data to GSFC. X-Band: Receive up to 80 Gbits of science each day at 105 Mbps. Record the received X-Band data on hard media, mail to GSFC and store for 30 days. S-Band: Housekeeping data-route selected virtual channels to GSFC in real-time, record up to 200 Mbits of data each day, and ftp recorded data to GSFC within one hour. Store for 30 days.
Hyperion	US		Hyperspectral Imager	.4-2.5	5	7.5 by 100	16	
Hyperion	US		Hyperspectral Imager	.48-.75	30	12.9	16	
MODIS	US	2000	Moderate Resolution Imaging Spectroradiometer	.4-14.4	250, 500, 1000	2330	16?	X-Band
SAR	US	2001/2002	Synthetic Aperture Radar	1.2575 GHz (L-band), 9.6 GHz (X-band) or 5.3 GHz C-band.	25	100	10	Downlink: Real-time and playback telemetry data simultaneously. Peak data rate: 2 x 150 Mbps @ X band; 200 kbps @ S band. Average data rate: Up to four 5-min passes per orbit for X band; one 5-min pass/day for S band.
AVHRR	US	1991	Advanced Very High Resolution	.58-12.4	1100	3000	12 Hours	Currently downlinked.

AVHRR/2	US	1994	Radiometer Advanced Very High Resolution Radiometer	.58-12.4	1100	3000	12 Hours	Currently downlinked.
AVHRR/3	US	1998	Advanced Very High Resolution Radiometer	.63-12.0	1100	3000	12 Hours	Currently downlinked.
AVHRR/3	US	1999	Advanced Very High Resolution Radiometer	.63-12.0	1100	3000		Currently downlinked.
AVHRR/3	US		Advanced Microwave Sounding Unit	89.0-191 GHz	16000	2200		
OrbView	US	1999	OrbView	.45-.90	4	8	3	\$200,000 fee for yearly downlink license.
OrbView	US	200?	OrbView	.45-.90	4	8	3	\$200,000 fee for yearly downlink license.
QBM	US		OrbView	.45-2.5	8	5	3	
QBP	US	1999	QuickBird	.45-.90	4	27	1-5	Downlink: X-band data rates of 300 Mbits/s to EarthWatch owned ground receiving stations.
SAR	US		Multispectral QuickBird	.45-.90	1	27	1-5	
RadarSat	Can	1995	Panchromatic Synthetic Aperture Radar	5.3 GHz (C- Band)	8-100	up to 500	24	Downlink: two parallel X-Band channels at 105 Mbits/s for real-time data and 85 Mbits/s of recorded data. ASF is a Ground Station.

Various restrictions and requirements are necessary for gaining access to satellite information as evident in Table 5-1. For X-band reception, there are only two receivers in Australia: one in Hobart – the TERSS facility – and another at Alice Springs capable of receiving the data. In other cases, such as with OrbView/SeaWiFS, a yearly access fee must be paid for commercial access. Along with the necessary hardware and access permission, a suitable reception, archiving and processing facility together with experienced personnel for operating the facility are required. Simpson's (1992) detailed review of the use of remote sensing and geographic information system (GIS) technologies in fisheries operations and management provides a good background to technical aspects of utilizing current technologies.

Given the costly nature of remote sensing and the high technology requirements in data reception and processing, it comes as no surprise that the agencies involved in operational fisheries (Table 5-2) are some of the major research agencies at the forefront of remote sensing science in the world. In this regard, this project is fortunate in having access to the one of the best remote sensing facilities here at the CSIRO Hobart site. This site, despite limitations in resources, is arguably one of the most efficient in the world and was rated as the second best site in supplying NASA satellite information for the global 1km project (China was rated number one but apparently pooled resources from 4 satellite reception sites). It has also received one of a few real-time research licenses from Orbimage for restricted access to data from Orbview-2 (ala SeaWiFS).

More importantly, but often overlooked, is that along with the hardware and software, successful remote sensing facilities have skilled and internationally-recognized remote sensing scientists who participate in global remote sensing initiatives. It is difficult to assess the contribution of such individuals but it is often the case that the viability of major projects may well hinge on one such individual. In the case of this project we have been very fortunate to have the participation of Dr John Parslow – one of Australia's principal marine remote sensing scientists – whose is a member of a number of international science teams working in support of current and future remote sensing missions.

Operational Fisheries Information Systems

In addition to the requirements for remote sensing data reception and processing detailed previously, establishing an operational system requires effective means of quickly processing and communicating relevant value-added remote sensing products to the outside world. Thus, the few well-established operational fisheries agencies have evolved over many years to produce products tailored to the needs of their clients (Table 5-2). In most cases each of these operations involves at least two groups: remote sensing and fisheries applications, with possibly a third group in the intermediate areas of oceanography and biological oceanography. Generally there is a bias in one of the fields depending on which group has taken the lead in establishing the service. This is evident from the type of products offered. Most of the services provide operational assistance with fisheries operations but in a few instances, the service provided is used for management purposes (e.g. Canada). This highlights one of the main management issues with new technology; namely that fishing operators and companies are quick to adopt technologies that will assist in reducing search effort and capture but management is unable (for a variety of reasons) to use these same technologies, or to account for the consequences of their adoption by operators.

Table 5-2 Operational fisheries agencies and services for fishing nations. Information sourced from Simpson (1992) and other promotional literature. (Note: We do not include our current project in this list.)

Country	Agency	Status	Fisheries Area	Technology	Information/Use	Comments
Australia US	CSIRO NOAA/NASA	Ongoing Early 1970s ...	Tuna Fleet Tuna Fleet	AVHRR AVHRR SST CZCS Wind	Online SST charts Charts (color) – operational fishing	Automated online access Thermal charts – 25-40% reduced search time. CZCS: Albacore, swordfish – 50% savings in search time
US	NOAA, Honolulu		Squid, salmon, albacore. N Pacific Transition. Subarctic Front W Canada	AVHRR	Thermal structure charts – operational fishing	
Canada				AVHRR CZCS airborne SST, CASI Aerial photos	Salmon & herring fishing effort & environment	Fisheries independent aerial surveys
USSR	Space Information Service	Ongoing	CIS fishing fleet – worldwide	METEOR KOSMOS	Daily data from 180 vessels + remote sensing. Isotherm, dissolved oxygen tracking, Statistical & dynamical models.	Daily-weekly recommendations sent to each fishing region (10 main ones)
Japan	JAFIC	Ongoing	Japanese Prefectures , Worldwide	AVHRR Research vessel Market info	5 day average SST contours, species, catch, size, gonad index + market info.	Combines complex information and assessments by experienced experts. Labor-intensive system relying on fax transmissions and hand-drawn contouring. NOAA APT receivers on most high-seas vessels Tuna forecasts based on 5- week prior history. Encourages use of remote
France	ORSTOM IFREMER	1982 – 1985	Mediterranean Sea, tropical	NOAA METEOSAT SPOT	SPOT (for shellfish farms). ARGOS for data	

Germany	European Space Agency program		Atlantic, W Africa. Tuna and aquaculture	ROSI MOS	transmission N/A	sensing amongst Pacific Island nations. N/A
Scandinavia	Danish Inst. Fish. Mar. Res.		Baltic Sea. Salmon	AVHRR Airborne sensors	Algal blooms, larval survival	Mainly used for coastal zone monitoring and aquaculture farming.
China	Various agencies		Yellow Sea, China Sea	FY-1A FY-1B	Operational forecasting. Red tides	A variety of forecasting methods are used.

Despite the enormous technical and operational difficulties involved in establishing an operational fisheries program, a number of commercial operations exist (Table 5-3). In two of these cases (NIWA, Orbimage) the operations are application arms extending from a core remote sensing program that support other research and applications. In the case of Orbimage, this core group was responsible for building and launching the OrbView-2 (ala SeaWiFS) satellite. ROFFS© (<http://www.roffs.com/>) is an entrepreneurial company in the US catering for the recreational market and commercial fishers. Their longevity and apparent success would appear to indicate that what they provide is considered to be useful by their clients. However, no objective assessments appear to exist for the success rate (of predictions) nor of the profitability of these operations. With so few commercial fisheries forecasting companies one would think that there would be scope for more to participate, but this appears not to be the case as active poaching of rival analysts has taken place. The conclusion we draw from this is that while most fishers gain some utility from remotely-sensed images alone, there are very few groups who have successfully taken the next step up to fisheries forecasting. Those that have achieved this elusive goal are highly valued.

Table 5-3 Commercial operational fisheries forecasting companies and agencies.

Country	Agency	Status	Fisheries Area	Technology	Information/Use	Comments
NZ	NIWA MAF Fisheries	Commercial. Ongoing?	Tasman Sea. Albacore, tuna, marlin.	AVHRR	Isotherm analysis charts, gradient analysis. Charts delivered by weather radio fax, mail, courier.	1992 prices: \$110-140/chart + optional extras (color, gradient analysis). Ref: Dr Michael Uddstrom, NIWA, PO Box 3047, Wellington.
US	ROFFS©	1987...	US inshore & offshore	Not specific	Custom charts for set areas, species, seasons	See: http://www.roffs.com/
US	Orbimage	1997...	Worldwide	OrbView-2 (aka SeaWiFS) AVHRR Altimeter	Plankton images + SST + weather and currents from sea-surface height	Email and fax delivery. See: http://www.orbimage.com/apps/marine/marine.html

SST and Ocean Color in Fisheries Applications

The use of sea-surface temperature (SST) in fisheries applications is well established (see previous sections) and it is appropriate at this point to present details of the SeaWiFS ocean color sensor in order to better understand its potential utility.

SeaWiFS (Sea-viewing Wide Field of View Scanner) is a multi-spectral ocean color scanner with high signal-to-noise ratio, designed to allow estimation of phytoplankton chlorophyll in oceanic waters from space. SeaWiFS operates with a 1.2 km pixel at nadir, and measures upwelling radiance in 6 visible and 2 near-IR bands. The sensor is owned and operated by a commercial company, ORBIMAGE, but NASA has carried out a bulk data purchase for research purposes. The research described here was carried out under a research license from NASA.

A series of calculations must be carried out in order to convert upwelling spectral radiance at the satellite into chlorophyll estimates. Atmospheric scattering can account for over 90% of the radiance reaching the sensor. The effects of atmospheric absorption and scattering, and reflection at the sea surface, must be accurately removed in order to obtain estimates of water-leaving radiance. The water-leaving radiance or reflectance depends in turn on the absorption and back-scattering of light within the water, due both to the water itself and various dissolved and particulate constituents.

In open ocean waters, the dominant optical constituents are phytoplankton and their degradation products. Consequently, there is a strong relationship between phytoplankton pigment concentrations and the water-leaving spectral reflectance. Based on simultaneous in situ measurements of water-leaving reflectance and chlorophyll concentrations, direct empirical relationships have been developed between the ratios of water-leaving radiance in certain visible bands, and pigment concentrations.

The SeaWiFS chlorophyll images used in this study were processed in Hobart using standard NASA algorithms developed by the NASA SeaWiFS Science Team, and provided as part of the SEADAS processing package (see links at: <http://SeaWiFS.gsfc.nasa.gov/SEAWIFS.html>). The SEADAS chlorophyll estimates are calculated using an empirical band-ratio algorithm (Aiken et al), which uses the ratio of normalized water-leaving radiance at spectral bands centered on 490 and 550 nm.

There are a number of potential sources of error in SeaWiFS chlorophyll estimates. The atmospheric correction procedure requires that the satellite sensor be calibrated very accurately. Because the atmospheric signal may account for over 90% of the total signal, even small calibration errors of 1% can lead to errors exceeding 10% in water-leaving radiance. The atmospheric correction algorithm must also make certain assumptions about the nature of the aerosols. Under some circumstances (e.g. absorbing aerosols), these have been shown to lead to significant errors.

The band-ratio algorithms assume a fixed relationship between chlorophyll and the spectral shape of water-leaving radiance. In reality, this relationship is affected by a large number of other variables: the size of phytoplankton cells (packaging effect), the pigment composition of phytoplankton, and the amounts of other optical constituents, especially non-algal particulates (NAP) and colored dissolved organic matter (CDOM). In open ocean waters, CDOM and NAP tend to covary with chlorophyll, but even there, recent evidence suggests some large scale variability. On continental shelves and coastal waters, CDOM and NAP can vary widely depending on river inputs and sediment resuspension, and the band-ratio algorithms may fail entirely (Parslow et al, 1998).

The NASA SeaWiFS algorithm has a goal of estimating chlorophyll in open ocean waters with a 30% error on a global basis. Given the various sources of error, it is not possible to be confident a priori that this will be achieved in a specified region or season. Regional differences in phytoplankton composition, or in concentrations of CDOM or NAP, could lead to increased error. These are likely to be exacerbated in continental shelf regions. Regional differences in aerosol composition have already been shown to cause significant errors.

Given these possible sources of error, it is important that the accuracy of SeaWiFS chlorophyll estimates is assessed directly by comparison with in situ measurements (ground-truth). NASA has encouraged an international program of calibration and validation of SeaWiFS estimates. The results reported here contribute to that international program, and directly assess the validity of the SEADAS algorithms in continental shelf and offshore waters off Australia's east coast (Figure 5-1).

The conventional method used to obtain ground-truth is to collect water samples from research vessels, filter these to collect phytoplankton, extract pigments, and measure chlorophyll using HPLC (high pressure liquid chromatography). This method has a number of drawbacks. Research vessels are expensive, and opportunities to collect ground-truth are limited, providing little spatial and temporal coverage. This is exacerbated by the presence of cloud cover, which may render most or all of a particular cruise useless. It is highly desirable that a sampling platform be used which can sample frequently or continuously over a wide region.

Chlorophyll measurements from bottle samples have another potential disadvantage. The chlorophyll estimate provided by SeaWiFS is based on upwelling radiance from a pixel over 1.2 km across. There may well be spatial variation within pixels. Under these circumstances, it is not clear that a 2 or 4 liter bottle sample collected somewhere within a pixel can be compared with the satellite average estimate.

In this study, we have adopted a different method for collecting SeaWiFS ground-truth, by deploying underway fluorescence sensors on fishing boats. Underway chlorophyll fluorescence sensors have long been used on research vessels as a way of estimating chlorophyll biomass. They have the advantage of covering variation in phytoplankton biomass on a wide range of time and space scales (Falkowski and Kolber, 1995). This variability is driven by a combination of large scale environmental factors and small scale biological and physical processes.

In particular, underway fluorescence measurements can resolve spatial variation both within pixels and between pixels, and provide regional and temporal coverage cost-effectively. By deploying fluorescence sensors on fishing boats (described in subsequent sections), we have been able to obtain much more temporal and spatial coverage at vastly less cost than would have been involved in using research vessels. Dickey et al (1993) stress the value of integrating data sets from moorings, ships and satellites in studying bio-optical phenomena over time scales varying from minutes to seasons.

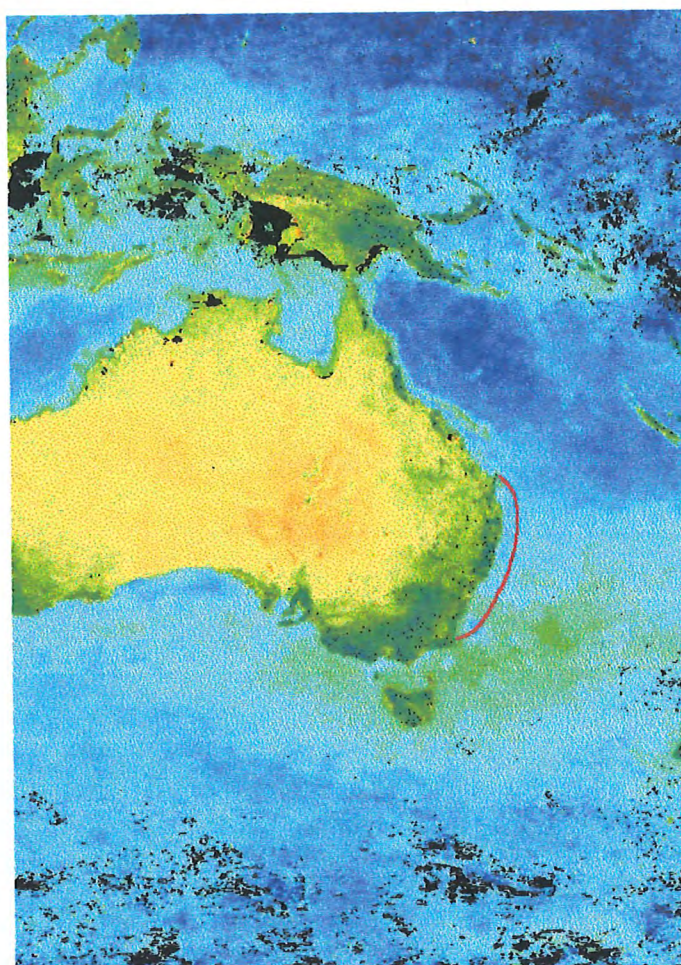


Figure 5-1 SeaWiFS composite image for the Western Pacific from 04 September to 28 October 1997 (the color scheme for the open ocean grades from blues for low chlorophyll, through to greens for high chlorophyll). The red line encloses the area the long-liners fished during this study. This image was provided by the SeaWiFS Project, NASA/Goddard Space Flight Centre.

Apart from Orbimage, we do not know of any agencies or commercial operations that utilize ocean color imagery in operational fisheries services (for shelf and high-seas fisheries), and even less of the utility of ocean color for fisheries applications. Here's what ROFFS© says about the respective utility of water temperature and ocean color (excerpt from <http://www.roffs.com/>, used with permission):

“MAPS OF OCEAN COLOR:

We do use ocean color and turbidity information for our analyses. The use of water color as an indicator of phytoplankton, ocean primary productivity, and fish as derived from satellites is in an experimental stage. One orbiting satellite (ADEOS) with an ocean color sensor was being used strictly for research purposes, but is no longer operational. With the launch of the SeaStar satellite, the SeaWiFS color data are available primarily for the scientific community. The cost of the data to commercial users is prohibitive. Scientists at ROFFS© have studied ocean color imagery intensively and have suggested some potential fishing applications on a limited basis. Be aware that the majority of the important ocean features observed with ocean color imagery were also observed with ocean surface temperature data. No one has shown that ocean color data, when compared with ocean temperature data, will provide better information for finding fish on an operational basis. The main problem with ocean color data derived from satellites, as with the sea surface temperature data, is cloud interference. ROFFS© has many years experience providing useful fishing forecasting analyses in areas plagued with clouds. While we still have many improvements to make, we have developed unique (and proprietary) techniques that allow us to differentiate between true ocean features and cloud artifacts. No other companies have our level of experience in developing operational products for areas where clouds are a problem. ...”

Thus, based on past studies we note here the three characteristics of the use (non-use) for fisheries application of ocean color compared to temperature:

- *Free access to ocean color is for strict research purposes and commercial access fees are high.*
- *Ocean color sensors are more sensitive to cloud effects (plus night time passes are not useful).*
- *The utility of ocean color, at regional scales, beyond what is achievable with SST, has not been established.*

However, there have been no studies to date that we are aware of which explicitly examine the potential utility of ocean color for fine-scale resolution of catch distributions in relation to environmental variability. Such a study conducted in this project is reported by Young et al (appended to this report).

Nature of East Australian Tuna Fisheries

While our initial interests were primarily with yellowfin (YFT – *Thunnus albacares*) and skipjack (SKJ – *Katsuwonus pelamis*) tunas; the project expanded (as explained previously) to include bigeye (BET - *Thunnus obesus*) and broadbill (BBL - *Xiphias gladius*). Yellowfin tuna still remains the dominant tuna species caught off eastern Australia (e.g. Campbell, 1999). In this section we examine the dynamics of the fisheries regionally (drawing upon the summaries of Hampton et al, 1999) and locally, and then we examine operational considerations with respect to the use of remote sensing in the each of the fisheries.

In reviewing the tuna fisheries off eastern Australia, the relevance of remote sensing is in helping us understand the spatial dynamics of stocks, both movement and recruitment, in relation to environmental variability. These are key uncertainties in the analyses of trends in abundances of yellowfin and other tuna stocks (e.g. Campbell, 1999). In the case of yellowfin tuna for instance, there are large interannual changes in computed abundance levels within the eastern Australia fishing zones but there is no evidence of a long-term trend amidst the substantial interannual variability (Campbell, 1999).

Regional Perspectives

Yellowfin Tuna (YFT)

Regionally, the YFT fishery extends along the Pacific Islands and SE Asia and includes the tropical and equatorial Pacific. Purse-seiners account for about 60% of the catch, of small YFT, with the rest of the catch, large adults, taken by longlines. Largest catches by the purse-seiners occur in the so-called *warm pool* off Papua New Guinea. Variations in catches are thought to be linked to ENSO (El-Nino Southern Oscillation) especially east of 160E which is at the edge of a zone of high purse-seine catches. Larger catches in this area occur during El-Nino when the normal upwelling system in the eastern Pacific slows or ceases and warm water conditions are established in central and eastern Pacific. Causal links between catch and ENSO may occur via environmental impacts, vulnerability of stock to purse-seines (due to changing thermal structure conditions) and variations in the size of stock itself through recruitment. In contrast, the eastern AFZ of Australia is hypothesized to have large recruitment during La Nina and low recruitment during El Nino conditions (Campbell, 1999). These complimentary observations suggest a possible scenario of a core distribution of stock that moves with the alternating water conditions during El Nino/La Nina events, with possible overflow of stock down the eastern AFZ during La Nina conditions, and consequently reduced catches east of 160E in the warm pool. Highest annual exploitation rates occur around Philippines/Indonesia and recruitment variations display both slow (decades variation in growth rates due to environment changes) and fast variability (yearly - ENSO). Impacts in most Western Central Pacific Ocean (WCPO) fishing areas appear to be low except for Area 3.

Bigeye Tuna (BET)

Juvenile BET are caught by purse-seines and adults via longlines. BET commands the highest sashimi prices for all tunas. This has spurred efforts on new fishing methods (deeper purse-seines, drifting FADS, deeper longline sets, live bait) which are now being adopted. The majority of catch occurs in equatorial waters with significant longline catches.

Skipjack Tuna (SKJ)

SKJ are caught primarily by purse-seines and pole-and-line, with smaller catches by artisanal fishers in eastern Indonesia and Philippines. The main fishery occurs east of PNG and is strongly influenced by ENSO events. During El-Nino greater portions of the catches occurs east of 160E. Catch per unit effort statistics are confounded as there has been a greater reliance on floating sets during the 1990's (up from 10% to 80% for USA, and up from 50-80% for Japan). Fishing effort appears to have increased and masks interpretation of catch per unit effort based on nominal effort measures (number of sets).

Local Perspectives

Oceanography of the study area

The tuna fisheries of eastern Australia are within complex ocean waters ranging from the tropical oligotrophic waters of the Coral Sea in the north, the swift energetic East Australian Current waters in the central region, to a mixture of tropical and subantarctic waters in the subtropical convergence zone of the south. The extent of the water masses, the strength of the East Australia Current and nature of the mixing in the subtropical convergence are all subject to both seasonal and interannual factors. Late in the Australian summer the East Australia Current is at its strongest and its waters can be carried in a series of eddying currents that extend as far south as the southern tip of Tasmania. In the winter it retreats northward as the winter westerlies drive subantarctic surface waters northward. Interannual variations can be even more pronounced: El Nino years produce relatively weak currents as the equatorial waters feeding the western Pacific are at their weakest. In contrast La Nina years appear to be characterized by higher temperatures along the eastern seaboard and extend further southward.

The fishery

The east coast domestic longline fishery extends from Eden on the southern coast of NSW to as far north as Cairns in northern Queensland and although concentrated within the 200-mile Australian Fishing Zone individual boats regularly fish beyond the zone. Presently, Mooloolaba, southern Queensland, is developing as a major landing and resupply port for the broadbill swordfish and tropical tuna fishery. Ulladulla and Bermagui are two other major ports further south which service more localized fishery operations along the NSW coast. Eden is the principal port for the purse-seine skipjack fishery although this is about to change with the impending closure of the cannery there. The catch ranges from a mixture of southern bluefin, yellowfin and bigeye tuna and broadbill swordfish in the south to a mixture of yellowfin and bigeye tuna and broadbill swordfish in the north (Ward in preparation).

Historical catch records (Figure 5-2) show that while yellowfin tuna catches dominate, since about 1993 there has been a rapid increase in catches of bigeye tuna followed by a dramatic increase in broadbill since about 1995. In terms of tonnage, the broadbill catches are now approaching that of yellowfin.

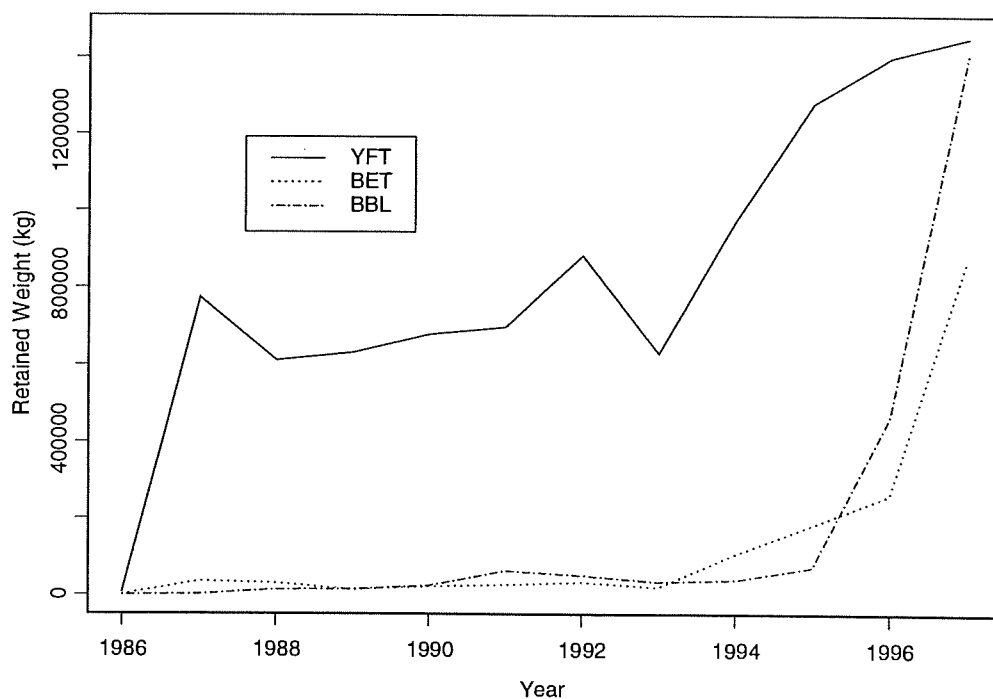


Figure 5-2 Yearly variation in retained weight of yellowfin (YFT), bigeye (BET) and broadbill (BBL) in the eastern Australian AFZ. Data drawn from Campbell (1999, Table 1.1).

The increasing capitalization of the fishery, evident from the rapid increases in the catches since the early 90's will demand more detailed knowledge of the distributional dynamics, especially of the new target species.

Catch Distributions

The distribution of Japanese fishing effort for tuna off eastern Australia (Figure 5-3) shows the highest densities of effort along the region of the continental slope extending from Sandy Cape (about 25°S) down to about 29°S. Off NSW, there is a conspicuous concentration of effort just outside of the South East Restricted Area. Between these two concentrated fishing areas, the effort is relatively low but there is some suggestion of a concentration around some of the offshore islands and seamounts associated with the Tasman Abyssal Plain and the Lord Howe Seamount Chain.

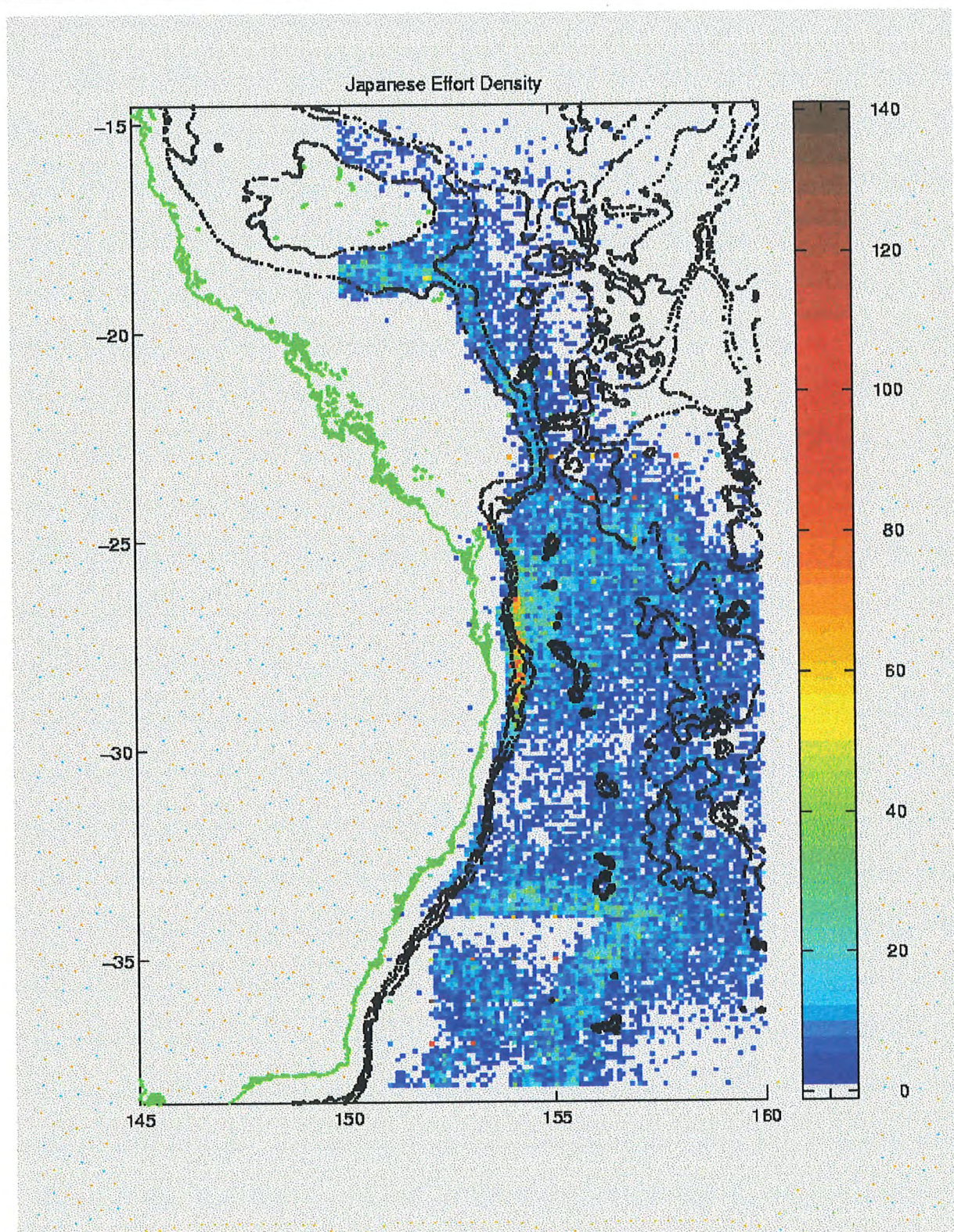


Figure 5-3 Distribution of Japanese longline fishing effort off eastern Australia indicated as the number of records of fishing logs summed over a 0.1 degree square block. Data records are from the AFMA logbook database up till and including mid-1997. Note the "hotspots" of supposed dense effort at integer values of latitude/longitude (a result of data being recorded to the nearest integer lat/lon), and some catches on land.

Yellowfin tuna are caught along the eastern Australian coastline, and as far south as southern Tasmania in warmer years (Figure 5-4). Fishery and tag recapture data indicate that the stocks off eastern Australia are the result of overflows of the main western tropical Pacific stock down the east coast of Australia aided by the southward flow of the EAC (Hampton and Gunn 1998). Catch distributions in the eastern AFZ (Figure 5-4) show a broad region in the tropical Coral Sea of high catches which concentrates into a narrow slope-bound stream down to the northern limit of the restricted zone. An offshore veering of the high catches trending in a north-east direction is also evident. We hypothesize this to be associated with the EAC current system evident from the mean temperature distribution off eastern Australia (Figure 5-5). There is also a suggestion of enhanced catches associated with the Lord Howe ridge system. As discussed previously, there is some evidence that the number of yellowfin in eastern Australian waters increase in La Nina years when the EAC is at its strongest.

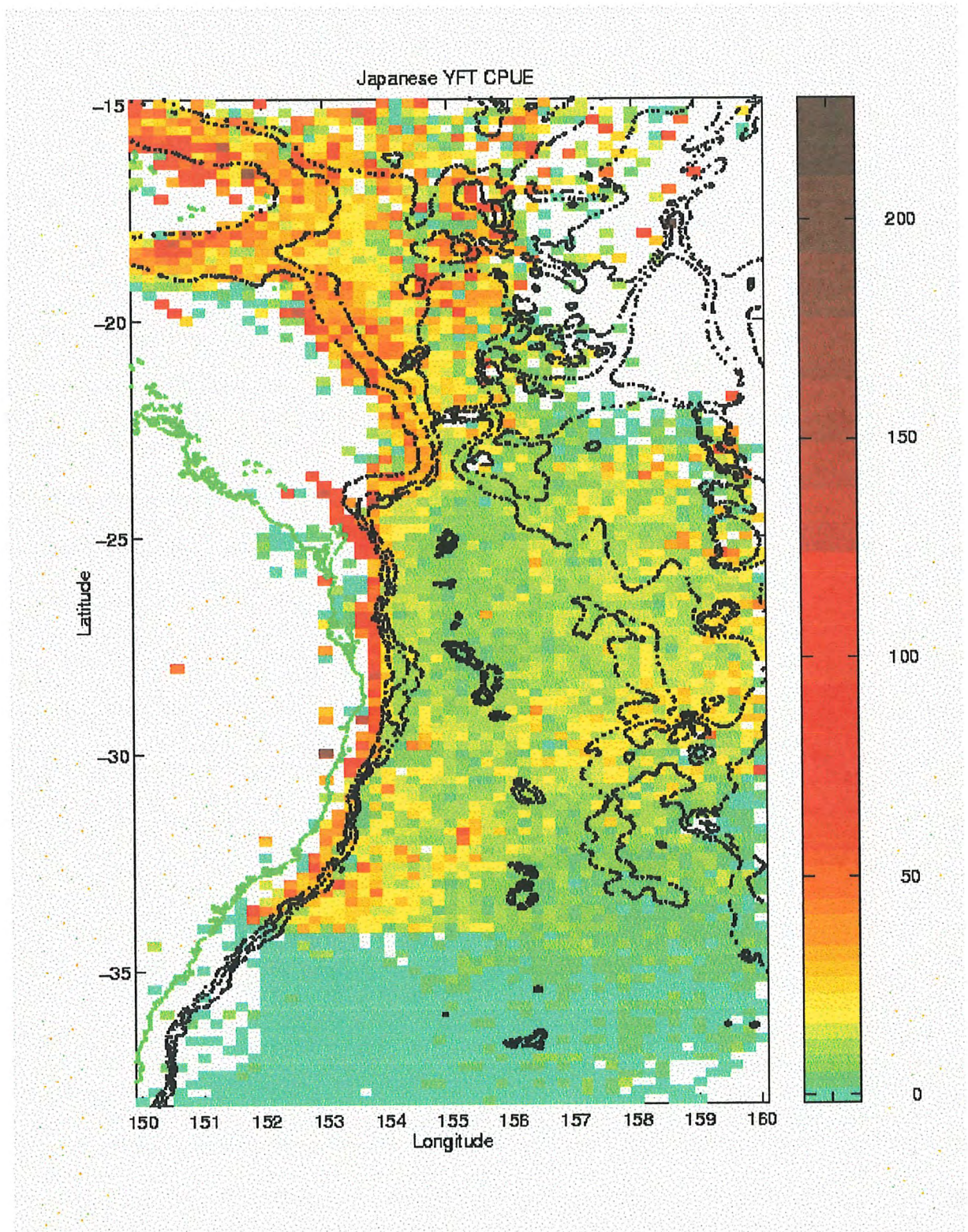


Figure 5-4 Average number of yellowfin tuna caught over a 0.2 degree square block computed from the Japanese fishing log records held in the AFMA database up till mid-1997. The average is the sum of catch counts divided by the number of records so no account has been taken of hook effort. This plot is merely to indicate the gross distribution pattern. The rather amusing plots of catches on land reflect some of the more visible uncertainties with this data.

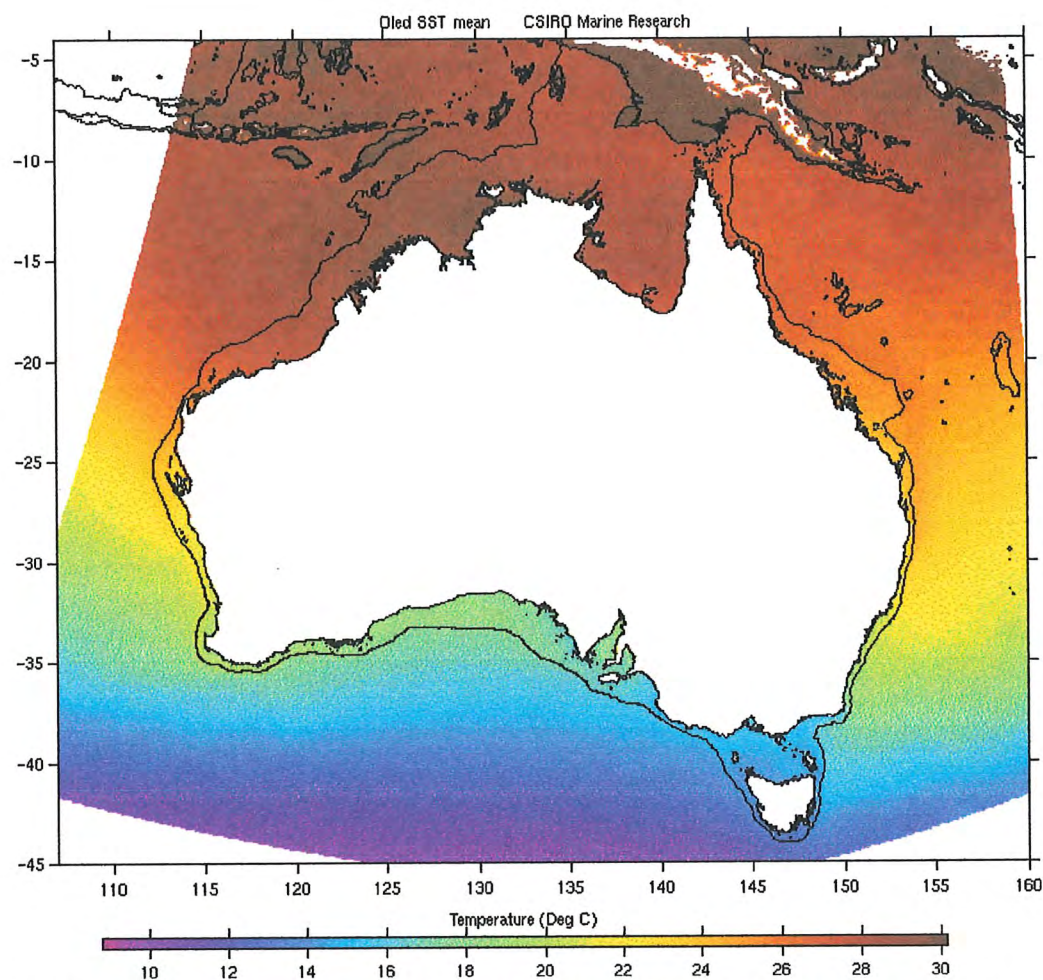


Figure 5-5 Mean temperature distribution around Australia computed by an optimal interpolation method for March 1991 to March 1997. (Ref: <http://www.marine.csiro.au/~griffin/OISST/>)

Catch data from both the domestic and foreign longliners indicate that bigeye tuna have similar movements to yellowfin although fewer of the former appear to travel as far south as the yellowfin (Figure 5-6). They tend to be caught in similar waters to swordfish but are found deeper in the water column. Highest catch rates (Figure 5-6) are located off the slope and continental rise region between about 25 and 30°S and near some of the offshore seamounts in that latitude band. Not surprisingly this is the region within which the deeper waters of the East Australia Current (EAC) flow as a jet along the continental slope/rise. We hypothesize that the concentration around the seamounts and offshore islands are the result of localized upwellings and enrichment – topographically-induced by interactions with the EAC. The second area of high catch rates is well offshore in the latitude band 30 to 34°S. This band is associated with the separation and offshore “recirculation” of the deeper waters of the EAC current (the surface waters of the EAC, and associated yellowfin catches, separate further south and in a narrower band – see Figure 5-4). In this band, highest catch rates appear concentrated around the seamounts (Derwent Hunter Guyot, Barcoo Bank and Taupo Bank), the Dampier Ridge and Lord Howe Rise structures. The apparent reduced catches off NSW are an artifact of the exclusion zone there.

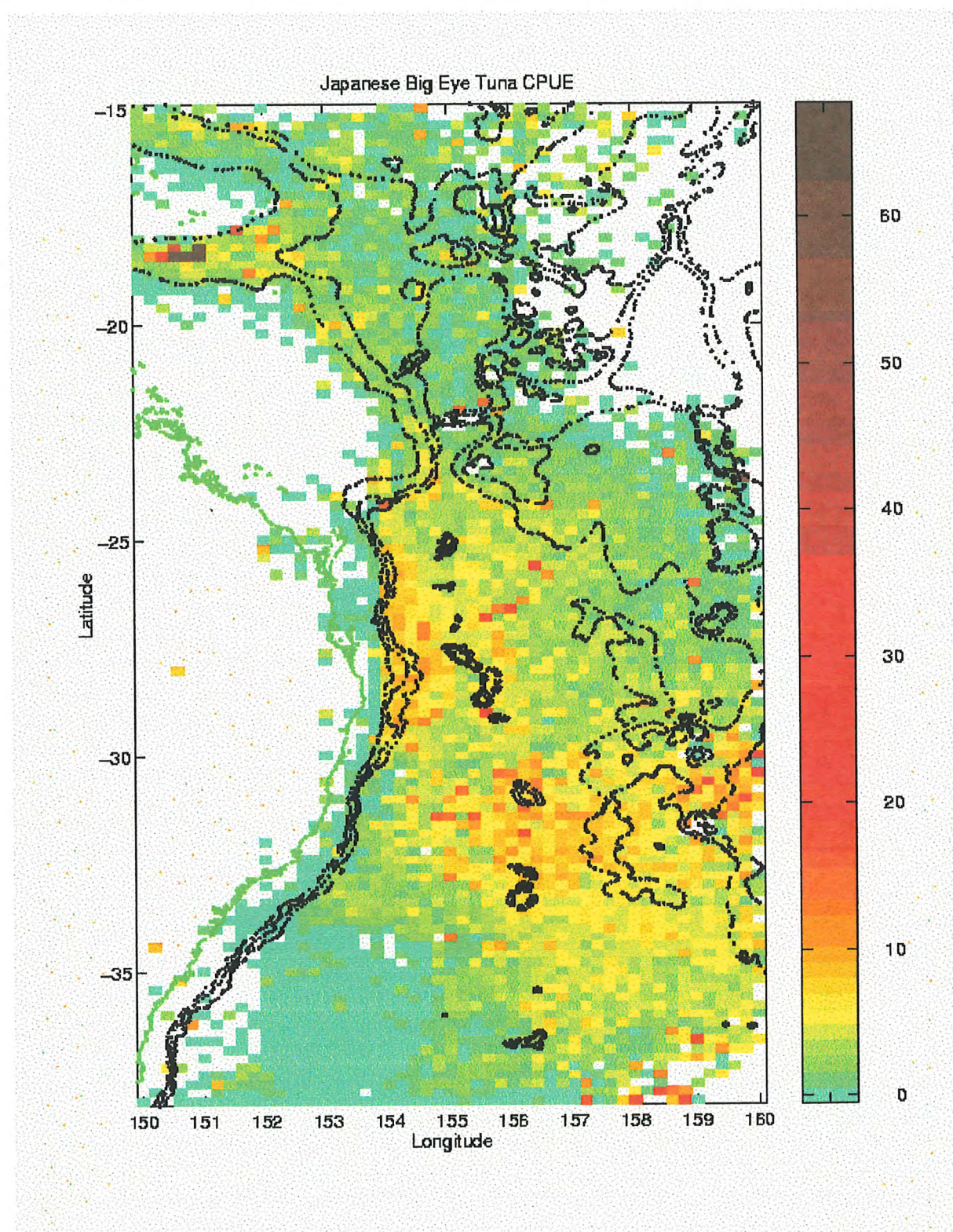


Figure 5-6 Average number of bigeye tuna caught over a 0.2 degree square block computed from the Japanese fishing log records held in the AFMA database up till mid-1997. The average is the sum of catch counts divided by the number of records so no account has been taken of hook effort. This plot is merely to indicate the gross distribution pattern.

Japanese longline catches in the southwest Pacific Ocean show that broadbill swordfish are distributed along the east coast of Australia to 45°S. The developing fishery for swordfish off southern Queensland suggests that the area between 20 and 30°S may be an area in which these fish concentrate. However, as fishing techniques develop the fishery has broadened its range indicating that the catches in the area may be the result of more intensive fishing. There is no tagging data from which movement patterns of these fish could be deduced. However, possible movement models include the existence of a separate stock along the east coast of Australia, which is self-replenishing, although the Japanese catch data indicates this is unlikely. Alternatively, there is a wider western Pacific stock that moves in and out of eastern Australian waters in response to enhanced feeding conditions resulting from changes in the regional oceanography, or to spawn. Large spawning females are caught off Mooloolaba for an extended period over the summer months (Young 1998).

6. METHODS

Catch data

Historical catch from AFMA's (Australian Fisheries Management Authority) database for both Australian and Japanese logbooks were used for the period from 1989 (this was the earliest year from which the satellite SST archive extended).

We used the reported noon time position as the location for the catch, thus there is an uncertainty in our analyses of the precise location of individual catches due to the long spatial scale of the longline sets (>100 km). The attributes of the catch record used comprised: the day, month, year, longitude, latitude, number of fish caught for given species, total weight of catch for given species, total number of fish caught (of all species) and number of hooks used.

Sea-surface temperature data

For the east coast operations, sea-surface temperature data were obtained from the excellent archive at the Remote Sensing Facility at the CSIRO Marine Laboratories. The Advanced Very High Resolution Radiometer (AVHRR) data, processed according to the method of Rathbone and Parslow (1997), used composites of images over a 15 day period and filtered with a histogram filter designed to eliminate cloud and to select a reasonable maximum temperature. Images were produced every 5 days using the 15 day filter window. For the west coast cal/val activities, AVHRR was received at the Western Australian Technology and Applications Consortium (WASTAC) facility and the Remote Sensing Services Section of the WA Department of Land Administration (DOLA). Processing methods for the WA data are detailed in the appended companion report edited by Pearce and Lynch (2000).

Each east coast image occupied a longitude range from 148.5 to 163.5°E and a latitude range from 21 to 46°S. The image resolution was 0.02 degrees in longitude and latitude (roughly 2.4km in north-south range). The image spatial range was originally selected to encompass a smaller area to cater for the longline fisheries off Ulladulla/Bermagui but was later extended north to cover the developing fishery off Mooloolaba as well as the more extensive offshore excursion by larger vessels taking part in the project. With the skipjack predictions for the warm 1999 summer the prediction range was further extended to track the rapidly migrating skipjack schools which proceeded south to Storm Bay off Hobart. Thus virtually the whole of the eastern Australian tuna fishery area was covered by the project.

The SST data files were manipulated to convert from the image format to a geographical format. This allowed the catch data to be registered to the closest (in time) image, which then allowed a temperature value to be assigned to the noon-time position of the catch record. Note that since the images are composited and filtered, the assigned values are not precise estimates of the temperature at the reported catch position or time (neither is the catch position for that matter as discussed before). However, they do represent a value that can be interpreted as being a value filtered in time (over 15 days) and space (to the nearest pixel at the ship's noon position).

Ocean color data

For a basic description of ocean color and processing of satellite ocean color data the reader is referred to: http://daac.gsfc.nasa.gov/CAMPAIGN_DOCS/OCDST/what_is_ocean_color.html

CZCS Data

The ocean color site (referred to above) also contains a good article describing the role of ocean color in examining the complex patterns of phytoplankton distribution caused by the interactions of currents and the bottom topography around Tasmania. The article reproduced below (with the kind permission of Dr James Acker of NASA's Ocean Color Data Support Team) shows one of the more spectacular images seen from the CZCS satellite (*Figure 6-1*) that captures a remarkable structuring of phytoplankton distribution by ocean currents. In many ways, this image provided the inspiration for our efforts in ocean color.

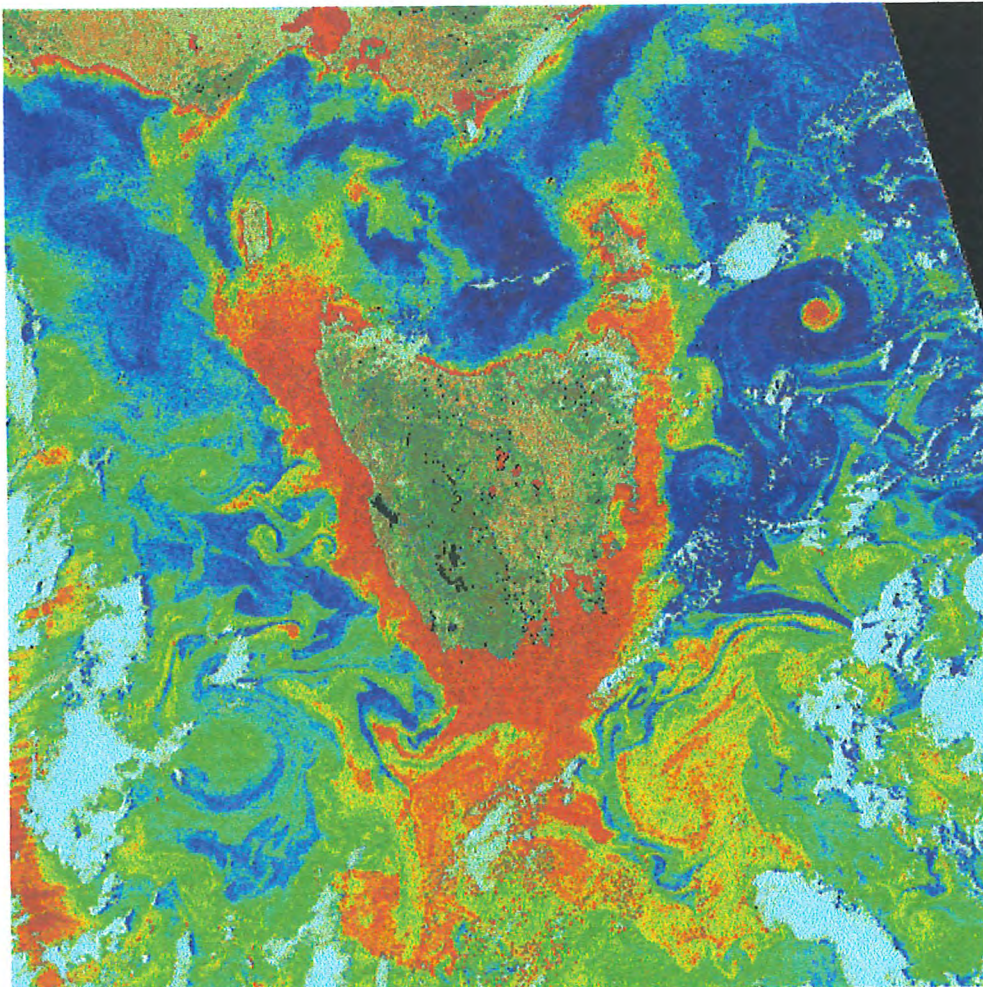


Figure 6-1 CZCS image of Tasmania and surrounding waters, obtained on November 27, 1981. The southern coast of Australia is at the top of the image, separated from Tasmania by Bass Strait. (Additional Notes: The spectacular clockwise-swirling waters with the intense reddish bullseye off the NE coast of Tasmania is likely to be a "cold-core" eddy which seems to have an accumulation, or alternately in-situ production, of phytoplankton at its core. The high productivity seen south of Tasmania may be due to the interaction of currents with the SE

Tasman Rise and Cascade Plateau. High apparent concentrations of phytoplankton in shelf waters could be biased by turbidity from other sources such as sediments and tannins – particularly off the west coast.)

“The CZCS was an instrument carried on the NIMBUS-7 satellite. It was designed to make precise measurements of the intensity of radiation in different portions (bands) of the color spectrum. These measurements indicated how much sunlight was being absorbed and how much was being reflected at (and from some depth beneath) the ocean’s surface. The small living plant cells that exist near the ocean surface—called phytoplankton—contain chlorophyll, the pigment that allows them to convert sunlight and carbon dioxide into the organic matter of their cellular structure. The more chlorophyll that is present at the surface, the “greener” the reflected light will be. At the same time, more red light will be absorbed. Thus, the measurements made by the CZCS allow a view of the patterns of phytoplankton in the ocean.

The image of the oceans around Tasmania is a “false color” image. False color means a color scale is used to indicate the approximate concentrations of phytoplankton in the water. In this color scale, yellows and reds indicate more phytoplankton, and greens and blues indicate less. Dark blue and purple indicate very low concentrations of phytoplankton in very clear ocean water.

It is obvious that the current interactions around Tasmania are very complex, and they shape the phytoplankton growing near the island into patterns that are constantly changing. The complexity of the patterns and the fact that they are always in motion makes it very difficult for the traditional methods of oceanography, conducted from a stationary ship, to make accurate estimates of the amount of phytoplankton in a given oceanic region. It is also difficult to determine how rapidly the phytoplankton in an entire region are growing. The process of photosynthesis in plants converts light and carbon dioxide to carbon in the cell. The rate at which carbon is produced by plants is called primary productivity, and it is one of the fundamental variables measured by biological oceanographers.

If scientists on a ship were trying to survey the waters around Tasmania, they could travel in a certain direction for days in clear water, and only a few kilometers away there might be a patch of higher primary productivity that the ship never encountered. On the other hand, a ship could travel in high productivity waters and not encounter any areas of low productivity. In either case the scientists’ picture of the biology around the island would be inaccurate. It is only by taking a view from space that the biological patterns in the whole region can be observed and measured, presumably allowing more accurate estimates of primary productivity. “

(Image and article reproduced with permission. The image was produced by the Coastal Zone Color Scanner Project at Goddard Space Flight Centre and obtained from the Goddard Earth Science Distributed Active Archive Center).

The complexity of the interactions, and the finescale structuring even out in the deep ocean, suggests that local catch success may be highly variable over short distances if fish species are influenced by ocean color. Lyne et al (1997) find that for SBT off eastern Tasmanian waters the consistency in catch rates of SBT is locally influenced by the structuring of water masses which in turn is conditioned by the relative flows of subtropical and temperate waters.

OCTS Data

During the course of the project, and with the repeated delays in the launch of SeaWiFS, Dr John Parslow actively negotiated with Japan's national space agency NASDA for access to the data from the ocean color satellite OCTS aboard the ADEOS platform, launched successfully in August 1996. A proposal for a Pilot Study to use OCTS to investigate its usefulness to Australian fisheries was eventually signed by heads of the then CSIRO Division of Marine Research, AIMS (Australian Institute of Marine Science), COSSA (CSIRO Office of Space Science and Applications) and AFMA. The proposal would have allowed this project access to the OCTS data. In addition to NASDA, the proposal also involved JAFIC (Japanese Fisheries Information Center) and EORC (Earth Observation Resource Center) from the Japanese side. An agreement form was processed and we expected to receive a DTL (Direct Transmission Link) for direct access to OCTS coarse-resolution data in addition to resources to process OCTS data. We were also negotiating to receive access to the fine-resolution data. Progress on the negotiations was slow but in the end the ADEOS platform suffered a massive power failure and all communications with the platform was lost towards the end of June 1997 about one month before SeaWiFS was eventually successfully launched. At that point we switched our attention to the receipt and processing of SeaWiFS data.

SeaWiFS Data

SeaWiFS data was received at the L-band receiving facility in Hobart under a Global Change research license from NASA. The data for the West Australian region were received by WASTAC (Western Australian Satellite Technology and Applications Consortium) on a non-operational basis (i.e. not in real-time). The WA data was used to complement the long-term AVHRR study being undertaken by Mr Alan Pearce on the temporal and spatial variability in the Leeuwin Current and its application to the fisheries of WA. The NASA SeaDAS data processing software was used to process SeaWiFS data; various upgrades to the software were implemented during the project. Some of the upgrades necessitated reprocessing of the entire SeaWiFS archive of daily images.

Delivery and installation of the new L-Band reception system (CSIRO funded) for the Hobart operations took place early in 1998. This required significant additional effort from the remote sensing group, but was rewarded with a substantial improvement in the reliability and quality of data reception. Twice daily SeaWiFS passes were acquired from January to June 1998, with very few passes lost. Earlier problems in processing were partially corrected by new navigation and calibration procedures provided by NASA. Monthly composite data were also processed.

In-Situ Ground Truth Data

In-situ ground truth data were collected from research cruises, fishing vessels, and dedicated field sampling in Western Australia. The WA sampling included a series of monthly cross-shelf transects, from the coast at Hillarys out west to 40km offshore, for temperature, chlorophyll, nutrients, salinity, light, phytoplankton, meteorology, solarimeter and zooplankton (underway and station sample – see details in appended report by Pearce and Lynch, 2000). The opportunistic collection of much of the ancillary WA data was in support of longer term objectives, of the WA investigators, of understanding seasonal and interannual fluctuations in recruitment and catch of important WA commercial fisheries. A dedicated research cruise was conducted in May 1996 to undertake biological investigations during the start of the tuna fishing season off south-eastern Australia. The cruise was a northward extension, to study east coast tuna, of a series of CSIRO cruises in the area east of Tasmania on the feeding and movement of southern bluefin tuna. Three days of this cruise contributed directly to the objective of this project on favorable fishing areas for east coast tuna. Other CSIRO cruises also collected optical and biological information as ground truth for SeaWiFS.

Following consultation with ECTUNAMAC potential participants for the field trials were discussed in conjunction with the Chairman of the East Coast Tuna Association – appointed by ECTUNAMAC to liaise with the project during this phase. Following this, visits to the ports of Mooloolaba, Ulladulla and Bermagui were made by project participants to discuss details of the project and invite interested parties to take part in the field trials. An initial list of 10 potential operators willing to participate in the catch prediction/economic assessment phase of the project was drawn up.

The economic performance assessment required for the project was discussed with operators. An initial logsheet designed to assess their fishing strategy both before and after they receive the catch prediction information was drawn up (Appendix B). These questionnaires were sent out by fax, initially about twice a week, and required participants to specify where they proposed to fish, what they expect to catch and market factors affecting their decisions. Predictions were to be sent only to those who returned the “before” questionnaire. These assessments would have allowed us to objectively determine whether the predictions altered expectations on where/what to fish plus it would have provided the post-hoc fishing information from which to assess the skill of the predictions. It soon became apparent that most operators were not inclined to fill out the forms, and this was compounded by problems due to the vagaries in timing of fishing trips and, more often than not, the operators urgent need for a prediction (within an hour or two, or by the next morning). Fax communications with vessels at sea was also a problem and an added cost. We reluctantly abandoned this objective attempt for a more subjective assessment involving close liaison with fishing operators and a more compact and streamlined logsheet (Appendix C) in which the operators were asked to indicate whether the catch information had been used in directing their operations. Thus, the assessments were less objective and quantitative.

With the larger operations, it was possible to setup communications with a central intermediary on land who would then relay information to their fleet. With the cooperatives we initially attempted sending information to the manager for distribution to the fleet – this was setup at Ulladulla and relied upon the system used at Ulladulla to disseminate SST images to the fleet. This unfortunately was not successful, as many of those who did use the predictions did not provide any feedback. Thus, reluctantly, in order not to distort the results of the project it was necessary to only provide predictions to those who regularly provided feedback. Catch predictions were sent out as attachments to email twice a week – the interval between predictions depended on cloud cover and quality of the SST images. Ad-hoc requests from certain operators were met as required. Attempts were made to provide imagery, or at least interpretations of the imagery, to those who could not receive email. In the case of the skipjack predictions, the color images were sent via email to a coordinator for a group of fishers. The coordinator would trace the color image and add shading before faxing it out to the vessels.

Information exchange between the scientists and operators occurred via a variety of means, and not as we had hoped primarily through the logsheet returns. Two operators provided prompt and detailed logsheet returns. One group provided location and catch information via Satcom C on an almost daily basis and communication with the group was primarily through their land-based operations center. Phone contact with the skippers occurred about once per week and concerned interpretations of the images and the skippers' recent experiences in relation to catches and the environment. Another group maintained close contact via mobile phone while heading out to sea, or while in mobile phone range at sea, and provided their private logsheet returns rather than the CSIRO logsheets. Other operators provided sporadic returns and infrequent contacts via phone or email. A total of over 300 catch returns were processed over the period of the field study. With the exception of the those few who diligently returned logsheets, much of the information exchange, and there was much more information exchange than is documented in the logsheets, is difficult to quantify. Phone communications for example dealt with details of how the SST and catch information were being used, or not used, weather information, what was being caught in relation to water conditions and anecdotal information on other catches and experiences in the local area. While difficult to quantify this sort of information was vital in understanding both the value and limitations of the information being supplied to the operators.

Underway Sampler

Two vessels taking part in the fieldwork were equipped with robust underway samplers that recorded temperature, salinity, fluorescence and vessel GPS position. ECTUNAMAC again decided which vessels would be equipped and these were Tonka owned by Jim Uttley more and operated by Mark Ebbels, and Elena Rosa (later replaced by Laurina P when Elena Rosa broke down) owned by Joy Puglisi and operated by John Hine.

As the underway sampling system was to be installed on commercial fishing boats we needed a simple, robust and compact instrument which would be reliable, useful to the fishers, provide data security and include procedures to reduce the effects of fouling.

The CSIRO Marine Instrument Group developed a highly effective low-cost underway sensor package specifically for this project. This package was used not only to provide chlorophyll fluorescence for SeaWiFS validation, but also to provide records of temperature and salinity as well as fluorescence throughout fishing operations, to aid in the understanding and prediction of stock distribution (see later sections).

In the following, we first describe the instrument package and the calibration and sampling methods, and then present the results, including both calibration of the fluorescence signal, and comparison of in-situ and SeaWiFS data, including an error analysis.

The final design of the flow-through sensor unit (Figure 6-2, Figure 6-3) used OEM C-T conductivity and temperature sensors (Falmouth Scientific Inc.) and a WETStar miniature fluorometer (WET Labs Inc). Seawater was supplied via a self-priming pump (ITT Jabsco Water Puppy 2000) and water flow was measured using a flow transducer (Farnell Electronic Components). Once installed, seawater flow was regulated to approximately 150ml/s through the C-T canister and 15ml/s through the fluorometer using flow restrictors and a bypass. Electronic solenoid valves (SMC VXZ-series) were used to switch between normal seawater supply and fresh water for sensor cleaning. A tap at the bottom of the sensor unit allowed water samples for calibration to be drawn while the system was running and for the unit to be flushed and drained while the vessel was in port.

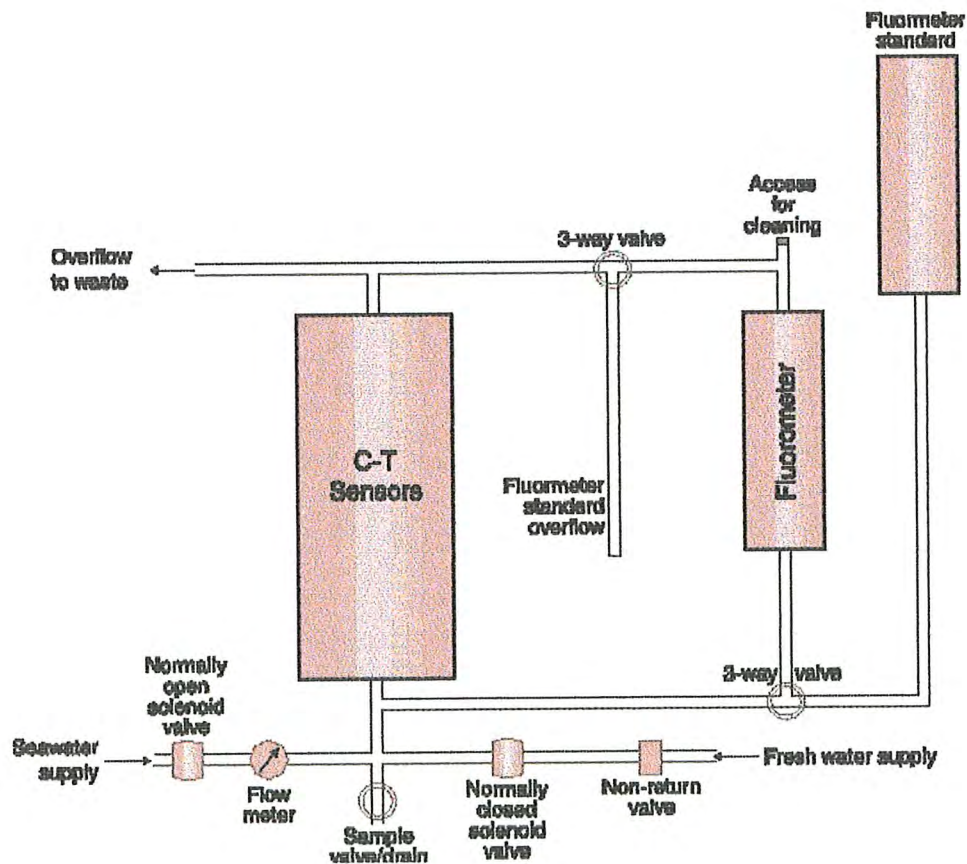


Figure 6-2 Schematic diagram of the flow-through sensor unit. A laptop computer mounted in the ship's bridge was used to control the valves and obtain data from the sensors, along with GPS from the ship's navigation system.

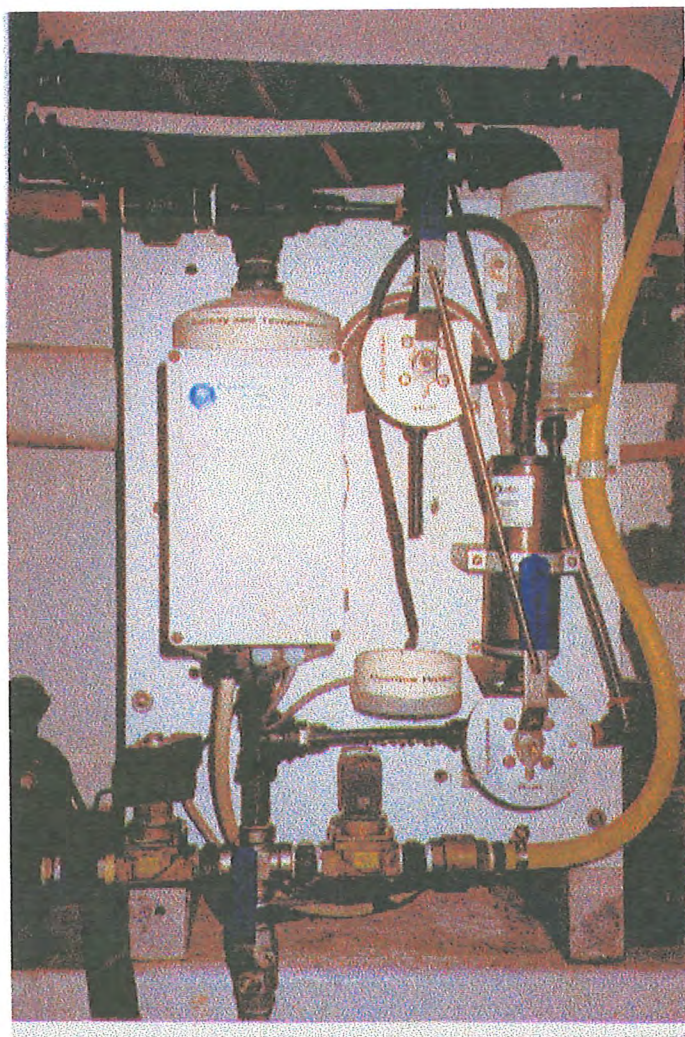


Figure 6-3 Scanned photograph of the underway sampler as mounted on *Tonka*. The intake to the system is via the tube to the right flowing into the bottom solenoid-operated valves. Water then passes through the large debubbling chamber, mounted on the left, before it flows through the sensors. The clear container in the top right is used to hold a calibration solution for the fluorometer. Apart from the calibration, control of the system is automated via a laptop computer mounted in the bridge of the vessel.

Both the C-T sensor and fluorometer were powered by a 12V DC supply and output analog voltage signals. These analog signals were cabled from the sensors in the vessels engine room to the wheelhouse where they were connected into a notebook computer fitted with a PCMCIA interface module (National Instruments DAQCard-500). This module converted the analog signals to digital values, which were subsequently scaled by the application software to derive actual temperature, conductivity and fluorescence measurements. In addition this module provided a counter interface channel through which the pulse output signal from the flow meter was measured. Position data from the vessels Global Positioning System (GPS) was also fed to the notebook computer through one of its standard RS232 communications ports.

The acquisition and display application, running under Windows 95, was developed using the LabVIEW Graphical Programming language (National Instruments). The application was designed not only to robustly acquire and log data, but also to display the data in a way that made it accessible and useful to the skippers. The application drove the system, acquired measurements from the various sensors every sixty seconds, stored the data to the computer hard disk along with water flow, time and position records and backed up the day file to floppy disk at midnight. It also displayed alarm warnings for low water flow and low salinity through the sensors and provided a means for the crew or observers to flag event marks in the data set corresponding to specific vessel activities such as gear setting, catch landed or calibration sample taken. Each of the measured parameters was presented on the computer screen in scrolling trend graphs, which displayed a six-hour history for each parameter.

Sample Collection for Sensor Calibration

Every one to two months a CSIRO observer spent a few days on each of the vessels to carry out equipment maintenance and collect samples. As well as seawater samples taken for pigment and salinity analysis, catch data and biological samples such as otoliths, stomachs and gonads from selected fish were collected.

Seawater samples were collected for pigment analysis by drawing 4l of water from the sample tap, filtering through a 47mm GF/F filter and storing the filter in liquid nitrogen until returned to the laboratory for analysis. Chlorophyll a concentration was determined spectrophotometrically using the trichromatic equations of Jeffrey and Humphrey (1975) with a GBC UV/vis 916 dual beam spectrophotometer. The sample extract was then analyzed for pigment composition (not discussed in this paper) by HPLC as described in Clementson et al. (1998).

Twelve salinity samples were collected each trip and returned to Hobart for analysis to check conductivity sensor calibration. In the laboratory, salinity was determined using a Guildline salinometer calibrated with IAPSO standard seawater.

Maintenance and fluorescence calibration

At the beginning and end of each observer trip, distilled water and a 500µg/l rhodamine standard were introduced to the fluorometer flow tube to obtain a zero and mid-range response to check for sensor stability and to enable standardization of fluorometer output between vessels. These standards were measured before and after cleaning the fluorometer to check for evidence of fouling.

Between observer trips, the skipper flushed the sensors with fresh water daily, to inhibit fouling. The system was designed using solenoid valves so that flushing could be triggered remotely using a switch in the wheelhouse. Every few days, the skipper or crew member also cleaned the fluorometer flow tube with a tubing brush through a T-piece on the top of the fluorometer. While in port the sensors were washed with fresh water and the system drained and left empty.

SeaWiFS data processing and analysis

Use of fluorescence sensors as a surrogate for pigment measurements does involve some disadvantages. The fluorescence signal is affected by factors other than phytoplankton concentration and composition (Stramska and Dickey, 1992): chlorophyll *a* fluorescence yield can vary up to three-fold depending on environmental conditions (Chekalyuk and Gorbunov, 1994).

In order to deal with this variation in fluorescence yield, we have essentially adopted a two-tier validation approach. Observers on the fishing boats collected and filtered water samples regularly when on board, and these were returned to the laboratory for pigment analysis. These chlorophyll estimates were then used to calibrate the fluorometers, and to correct for diel variation in fluorescence yield. These calibrations and corrections were then applied to the underway fluorescence data to produce a geo-referenced time series of fluorescence-based chlorophyll estimates along the fishing boat cruise track on each day. These values were in turn compared with SeaWiFS chlorophyll estimates on that track on the same day.

Maintenance of sensor calibration on volunteer platforms such as the fishing boats is not straightforward. We paid particular attention in the design of both the instrument package and the protocols to the need to maintain calibration of the instrument. This depended heavily on the cooperation of the skipper and crew, and the success of this project is testament to their care and attention.

CZCS Ocean Color Data Processing

Attempts were made to assess the potential utility of ocean color by analyzing the archived series of images from the CZCS sensor. For a few months in early 1986 coregistered images of SST and ocean color were available and we decided to examine these series to determine if ocean color could provide additional information beyond what was available from SST.

Basic correlations between SST and chlorophyll show the expected base trend of low chlorophyll in warm waters, high chlorophyll in cold waters with intermediate maxima in mixing zones (Figure 6-4). However, this trend is not consistent between months (cf. Figure 6-5) where the base trend is not as evident.

April 86 - T vs Chl

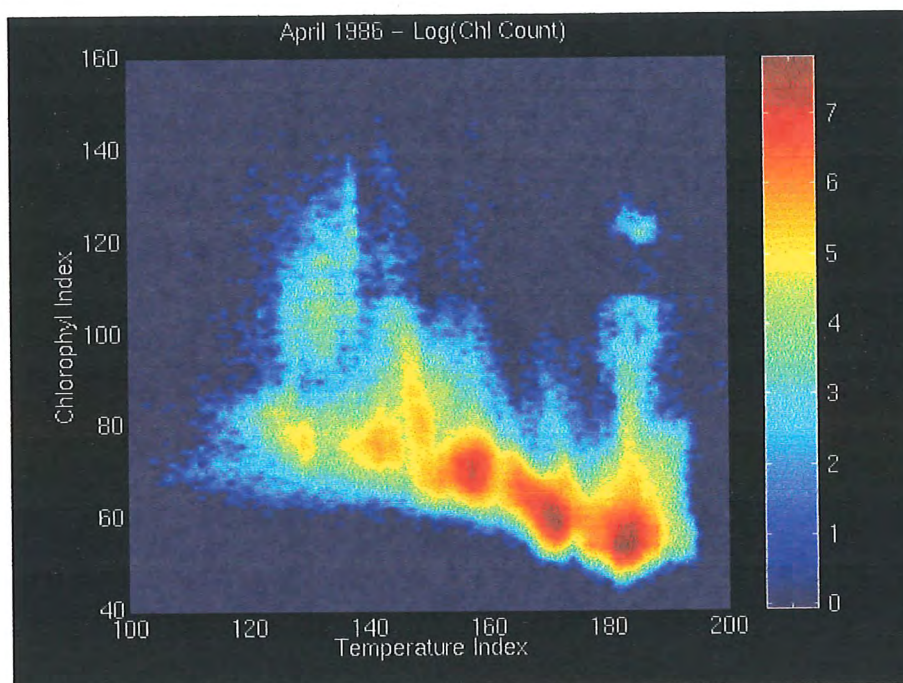


Figure 6-4 Temperature vs chlorophyll image for April 1986 off eastern Australia. The color coding shows the density of observations – most observations occur in oligotrophic waters of high temperature and low chlorophyll.

June 86 - T vs Chl

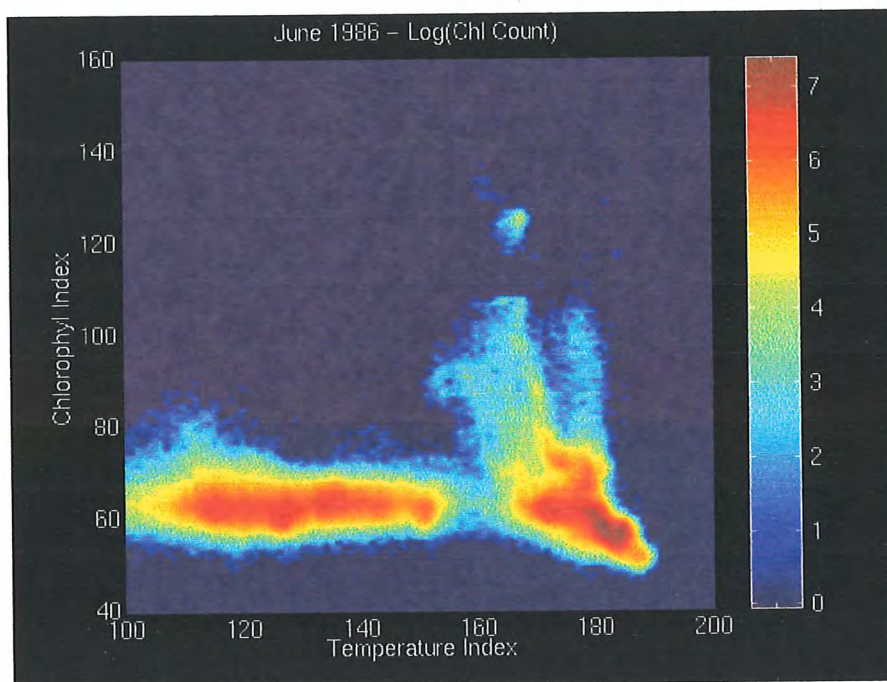


Figure 6-5 Temperature vs chlorophyll image for June 1986 off eastern Australia.

Part of the problem with the correlations, and more specifically with the CZCS image is the so-called electronic overshoot problem evident in the CZCS image when compared to a companion SST image (Figure 6-6). The overshoot causes saturation of the sensor optic electronics due to the high reflectance from clouds and it takes time for the optics to renormalize when the cloud saturation is removed. As the sensor scans from west to east this shows up in the CZCS image as a streak running from the eastern edge of clouds (and land – which also causes saturation of the sensor) as evident in Figure 6-6.

CZCS April 86 - T & Chl

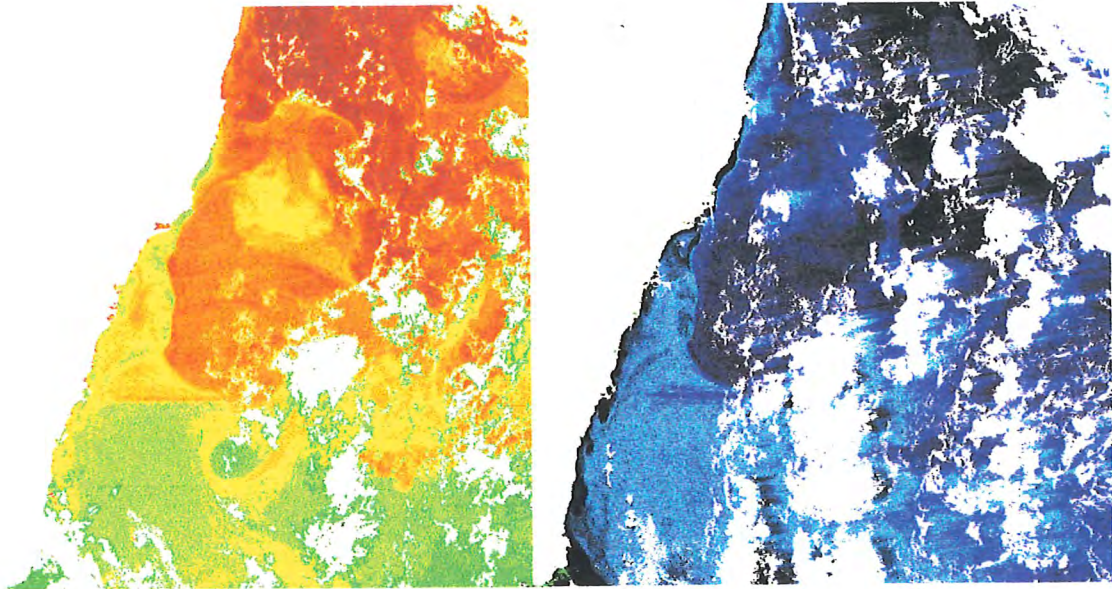


Figure 6-6 Coregistered SST (left image) and CZCS chlorophyll (right image) for April 1986. Note the greater cloud masking and the "streaking" on the eastern cloud edges in the CZCS image.

The standard approach to this problem is to mask out the overshoot areas but as can be seen in Figure 6-6 this could result in substantial loss of imagery. We attempted to develop a procedure for correcting the overshoot – not an easy problem as no one appears to have developed such a procedure after more than a decade of analyzing CZCS imagery (*in retrospect, we were ambitious in even attempting to develop a procedure*). The procedure we developed examined the overshoot as a function of saturation time (basically the cross-scan run length of cloud) and the filtered observed overshoot response. Ideally this should provide a two-dimensional response surface which could then be used to correct the original image. A matrix of the overshoot signal as a function of the cloud cover was formed taking into account the background signal to which the signal tended. A median filter was applied to this matrix to smooth out sharp variations.

A derived response (Figure 6-7) shows a highly non-linear surface with overshoot and undershoot (responses higher or lower respectively than what they should be) and "ringing" after the initial response. Corrections to the image using this response surface did improve the image to give a greater usable area of imagery. However the corrections applied did not appear to be valid for areas near land and in situations where the cloud cover was highly patchy. Thus, the overshoot matrix derived from a segment of the image did not capture the range of overshoot behavior or that the methodology used was not generic enough. Rather than continue work on this difficult problem we made a conscientious decision to refocus our efforts towards the newer ocean color datasets, which do not have this overshoot problem.

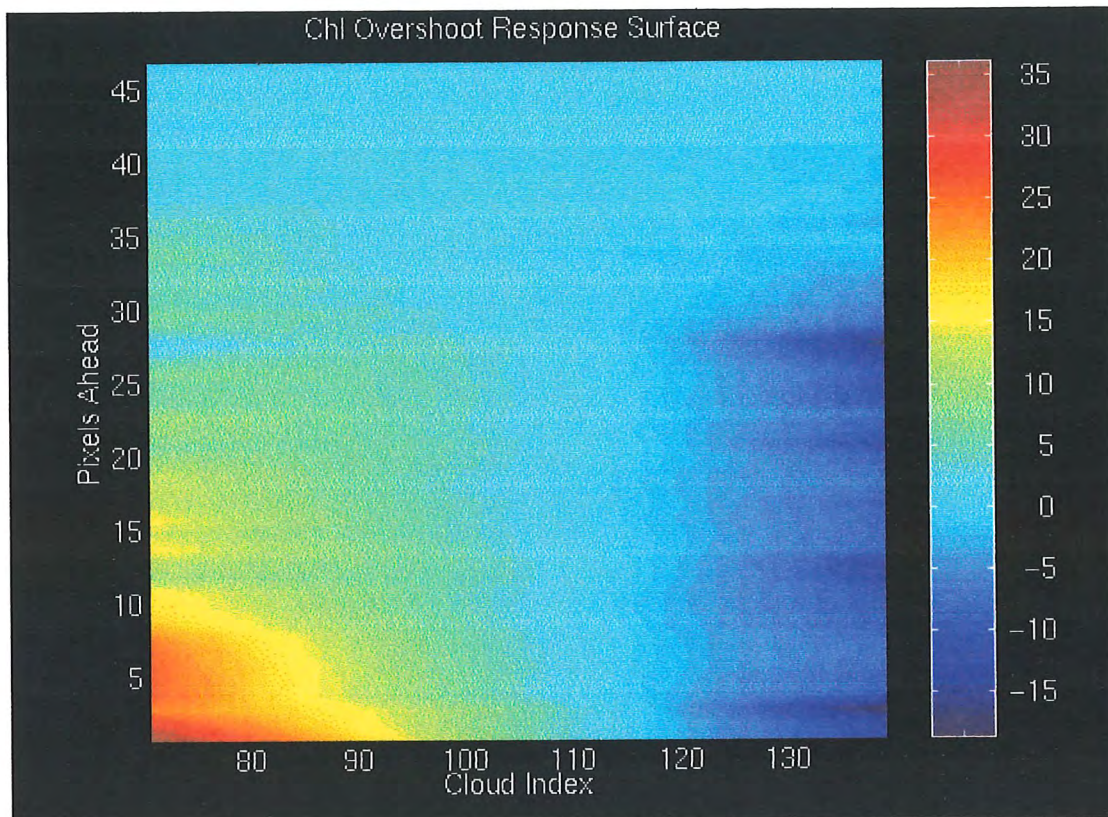


Figure 6-7 Two dimensional response surface of CZCS electronic overshoot as a function of an index of cross-scan cloud (basically the length of cross-scan cloud in pixels) and the distance from the eastern cloud edge. A positive response (red-light blue) indicates that the measured chlorophyll value/index is higher than values outside of the immediate overshoot-affected region.

Given the problems with the CZCS data (and the high cost of real-time SeaWiFS imagery), our approach with the catch prediction phase was to concentrate on developing innovative methods for using SST data and our intention with the catch prediction was to post-hoc analyze the potential benefit SeaWiFS ocean color data could provide.

CATCH DISTRIBUTION ANALYSES

Analyses of catch distribution statistics were conducted at two scales of interest to this project:

Regional Scale: This analysis encompassed the entire region of the study extending from approximately 20°S to 45°S and from inshore waters out to 163°E. Confidentiality restrictions prevent us from detailing the analysis methodology here but the outputs of this analysis are the catch predictions supplied in near real-time to the operators participating in the field trials. The field trial period extended from approximately August 1997 to February 1998 (some predictions still continued through March and April 1998), and the project was later commissioned by AFMA/AFFA to provide predictions for minimizing SBT by-catch from July-September 1998. Assistance was also been provided to the skipjack fishery for the 1999/2000 skipjack fishing season in part-exchange for the collection of detailed personal logbook records of Mr Pat Broder and his father.

At the regional level, a number of strategies to objectively assess the utility of remote sensing were examined:

1. Using SST and other available data such as catch statistics to develop predictions that were tested by fishers and carry out post-hoc analyses on 1997 catches of yellowfin.
2. Assessment of the predictability of ocean color using SST and other available information.
3. Subjective assessments based on information supplied by fishers.

After an initial consultation period with fishers, predictions were carried out for the following species and areas:

Species:

YFT – yellowfin tuna

BET – Bigeye tuna

BBL – Broadbill tuna

SKJ – Skipjack tuna

(SBT – Southern bluefin tuna, predictions carried out independently for AFMA and AFFA on SBT by-catch minimization project)

Areas [longitude range and latitude range in brackets]:

- | | | |
|---|--------------|-------------------|
| 1 | Northern Qld | [153 160 -25 -21] |
| 2 | Southern Qld | [153 160 -30 -23] |
| 3 | Northern NSW | [150 156 -36 -30] |
| 4 | Southern NSW | [148 154 -40 -33] |
| 5 | Tasmania | [148 154 -44 -40] |

In addition SST composites were supplied for each of the areas. These images were composited over a number of days (usually about 3 days) to overcome problems of cloud cover especially for the northern tropical areas. These improved the clear-area areal coverage over single daily images as supplied by the remote sensing facility in Hobart to its clients.

Finescale (see appended report by Young et al for details): At approximately two-monthly intervals CSIRO observers spent periods of up to a week on board the two fishing vessels equipped with the underway sensors. On these trips the observers recorded and identified all

fish caught against the time at which they were caught. As time could be related directly to GPS position the former became a proxy for position. Size and biological details for all fish caught by the longlining operation were also recorded. In the laboratory observer data were matched with the underway files to link individual fish with all contemporaneous data collected. The observers also collected samples of chlorophyll and salinity to calibrate the sampler and the SeaWiFS ocean color satellite.

Transect data were used in the following ways: Off Mooloolaba we used the steaming transect out to the fishing area for each fishing trip on which there was an observer to document changes in the surface characteristics (in this case surface temperature, salinity and fluorescence) of the water. This data set was not repeated for the southern zone as fishing was generally relatively close to the coast. To provide a seasonal comparison of the surface waters in which the longliners fished during the study we used a mean of the underway data from the first set of each fishing trip regardless of whether an observer was on board or not. The underway data was supported by satellite sea surface temperature imagery provided by the NOAA AVHRR satellite although cloudy conditions limited the usefulness of satellite imagery for periods of the study (see data analysis). Ocean color satellite imagery from the SeaWiFS (Sea-viewing Wide Field of View scanner) satellite was also cloud-affected so was not used in the statistical analyses but was used in the description of the study area.

We obtained information on the vertical structure of the water column for both areas from two oceanographic cruises completed during the course of the study. The first, in May 1996 by CSIRO's research vessel MRV Southern Surveyor described the area of the southern portion of the fishery between 35 and 37 degrees South (Young et al in prep). The second cruise, in March 1999 by the Oceanographic Research Vessel Franklin under CSIRO's Dr Ken Ridgway, examined the vertical structure of the waters covering at least part of the Mooloolaba fishery. Dr Ridgway made available vertical cross-section data of temperature and salinity through the main fishing area off southern Queensland to a depth of 500 m. He also provided surface current data for the region during the period of the cruise.

We examined the relative effects of physical and environmental factors on catch rates of broadbill swordfish, yellowfin tuna and bigeye tuna with visual examination of scatter plots followed by generalized linear (GLM) and generalized additive (GAM) models. Catch rates were examined against the set of variables defined in (Table 6-1). Forward stepwise regressions were applied to the GLMs to determine the statistically significant terms in decreasing order of significance. GAMs were fitted to the significant terms to determine the nature of the response to the variables.

We assumed that each longline set was relatively stable horizontally on the basis that even if the line moved it moved in relation to the prevailing currents effectively staying with the same body of water. For this analysis we only used the underway data from the hauling period. We divided each haul into approximately equal segments composed of approximately 200 hooks. The catch data was standardized to the number of fish per 200 hooks. Two comparative studies were undertaken: in the first all 139 records for both areas (Mooloolaba and Bermagui) were used while in the second analysis, a detailed fine-scale analysis was run on the Mooloolaba data. The Bermagui data was not examined separately due to the small sample size.

Table 6-1 Descriptions of factors and ranges used in GLM and GAM analyses

Factor	Description	Range	
		Mooloolaba	Bermagui
Area	Mooloolaba coded as 1, Bermagui as 2	Latitude 25 05 to 27 07 Longitude 151 31 to 155 18	Latitude 28 48 to 33 26 Longitude 150 20 to 154 18
Year	Years during which data were collected	1997-1999	1997 – 1998
Month	Month of the year during which data were collected	All months except May, September, October and December	February, September and November only
Moon phase	New moon coded as 1, first quarter as 2, full moon as 3, last quarter as 4	1-4	2 – 3
Wind speed	Average wind speed in knots recorded on vessel during the hauling of each set	1 – 20	5 – 10
Set	Each complete hauling operation of all hooks deployed. Consecutive numbers are given for each set for each fishing trip	1 – 5	2
Subset	Consecutive 2 hour hauling period or part period during the hauling of each set	2 – 6	2 – 5
Temperature	Median value of sea surface temperature for each subset in degrees Centigrade	20.94 – 31.07	19.38 – 25.45
Salinity	Median value for sea surface salinity for each subset in parts per thousand	34.97 – 35.82	35.19 – 35.73
Fluorescence	Median values for sea surface Fluorescence for each subset in standard units	-0.0564 – 0.6646	0.0804 – 1.0319
Distance to temperature front	Distance from subset position to nearest sea surface temperature front. If no front was present, distance was set at 100 nm	3 – 40	0 – 12

7. RESULTS

SST Validation

In the WA field studies, SST validation was conducted by initially comparing different methods of measuring the in-situ surface temperature (bucket, SDL at 1m, SDL max, thermistor, underway instrument), and subsequent comparing satellite-derived SSTs and bucket temperatures. The different in-situ measurements were all highly correlated (correlation coefficients were in excess of 0.96); highest differences in the surface measurements occurred under low wind conditions in summer. Temperature differences greater than 0.5°C tended to occur when wind speeds were less than 5 m/s. Seasonal temperature ranges were larger near the coast (7 to 8°C) than offshore (about 3°C). Comparisons of in-situ measurements with satellite-derived SST was made using the McMillin and Crosby (1984) and the Non-Linear SST (NLSST) algorithms. Correlations between the bucket temperatures and satellite-derived SSTs were good (correlation coefficients over 0.94 for both) but the McMillin-Crosby values had a smaller bias (0.19 cf. 0.36°C for NLSST) and less scatter. 65% of the McMillin-Crosby SSTs fall within 0.5°C of the bucket temperatures, and 88% within 1°C, while the corresponding statistics for the NLSST are 62% and 86%. Differences of over 2°C, and over 5°C occasionally, which we presume is due to undetected high-altitude cloud effects.

Underway System: Instrument Performance

The sensor packages onboard the two fishing vessels proved to be robust and reliable. Both instruments operated with very little down time after installation, and data were collected on almost all days when the vessels were at sea, over a period of 15 months. Both data logging and maintenance were automated as far as possible, to minimize disruption to fishing operations, and this appears to have been successful.

The biggest cause of data loss was entrainment of air bubbles into the underway system. When fishing boats are punching into rough seas, the intake can come clear of the water. The simple debubbler installed in the system was unable to cope with the resulting high rates of air intake, and air bubbles reach the sensor. Contamination of this kind can be easily identified by the resulting high noise in the salinity signal. A running estimate of the salinity noise has been used to flag and discard all affected data. By the nature of long-line fishing operations, periods of fast travel into waves are usually followed by periods of slow travel with the waves, so that data loss is restricted to limited periods, even in bad weather.

It was unclear when we started whether it would be possible to maintain sufficient accuracy in underway fluorescence measurements on fishing boats to provide useful ground truth for ocean color satellites such as SeaWiFS. We were particularly concerned about the effects of fouling and sensor drift, as well as the natural variability in fluorescence yield.

We have relied on measurements with distilled water and rhodamine dye to monitor the instrument calibration (baseline and sensitivity) over time. Concentrated 10 ml rhodamine standards were taken by the observers, and diluted to 500 ml immediately before calibration. Analysis of replicates suggests errors in standard concentration were less than 2%. The rhodamine signal decays after introduction to the fluorometer, but measurements were recorded in the first minute after addition, introducing at most an uncertainty of a further 2%.

One sensor (installed on vessel Tonka), showed a significant decline in both the milli-Q and rhodamine standard voltage over time. A linear trend was fitted through these data, and used to correct the fluorometer voltage at intervening times. The second sensor, installed on Laurina P, showed no mean drift in baseline or sensitivity. The residuals from regressions through these data indicated a mean baseline variation of about 0.01 volts (corresponding to about 0.02 mg Chl m⁻³), and a relative variation in sensitivity of about 5% for Tonka, and 10% for Laurina P.

Distilled water blanks obtained by the observers before and after cleaning the sensor generally agreed well, indicating that fouling was controlled by freshwater flushing and brushing. Two exceptions are thought to have been due to a failure to clean and flush the sensor after the vessel returned to port. However, data collected by the observers are not adequate to eliminate the possibility of fouling. We plan to modify the automatic flushing procedure in the future so that distilled water baseline voltages are acquired at frequent intervals in the absence of observers.

Converting Fluorescence to Chlorophyll

The rhodamine calibration was used to convert the underway fluorescence voltages to a standardized fluorescence value, F_s . We then compared these standardized fluorescence values with spectrophotometric Chl a values C_s obtained from coincident underway samples collected by observers. In this comparison, we combined data from both instruments. The northern vessel operated in oligotrophic sub-tropical waters, with chlorophyll values from 0.03 to 0.3 mg m⁻³, while the southern vessel operated in temperate / subtropical shelf waters, with chlorophyll values from 0.1 to 1.5 mg Chl a m⁻³. This resulted in 111 (F_s , C_s) pairs.

Errors in the data are approximately log-normal, so that it is appropriate to compare $\ln F_s$ with $\ln C_s$. However, there is a small but non-zero additive offset, due presumably to the difference between measurements in distilled water and seawater. After correction for this offset, we found that $F_s + 0.05$ was proportional to C_s . As we wish to predict C_s from F_s , we looked to estimate the ratio $A = C_s / (F_s + 0.05)$. We therefore looked at variation in $\ln(A) = \ln(C_s / (F_s + 0.05))$. Values of $\ln(A)$ showed considerable variability over the whole data set.

We investigated a range of environmental factors which might influence $\ln(A)$. However, the only consistent factor was time of day which showed a highly significant effect (Figure 7-1). We represented this dependence as

$$\ln(A) = a + b \cdot \cos(2 \cdot \pi \cdot (h - h_0) / 24),$$

where h is hour of the day (local time). Least squares estimates of a , b and h_0 were $a = 0.139$, $b = 0.317$, $h_0 = 11.8$ h. The diel variation is highly significant ($P < 1.E-08$). The time of peak $\ln(A)$ (minimum fluorescence yield) is not significantly different from noon. Diel variation in chlorophyll-a and in fluorescence yield per unit chlorophyll has been recognized for many years (e.g. Kiefer, 1973, Marra, 1997) and may be subdivided into three components: photoinhibition, photoadaptation and growth (Marra, 1997).

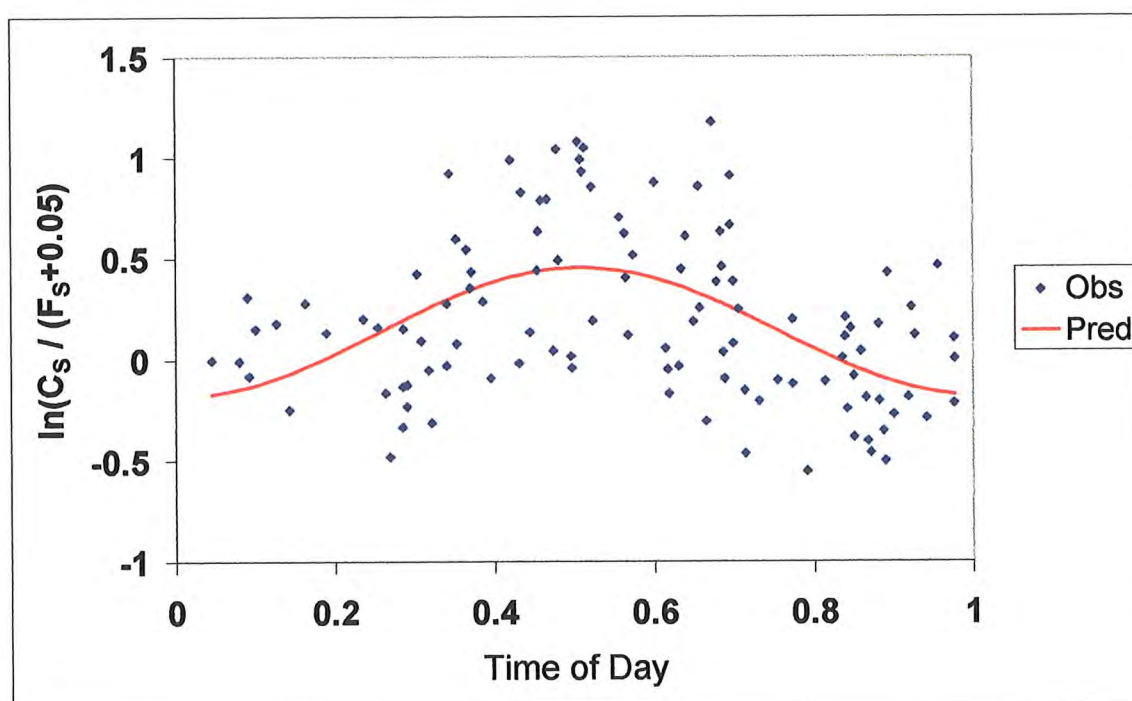


Figure 7-1 Values of $\ln(C_s / (F_s + 0.05))$ vs time of day. The red curve represents the fitted cosine curve allowing for diel variation in chlorophyll-fluorescence yield.

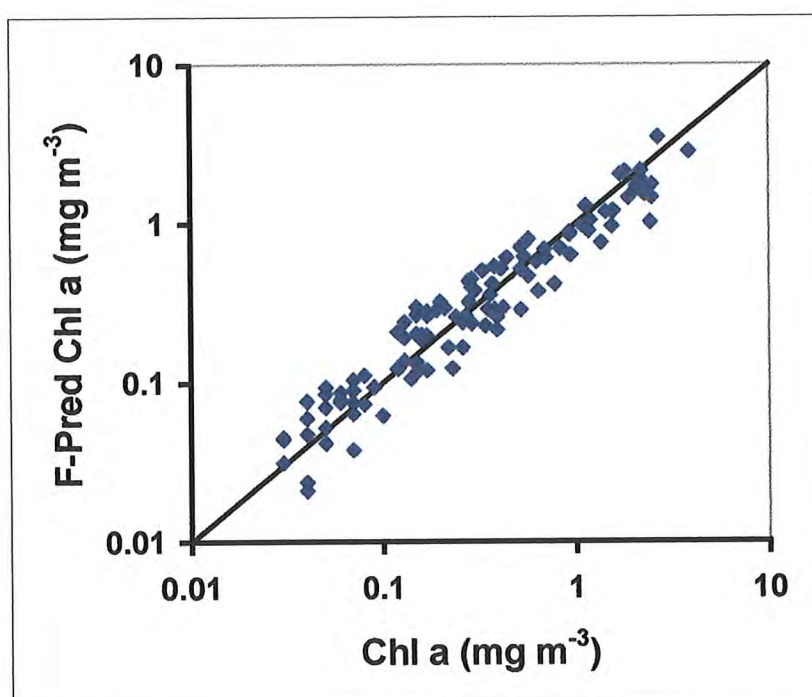


Figure 7-2 Predicted chlorophyll a (C_F) vs observed spectrophotometric chlorophyll a.

The residual MSE in $\ln(A)$ is 0.126, and the residual standard deviation is 0.355. This is still substantial; it means that, after correcting for diel variation, we can only predict chlorophyll from fluorescence with about 35% accuracy. However, this is not too surprising, given the variability in chlorophyll-specific fluorescence yield encountered in previous studies. Many studies report on a range of physiological and environmental factors that affect chlorophyll a and fluorescence yield. Examples include chlorophyll synthesis and zooplankton grazing (Le Bouteiller and Herbland, 1982), nutrient stress (Kiefer, 1973b), temperature and photoperiod (Hitchcock, 1980), light intensity, season and community generation time (Stramska and Dickey, 1992), population composition (Marra, 1997) and a coupling between photodensity and diurnal physics (Doney et al, 1995).

The fluorescence based chlorophyll C_F was calculated as:

$$\ln(C_F) = \ln(A) + \ln(F_S + 0.05),$$

with $\ln(A)$ corrected for time of day. Despite the residual error, the agreement of predicted and observed chlorophyll over a wide dynamic range (2 orders of magnitude) across both sensors is compelling (Figure 7-2). This calculation was then applied to all standardized underway fluorescence data.

Comparison of Fluorescence-Based Chlorophyll and SeaWiFS Chlorophyll.

Daily SeaWiFS data for the period September 1997 (after launch) to June 1999 were acquired in Hobart and processed to georeferenced remapped chlorophyll images at full resolution using SEADAS software. SEADAS algorithms and satellite sensor calibration coefficients were modified a number of times after launch. The comparisons here are based on chlorophyll estimates C_{SAT} obtained using algorithms current as of June 1999.

For each day where underway fluorescence data were acquired, the corresponding SeaWiFS image was assessed. Many images were rejected because the area occupied by the fishing boat was affected by cloud cover. Over the period September 1997 to June 1998, a total of 26 images off New South Wales were identified where underway fluorescence data were available in clear regions.

For each 24 hour period, the underway data (with GPS locations) were matched with SeaWiFS pixels. For each SeaWiFS pixel, the arithmetic mean of the fluorescence based chlorophyll estimates C_F in that pixel was computed. In order to check on the variation within pixels, the standard deviation of $\ln(C_F)$ (coefficient of variation of C_F) within each pixel was also calculated. We found that this CV was typically quite low, about 10%, in this region. This is reassuring, as it suggests that despite strong gradients in chlorophyll (see Figure 7-3), point samples provide a good estimate of pixel average chlorophyll.

We also computed the CV of SeaWiFS chlorophyll estimates C_{SAT} over the 3x3 set of pixels centered on each match-up pixel. This allowed us to discard pixels associated with strong local gradients, especially those close to the coast.

The SEADAS algorithms also set a number of quality flags for each pixel, which indicate cases where the atmospheric correction algorithm may have failed, or where the water-leaving radiance spectrum is inconsistent. These flags were also preserved in the match-up data set.

Over the 26 clear images, we obtained 4419 same day pixel match-ups between SeaWiFS pixels and underway data. After we discarded pixels where SEADAS flags were set, and pixels with high CV for C_F (CV > 30%) or C_{SAT} (CV > 40%), 3365 match-ups remained.

These same-day match-ups include in-situ vs satellite pairs with up to 12 hour time difference between the in-situ measurement of C_F and the satellite overpass. This elapsed time could lead to errors due to either horizontal advection, vertical mixing, or changes in phytoplankton biomass. To see whether this affected the statistical comparison of C_F and C_{SAT} , we also considered only data collected within 4 hours of the satellite overpass. This reduced the number of match-ups to 960.

This is still a much larger match-up set than can be obtained by conventional techniques. Collection of point pigment samples would have resulted in at best a few match-ups on clear days. In partly cloudy conditions, research cruises often return only a small number of match-ups over a 2-week cruise. Thus, it would not be possible to maintain a research vessel at sea to collect ground-truth samples for the number of sea days obtained from the fishing boats.

For each match-up set, we computed the mean and standard deviation of the error $\ln(C_{SAT}) - \ln(C_R)$. We can think of the mean as a (multiplicative) bias, and the standard deviation as a coefficient of variation. These are shown in Table 7-1. Interestingly, there is relatively little reduction in the standard deviation as we impose more stringent match-up criteria. However, there is a significant reduction in the bias as we restrict the match-up window from ± 12 h to ± 4 h. The satellite chlorophyll estimates are on average lower than in-situ estimates by over 30%, but this bias is halved if match-ups are restricted to a 4 hour window.

Table 7-1 Mean and standard deviation of the error $\ln(CSAT) - \ln(CF)$ for the indicated match-ups.

Match-up Criteria	# match-ups	Mean	Std Dev.
All	4419	-0.36	0.59
No flags, low CV	3365	-0.33	0.50
No flags, low CV, within 4h.	960	-0.17	0.46

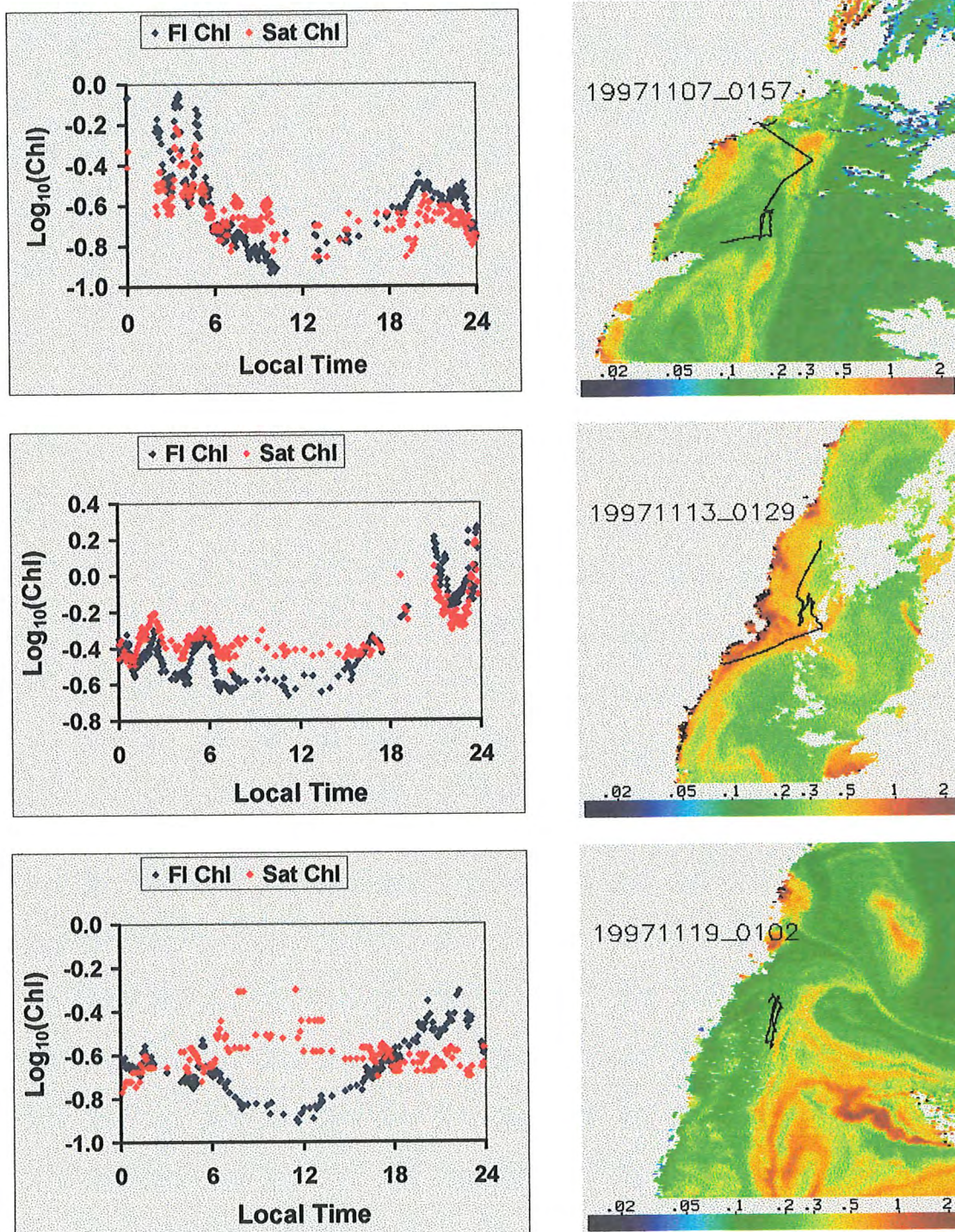


Figure 7-3a Comparison of C_F and C_{SAT} for three images off the NSW coast (7, 13 and 19 November 1997).

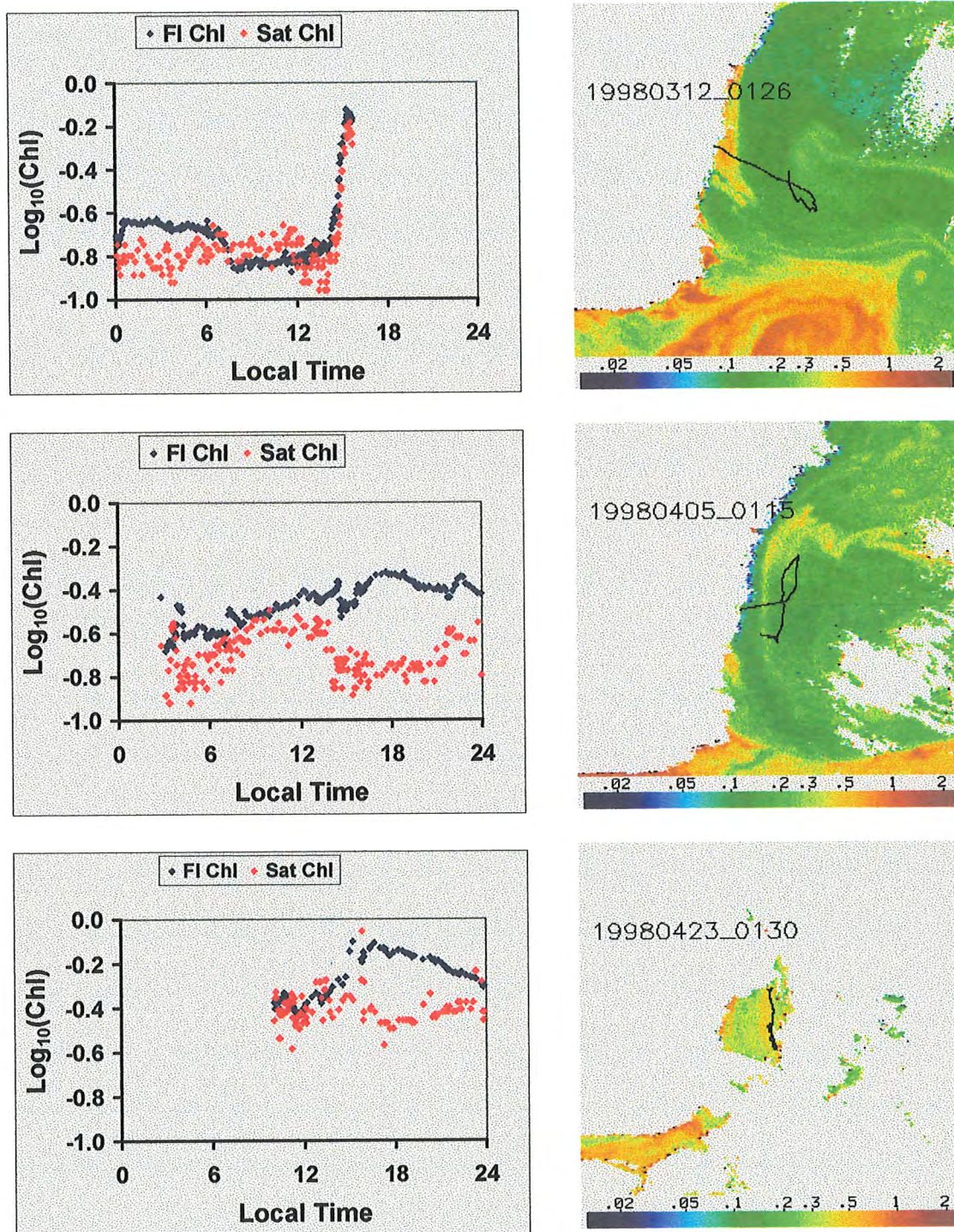


Figure 7-3b Comparison of C_F and C_{SAT} for three images off the NSW coast (12 March, 5 April, 23 April 1998).

Six examples of match-ups for individual images are shown in Figure 7-3. $\log_{10}(C_F)$ and $\log_{10}(C_{SAT})$ are plotted vs time alongside the corresponding SeaWiFS image with cruise track superimposed. The comparison on 7 November shows very good agreement through a wide dynamic range, as the boat passed through a series of high chlorophyll filaments on the continental shelf. The comparison on 13 November also shows good agreement as the boat crosses filaments offshore and finally enters higher chlorophyll water on the inner shelf. The dynamic range is much smaller on 19 November, and the comparison suggests a diel signal in C_F which is not adequately corrected. The same discrepancy is also evident on 13 November.

The comparison on 12 March shows good agreement throughout daylight hours, especially as the boat enters the high chlorophyll zone on the inner shelf. On 5 April, agreement is reasonable up until about 1300h, but there is poor agreement after this time. This may be due to rapid advection or possibly problems with atmospheric correction. The match-up on 23 April again shows good agreement around the satellite overpass, but poor agreement some hours later.

Evaluation of SeaWiFS accuracy.

Given that there are significant residual errors in predicting chlorophyll from fluorescence, it is not straightforward to translate the differences between C_{SAT} and C_F into absolute errors in SeaWiFS chlorophyll estimates. The following simple error model can be used to interpret the results. Assume

$$\ln(C_F) = \ln(C_S) + \varepsilon_F,$$

$$\ln(C_{SAT}) = \ln(C_S) + \varepsilon_{SAT} + \text{bias},$$

where ε_F and ε_{SAT} are random errors with variances σ_F^2 and σ_{SAT}^2 . From the fluorometer calibration, we know $\sigma_F^2 = 0.126$. If we assume that ε_F and ε_{SAT} are independent, then

$$E\{\ln(C_{SAT}) - \ln(C_F)\}^2 = \sigma_F^2 + \sigma_{SAT}^2.$$

For the ± 4 hour match-up,

$$E\{\ln(C_{SAT}) - \ln(C_F)\}^2 = 0.212.$$

It follows that $\sigma_{SAT}^2 = 0.086$, or $\sigma_{SAT} = 0.29$.

According to this model, SeaWiFS is estimating chlorophyll with a CV of about 30%, which is the NASA target. However, our analysis shows a bias of about -17%.

The automated underway sensor packages described here have operated successfully in a difficult environment over a period of 15 months. This is attributable to robust design and automation of data logging and maintenance. The support of the vessel masters and crews is obviously critical, and this has been encouraged by the provision of a real-time color display. The package could be deployed on merchant vessels as well as fishing vessels.

We consider that regular calibration with both a fluorescence standard (such as rhodamine) and coincident pigment samples is essential if underway fluorescence is to be converted to chlorophyll estimates with acceptable (and known) accuracy. Our analysis shows that it is important to account for day-night differences in fluorescence yield. The accuracy achieved here in fluorescence-based chlorophyll estimates ($CV = 35\%$) might be considered marginal for sea-truth of ocean color algorithms, which aim to achieve accuracy in CASE 1 waters of the same order. However, CASE 1 algorithm errors in continental shelf waters may be considerably larger (Parslow et al., 1998).

The automated underway fluorescence packages offer the additional advantages of scaling up from point pigment samples to satellite pixels, and providing much greater spatial and temporal coverage than is possible from bottle samples on research vessels. The number of match-ups attained in this project is far greater than could be obtained from conventional sampling on research vessels, and has permitted a rigorous analysis of the satellite performance. The total expenditure on the satellite calibration component of this project would cover only a few days of research vessel costs.

Our results suggest that the SeaWiFS chlorophyll algorithm is achieving a target CV of about 30% in outer shelf and open ocean waters off NSW, although there is also a bias of about -17% . We suggest that SeaWiFS chlorophyll estimates can be used with confidence in these regions. Of course, caution must still be exercised in interpreting SeaWiFS chlorophyll estimates in waters affected by coastal runoff (Parslow et al., 1998).

Logbook Returns from Participants

Over the period of the field study, the returns from participating operators (Figure 7-4) shows consistently good returns from about half of the participants. Not surprisingly, the computed total weight of catch (Figure 7-5), during the period of this study, is to a large extent correlated with the number of logsheet returns (and hence the amount of effort). While a few operators provided consistent returns, to the point where a group of operators were sending almost daily returns via Satcom C, a significant proportion of participants did not consistently provide returns throughout the period of the study. This can partly be attributed to a number of operating factors such as vessel breakdowns and weather restrictions on small vessels. It is fair to say that those operators who kept in good contact with project scientists, either by regularly phoning and discussing their experiences, through project scientists participation on vessels, or through discussions during the visits by scientists to ports, were highly successful in their operations. This is true of nearly all operators taking part in this project and certainly applies to those with the highest catch returns (Figure 7-5). Subjectively, the common element of a successful operator was a willingness to learn and use an integrated combination of information provided by project scientists (be it information on catch prediction or SST images) with the operator's experiences. In other words, those that obtained synergistic value from remote sensing by combining it with their field experiences gained most from the project. Those that relied on one or the other aspects did not do as well. These subjective assessments are hard to quantify and we discuss the reasons later.

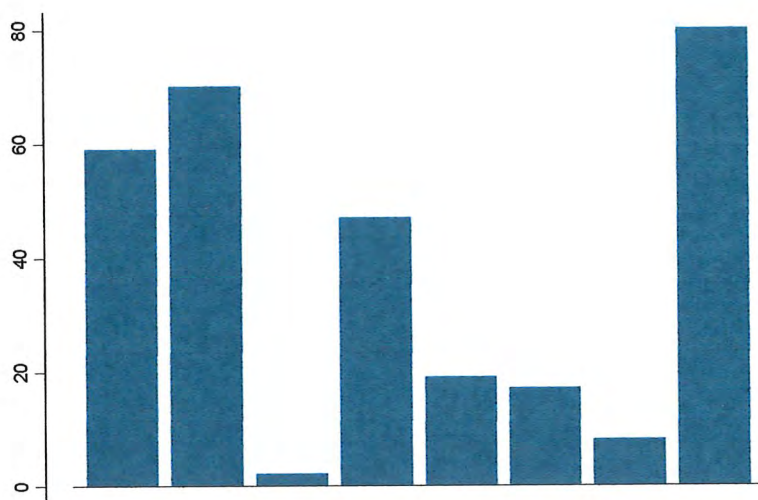


Figure 7-4 Bar chart of number of logsheet returns over the period of the field study for each of the 8 main participating operators (operator's identity deliberately undisclosed in the graph).

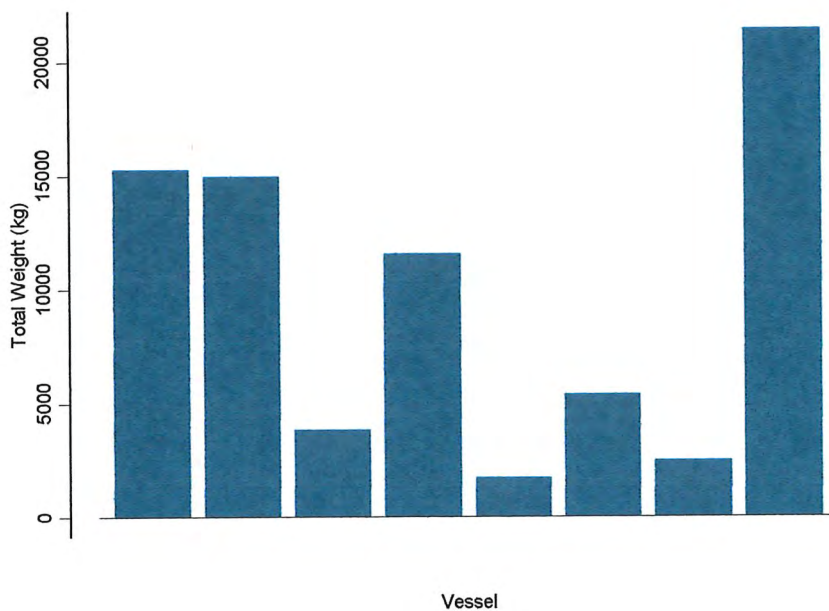


Figure 7-5 Bar chart of total weight of fish caught during the period of the field trials by the 8 participating fishing operators (Note: Vessel identifications have been deliberately omitted but relative locations in the bar chart are the same as in Figure 7-4)

While the focus of this project is primarily on the 4 target species (YFT, BET, BBL, SKJ) a number of other species were caught by participating operators (Figure 7-6). Among the target species, the nominal average size caught spans a relatively narrow range for yellowfin and bigeye tuna compared to broadbill. The size range of fish is of interest as it is well known that different sizes of the same species of tuna may have evolved different environmental preferences (e.g. see Lyne et al 1997 for SBT size-related preferences). This has implications for the catch prediction, and fine-scale analysis, as we did not stratify the predictions to take account of size-related aspects. While taking size into account in the predictions was possible, the basic logbook data does not generally have sizes recorded although an index of size can be computed if both numbers of fish and total weights by species are recorded. Thus, our broadbill predictions may not be satisfactory considering the range of sizes caught by the fishery.

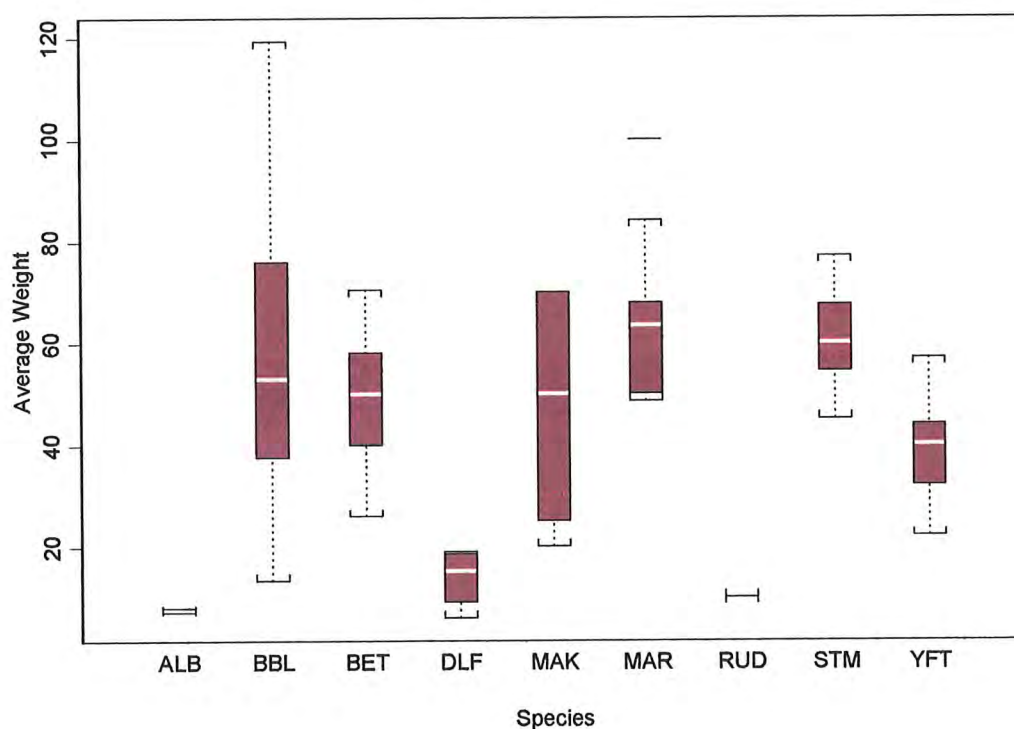


Figure 7-6 Box-and-Whiskers plot of the average weight (kg) of various species of fish caught (in each shot) from logsheet records returned during the catch prediction phase of this project. Acronyms are: ALB=albacore, BBL=broadbill, BET=bigeye tuna, DLF=dolphin fish, MAK=mako shark, MAR=marlin, RUD=rudder fish, STM=striped marlin, YFT=yellowfin tuna. The filled bar encompasses the quartiles of the data with the median embedded as a line. The "whiskers" encompass the extremities of the data distribution and outliers are shown individually outside of the "whiskers".

The other point to make on the catch mix is that most catches comprise two or more species. We examined this mix by conducting a principal component analysis of the catch composition using both the covariance and correlation methods (the covariance method is sensitive to catch levels (of the different species) while the correlation method tends to emphasize normalized patterns). The results for the covariance method (Figure 7-7) shows that, if emphasizing catch sizes, two components dominate catch composition: the first is a composition of yellowfin and broadbill while the second mode is one of negative elements (non-catches) of broadbill and marlin associated with a positive element (catches) for yellowfin. So, the dominant component shows a mixed catch - highest in yellowfin and broadbill with lower catches of striped marlin and bigeye tuna. There is a suggestion that bigeye catches are in fact overshadowed by catches of striped marlin. With the correlation method (Figure 7-8), which emphasizes normalized patterns, the first two components are not as dominant and furthermore the first dominant mode shows a diverse range of species (in fact all species) being caught including the target species. The second mode is a mixture dominated by non-target species. From an operational viewpoint where catch levels do matter, the covariance method, which shows the yellowfin-broadbill association, is more relevant and suggests that current targeting practices are effective at catching a combination of yellowfin and broadbill.

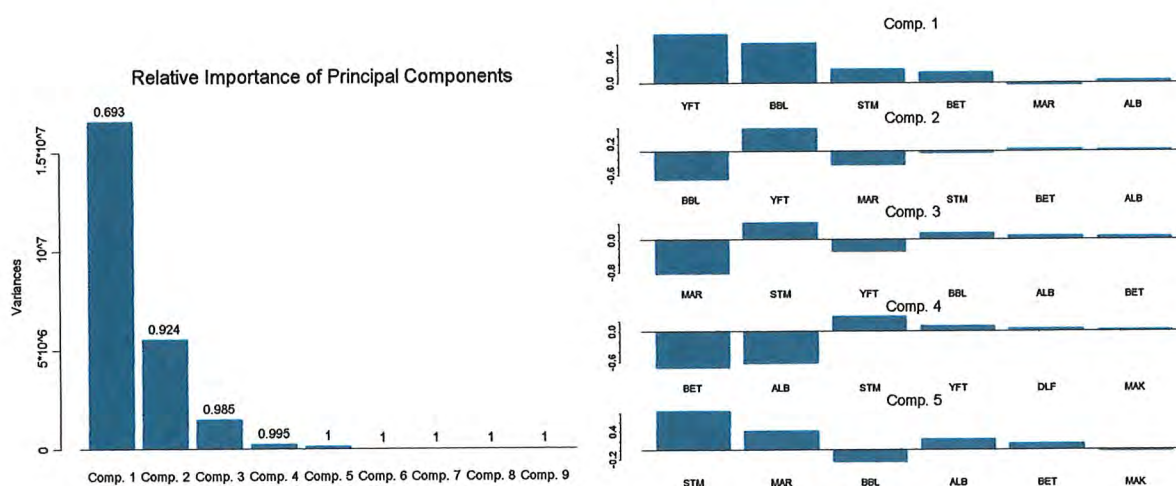


Figure 7-7 Principal component analysis, covariance method, results for the composition of species recorded in the catch logs. The relative importance of the components in terms of variance explained by each component is shown on the left and the component loadings on composition of catch are on the right.

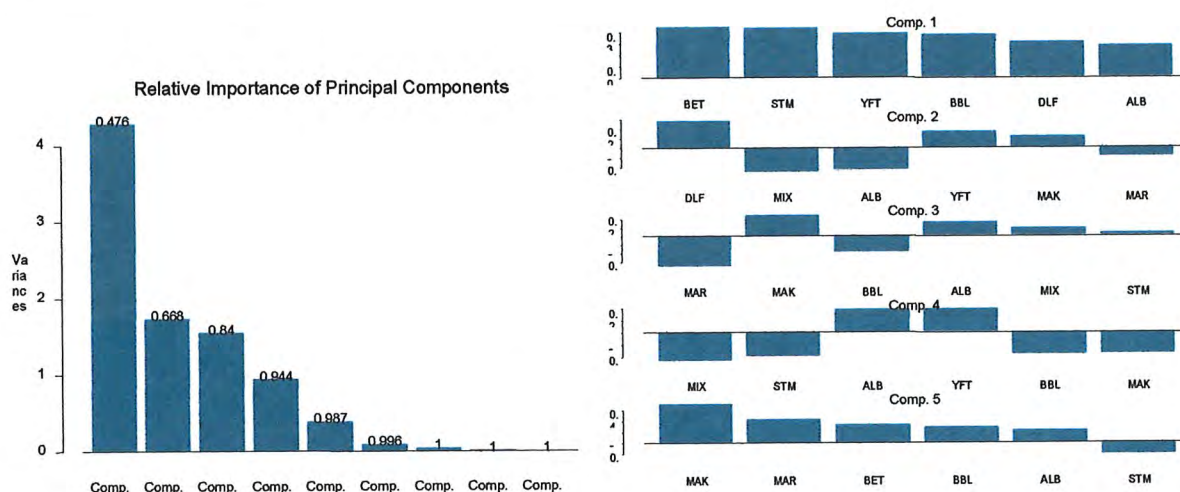


Figure 7-8 Principal component analysis, correlation method, results for the composition of species recorded in the catch logs. The relative importance of the components in terms of variance explained by each component is shown on the left and the component loadings on composition of catch are on the right.

Catch Predictions

In the previous section the synergistic value of the catch predictions was emphasized. This was to highlight the fact that while the gross distributional dynamics of fish maybe captured by statistical predictions, it can never be perfect and what is provided must be interpreted in an informed manner. Remote sensing by itself or in combination with historical catch data will not be sufficient. In the following subsections we will discuss the key issues, in our experience, on the use of the catch prediction information and assessments of the technical utility of the predictions. We will examine an objective approach, various case studies and comments by operators on the utility of the predictions.

Catch Predictions – An Objective Assessment

Given a catch prediction method, it would seem reasonable to simply test, at first, how the predictions compare with observations. Such plots are shown in Figure 7-9, for month-by-month comparison, and in Figure 7-10 for an overall comparison across all months. While there's a fuzzy positive trend of increasing predicted and observed catches, there is considerable scatter in the comparisons. A number of factors contribute to this:

- Longlines operate across a length of up to 120km and during the soak period, apart from movement of the longline, fish caught on the line may potentially have come from an extensive buffer region (which needs to reflect the fish's movement in the soak time, plus ocean currents etc) surrounding the longline. Thus the location of the longline as recorded on the logsheets does not reflect the true potential catch location or effective swept area (swept by the fish movement and longline).
- The time at which fish are caught, usually known only to within a day, may not correspond to a time at which clear satellite image for the area is available (because of cloud problems and satellite pass times). Also, if high catches occur on one or the other side of highly dynamic fronts, large spatial shifts in catch distributions are possible at a particular location making it difficult to relate catch predictions to precise environmental conditions.
- Sea surface temperatures, as observed by satellites, can potentially contain daily variations caused by surface heating and cooling, especially for highly stratified waters of the EAC, and during summer (see the appended report on the WA sampling results). In the tropical areas, high altitude cloud effects can also contribute to inaccuracies, and areal coverage available.
- Some positions recorded in the logsheets may be in error; the ones falling on land are obvious but not so obvious are the ones which are in the fishing area but erroneous. A number of positions are also recorded to the nearest integer latitude/longitude as shown previously.

It is impossible to take into account the vast number of factors that contribute to catch success or failure; these include not only the environmental water condition influence on fish distribution and the ecological aspects of the fish movement, migration and feeding (e.g. moonphase), but also such influences as the skipper's experience, weather, fishing gear, depth of set and bait. Thus high variability of the sort seen in Figure 7-10 can be expected and the aim of the catch prediction is to examine whether remote sensing information can assist in narrowing down the potential catch area despite the myriad of uncertainties and complications.

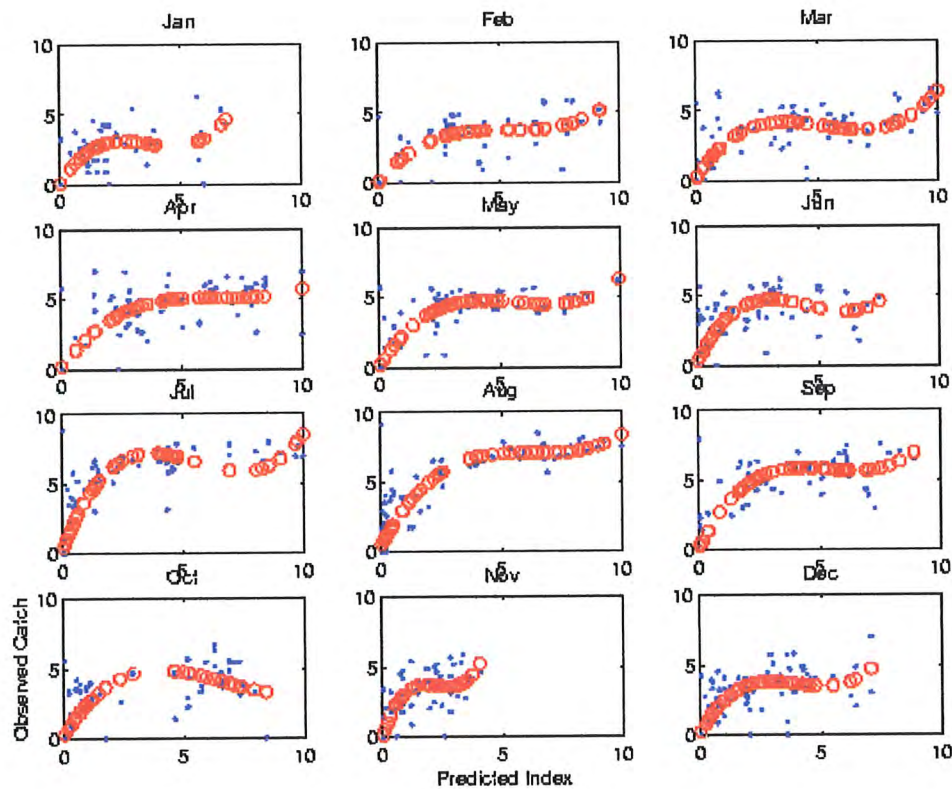


Figure 7-9 Monthly plots of predicted catch index versus (log transformed) observed catch index. A 3rd order polynomial regression fit is plotted in each panel *for reference only – it is heavily biased in some plots.*

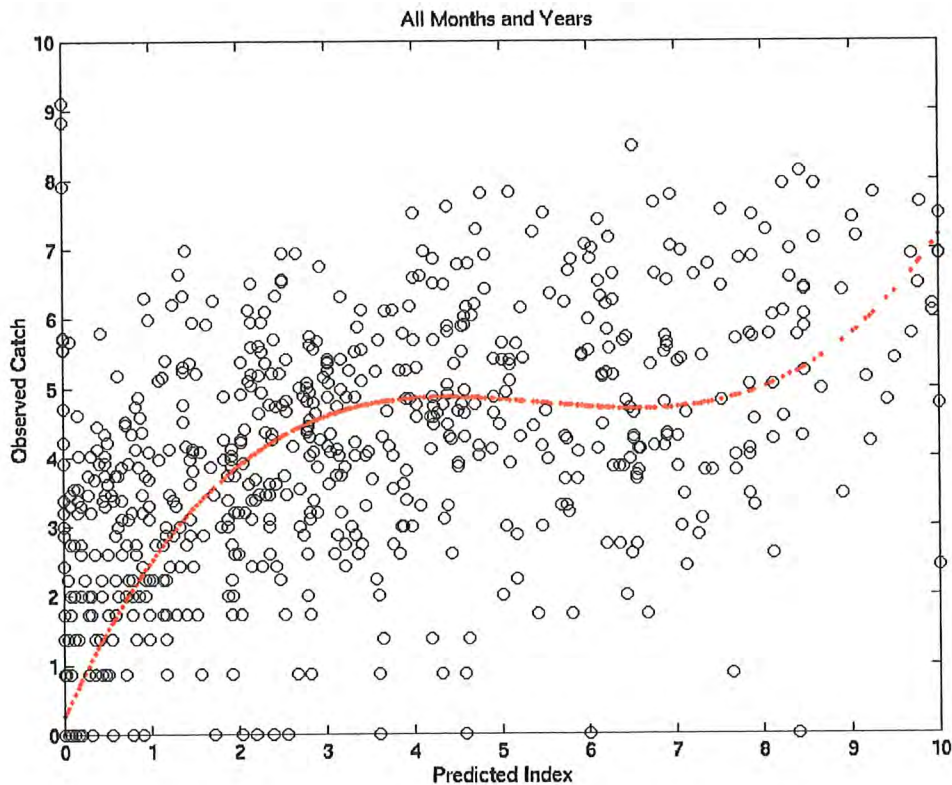


Figure 7-10 Comparison of predicted catch index with observed index for all years from 1992-1997 inclusive. Predictions were conducted for the east Australian yellowfin tuna fishery using historical catch and remote sensing data. In the predictions, the test year is excluded in formulating the predictions. Comparisons were conducted only for the offshore fishery (waters deeper than 2000m) and each comparison point represents monthly medians of catches and predicted indices. A 3rd order polynomial regression fit is shown *for reference only*.

One final point worth noting about Figure 7-10 is the relatively high observed catches recorded in most months where the predicted catch index is larger than about 3. This suggests that where the prediction indicates large catches, observed catches will most likely also be large – but not necessarily increasing with the catch index. Thus, the catch index can serve primarily to identify the “core” areas of expected high catches. In retrospect, this is primarily how the predictions were used – to identify suitable target areas of expected high catch, rather than simply targeting the areas of highest catch index.

Catch Predictions - Case Study

In this section we compare the fishing activities and catches of 3 operators that utilized the catch predictions during a 5 day period in the beginning of December 1998. Vessel names and identities are not disclosed and we simply refer to the 3 vessels as A, B and C. Each of the operator's land office were supplied with the catch predictions but it likely that the operators were basing their fishing strategy on the prediction period prior to the one being examined here. The catches of the operators during this period Table 7-2 show a number of features:

1. Despite the target species being supposedly yellowfin, bigeye and broadbill, a range of other species, notably marlin and striped marlin, were caught.
2. Vessel B catches were predominantly marlin.
3. Vessels A and B have relatively low catches of yellowfin and all vessels had good catches of broadbill.

Table 7-2 Total weight (kg) of various species of fish caught by 3 operators during a 5 day period in December 1998 off Mooloolaba. For a description of acronyms see Figure 7-6.

Vessel	Shots	BBL	BET	MAR	MIX	STM	YFT
A	2	1085	200	-	80	300	240
B	4	1180	100	2851	-	-	600
C	4	1573	138	-	-	1015	1524

The locations of the vessels in relation to the supplied sea-surface temperature and catch predictions (Figure 7-11) reveals that most of the shots by the operators, in particular vessels A and B, are in areas that the predictions identifies as being poor index areas for the target species. Only vessel C it seems has followed the catch predictions. Thus the respective catch (or non-catch) of the target species, especially yellowfin, to a large extent, can be construed to confirm (albeit in an inverse way) what the predictions were identifying. So, why were some operators not in the target areas? A number of explanations are possible but a likely one is that: at the beginning of the catch prediction phase, project scientists spoke to most operators about the new generation of ocean color satellites and how the information from ocean color could be used in fishing operations. The message given to operators was that because ocean color satellites could identify the clarity of water, and given the operators observations of high catches in clear "tuna water", there was potential of using this new information for targeting catch areas. In ocean color images, the clear areas are identified as blue and the "dirty water" areas are identified as orange-red areas. When the colored catch predictions were supplied to operators a number of them confused the colors on those images with those of ocean color images - despite written and verbal explanations when the catch images were delivered. In the catch images, blue areas are identified as being poor catch areas and reds are the high catch areas. The catch images mimic some of the features of ocean color but the color schemes are reversed in terms what they mean for catch success. In speaking to operators there was definite confusion, at least in two operators who used the image, as to what the colors meant; these operators reversed the meaning of the colors on the catch predictions. Other examples, similar to the above, of operators fishing in non-target areas exist.

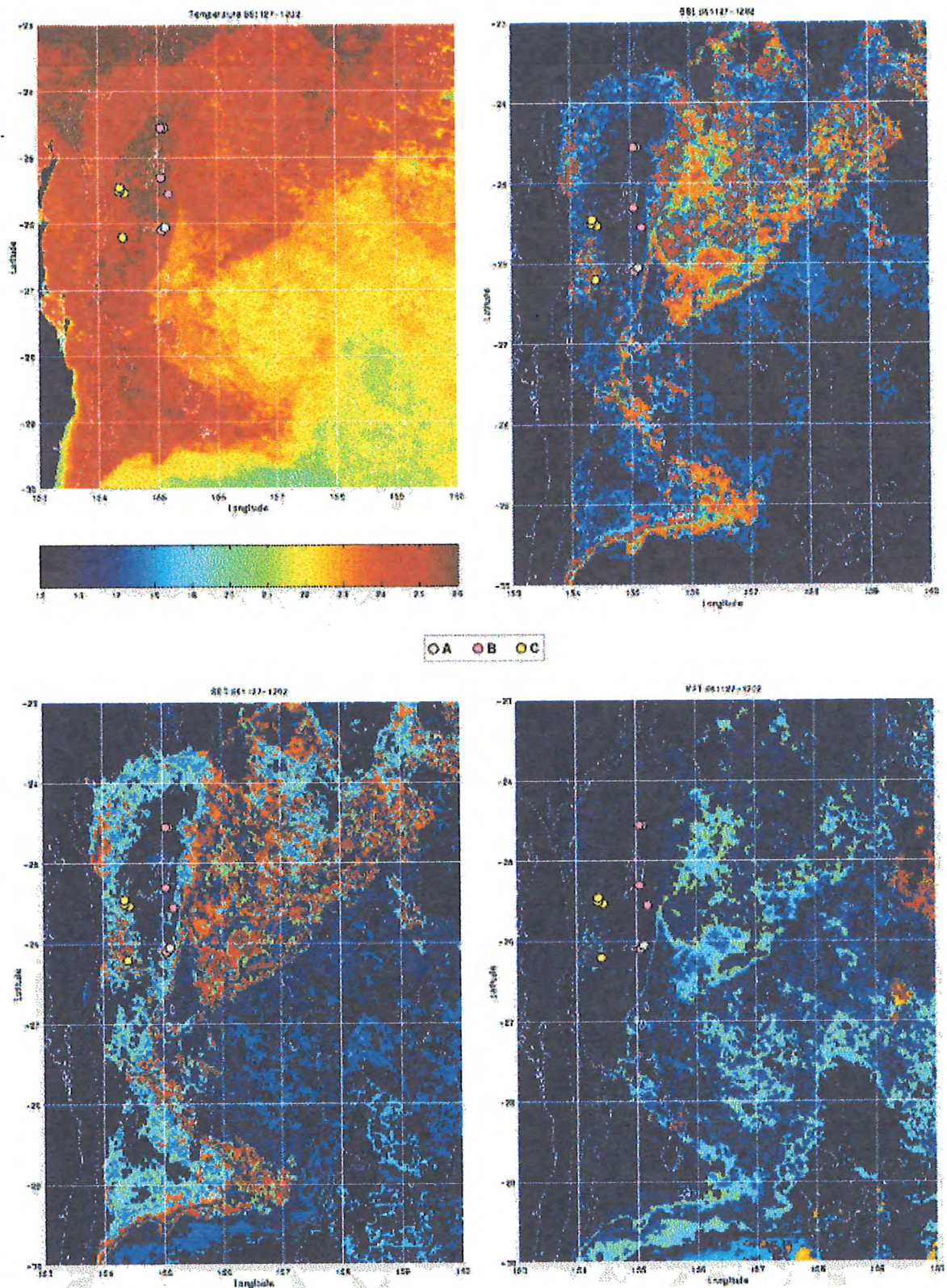


Figure 7-11 Example set of SST and prediction images for early December 1998 with the location fishing shots of 3 participating vessels overlaid on the images (note each image is normally supplied separately rather than as a single set as displayed here). In the predictions, the predicted index is coded according to the rainbow scheme with brown/red corresponding to high indices and blue to a low (or zero) index. Bathymetric contours are also noted on the images.

Catch Predictions – Information from Ocean Color

Given the difficulty of assessing predicted and observed catches, even in post-hoc analyses, another approach to assessing the additional value of ocean color is to determine what features (of relevance to catch predictions) in ocean color are not deducible from SST. In other words, how well can we predict relevant ocean color features given SST. Visually, there is a high degree of subjective correlation between ocean color and SST (see for example Figure 6-6 and various SeaWiFS-ocean color image sets on the remote sensing website at <http://www.marine.csiro.au>). Classic theories of the coevolution of temperature and phytoplankton features in the ocean (e.g. Lyne, 1983) suggest that at a certain critical scale, that depends on the growth rate of phytoplankton and the diffusion rate of tracers in the ocean, different processes control the evolution of phytoplankton features. Below this scale which is about several kilometers for typical open ocean phytoplankton and diffusion (Lyne, 1983), biological processes dominate whereas above this scale physical processes dominate. In other words, if these theories hold true, we can expect to see high coherence between temperature and phytoplankton features certainly at regional scales of 100's km.

The usual approach in demonstrating this theory relies upon analyses of the spectrum of temperature and phytoplankton. This (linear) approach is not entirely satisfactory as there is no guarantee that features at large scales do in fact correspond - as small shifts in spectra, not to mention phase, can substantially alter the actual spatial pattern. We approached the problem by directly predicting the actual features of phytoplankton as visible in the ocean color images. For the test we used a relatively clear set of images from 3rd September 1998. The SST image (Figure 7-12) shows the expected latitudinal grading from warm tropical waters down to the cool waters off Tasmania. A strong narrow East Australia Current is visible in the image flowing down from a broad headwater region off about Brisbane to a narrowing jet off New South Wales which disintegrates into mixed regions off southern New South Wales. The observed ocean color image (Figure 7-13) shows broad low phytoplankton regions in the tropics and the East Australian Current region but high values in the mixed region, in Bass Strait and the coastal band (which may not be entirely phytoplankton but could additionally be due to sediment and/or dissolved organic matter). In the open ocean, the high productivity regions are presumed to be due to the mixing of warm nutrient-depleted tropical ocean waters with cool nutrient-enriched temperate waters from the south and/or from the hydrodynamic turbulent mixing instabilities at the edge of strong eddies or current jets.

Visually, the predicted ocean color image (Figure 7-13) is remarkable in not only showing these expected regional trends but in faithfully mimicking broad spatial features of the observed image including surprisingly good predictions of the finer-scale coastal structures. As expected from theory, the fine-scale ocean features visible in the observed image appear as "smeared" or diffused features in the prediction. The Tasmanian coastal features are broader and not faithfully captured implying that the coastal processes off Tasmania are different to those off East Australia and that the regional prediction is dominated by (the longer area of) the mainland coast. While the discrepancies were of second-order interest, the predictions could be improved by allowing for latitudinal variations in coastal processes and by a double-scale prediction approach for the fine-scale open-ocean features. In the latter case, fine-scale open-ocean features caused by strong current mixing, and not dominated by phytoplankton growth processes, could possibly also be predicted but would require a predictor attuned to local processes.

The prediction scheme we used for the ocean color images is essentially the same as that used for catch predictions (although the full prediction scheme in this case is not normally used in the catch predictions due to data problems). What this implies is that if ocean color is important in explaining catch, that aspect should be captured in the catch prediction scheme. Which all leads us to the ironic conclusion that at broad regional scales ocean color adds little value to information derivable from sea-surface temperature. While the conclusion may not, and probably does not, hold at fine scales, it is nonetheless one of the remarkable findings of this study which also confirms the conclusions by ROFFS (discussed previously).

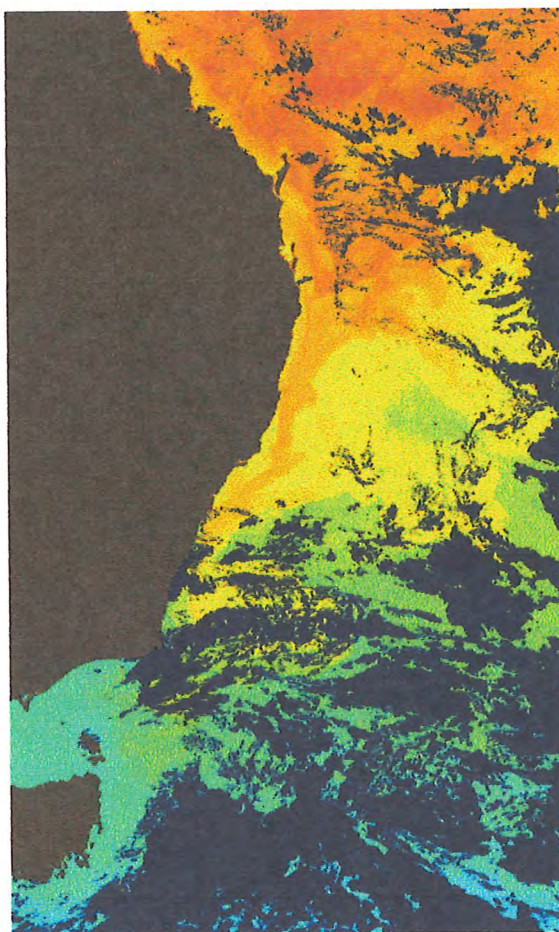


Figure 7-12 Sea surface temperature image for 3rd September 1998, used of predict ocean color. Dark blues areas correspond to cloud cover and the land masks are in brown.

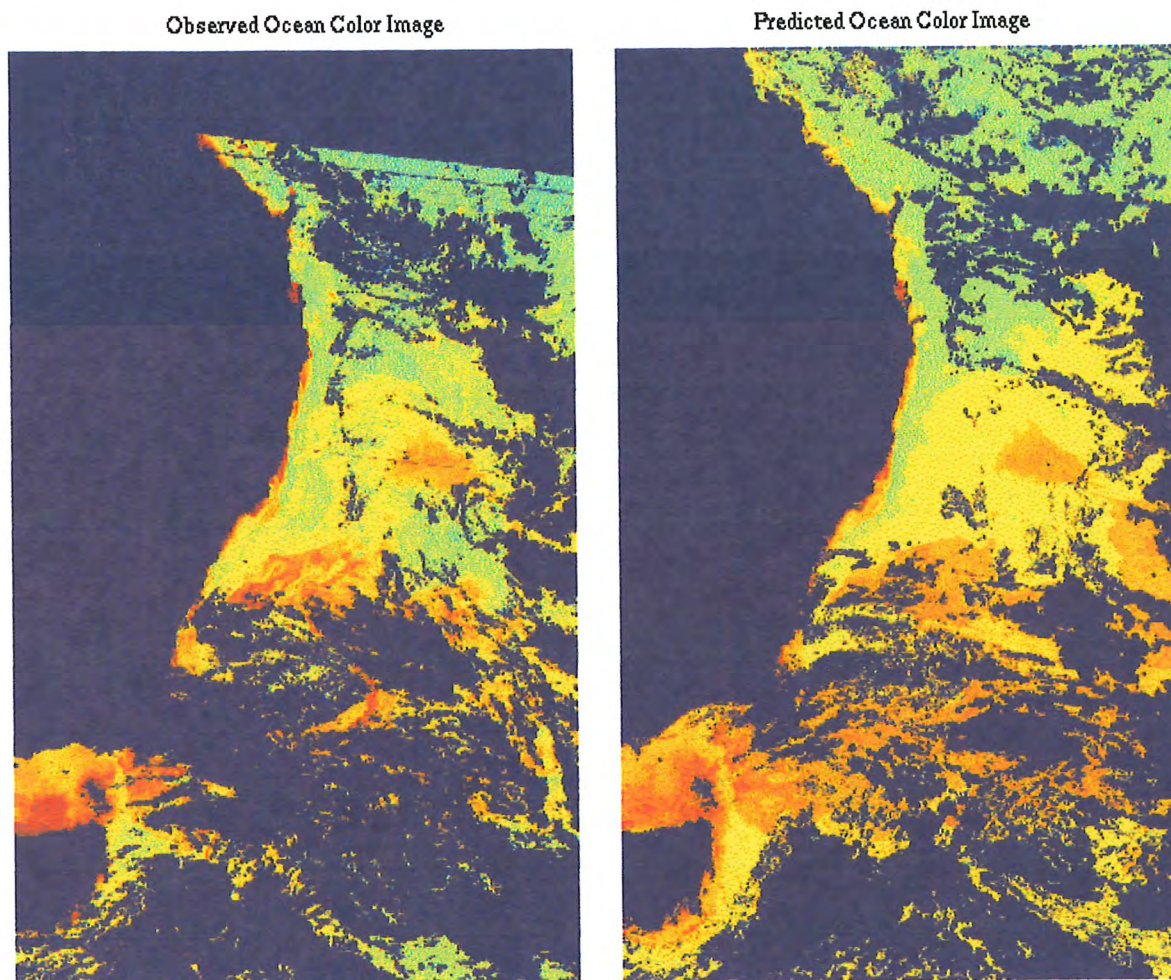


Figure 7-13 Observed SeaWiFS chlorophyll image (left) and predicted (right) for 3rd September 1998. Predictions are based on sea surface temperature (Figure 7-12) from a separate satellite pass on the same day. Note the more extensive cloud cover effects in the observed chlorophyll image. Dark blue areas correspond to cloud cover or land and high phytoplankton areas are in red/orange and grade down to lower values from yellow, green, cyan to blue.

Catch Predictions – Subjective Information from Operators

Comments provided by a number of operators as part of their information returns provide clues on the usefulness or otherwise of remote sensing information, and catch predictions, on their operations and catch success.

We have previously mentioned the problems in interpretation of the meaning of the colors used in catch predictions. This was a particular problem early on in the catch prediction phase. In one instance we plotted up the position of a (non) catch location for an operator who reported that it was the worst catch on record only to find that they were fishing in the midst of an area colored blue in the predictions to indicate that catches were likely to be low there. Our discussions with the operator confirmed this use of the image as the reason for the low catches (and inadvertently provided a good ground truth point for the predictions).

Operator skill in interpreting the local environment is also a key factor as evident from the detailed information provided by one operator. In several instances the operator coincidentally fished in the same local area as other operators who were also receiving the catch predictions. In a number of cases, the operator reported that the other (more experienced) operators who were fishing next to him were catching a few tons of fish while he was struggling to get a decent catch. We interpret this to be due to either the experience of the other operators in understanding the local environment and/or fishing techniques, and that finescale effects do matter.

One experienced operator who understood the local environment well reported fishing on the warm side of a front in defiance to the predictions which were showing better catches on the other side of the front. He later fished on the side indicated by the image and reported far better catches there. (This was verified by a CSIRO staff).

As a general observation, there is a consistent theme in discussions with operators and from their feedback that they wanted to know what lay behind the predictions and that they were uncomfortable in putting their faith (and livelihood) as to where the best catches were. A number of these operators used the composite sea-surface temperature images along with the predictions to try and understand why particular areas were being marked as good or bad. In this way, these operators have built up their knowledge of the good fishing areas. This was an unexpected outcome of the catch predictions and it was reflected in the Remote Sensing Facility of CSIRO signing up a number of new customers for their sea-surface temperature image products and requests for composite temperature images (rather than the daily ones routinely supplied).

A few general conclusions can be made from the comments provided by operators and from observations of the quality of the SST and predictions:

- SST data in the northern portion of the viewing area (up to about 20° S) was often contaminated by high-level cloud which the cloud identification algorithm found hard to identify and eliminate. Composited images for that region were often of "motley" appearance and this directly affected the quality of the predictions (because of the poor quality of historical images used for prediction, and because of the poor quality of the actual images used in the prediction).
- In contrast the area off NSW was not as affected and given the strong gradient in water conditions caused by the energetic elements of the East Australia Current, both the quality of the SST and the predictions were not as affected as the tropical areas.
- While the quality of the predictions was better off NSW, it does not necessarily imply that it was of greater value to operators for reasons that a) operators were already receiving satellite SST images via the co-op (from CSIRO Marine Research Remote Sensing Facility) and most had developed their local knowledge of the association between catches and SST and, b) these operators also generally did not venture off, or far off, the continental shelf. Subjectively, it would appear that the SST images and predictions were of much greater value to the northern operators. Indeed, proof of this is the fact that many of the new subscriptions for SST products came from the northern operators.

8. FINE-SCALE RESULTS

Summarizing the results of the appended report by Young et al:

Using a combination of generalized linear and generalized additive models, both fine and broad scales were found to be significant in relation to catches of all 3 species (broadbill, yellowfin and bigeye). We found that area, followed by month and fluorescence, were significantly related to broadbill swordfish catches. In the second model (using just Mooloolaba data), salinity, fluorescence, nearness to front, year and moon phase were significant. The catch rate of yellowfin tuna was significantly related to area followed by month, fluorescence, moon, sea surface temperature and wind speed. The catch rate of bigeye tuna was significantly related to fluorescence followed by salinity, nearness to front and moon phase. Using only the Mooloolaba data, surface salinity and fluorescence are both significant for all 3 species. Our results demonstrate that the use of the underway sampler for measuring fluorescence and salinity, together with an awareness of the position of fronts, has the potential to increase our understanding of the local distribution of tuna in waters off eastern Australia.

9. BENEFITS AND ECONOMIC EVALUATION

The economic value of SST images and catch predictions has both public and private components. The public value arises from benefits and costs to society at large and may be assessed in part via the impact of such information on management agencies, their strategies and their effectiveness in achieving specified objectives. The private value to fishing firms from receipt of new information arises from its effect on the costs and revenues associated with fishing.

Economic benefits to fishing firms result from reduction in search costs and from increased revenue associated with larger catches. A complete analysis would involve assessing how these things change over time but this is beyond the scope of the present study. The economic component of the SeaWiFS project is focussed on shortrun net benefits to fishing firms, however. Therefore, attempts were made by the researchers to obtain from fishing firms, the cost and revenue data necessary for rigorously assessing the private economic value of the catch predictions and SST images during the period in which these were provided to participants.

In principle, several measures of shortrun private economic value are possible, provided that the necessary data are available. The first is associated with whether fishers change their fishing plans in response to the receipt of new information (in this case, the information takes the form of up-to-date composite SST images and forecasts of catches of selected species in the various sectors of the study region). Fishers were asked to provide data on: a) their expected catches and fishing locations immediately prior to receiving the additional catch and SST information and b) their expected catches and fishing locations immediately after receiving the information. Such data would have been useful for evaluating the expected value of the information at the time fishing voyages were being planned. This, in turn, would have given insights into the decision-revision process that fishers engage. As subsequent events unfold, it would also provide a basis for assessing the forecast errors that resulted from the information-induced revision, as compared to the forecast errors that have arisen in the absence of such information.

Regrettably, although qualitative assessments were provided by fishing firms, it was not possible to secure the detailed quantitative information necessary for a more rigorous analysis.

The second measure of shortrun private economic value is to compare fishing performance of the same firms in different periods. This clearly requires provision of the extra information to firms in some periods but not in others. An obvious problem with this measure is that environmental and market conditions can vary substantially across periods, causing problems with attributing changes in costs and revenues to the availability of the information.

A third measure of value is to compare, during a particular period, the performance of firms that have access to the information with those that do not. This has the advantage of standardizing environmental and market conditions but does not account for differences among firms that influence fishing success.

In the SeaWiFS Study we are limited to quantitative measures of shortrun private economic value of the second and third types. Before enumerating these, however, it is worth reporting the qualitative responses of fishing firms.

Of the 10 vessel skippers who provided some of the requested feedback seven found the prediction and/or the SST images to be useful and a cause for changing their planned destinations. Five of these skippers were very keen to consult the images before leaving port and requested updates when out at sea. The four fishers who provided the most regular and detailed feedback requested continuation of provision of images beyond the life of the project, indicating a willingness to consider contributing to the cost of same. Interviews with these skippers were fruitful in detailing the source of benefits to fishing firms, although quantitative records are not available. The source of benefits put forward include the following:

1. Reduction in search time (both vessel and aerial, where used) in locating target species or water masses with favorable temperature and color
2. Reduction in uncertainty of locating target species with consequent reduction in sea time
3. Reduction in uncertainty of timing of fishing trips to avoid bad weather and take advantage of good weather
4. Related to 2., improved direction of search aircraft when used, with subsequent reduction in search costs
5. Location of higher concentrations of target species, leading to increased revenue
6. Location of target species in areas previously not considered, thus expanding the perceived fishing grounds.

10. DISCUSSION

At this point it is appropriate to recall Blackburn's criteria for a successful fisheries oceanography project and to address each of these in turn:

- 1) Continuous data gathering and mapping of temperature and other ocean properties
- 2) New instrument technologies for ocean observations
- 3) Skill in inducing relationships between tuna distributions and ocean properties
- 4) Organizing the flow of information between fishers and oceanographers (scientists)

Satellite imagery nowadays provide unprecedented coverage of the oceans, but still subject to cloud, and during this project we have collected comprehensive integrated datasets for remote sensing validation both off Western Australia and eastern Australia. In fact the problem now is not so much data gathering and mapping as such but given the plethora of satellite sensors available, or about to be launched, it is more in acquiring, processing and managing, the right datasets of appropriate resolution and quality to address problems of interest. While it is quite feasible to think that small organizations or groups can amass the necessary infrastructure and ongoing support in future, this is not the case for the current range of sensors especially the new ocean color, and other high-bit-rate multi-spectral, sensors. This project provides an outline of the elements required for successful development and evaluation of remote sensing systems, in particular ocean color, for fisheries operations. We have shown that smarter use of SST for fisheries operation activities can provide worthwhile gains, for less effort, than the substantial human resource and infrastructure investment required to collect ocean color data. This is not to preclude the option under which efficiency gains from alternate uses of ocean color (e.g. for studying links between productivity, fisheries and ecosystem structure and function), or any other sensor data for that matter, may make this new data attractive for use in fisheries. Thus, quality assurance and active maintenance of calibration/validation including algorithm development are key activities that must be accounted for **up front** in considering the use of any new sensor. Such facilities are most often only available in large government-funded agencies and even then only in a subset that have a clear vision and commitment to support these new endeavors.

The Automated Underway System is another example of innovation, which resulted in substantially more calibration comparisons with satellite data, and furthermore provided an unexpected tool in assisting with fine-scale fisheries operations. This new tool has acted as a catalyst drawing together, in much the same way that satellite data does, industry and scientists. Scientists participating on the field trips were able to directly impart knowledge of ocean processes to operators and at the same time were able to observe first hand operational aspects of the fisheries. The primary use of the system, namely for calibration and validation has resulted in new insights and procedures for accounting for diel variation of fluorescence in the ocean off eastern Australia. Furthermore, this unit has the potential for numerous applications where continuous underway data would be of use in calibration and validation, such as collecting data from trans-ocean merchant tracks, or for coastal studies using small vessels. It encourages us to seek new ways of routinely obtaining, from vessels of opportunity, what are otherwise very expensive research data.

Our catch prediction methodology encapsulates many elements of our understanding of fish distributional dynamics and its pragmatic application to assist in fisheries operations. Here again innovative catch prediction techniques (not part of the objectives) in analyzing a properly constituted archive of satellite and fisheries data, and lessons from the painstaking history of pioneers in the field, have borne fruit. This methodology will offer fresh insights into the spatial dynamics of tuna. It also offers us the ability to more wisely utilize existing data such as SST. Much more development of the method is feasible, and necessary, but even at this early stage it has demonstrated that remote sensing is of considerable value especially for developing fisheries. As Murphy's Law would have it, the need for good predictions were in the northern region where the satellite data and associated predictions were bad at times. So a critical improvement in the future is in cloud masking or better atmospheric correction algorithms for SST in the tropical areas. Once this is accomplished we can then investigate improved methods for understanding the distribution of fish, particularly of yellowfin tuna – without good environmental data, attempting to improve upon the predictions is difficult, and probably futile.

While there was good flow of information between scientists and fishers, aided by the innovative underway system and catch predictions, it is a fair assessment that we were not able to collect rigorous and quantitative information to properly assess the value of remote sensing for fisheries operations. This was not for lack of trying on the part of both the scientists and the participating fisheries operators. However, two developments arising from the project provide conclusive proof of the utility of remote sensing: the first was an unexpected rush of new subscribers for the SST products of the CSIRO Remote Sensing Facility, and the second is industry interest in exploring options for extending the uptake of remote sensing technology. A further development is the preliminary use of the technology by AFMA/AFFA in its attempts at minimizing the by-catch of SBT in 1999. Subjectively, there were many improvements attributed to the use of remote sensing and catch predictions; the economic returns of any one of these was perceived to be far in excess of current costs to subscribing for remote sensing products such as SST images.

As in most scientific endeavors, there are potential advantages and disadvantages in new developments or technologies. Better fishing technologies can potentially enhance operator return but it can also lead to various problems for the fisheries (higher catches, targeting of higher value fish, extended fishing range and season for non-quota species), unrealistic expectations (which can show up as premature infrastructure investment), assessment problems (as in determining how effort is affected by new technologies and fishing operations) and management problems (in coming to terms with the management implications of new technologies). As history shows, new technologies and ideas follow the path from scientists to industry and then to management, with management often coming in late to deal with problems created by the new technology. This is not to say that industry is irresponsible in the use of new technologies - on the contrary, most operators are very concerned with the longterm future of their industry. The opportunity is here now for management to come to grips with the use of remote sensing and other technologies in enhancing the long-term sustainability of Australian fisheries and ecosystems. This project hopefully provides a useful starting point for these endeavors.

11. CONCLUSIONS AND FURTHER DEVELOPMENT

We set out to develop, evaluate and apply remote sensing data to Australian fisheries with the specific application focussed on the east coast tuna fisheries. One undeniable conclusion of this work is that there are considerable synergies to be gained from involving industry in both data gathering and exchange of knowledge. Satellite sea-surface temperature data is indispensable in fisheries operations. Operators who are aware of this are capitalizing on the information and others involved in this project are also now utilizing the information. There is a clear need for an educational process to further the use of remote sensing information for the benefit of operators and managers.

Being smarter about how we use existing data can offer considerable benefits as we demonstrate with our catch prediction methodology. However, such insights rely upon a long history of information on both the environment and the resource. With remote sensing data, quality control via dedicated calibration/validation activities are vital and the need for such activities must be carefully considered and budgeted for especially for the new range of high data rate multi-spectral sensors – of which SeaWiFS is one. At regional scales, ocean color adds little additional value to information obtainable from SST for fisheries operations. Better atmospheric correction and cloud detection algorithms for the tropical ocean areas promise to add even more value to the existing SST datasets. The foundation of enhanced understanding of environmental influence on fisheries begins with good quality environmental data.

While there is scope for developing the catch prediction methodology, operators need to use both regional and local knowledge in their operations. The automated underway system can provide local information while at the same time collecting valuable information for ground-truthing satellite data and fine-scale catch information. Progress in utilizing the new generation of satellite sensors will we expect rely increasingly upon better use of ships of opportunity, such as fishing vessels, as these can offer a more comprehensive data collection capacity than dedicated research ships (for some types of data). However, it is vital that a close liaison is maintained with the vessels and that robust data collection strategies are developed.

One of the ultimate tests of whether this project has been successful is in whether industry is utilizing remote sensing information for their operations. In this respect we can claim, from the uptake of SST information by operators, to have been successful with at least those operators who took part in the trials. Our negative findings with respect to regional ocean color are also an important contribution but this was for a limited test and only for large scales. Analyses of finescale results suggest that the conclusion may not hold (as we expect) at small scales especially for bigeye tuna.

Finally, we need to be conscious of history in respect of new technologies whether it be cars, computers, or as we are currently witnessing, the internet. History teaches us there are defined phases in the uptake and application of new technologies and those at the end of what is usually the final phase – management – must come to grips with the implications of the technology as early as possible, especially in respect of the impact of the technology on resources (including the environment).

12. REFERENCES

- Aiken, J., G.F. Moore, C.T. Trees, S.B. Hooker and D.K. Clark. (1995) The SeaWiFS CZCS-Type Pigment Algorithm. SeaWiFS Technical Report Series 29, NASA.
- Allan, R., Lindsay, J. and Parker, D. (1996) El-Nino Southern Oscillation & Climatic Variability. CSIRO Publishing. Collingwood, Australia. 405pp.
- Barbieri, M.A., Yanez, E., Farias, M. and Aguilera, R. (1989) Determination of probable fishing areas for albacore (*Thunnus alalunga*) in Chile's central zone. In Quantitative remote sensing: an economic tool for the nineties, IGARSS '89, Vancouver, BC, Canada. pp. 2447-2450, 10-14 July 1989.
- Barkley, R.A., Neill, W.H. and Gooding, R.M. (1978) Skipjack tuna *Katsuwonus pelamis*, habitat based on temperature and oxygen requirements. *Bull. Fish.* 76: 653-662.
- Borstad, G.A., Brown, R.M., Truax, D., Mulligan, T.R. and Gower, J.F.R. (1982) Remote sensing techniques for fisheries oceanography: examples from British Columbia. *NAFO Sci. Coun. Studies* 4:69-76.
- Breaker, L.C. (1981) The application of satellite remote sensing to west coast fisheries. *J. Mar. Tech. Soc.* 15:32-40.
- Campbell, R. (1999) Long term trends in yellowfin tuna abundance in the South-West Pacific – with an emphasis on the eastern Australian Fishing Zone. Final Report to AFMA. Eastern Tuna & Billfish Management Advisory Committee. Fisheries Research Series. February, 1999. 97pp.
- Campbell, R.A., Polacheck, T. and Ishizuka, Y. (1992) Longline catch rates as indices of abundance of southern bluefin tuna. Unpublished report prepared for the SBT Trilateral Scientific Meeting.
- Campbell, R.A. and Tuck, G. (1996) Spatial and temporal analyses of SBT fine-scale catch and effort data. Working paper presented at the 2nd CCSBT Scientific Meeting held August 26 - September 6, 1996. Hobart, Australia.
- Campbell, R.A., Tuck, G., Tsuji, S. and Nishida, T. (1996) Indices of abundance for SBT from analysis of fine-scale catch and effort data. Working paper presented at the 2nd CCSBT Scientific Meeting held August 26 - September 6, 1996. Hobart, Australia.
- Castillo, J., Barbieri, M.A. and Gonzalez, A. (1996) Relationships between sea surface temperature, salinity, and pelagic fish distribution off northern Chile. *ICES J. Mar. Sci.* 53(2):139-146.
- Caton, A.E. (ed) (1991) Review of aspects of southern bluefin tuna biology, population and fisheries. In: Deriso, R.B. and Bayliff, W.H. (eds.) World meeting on stock assessment of bluefin tunas: strengths and weaknesses. Inter-American tropical tuna commission Special Report No. 7. La Jolla, California.

Caton, A.E. and Williams, K.F. (1996) The Australian 1994-95 and 1995-96 southern bluefin tuna seasons. BRS Working Paper; August 20, 1996. Canberra.

Chekalyuk, A.M., Gorbunov, M.Y. (1994) Diel variability of in vivo chlorophyll fluorescence in near-surface water layer. SPIE Ocean Optics XII, **2258**, 140-151.

Clementson, L.A., Turnbull, A.R., Bonham, P.I. and Parslow, J.S. (1998) Changes in pigment and spectral characteristics of the toxic dinoflagellate *Gymnodinium catenatum* during bloom conditions. SPIE ocean Optics XIV (this volume).

Clementson, L., Parslow, J.C., Griffiths, B., Lyne, V.D., Mackey, D.J., Harris, G.P., Mackenzie, D., Bonham, P., Rathbone, C. and Rintoul, S. Controls on carbon flux in the Australasian section of the Subtropical Convergence. Deep-Sea Research. (in press).

Dickey, T., Granata, J., Marra, J., Langdon, J., Wiggert, J., Chai-Jochner, Z., Hamilton, M., Vazquez, J., Stramska, M., Bridigare, R., Siegel, D. (1993) Seasonal variability of bio-optical and physical properties in the Sargasso Sea. J. Geophys. Res., **98**(C1), 865-898.

Doney, S.C. (1995) Photochemistry, mixing and diurnal cycles in the upper ocean. J. Mar., **53**, 341-369.

Edwards, R.J. (1979) Tasman and Coral Sea ten year mean temperature and salinity fields, 1967-1976. CSIRO Division of Fisheries and Oceanography. Reprint No. 1046. Marine Laboratory, Cronulla, Sydney.

Falkowski, P.G., Kolber, Z. (1995) Variations in chlorophyll fluorescence yields in phytoplankton in the worlds oceans. *Aust. J. Plant Physiol.*, **22**, 341-345.

Fiedler, P.C. and Bernard, H.J. (1987) Tuna aggregation and feeding near fronts observed in satellite imagery. *Cont. Shelf Res.* **7**(8): 871-881.

Fiedler, P.C., Smith, G.B. and Laurs, R.M. (1985) Fisheries applications of satellite data in the eastern North Pacific. *Fish. Rev.* **46**:1-13.

Hampton, J., Lewis, A. and Williams, P. (1999) The western and central Pacific tuna fishery: Overview of the fishery and current status of tuna stocks. Report: Oceanic Fisheries Programme, Secretariat of the Pacific Community. Noumea, New Calendoncia. August, 1999. pp. 19-28.

Hearn, W.S. and Polacheck, T. (1993) Estimating SBT age-at-length relations from the 1960's and 1980/90's. 12th Trilateral Scientific Meeting on SBT. Report No. SBFWS/93/14.

Hitchcock, G.L. (1980) Diel variation in Chlorophyll *a*, carbohydrate and protein content of the marine diatom *Skeletonema costatum*. *Mar. Biol.*, **57**, 271-278.

Humphrey, G.F. (1969) Perspectives of fisheries and oceanographic research in Australia. In: Bulletin of the Japanese Society of Fisheries Oceanography, Special Number (Professor Uda's Commemorative Papers). pp. 43-47.

Hynd, J.S (1968) Sea surface temperature maps as an aid to tuna fishing. *Aust. Fish. News.* **27**(5), 23-29.

-
- Hynd, J.S (1969) Isotherm maps for tuna fishermen. *Aust. Fish.* 28(7), 13-22.
- Hynd, J.S. (1974) An unusual bluefin season for N.S.W. *Aust. Fish. Newsl.* 33(4), 9-11
- Jeffrey, S.W. and Humphrey, G.F. (1975) New spectrophotometric equations for determining chlorophylls a, b, c₁ and c₂ in higher plants, algae and natural phytoplankton. *Biochem. Physiol. Pflanzen*, 167, 191-194.
- Kiefer, D. A. (1973a) Fluorescence properties of natural phytoplankton populations. *Mar. Biol.*, 22, 263-269.
- Kiefer, D. A. (1973b) Chlorophyll *a* fluorescence in marine centric diatoms: responses of chloroplasts to light and nutrient stress. *Mar. Biol.*, 23, 39-46.
- Laurs, R.M., Fiedler, P.C. and Montgomery, D.R. (1984) Albacore tuna catch distributions relative to environmental features observed from satellites. *Deep Sea Res.* 31(9): 1085-1099.
- Laurs, R.M. and Lynn, R. (1977) Seasonal migration of north pacific albacore, *Thunnus alalunga*, into North American coastal waters: distribution, relative abundance, and association with transitional waters. *Fish. Bull.* 75(4): 795-822.
- Le Bouteiller, A, Herbland, A. (1982) Diel variation of chlorophyll *a* as evidenced from a 13-day station in the equatorial Atlantic Ocean. *Ocean. Acta*, 5(4), 433-431.
- Lyne, V.D. (1983) The role of hydrodynamic processes in planktonic productivity. Ph.D. Thesis, Dept. of Civil Eng., Univ., of W.A., 271 pp.
- Lyne, V.D., Scott, R., Gray, R.A. and Bradford, R. (1997) Quantitative Interpretation of Fine-scale Catch-Per-Unit-Effort for Southern Bluefin Tuna off South Eastern Australia Final Report to Fisheries Research Development Corporation. CSIRO Marine Research, Hobart, Australia. 88pp.
- Marra, J. (1997) Analysis of diel variability in chlorophyll fluorescence. *J. Mar.Res.*, 55, 767-784.
- Maul, G.A., Williams, F., Roffer, M. and Sousa, F.M. (1984) Remotely sensed oceanographic patterns and variability of bluefin tuna catch in the gulf of Mexico. *Oceanologica Acta* 7(4): 469-1099.
- Parslow, J.S., Clementson, L.A., Turnbull, A., McKenzie, D. (1998) Bio-optical characteristics of oceans around Australia. *Ocean Optics XIV*, November 1998, Hawaii.
-
- Ramos, A.G., Santiago, J., Sangra, P. and Canton, M. (1996) An application of satellite-derived sea surface temperature data to the skipjack (*Katsuwonus pelamis* Linnaeus, 1758) and albacore tuna (*Thunnus alalunga* Bonaterre, 1788) fisheries in the north-east Atlantic. *Int. J. Remote Sensing* 17(4): 749-759.
- Rathbone, C. and Parslow, J. (1997). Histogram space and time neighborhood filtering technique. (Draft publication).

Rochford, D.J. (1981) Anomalously warm sea surface temperature in the western Tasman Sea, their causes and effects upon the southern bluefin tuna catch, 1966-1977. CSIRO Division of Fisheries and Oceanography. Reprint No. 1249. Cronulla, Sydney.

Rochford, D.J. (1983) Origins of water within warm-core eddies of the western Tasman Sea. *Aust. J. Mar. Freshw. Res.*, 34, 525-34.

Tuck, G., Campbell, R.A., Tsuji, S. and Nishida, T. (1996) Synopsis of southern bluefin tuna data files from Japanese longliners. Information paper presented at the 2nd CCSBT Scientific Meeting held August 26 - September 6, 1996, Hobart, Australia. Paper SBFWS/96/20.

Warashina, Y., Nishikawa, S., Tsuji, S., Ishizuka, Y and Suzuki, Z. (1989) Environmental conditions and formation of longline fishing ground for southern bluefin tuna in the areas off South Africa. *Indo Pacific Tuna Program. V.7. Paper IPTP/89/GEN/17. 143-155.*

Wyrтки, K. (1962) Upwelling in the region between Java and Australia during the southeast monsoon. *Aust. J. Mar. Freshw. Res.*, 13(3), 217-225.

Yamanaka, I. (1978) Oceanography in tuna research. *Rapp. P. -v. Reun. Cons. Int. Explot. Mer*, 173, 203-211.

Young, J.W. and Lyne, V.D. (1993) Ocean conditions affect Tasmanian tuna aggregations. *Australian Fisheries*. 52(6). 24-26.

Young, J.W., Bradford, R.W., Lamb, T.D. and Lyne, V.D. (1996) Biomass of zooplankton and micronekton in the southern bluefin fishing grounds off eastern Tasmania, Australia. *Marine Ecology Progress Series*. 138, 1-14.

APPENDIX A INTELLECTUAL PROPERTY

Intellectual property relating to the generic catch prediction is vested in CSIRO and in principle agreement on this was provided by FRDC (through Mr Alex Wells) and the then ECTUNAMAC. Intellectual property relating to the design, manufacture and operation of the underway system is owned by CSIRO.

APPENDIX B INITIAL LOGSHEET

BEFORE EXTRA CSIRO INFORMATION RECEIVED

Given the information you already have on seawater temperature, weather and market conditions, please indicate:

1. Where you would choose to fish if you were to depart now?

- centre of search area(s) in order of locations to be searched

latitude

longitude

- size or diameter of search area

miles diameter

OR

square miles

2. Expected catch (number of fish per shot).

small

yellowfin

big eye

broad bill

medium

large

3. What market factors have influenced your decision?

AFTER EXTRA CSIRO INFORMATION RECEIVED

Now that you have received the extra information from CSIRO based on ocean color images and historical catches:

4. Will you change where you will steam to?

 yes no

→ go to question 7

centre of search areas
in order of locations

latitude	longitude

size or diameter
of search area

	OR	
miles diameter		square miles

5. Expected catch (number of fish per shot).

small	<input type="text"/>	<input type="text"/>	<input type="text"/>	<input type="text"/>
	yellowfin	big eye	broad bill	
medium	<input type="text"/>	<input type="text"/>	<input type="text"/>	<input type="text"/>
large	<input type="text"/>	<input type="text"/>	<input type="text"/>	<input type="text"/>

6. What are the cost implications of these changes, if any?

7. Have any market factors changed since filling out the form with questions 1-3 or is your decision revision based only on the extra information from CSIRO?

<input type="checkbox"/> yes	<input type="checkbox"/> no	<input type="checkbox"/> yes	<input type="checkbox"/> no
market changes		extra information from CSIRO	

What are the market changes?

APPENDIX C LOGSHEET – VERSION 2

CSIRO Marine Research: East Coast Tuna Fisheries Remote Sensing/Ocean Colour/Fishing Effort Proj

BOAT _____ DATE _____
 SKIPPER _____ PORT OF DEPARTURE _____
 SHOT # FOR TRIP _____

EXPECTED CATCH (number of fish per shot)									
BEFORE	Yellowfin	Big-Eye	Broadbill	Other	AFTER	Yellowfin	Big-Eye	Broadbill	Other
CSIRO DATA					CSIRO DATA				
small					small				
medium					medium				
large					large				
DID YOU CHANGE COURSE AFTER RECEIVING THE CSIRO DATA? YES [] NO []									
FISHING DETAILS					What market factors influenced your decision to fish here?				
	TIME (24h)	POSITION Latitude Longitude		Water Temp (degreesC)	_____ _____ _____ _____				
Start Set									
End Set									
Start Haul									
End Haul									
ACTUAL CATCH DETAILS									
FISH SPECIES	NUMBER	WEIGHT (kg)	COMMENTS ON SIZE/CONDITION etc.						
Yellowfin									
Broadbill									
Big Eye									
Skipjack									
Bluefin									
Albacore									
Marlin									
Striped Marlin									
Swordfish									
Others									

ADDITIONAL INFORMATION

GEAR DETAILS

Mainline Length (km)			
# Beacons set			
# Buoys set			
# Hooks per buoy			
TOTAL # HOOKS			
TOTAL # LIGHTSTICKS			

SEA CONDITIONS

Wind Direction/Speed (kn)			
Current Direction/Speed (kn)			
Sea Direction			
Sea Height (m)			
Moon Phase			
Cloud Cover			/8

	Start	Finish
SALINITY		
FLUORESCENCE		

ANY OTHER COMMENTS? (eg. Water colour/clarity, bird activity, surface fish etc.)

PLEASE FILL ONE SHEET PER SHOT
 Once you have filled out the form, please fax back as soon as possible to:
 CSIRO Marine Laboratories Fax: (03) 62325199 Attention: Kim Woolley or Rosemary Bailey

APPENDIX D FIELD VESSEL STUDIES

Study A:

Alan Pearce et al: Seasonal and cross-shelf variability of physical, chemical, optical and biological properties off Perth, Western Australia: 1996-1998

Study B:

Jock Young et al: A two boat study of the relationship between swordfish and tuna catch rates and fine- and broad-scale physical and environmental variables off eastern Australia

Study A

Seasonal and cross-shelf variability of physical, chemical, optical and biological properties off Perth, Western Australia: 1996-1998

Final Report on the Western Australian phase of Project 94/045 to the Fisheries Research and Development Corporation

(Addendum to “**Development application and evaluation of the use of remote sensing data by Australian fisheries**”, CMR Report MR-C 96/12 by V.Lyne)

Compiled by
Alan Pearce, CSIRO Marine Research, Perth
Mervyn Lynch, School of Physical Sciences, Curtin University, Perth

With contributions from
Matt Boterhoven, School of Physical Sciences, Curtin University
Helen Chedzey, School of Physical Sciences, Curtin University
Jim Davies, School of Physical Sciences, Curtin University
Peter Fearn, School of Physical Sciences, Curtin University
Dan Gaughan, Fisheries WA
Stuart Hellen, Dalcon Environmental, Perth
Brendon McAtee, School of Physical Sciences, Curtin University
Brian Osborne, School of Physical Sciences, Curtin University
Luke Twomey, School of Environmental Biology, Curtin University
Wilma Vincent, School of Environmental Biology, Curtin University

CSIRO Marine Laboratories, Marmion, Western Australia

August 2000

CONTENTS

Section 1: Background	page 1
Section 2: The transect	2
Section 3: Surface temperature and salinity	5
Section 4: Radiometer	15
Section 5: Chlorophyll and nutrients	18
Section 6: Light	44
Section 7: Meteorology	58
Section 8: AVHRR imagery	59
Section 9: SeaWiFS imagery	83
Section 10: Phytoplankton	93
Section 11: Zooplankton	97
Section 12: Solarimeter	102
Section 13: Conclusions and future work	109
Acknowledgements	110
References	111

Section 1: Background (Alan Pearce and Mervyn Lynch)

These field studies formed part of a much larger Fisheries Research and Development Corporation (FRDC) project entitled "Development, application and evaluation of the use of remotely sensed data by Australian fisheries" managed by Dr Vincent Lyne and Dr John Parslow (CSIRO Marine Research, Hobart). The project was scheduled to commence in early 1994, but was delayed for almost 3 years by setbacks in the launch of the new ocean-colour satellite sensor SeaWiFS.

Surface validation studies for the Advanced Very High Resolution Radiometer (AVHRR) and SeaWiFS satellite sensors were undertaken along monthly cross-shelf transects off Hillarys marina (northern Perth metropolitan waters) between October 1996 and December 1998. While the main external funding was provided by FRDC, much personnel and in-kind support has come from CSIRO and Curtin University.

The objectives of the Western Australian field component of the project may be summarised:

- 1) To measure the seasonal and cross-shelf variability of sea-surface temperature (SSTs), bio-optical and biological properties of the near-surface waters across the continental shelf off Hillarys;
- 2) To relate these *in situ* observations to satellite measurements of ocean temperature and bio-optical properties.

The transect measurements have also shown the spatial and temporal variability of the coastal water properties off Perth, strengthening our understanding of demonstrated links between oceanic processes and recruitment to a number of commercial fisheries along the Western Australian coast, notably the western rock lobster (Pearce and Phillips 1994) and some fin-fisheries (Lenanton *et al.* 1991, Caputi *et al.* 1996).

This report documents the sampling and analytical methods used in the project and summarises the main results over the 27-month period, with emphasis on the SST and ocean colour data. Each of the topics is dealt with in a separate section, followed by the diagrams for that section. Some of the ancillary observations are still being analysed and are only briefly discussed here. Many of the measurements were essentially simple and within the constraints of the allotted budget which largely funded for the boat charter and some sample-analysis costs.

The vessel used was the *Lionfish II* chartered from the Perth Diving Academy; the boat is 18 m long, has a cruising speed of 16 knots and a capacity of up to 30 passengers, with an appropriately large deck area ideal for handling the various items of equipment. All of the equipment used was either provided by our institutions or borrowed, and field personnel time was provided by staff from CSIRO Marine Research, Curtin University (including a willing band of students) and Fisheries WA.

Section 2: The transect (Alan Pearce and Mervyn Lynch)

The transect consisted of 9 stations H0 to H40 (Figure 2.1, Table 2.1), extending to 40 km offshore (the numerical suffix denoting the distance from the coast in km). The latitude was selected to ensure safe passage through a gap in the Whitfords Reef system off Hillarys Marina.

Table 2.1: Station positions along the Hillarys transect along latitude 31°49.9'S (31.83°).

Station	Longitude	Nominal Depth (m)
H0	115°43.8'E (115.73°)	6
H5	115°41.0'E (115.68°)	14
H10	115°37.9'E (115.63°)	29
H15	115°34.7'E (115.58°)	36
H20	115°31.6'E (115.53°)	39
H25	115°28.4'E (115.47°)	41
H30	115°25.3'E (115.42°)	45
H35	115°22.1'E (115.37°)	47
H40	115°19.0'E (115.32°)	86

On the outward leg of the transect, both surface and profile measurements were taken at each station. The homeward leg was a continuous run, except for (from March 1997) a repeat stop at H5 for a comparison of the morning and afternoon conditions. On the first two transects in October and November 1996, surface samples were taken at each station but vertical temperature/salinity profiles only at every second station; thereafter, the full suite of measurements was made at each station.

Throughout each trip, ocean surface temperature, conductivity and fluorescence were recorded continuously. The round trip typically took about 5 hours, departing the quayside at 9am local time. Station positions were given by the vessel's GPS and water depths using the depth-sounder.

The relevant satellite daytime overpass times are NOAA-14/AVHRR (1400 to 1600 hours) and SeaWiFS (about noon), so all were either during or within a couple of hours of the transect measurements. While attempts were made to run the surveys on days when the sea was reasonably calm and the skies clear, both personnel and boat commitments necessitated occasional trips in adverse or cloudy conditions. On only one occasion (August 1998) did weather conditions prevent the complete transect to H40 being completed.

The transect dates, instrumentation and measurement details are provided in **Table 2.2**.

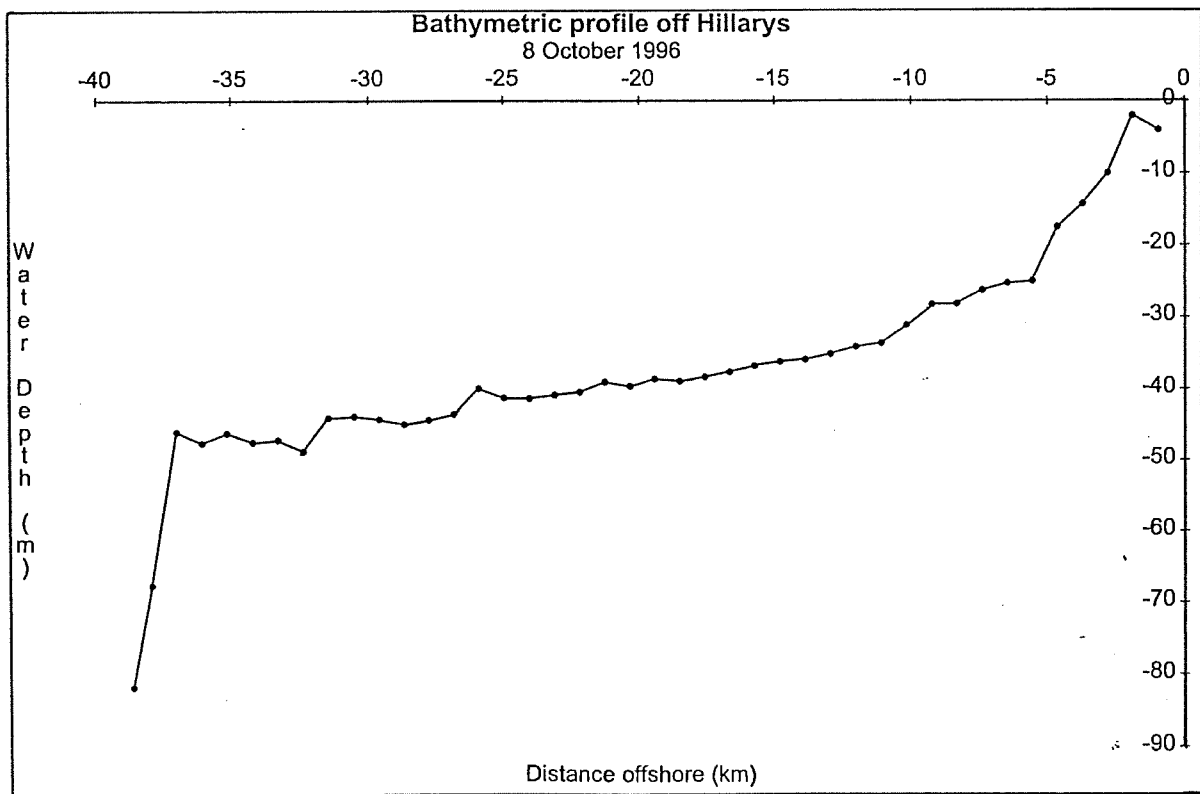
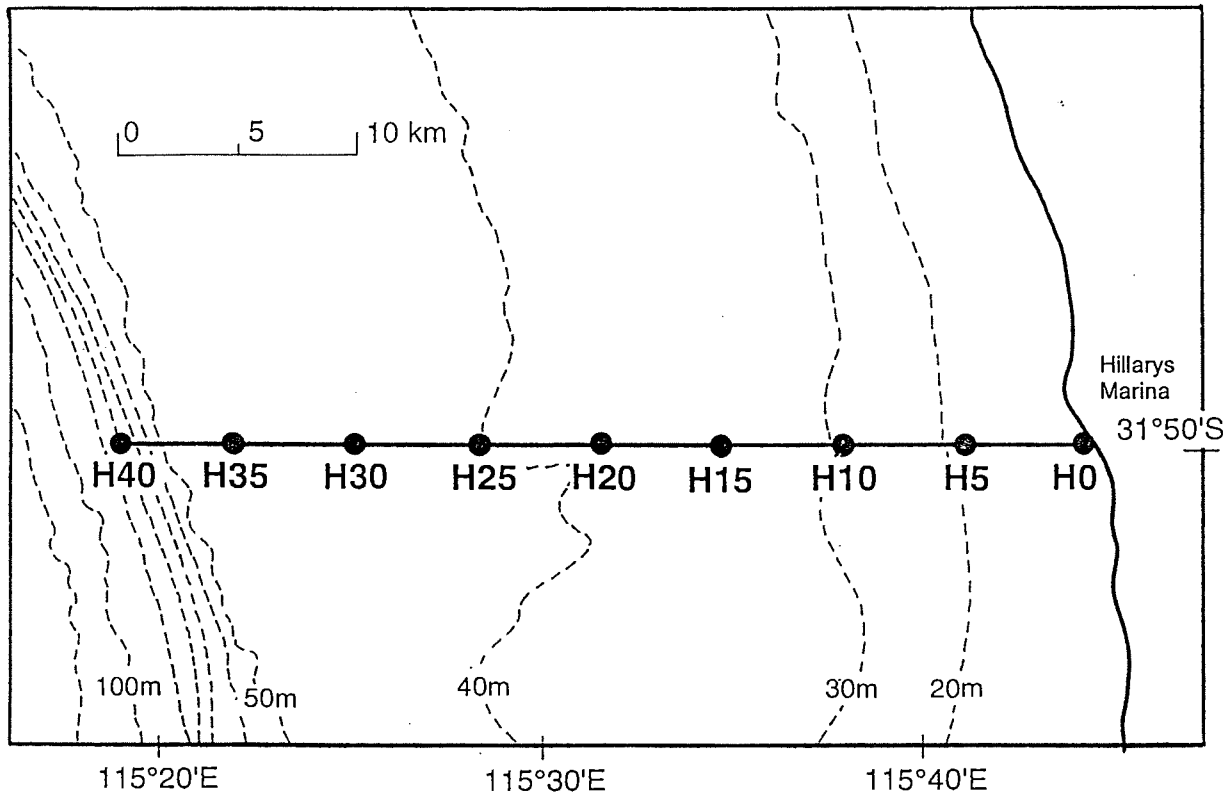


Figure 2.1: (a) Location chart showing the positions of the nine stations along the transect, with a simplified bathymetry (depths in metres) derived from the National Bathymetric Survey Series chart. (b) Bathymetric profile along the transect derived from the vessel's echo-sounder, with readings being taken manually at 1/2 nautical mile intervals.

Date	DayNo	Bucket	SDL	YSI	TASCO SST	Therm- istor	Chl-a	Nutr.	Secchi Depth	LICOR	INF300	Wind	Air Temp.	Phytop.	Zoop.	NOAA AVHRR	Sea- WiFS
8-10-96	96282	Y	Y	Y			Y		Y	Y		Y	Y	Y	Y		
11-11-96	96316	Y	Y	Y	Y		Y			Y		Y	Y	Y	Y	Y	
10-12-96	96345	Y	Y	Y	Y		Y		Y			Y	Y		Y	Y	
13-01-97	97013	Y	Y	Y	Y		Y		Y			Y	Y	Y		Y	
17-02-97	97048	Y	Y	Y/2	Y		Y		Y			Y	Y	Y			
19-03-97	97078	Y	Y	Y	Y		Y		Y			Y	Y	Y	Y	Y	
21-04-97	97111	Y	Y	Y?	Y		Y		Y			Y	Y	Y	Y		
21-05-97	97141	Y	Y		Y		Y		Y	Y		Y	Y	Y	Y?	Y	
16-06-97	97167	Y	Y		Y							Y	Y			Y	
21-07-97	97202	Y	Y	Y	Y		Y		Y	Y		Y	Y	Y	Y	2Y	
20-08-97	97232	Y	Y	Y	Y		Y			Y		Y	Y	Y		Y	
17-09-97	97260	Y	Y	Y	Y		Y	Y		Y		Y	Y	Y	Y	Y	
14-10-97	97283	Y	Y	Y	Y	Y	Y	Y	Y	Y		Y	Y	Y	Y	Y	
18-11-97	97322	Y	Y	Y	Y	Y	Y	Y				Y	Y	Y	Y	Y	
15-12-97	97349	Y	Y	Y	Y		Y	Y		Y		Y	Y	Y	Y	Y	X
19-01-98	98019	Y	Y	Y	Y	Y	Y	Y	Y	Y		Y	Y	Y		2Y	Y
16-02-98	98047	Y		Y	Y	Y	Y	Y	Y	Y		Y	Y	Y	Y	2Y	(Y)
17-03-98	98076	Y	Y	Y	Y	Y	Y	Y	Y	Y		Y	Y	Y	Y	Y	Y
21-04-98	98111	Y	Y	Y	Y	Y	Y	Y	Y	Y		Y	Y			Y	(Y)
19-05-98	98139	Y	Y	Y	Y	Y	Y	Y	Y	Y		Y	Y	Y	Y		(Y)
23-06-98	98174	Y	Y	Y	Y	Y	Y	Y	Y	Y	Y	Y	Y	Y	Y	Y	Y
15-07-98	98196	Y		Y	Y	Y	Y	Y		Y	Y	Y	Y	Y	Y	Y	(Y)
26-08-98	98238	Y	(Y)	Y	Y	Y	Y	Y		Y	Y	Y	Y	Y	Y		(Y)
23-09-98	98266	Y		Y	Y	Y	Y	Y		Y	Y	Y	Y	Y	Y	Y	Y
20-10-98	98293	Y	Y	Y	Y	Y	Y	Y	Y	Y		Y	Y	Y	Y	Y	Y
10-11-98	98314	Y	Y	Y	Y	Y	Y	Y	Y	Y	Y	Y	Y	Y	Y		(Y)
9-12-98	98343	Y	Y	Y	Y		Y	Y	Y	Y	Y	Y	Y	Y	Y	Y	(Y)

Notes: (1) For SeaWiFS X means poor image; (Y) partly clear; Y signifies good clear image
(2) For AVHRR: Y shows cloud-free images over the transect area; 2Y indicates 2 overlapping images on the same day.
(3) In YSI column: Y/2 indicates only one (outward or homeward) leg was obtained
(4) 26-8-98 transect: the survey ended at station H25 because of rough conditions offshore

Section 3: Surface temperature and salinity (Alan Pearce and Brian Osborne)

"Surface" temperature was measured by a number of techniques differing in sensor type, depth of water sampled and sampling frequency. These temperature measurements have been used for validation of satellite-derived sea-surface temperatures (SSTs) from the Advanced Very High Resolution Radiometer (AVHRR) on the NOAA series of satellites, as well as providing the oceanographic background to the optical and biological measurements along the transect. The conductivity/salinity data have not yet been fully analysed so are only briefly dealt with here.

3.1 Data and methods

Underway measurements

Temperature and conductivity (as well as fluorescence -- see Section 5 below) were logged continuously using a YSI-3500 Water Quality Monitor (#94J23550) with Flow-through Cell (model 3550 #94H22278) recording onto a laptop computer at 5-second intervals, together with time and GPS position. With a boat speed of about 16 knots or 8 m/s, this represents an along-track sample about every 40 m. The seawater intake for the deckhose was nominally about 50cm below the water surface, but may have been shallower when the boat "planed". The YSI failed during the first transect in October 1996 (power supply), and instrument problems in early 1997 meant that no underway data are available for April to June of that year. The rated accuracy of the temperature measurements is $\pm 0.2^{\circ}\text{C}$.

The logged underway datafile was split into separate outward and homeward legs, and averages were then computed for 0.001° longitude (nominally 100m) segments to reduce and summarise the data.

On-station surface temperature/salinity

a) "Bucket" temperature

At each station, "bucket" samples were taken using a 15-litre plastic bucket scooping water from the top 30 cm or so, some distance away from the engine cooling-water outlets. The bucket was brought on deck into the shade and the temperature noted immediately using a mercury thermometer graduated to 0.1°C . A salinity sample was then taken by decanting seawater from the bucket into a plastic jug, the glass sample bottle and cap being rinsed three times with this water and the bottle then filled to the base of the neck and stored. Salinities were later measured with an Autolab salinometer in the CSIRO Marmion or Hobart laboratories; rated accuracy is ± 0.003 ppt.

The mercury thermometers were calibrated in a laboratory tank against reference thermometers reading to 0.01°C . The estimated accuracy of the bucket temperatures is $\pm 0.1^{\circ}\text{C}$, with perhaps a similar "error" resulting from possible temperature changes within the bucket between taking the sample and reading the temperatures.

b) "Hard-hat" temperature

Near-surface water temperature were also measured by a YSI model 44032 thermistor housed in a buoyant, modified construction helmet ("hard hat"), supplied to Curtin University by Dr Peter Minnett, RSMAS, University of Miami. The helmet floated upside down so that the thermistor

was kept at a near constant depth of 5 to 10 cm. The cable used as part of the resistance circuit to the boat was buoyed by floats, allowing the helmet to drift 5 to 10 m clear of the vessel. This instrument was first deployed in October 1997.

The thermistor's resistance was measured by a Metrix 55 multimeter and converted to water temperature through a calibration equation based on tabulated temperature-resistance data provided by the thermistor's manufacturer:

$$T = -1.2037 * \log(R)^3 + 23.999 * \log(R)^2 - 196.08 * \log(R) + 529.85$$

where R is the resistance in ohms. While no independent test of the manufacturer's calibration has been performed to date, the hard-hat temperature values generally agreed with the other surface measurements within 0.1° – 0.2°C (some of this difference can be attributed to the different depths and areas sampled by the instruments). Minnett (personal communication) quotes an estimated accuracy for the hard hat thermistor of 0.01 to 0.05°C.

After deployment, the resistance values were measured at 1-minute intervals for four minutes, the range giving information on acclimatisation behaviour and sea surface temperature variability. The thermistor achieved thermal equilibrium with the water within the first two or three minutes of its immersion so the station mean temperature was then derived by averaging the 3- and 4-minute values.

c) Submersible Data Logger

Vertical temperature/salinity profiles were obtained at each station using a Yeokal Submersible Data Logger (SDL; model 606, serial number 66) sampling at 1 second intervals and recording internally onto solid-state memory. The rated temperature accuracy is ±0.1°C, conductivity ±0.02 mmho/cm.

The SDL was lowered into the water by rope from the bow of the vessel and held within the top 50 cm for about a minute to stabilise the sensors and provide good "surface" data. It was then lowered by hand at a speed of about 1 m/s to touch the seabed at all stations (except H40 where the depth was too great), and raised again to the surface. It was held at the surface for a minute before being brought back on board. During the first two transects, profiles were only taken at stations H0, H10, H20, H30 and H40. The SDL failed in February, July and September 1998 and the pressure sensor was unreliable during the August 1998 transect, so the pressure/depth information for those transects was unusable.

The datafiles were examined visually to separate the data into down- and up- profiles, and the 1 m depth-averages computed separately. To allow for any thermal structure within the upper 1m layer, the highest individual temperature in that layer was also noted.

3.2 Results and Discussion

Comparison of methods

Despite the "surface" temperature being sampled by a variety of methods over the 27-month period, there was a very high correlation between the different measurements (**Table 3.1**). Because the bucket temperature was the simplest to carry out, was from a well-identified part of

the water column (top 30 cm) and was the only measurement available for all stations on every transect, it has been selected as the "reference" for this analysis, with the 1m averaged SDL as second choice representative of the top 1m of water.

Table 3.1: Correlation between the various surface temperature measurements. The second column has the 1m averaged temperatures from the SDL while the following column has the highest individual reading from the instrument, presumed to be the temperature nearest the water surface.

	Bucket	SDL (1m)	SDL (max)	YSI	Thermistor
Bucket	1.000	.989	.991	.991	.982
SDL (1m)		1.000	.999	.993	.969
SDL (max)			1.000	.994	.974
YSI				1.000	.981
Thermistor					1.000

The scatter-plot of bucket temperatures against the 1m SDL values (**Figure 3.1a**) indicates that the bucket tended to give higher readings than the SDL as would be anticipated from the shallower layer sampled by the bucket -- this can also be seen in the cross-shelf temperature profiles in **Figure 3.2**. The noticeably higher bucket temperatures were in February, March, August, September and November 1997 (**Figure 3.2a**), and in March, November and December 1998 (**Figure 3.2b**). The highest difference was just over 1°C in December 1996 when the wind speed was less than 2 m/s; using the warmest SDL temperature instead of the 1m averages made little difference. Plotting the Bucket-minus-SDL temperature against wind speed (not shown here) indicated that temperature differences greater than 0.5°C tended to occur when the wind was less than about 5 m/s; above this wind speed, vertical mixing was presumably breaking down much of the stratification in the near-surface layer.

Surface salinity was measured only by the bucket sample and the SDL (the YSI conductivity data have not yet been analysed). The correlation between the two measurements over the full period is 0.976, with the bucket generally giving somewhat lower salinities than the SDL (**Figure 3.1b**); this is probably due to limitations of the SDL conductivity sensor. It is evident from **Figure 3.3** as well that the SDL was generally reading higher than the bucket salinities, but in most cases the cross-shelf structure was faithfully reproduced.

Seasonal and cross-shelf surface temperature variability

The cross-shelf temperature gradient showed a marked seasonal reversal (**Figure 3.2**). In summer, the inshore temperature was higher than that further out because of heating in the shallow nearshore waters; the lower temperatures mid-shelf represented the Capes Current (Pearce and Pattiaratchi 1998) bringing cooler water from the south, and the water then warmed

slightly into the (weak) Leeuwin Current near the shelf-break (January to March of both years -- **Figure 3.2** -- see also the satellite images in **Section 8**).

With heat loss to the atmosphere in autumn and the Capes Current waning, the nearshore waters cooled rapidly while the warm Leeuwin Current maintained relatively high temperatures along the outer shelf, so there was on occasion a 6°C temperature rise between the nearshore waters and the Leeuwin Current (as in June 1998, **Figure 3.2b**). As the water warmed again in spring, this gradient reduced so that by November/ December the summer regime had been restored.

As a consequence of both the inshore heating/cooling cycle and the seasonal strengthening of the Leeuwin Current along the outer shelf, it is clear that the annual temperature cycle was much higher inshore than offshore. By following the markers for station H0 in **Figure 3.2** (*i.e.* the left-hand end of each of the monthly segments), the inshore water was warmest at 23° to 24° in January and coolest at 16° to 17°C in June/July. By contrast, the water near the shelf-break, represented by station H40 at the right-hand end of each monthly segment, reached its peak of 23°C only by March/April/May as the Leeuwin Current strengthened, and fell to about 20°C in August/September.

The salinity transects (**Figure 3.3**) present a similar picture, with most of the variability occurring near the coast. In summer the coastal water had a high salinity well exceeding 36 ppt because of evaporation, so there was a pronounced gradient with the salinity falling offshore. By late winter and autumn, the inshore salinity had dropped to about 35.3 ppt due to precipitation and runoff in the wet winter months, with an anomalously low measurement of 35.0 ppt at H0 in September 1997 (there had been no local rainfall for a week, so the reason for this is not clear ... possibly a pulse of Swan River water drifting northwards?). At H40, on the other hand, summer and winter salinities were respectively about 35.7 to 35.9 ppt and 35.5 ppt, with relatively little seasonal variation.

The surface T/S plot (**Figure 3.4**) shows that the bulk of the shelf water was in the temperature and salinity ranges of 17° to 23°C and 35.4 to 36.2 ppt respectively. Higher salinities were due to inshore evaporation in summer, and the lowest temperatures (with matching low salinities) were again near the coast in winter.

Vertical thermal structure

The SDL temperature and salinity profiles are not presented in detail here. There were on occasion large temperature differentials between the surface and bottom SDL measurements (**Figure 3.5**), many of these being from surface warming during the summer months. Sometimes, however, the inshore and offshore waters were both well-mixed vertically and there was a strong thermocline of 2 to 3° at the mid-shelf stations, suggesting upwelling due to flow curvature around Rottneest Island in the wake of the Capes Current, as found by Alaei *et al.* (1998).

3.3 Conclusions

Despite the different types of measurements coupled with the presumed small-scale surface temperature variability, agreement between the results from the different temperature sensors was reasonably good. In the shallow near-coast waters, air-sea heating and cooling dominate the temperature, while the Leeuwin Current modulates the temperatures near the shelf-break some 40 km offshore (**Figure 2.1**); the annual temperature cycle near the coast (7 to 8°C) is therefore much larger than that offshore (about 3°C).

There is also a well-defined salinity pattern. The nearshore salinity rises sharply in summer due to evaporation, so that the annual salinity change near the coast is almost 1 ppt compared with about 0.3 ppt at the shelf-break.

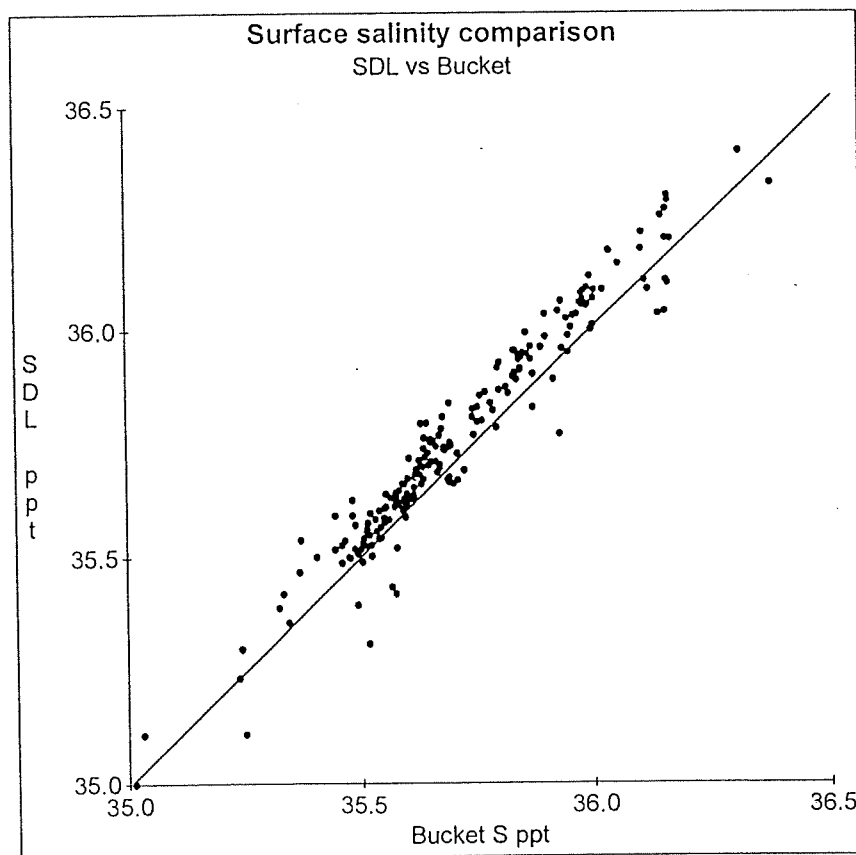
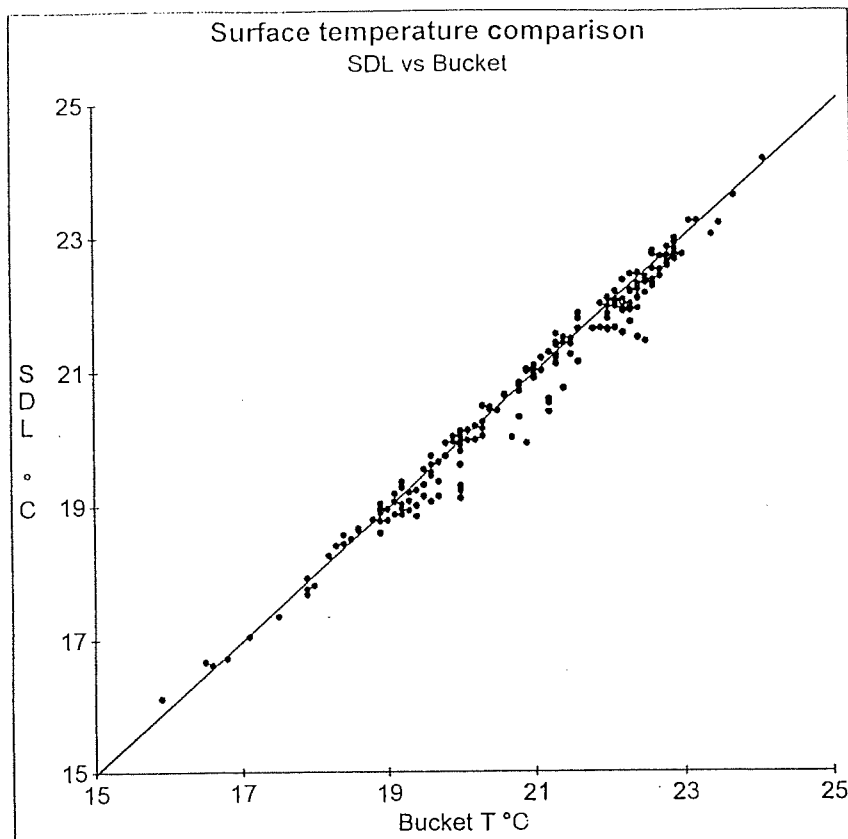


Figure 3.1: Scatterplots of (a - top) bucket SST vs SDL 1-m averaged temperature and (b - bottom) bucket salinity vs SDL 1-m averaged salinity for all 27 transects.

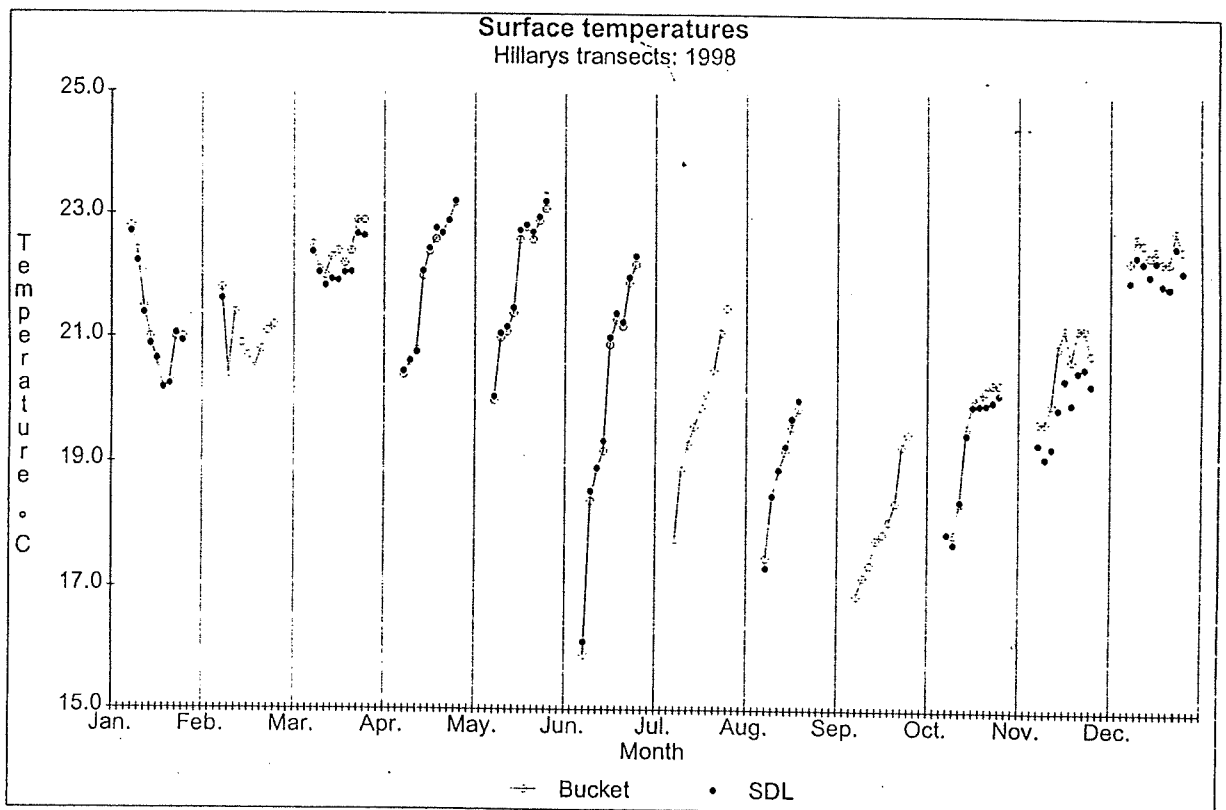
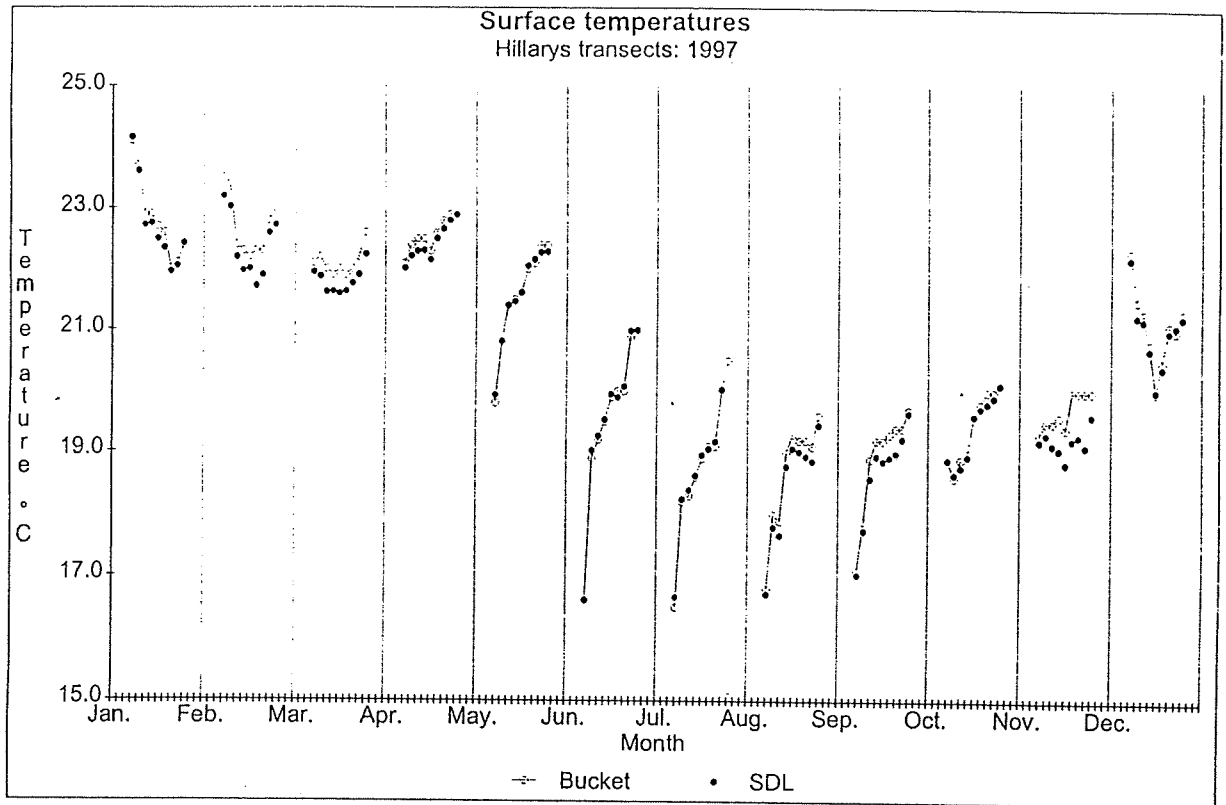


Figure 3.2: Cross-shelf surface temperature transects for (a - top) 1997 and (b - bottom) 1998 using the bucket (joined open circles) and SDL 1m averages (closed circles). Each segment represents a monthly transect, and the stations are along the segment with H0 (inshore) on the left and H40 (offshore) on the right.

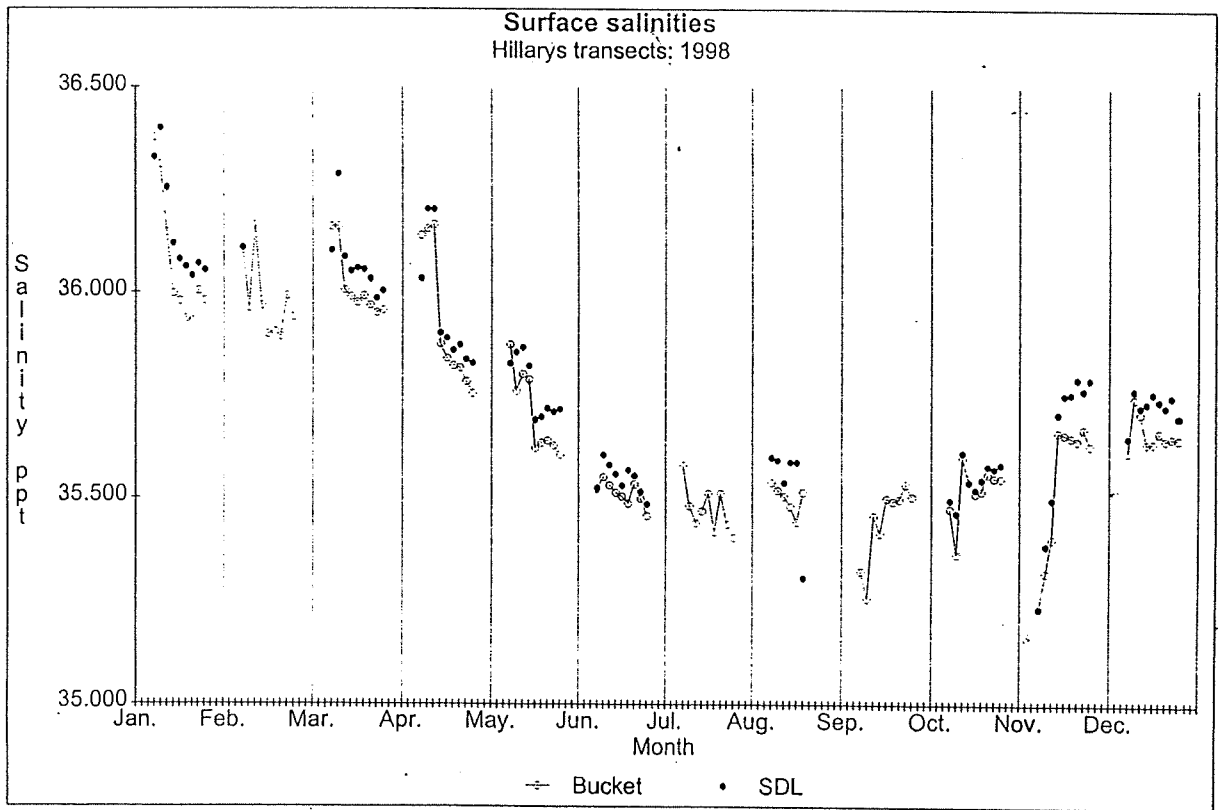
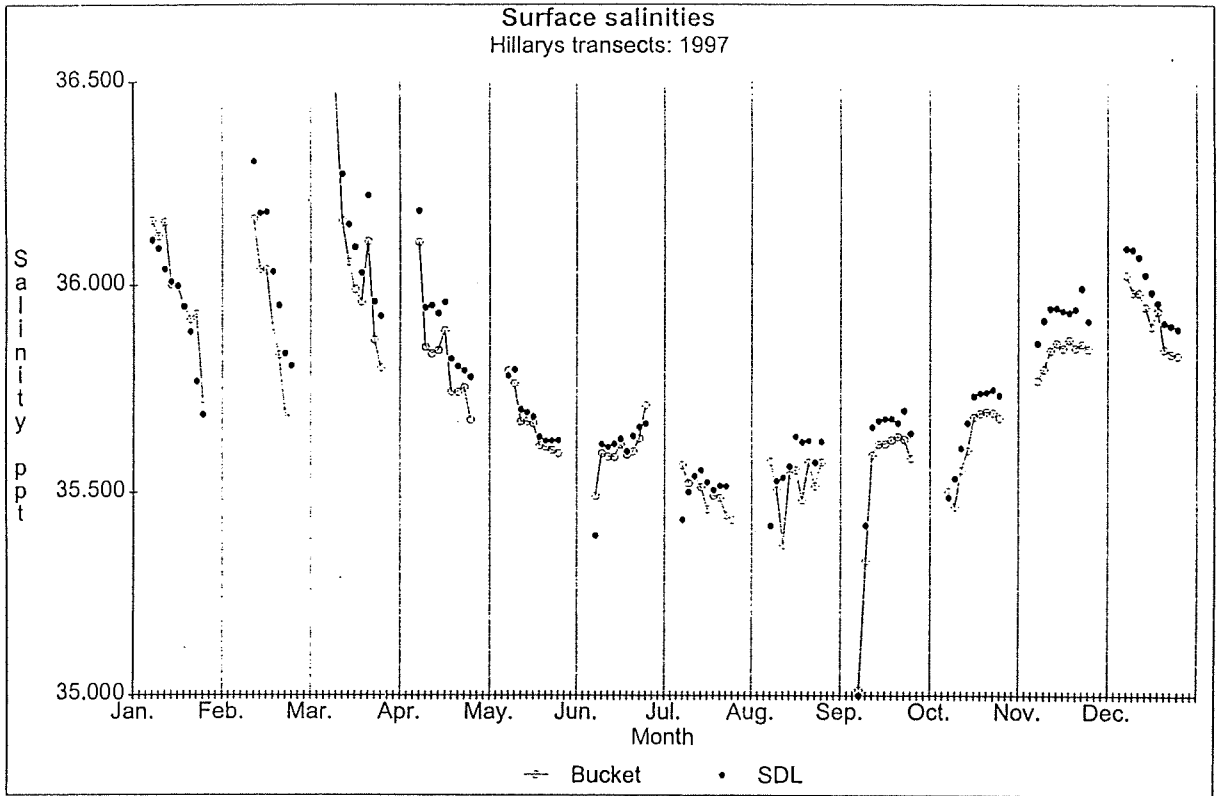


Figure 3.3: Cross-shelf surface salinity transects for (a - top) 1997 and (b - bottom) 1998 using the bucket (joined open circles) and SDL 1m averages (closed circles). Each segment represents a monthly transect, and the stations are along the segment with H0 (inshore) on the left and H40 (offshore) on the right.

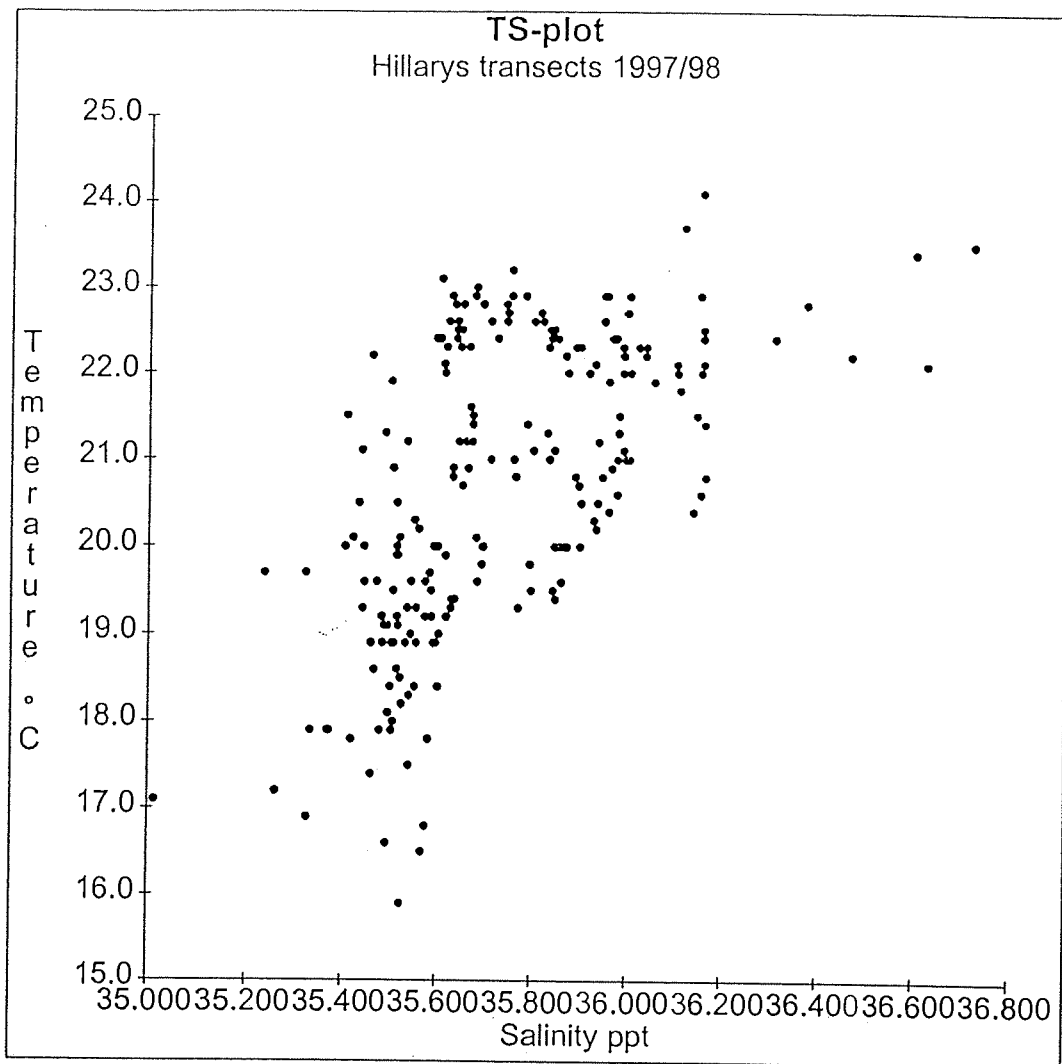


Figure 3.4: T/S scatterplot of the surface waters between October 1996 and December 1998.

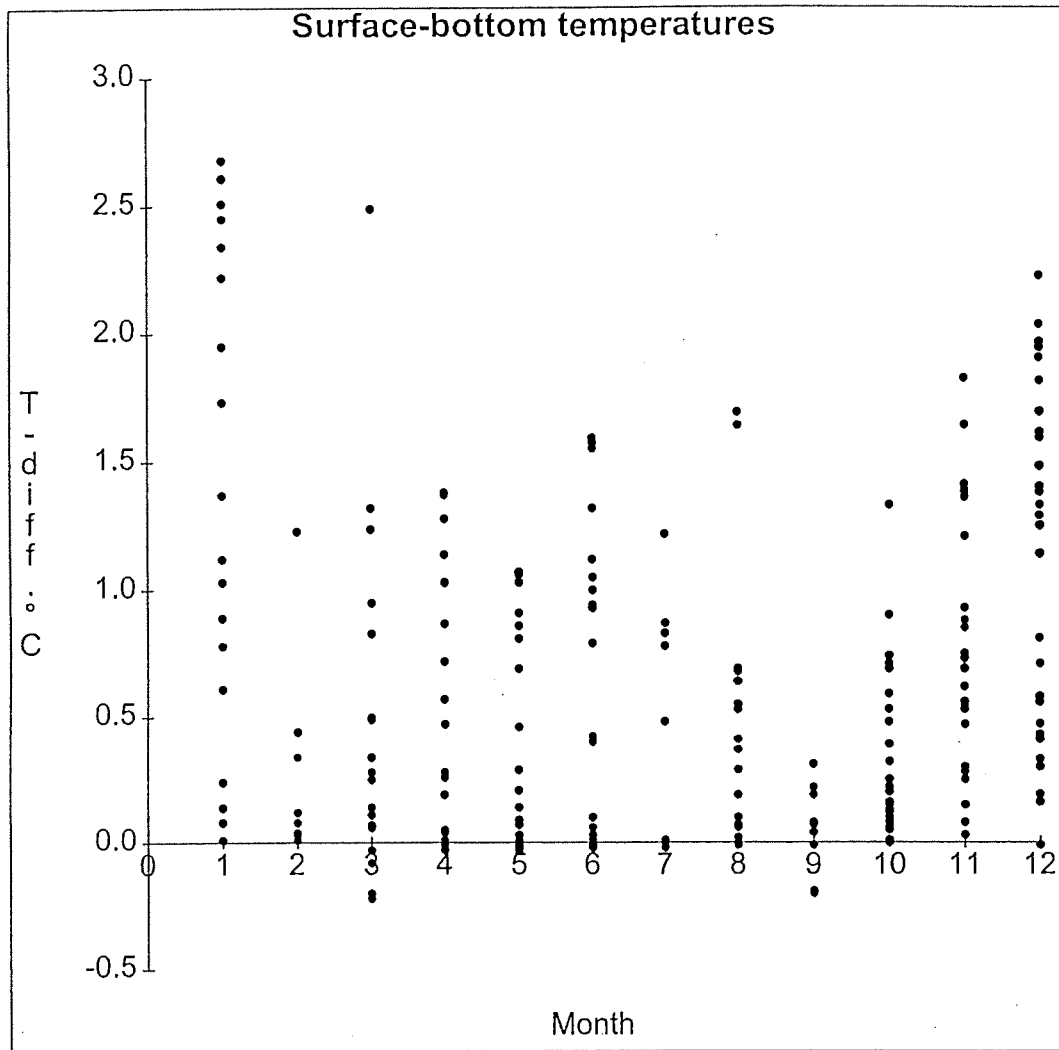


Figure 3.5: Vertical temperature differences between the water surface and seabed, derived from the SDL 1 m averages, plotted against the month (1 to 12).

Section 4: Radiometer (Brendon McAtee, Alan Pearce, Matt Boterhoven, Jim Davies, Mervyn Lynch)

During the Hillarys transects, "skin" sea-surface temperatures were measured from the boat using a hand-held thermal radiometer, to sample the micro-layer which emits the thermal radiation received by satellite thermal infrared sensors. Because of radiative cooling processes, the skin temperature is typically a few tenths of the degree cooler than the "bulk" layer below, which is sampled by the other techniques such as the bucket. The quality of the measurements improved during the surveys through the introduction of (and subsequent refinements to) a black-cone calibration instrument in January 1998 (McAtee 1999b).

4.1 Instrumentation and methods

The TASCOR radiometer (Model THI-500, Serial Number 526191, probe 428108) used during the surveys is a hand-held instrument with a temperature range of -50° to 500°C , a nominal accuracy of $\pm 2^{\circ}\text{C}$ (between 0° and 200°C) and a repeatability of $\pm 0.5^{\circ}\text{C}$. There is a temperature drift of $\pm 0.1^{\circ}\text{C}$ per degree, although the rate of change of ambient temperature also appears to have an effect. The wavelength sampled is 8 to $12\mu\text{m}$, and the angular field of view corresponds to about 60 cm at the sea surface from a typical viewing position (at 45°) on the aft deck of the boat.

The radiometric and bulk temperature measurements were recorded using several different techniques to compare the skin and bulk temperature measurements. After some initial experimentation, the following sequence of SST measurements was settled on for each station (McAtee 1999a):

(i) As the vessel stopped, the TASCOR radiometer was used to measure the temperature of the wake of the vessel in order to provide a radiometric estimate of the bulk temperature of the ocean. Initial comparisons between this "wake" reading and the subsequent SST measurement (see (iii) below), showed very little difference between the two temperatures. SSTs measured from the bow of the boat were also very similar to the wake temperature measurement.

(ii) The "hard-hat" thermistor (described in **Section 3**) was then deployed from the stern of the boat. Resistance measurement readings were taken and converted to an ocean temperature via a regression equation at each minute over a four minute period. The ocean temperature assigned for the station was then recorded as the average of the temperatures measured at 3 and 4 minutes.

(iii) An SST measurement using the radiometer was then made directed at 45 degrees below the horizontal, followed by a sky temperature reading with the radiometer directed 45 degrees above the horizontal. The sky temperature was used to correct the measured SST for sky radiance.

(iv) A bucket sample was collected (see **Section 3**) and the skin temperature was measured using the radiometer. The water in the bucket was then agitated in order to destroy the skin layer and another radiometric estimate (now assumed to be the bulk temperature of the bucket

sample) was taken. At the same time, a mercury thermometer was used to measure the bulk temperature.

(v) Finally, the temperature of the blackbody calibration unit (first used in December 1997) was measured both by the radiometer and a mercury thermometer, these measurements being later used to calibrate the radiometric data set for the day.

Ignoring the first two transects when the results were very erratic, radiometric measurements were made in all months except for February, March, April and December 1997, and the August 1998 transect was cut short due to bad weather.

4.2 Results and discussion

The suite of measurements taken at each station encompassed both the skin temperature using the radiometer and the bulk temperature measured by several different methods; for reasons given earlier, the bucket temperature is taken to be the most consistent and reliable technique for present purposes.

Graphs of all the individual transect plots are presented in McAtee (1999a). Examination of the differences between the radiometer (skin) temperatures and the various bulk temperature estimates does not consistently show the expected small cooling of the thin surface skin. About 30% of the skin-minus-bulk (bucket) differences were in the expected range of 0° to -0.5°C, but an equal proportion showed the skin temperature warmer than the bulk by that amount. Over 20% had the skin temperature unrealistically (?) cool by more than 1°C, even exceeding 2°C on 4% of occasions. It appears therefore that the present techniques of radiometer and/or bulk temperature measurements are probably inadequate for reliably deriving the skin-bulk temperature difference. McAtee (1999a) estimated that the theoretical uncertainty of the radiometer measurements for 1998 (with the specified calibration procedures) was between 0.5° and 0.9°C.

The problem of skin-bulk temperature measurements would therefore seem to lie in:

- 1) Natural small-scale patchiness of the water around the boat; the radiometer, bucket and hard-hat measurements were all made from different parts of the boat and at different times.
- 2) The non-uniform nature of the sea surface, which is constantly varying due to waves (on a variety of scales from capillary waves to wind-waves and large swell), sun-glint, spray, and the irregular breaking down of the water skin by small-scale variability in the wind. These factors are, of course, also encountered by radiometer measurements from the satellite but would be averaged out over the larger viewing area (pixel size of a square kilometre).
- 3) Inherent inaccuracies in the various methods of bulk temperature measurement. The hard-hat thermistor should potentially provide the best estimate because of the fixed depth below the surface, the proximity to the water surface (about 5 cm), the accuracy of the calibrated thermistor, and the continuous sampling over a few minutes. However McAtee (1999a) concluded that the generally close agreement between the bucket and hard-hat temperatures provided some confidence in both these measurements.

4.3 Conclusion

The SST datasets gathered during the surveys have indicated that the present techniques have probably been of insufficient precision to reliably determine the true ocean skin temperature and thus also the skin-minus-bulk temperature difference. The results will be re-examined in more detail to try and resolve some of the discrepancies. For future fieldwork, it is recommended that the radiometer readings be taken viewing the same water surface and at the same time as the hard-hat measurements are made, and preferably noting a sequence of readings of both instruments rather than a single spot measurement. The radiometer calibration procedures outlined by McAtee (1999b) should also be followed.

Section 5: Chlorophyll and Nutrients (Peter Fearn, Alan Pearce, Luke Twomey and Merv Lynch)

Chlorophyll is one of the primary products of satellite ocean colour sensors, being an indication of the phytoplankton density and distribution and hence indirectly the biological productivity of the ocean. It is also the first biological quantity to be measurable by satellite remote sensing. In addition to sampling for chlorophyll, we have taken the opportunity to measure the basic nutrients (nitrate, silicate and phosphate) to assist in understanding some of the biochemical processes operating across the continental shelf off Perth. This summary will focus on the chlorophyll data.

5.1 Data and methods

Water samples for chlorophyll and nutrient analyses were taken at each station, and fluorescence was recorded underway along both the outward and homeward legs of each transect.

Underway measurements

The underway sampling system, described above in **Section 3**, includes a fluorometer which logged underway fluorescence from a depth of about 50 cm onto a laptop computer at 2-second intervals. Initially, a Turner Designs Field Fluorometer Model 10 (no serial number evident) was used, but in December 1997 this was replaced by a Wet Labs Wetstar Fluorometer (WS3S-342P serial # 9710004).

As described in **Section 3**, the outward and homeward transect records were separated. During the last 4 surveys (September to December 1998), vertical fluorescence profiles were taken at station H25 (only) by passing the water from the vertical-pump hose through the onboard fluorometer, and assuming a constant rate of lowering vs depth. At each station, the YSI fluorescence reading was noted at about the time that the pumped sample (see below) was taken, and a regression relationship derived for converting the logged fluorescence values could be converted to chlorophyll concentrations. It was noticed that, on occasion, there was a "spike" in the fluorescence as the boat stopped on station -- the reason for this is not presently clear. Initially, all the pumps, filters, etc were separate entities, but an instrument box was constructed in September 1997 which greatly facilitated both handling and setting-up of the equipment on each transect. The fluorescence and conductivity sensors were both thoroughly flushed with clean water after each transect.

On-station chlorophyll samples

Using a pump and hose system, 4 to 5 litre samples were collected from a vertical haul of the hose over the upper 18 m of the water column (7.5 m at H0), yielding vertically-integrated samples from which chlorophyll and nutrient samples were taken. Chlorophyll samples were extracted from 1 to 2 (and later 5-litre) volumes of the integrated sample using GFC filters (47mm diam, 0.45µm) which were stored in test-tubes in the dark and chilled.

Back at the laboratory, each GFC filter was placed in a 10 ml test-tube, and 8 ml of a 90% acetone solution added. The sample was then sonicated for 10 minutes in an ultrasonic bath to break down the cells, and stored in a freezer overnight. The sample was filtered again through a GFC filter into a clean 10 ml test-tube.

These samples were analysed using both a Varian DMS-90 UV/VIS spectrophotometer (serial # 1311105) and the Turner fluorometer described above. A 90% acetone solution was initially used in both the reference and sample cuvettes on the spectrophotometer; the absorbance was read and the machine zeroed at each wavelength. Each chlorophyll sample was then inserted into the sample cuvette in the spectrophotometer and the concentrations read at 480, 510, 630, 647, 664 and 750 nm wavelengths. Each sample was then returned to its test-tube for fluorometer analysis. Periodically (after 10-15 samples), the 90% acetone sample was again placed in the sample cuvette and the "blank" reading noted.

After the spectrophotometer analyses, the test-tube samples were also read on the Turners Fluorometer to give the fluorescence, 3 drops of 1-normal hydrochloric acid added (to separate the chlorophyll from the other pigments) and the samples were read again.

The chlorophyll concentrations were derived as follows:

- 1) The raw spectrophotometer readings at wavelengths 750, 664, 647, 630, 510, 480 nm were corrected by subtracting the average of the starting and ending blank readings.
- 2) A proportionality factor F1 was computed as the ratio of the volume extracted (ml) to the filtered volume (litres).
- 3) Chlorophyll-*a* = $(11.85 * (R664-R750) - 1.54 * (R647-R750) - 0.08 * (R630-R750)) * F1$
- 4) Chlorophyll-*b* = $(21.03 * (R647-R750) - 5.43 * (R664-R750) - 2.66 * (R630-R750)) * F1$
- 5) Chlorophyll-*c* = $(24.52 * (R630-R750) - 1.67 * (R664-R750) - 7.60 * (R647-R750)) * F1$
- 6) Carotenoids = $(7.6 * (R480-R750) - 1.49 * (R510-R750)) * F1$
- 7) Total chlorophyll was the sum of Chlor-*a* + Chlor-*b* + Chlor-*c*.
- 8) Using the fluorescence method, the chlorophyll concentration was calculated by the difference between the fluorescences (corrected for the blank readings) before and after the addition of the acid:

It is suspected that the December 1996 & January 1997 chlorophyll data may be poor due to unreliable blanks in the spectrophotometer. When the instrument was serviced after the May 1997 transect, it was found that the light source lamp had deteriorated and left deposits in the quartz envelope. The large drift in the blank readings in December 1996 and January 1997 may have been due to these deposits; after this initial depositing, the lamp may have stabilized and then appeared to be functioning normally.

INF300 Profiler

The natural fluorescence of phytoplankton may be used to derive the vertical chlorophyll concentration profile (Chamberlin *et al.* 1990, Chamberlin & Marra 1992) and hence estimate the phytoplankton load in the ocean. The Biospherical INF300 instrument (serial # 9517) measures

depth, scalar PAR (photosynthetically active radiation) and upwelling radiance at wavelengths greater than 650 nm, 683 nm being the peak emission wavelength for chlorophyll a. The instrument's sampling rate is one measurement (or suite of different measurements) per second. It was kindly loaned by the Australian Institute of Marine Science, and was first used in June 1998. The instrument was calibrated annually by the manufacturer.

The INF300 was lowered into the water on the sunny side of the boat. The rate of lowering or raising the instrument is believed to have a significant effect on the accuracy of the measurements, and the generally accepted practice is a lowering rate of no more than 1 m/s. The Ocean Optics Protocols for SeaWiFS Validation (Mueller & Austin 1995) suggest that the speed at which the instrument is lowered or raised through the water column should yield at least two, preferably six to eight, samples per metre. There can be a significant difference between the results derived from measurements made during the downcast and upcast of the instrument, as evident in the chlorophyll profile for station H0 on 23rd June 1998 (**Figure 5.1a**) producing an offset of up to 0.4 mg m⁻³ in chlorophyll concentration in this case. We found that lowering the instrument to predetermined depths, typically every 1 or 2 m, and holding the instrument at each depth for a period of around 20 seconds allowed the instrument to stabilize and additionally permitted averaging of properties at that depth. The instrument was lowered to near the sea floor, or to a maximum depth of about 50m, the length of the deployment cable. Once the instrument had reached its maximum depth it was raised quickly to the surface.

Figure 5.1b shows the chlorophyll profile for the same station and data as **Figure 5.1(a)**, where the spread of points within each cluster may be used to estimate the uncertainty in chlorophyll concentration. We also found that lowering the instrument much slower than about 1 m/s helped to provide a reasonable average measurement at each depth. **Figure 5.2** shows the INF chlorophyll and temperature profiles for station H35 on 23rd September 1998. The reason for the abrupt increase in chlorophyll concentration near 50 m in **Figure 5.2a** is unclear -- the instrument was close to the sea floor so it may have been detecting reflectance from sea grass, or perhaps the instrument was tilting due to drift and therefore detecting a change in radiance and/or PAR irradiance.

Nutrients

Using the vertically-integrating pump sampler described above, 4 to 5 litre samples were collected from a vertical haul of the hose from the upper 18 m of the water column (7.5 m at H0). A 10 ml water sample was extracted using a syringe, filtered through GFC (glass-fibre) filters to remove particulates, and then injected into two sample tubes which were chilled in an ice-filled Esky (until the July 1997 transect, when they were frozen to -86°C). From the February 1998 transect, replicate nutrient samples were taken at each station.

Back at the Laboratory, the samples were frozen and later analysed for nitrate, silicate and phosphate concentrations on a Technicon AutoAnalyser II in the Marmion Laboratory (September 1997 to January 1998 transects) and in the Hobart CSIRO Marine Research Laboratories

(February to December 1998). The first batches of samples prior to September 1997 were unfortunately lost due to poor storage and handling procedures. Replicate samples were taken from February 1998. The detection limits were 0.03 μM for nitrate and phosphate and 0.07 μM for silicate.

5.2 Results and Discussion

Chlorophyll concentrations off Hillarys were highly variable in both space and time (**Figure 5.3**). On the open continental shelf (say from station H10 onwards), chlorophyll levels were typically 0.1 to 0.2 $\mu\text{g/l}$ in summer, increasing by a factor of 2 to 4 in winter. Concentrations near the coast were clearly higher in all seasons, often exceeding 0.5 $\mu\text{g/l}$ at the first two stations H0 and H5, and exceeding 1 $\mu\text{g/l}$ in October 1997 and June 1998; the highest values recorded were about 2.5 $\mu\text{g/l}$ at H0 in June 1998.

Helleren and Pearce (in prep.) analysed the relationship between the fluorometric and spectrophotometric methods using the Hillarys data from October 1996 to June 1998, finding a high correlation of 0.92 between the two techniques (**Figure 5.4**). Averaging over each calendar month along the whole 9-station transect shows a clear annual cycle (**Figure 5.5a**), with highest concentrations between May and September and a distinct peak in June due to the very high values at H0 in June 1998. Examining the cross-shelf variability in more detail, the raised chlorophyll levels at the coastal station H0 are evident throughout the year, but there was also an interesting increase in chlorophyll at the midshelf stations H20 to H30 especially during winter (**Figure 5.5b**) -- the reason for this is unclear at present, but is unlikely to be related to the summer upwelling in the wake of Rottnest Island discussed above.

Vertical chlorophyll profiles were measured using the INF instrument; the complete set of chlorophyll and temperature data are presented in Fearn (1999). The average chlorophyll concentration for each profile for all depths below 2 m has been calculated, with no attempt to bin the data into separate depths. It is assumed that the rate of lowering the instrument was uniform.

The average chlorophyll concentration values are shown plotted in **Figures 5.6 to 5.13**, together with the spectrophotometrically- and fluorometrically-derived chlorophylls and the SeaWiFS chlorophyll concentrations. The NASA specified accuracy for the standard SeaWiFS Case I water chlorophyll product is $\pm 35\%$. The best dates to show comparisons between SeaWiFS and *in situ* chlorophyll measurements are those where the SEADAS quality control flags are 0 for the deep water stations. Error bars have been displayed on the plots corresponding to these dates.

It is clear that for the nearshore waters the chlorophyll concentration has not been determined accurately by the SeaWiFS sensor and associated processing algorithm. This is to be expected as some of the water-leaving radiance signal may have been due to reflectance from the shallow sea floor, and the standard SEADAS chlorophyll concentration processing algorithm does not take shallow water effects into account. It may also have been due to the presence of optical constituents other than phytoplankton and associated detritus, making the nearshore waters Case

II, which are more optically complex and therefore standard products (such as chlorophyll concentration) cannot be obtained using the same processing schemes as in simpler Case I, open ocean waters. The distance from shore at which this abrupt change in SeaWiFS measured chlorophyll concentration occurred seems to differ on different transect dates. For example, results of the 15th July 1998 indicate that the SeaWiFS product was the same as the in-situ chlorophyll products by the 5 km station. However, results from dates such as 10th November 1998 and 21st April 1998 show the abrupt change in the SeaWiFS chlorophyll product occurring close to the 15 km station.

The NASA specified accuracy for the standard SeaWiFS case I water chlorophyll product is 35 %. The best dates to show comparisons between SeaWiFS and in-situ chlorophyll measurements are those where the SEADAS quality control flags are 0 for the deep water stations. Error bars have been displayed on the plots corresponding to these dates.

19th January 1998 - The fluorescence measurements compared very well to the SeaWiFS data, and the spectrophotometrically measured chlorophyll compared well at most stations. The SeaWiFS product was higher than the others for most stations.

17th March 1998 - The fluorescence measurements were closest to the SeaWiFS estimates, but both the fluorescence and spectrophotometer data were within the 35% limits.

19th May 1998 - The spectrophotometer values compared best with SeaWiFS.

15th July 1998 - The SeaWiFS values were the lowest at most stations. The spectrophotometer values were closest to SeaWiFS, but the fluorometer values were above the 35% limits. The INF300 values tended to be lower than all other chlorophyll concentration values: the only INF300 value within the 35% limits was at the 40 km station.

26th August 1998 - There were no *in situ* data for the deep water stations as the seas were too rough for sampling.

23rd September 1998 - Both the fluorometer and spectrophotometer values compared well to the SeaWiFS values. The INF300 measured chlorophyll values were much smaller.

20th October 1998 - The spectrophotometer values were closest to the SeaWiFS values; the fluorometer values were above the 35% limits and the SeaWiFS values were the lowest at most stations.

All data corresponding to dates and stations where SEADAS quality control flags were equal to zero were extracted from the data base and analyzed. Comparing the fluorometer and spectrophotometer data for only those stations where the SEADAS flags were zero shows a strong correlation of 0.94 (**Figure 5.14**). When the SeaWiFS data are compared to the fluorometer (**Figure 5.15**) and spectrophotometer data (**Figure 5.16**) in turn, there is less correlation evident. The limits of $\pm 35\%$ of the SeaWiFS chlorophyll values are indicated by dashed lines; data points falling outside these lines may be considered to not support the ground truthing exercise. If, however, one includes uncertainties of 10% for the *in situ* data then some of the near outliers may be included to support the SeaWiFS chlorophyll product validation.

The INF300 was only available for part of the transect program. There were enough measurements made however to indicate that it was producing chlorophyll concentration values lower on average than the other three sources. The instrument was re-calibrated in March 1998, however this does not seem to have changed the relative difference between the INF300 chlorophyll values and the other *in situ* measurements. Nevertheless, the INF300 however should provide the best vertical resolution within the water column in terms of chlorophyll measurements. It may be possible to use the *in situ* measurements to rescale/calibrate the INF300 measurements and thus produce more accurate chlorophyll profiles.

The depth-averaged nutrient concentrations are not discussed here in any detail; like the chlorophylls, they were highly variable (**Figure 5.17**). In line with some previous work in Marmion Lagoon (Pearce *et al.* 1985), nitrate concentrations displayed a seasonal pattern with highest values (and greatest variability) during the winter months. On some occasions the concentration was highest near the coast (especially the very high peak in June 1998 -- **Figure 5.17b**, which coincided with the chlorophyll peak in **Figure 5.3b**), but at other times (e.g. April and May 1998) the offshore nitrate concentrations were higher. Apart from isolated peaks, the concentrations across the shelf were less than 0.5µM; many were below the detection limit of 0.03µM.

Silicate concentrations were also variable and showed a winter maximum (**Figure 5.18**), with offshore waters having generally higher silicate levels than the nearshore waters. There was little seasonal variation in phosphorus (**Figure 5.19**); concentrations were about 0.10 µM except for elevated levels at the coast in May, June, August and October 1998. It appears that the samples analysed at Marmion (pre-February 1998) were appreciably higher than those after that date which were processed in Hobart, and the reason for this is still being followed-up.

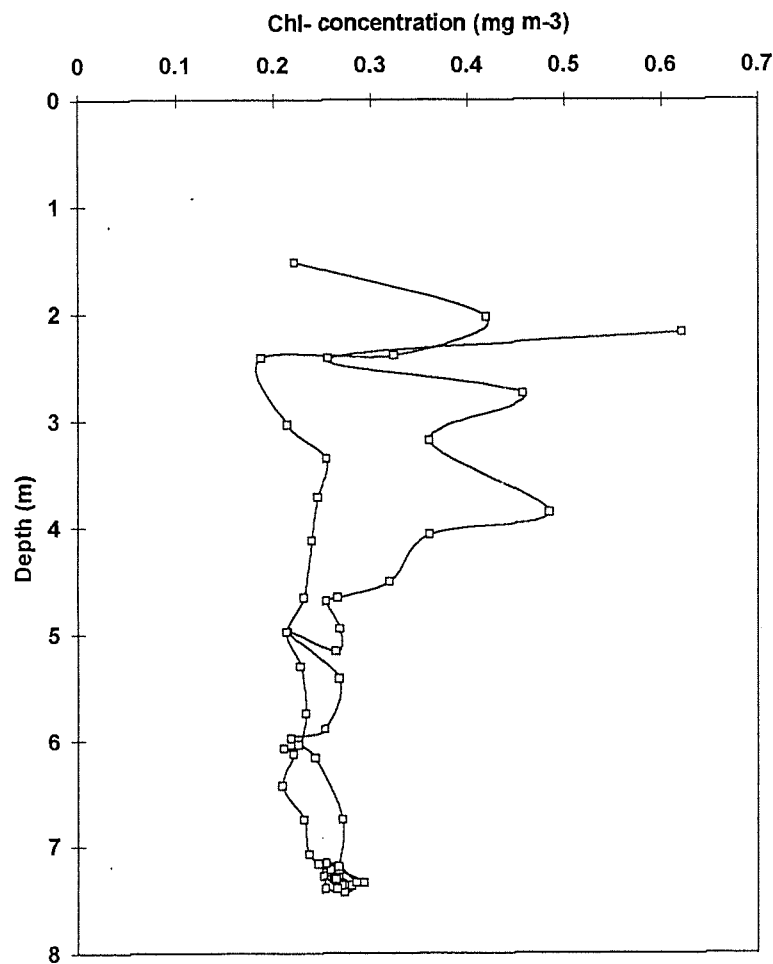
5.3 Conclusions

Although there were differences between the *in situ* (spectrophotometrically- and fluorometrically-derived) chlorophylls, the INF300 measurements and the SeaWiFS chlorophyll concentrations, for most transects they all tended to display similar cross-shelf patterns. This is encouraging, although the uncertainty in the SeaWiFS data was at times rather large when compared to the *in situ* measurements and there is a need to investigate reasons for the differences. The standard SEADAS algorithms are designed to produce chlorophyll concentrations in open ocean (*i.e.* Case I waters) and one would not expect the "standard" SEADAS chlorophyll product always to be accurate in the shallow, more optically complex, coastal waters.

One of the main strengths of satellite data is that it provides an overall picture of variations/patterns in the chlorophyll distribution in our coastal waters at a relatively high temporal resolution. Even if on occasion the absolute concentration is not within the specified accuracy hoped for, the relative concentrations do appear to be valid, and one may therefore use satellite data to monitor spatial variations and to help understand circulation patterns. Also, as was demonstrated during the transect of 26th August 1998, it is sometimes not possible to obtain in-situ samples. The satellite will provide data, subject to atmospheric conditions, on a daily basis. On the

other hand, only in-situ sampling enables one to measure vertical profiles of chlorophyll concentration. To date, this has not been shown to be possible from space-based sensors. One would conclude that both in-situ sampling and satellite remote sensing may complement each other.

Fluorometer: Chlorophyll-a Profile
23 June 1998: Hillarys - 0



Fluorometer: Chlorophyll-a Profile
23 June 1998: Hillarys - 0b

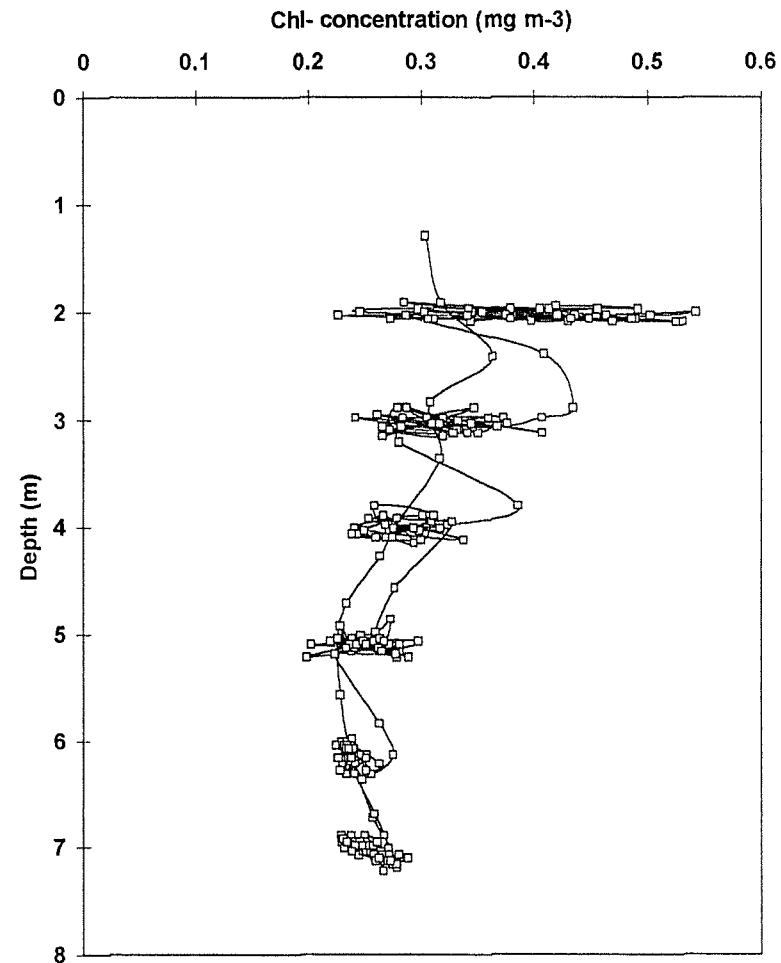


Figure 5.1 (a - left, b - right) Chlorophyll profiles measured using the Bispherical INF300 instrument. Figure (a) is a dramatic example to highlight the difference between the upcast and downcast results. Figure (b) shows the effect of holding the instrument at 1 m intervals for periods of approximately 20 to 30 seconds each.

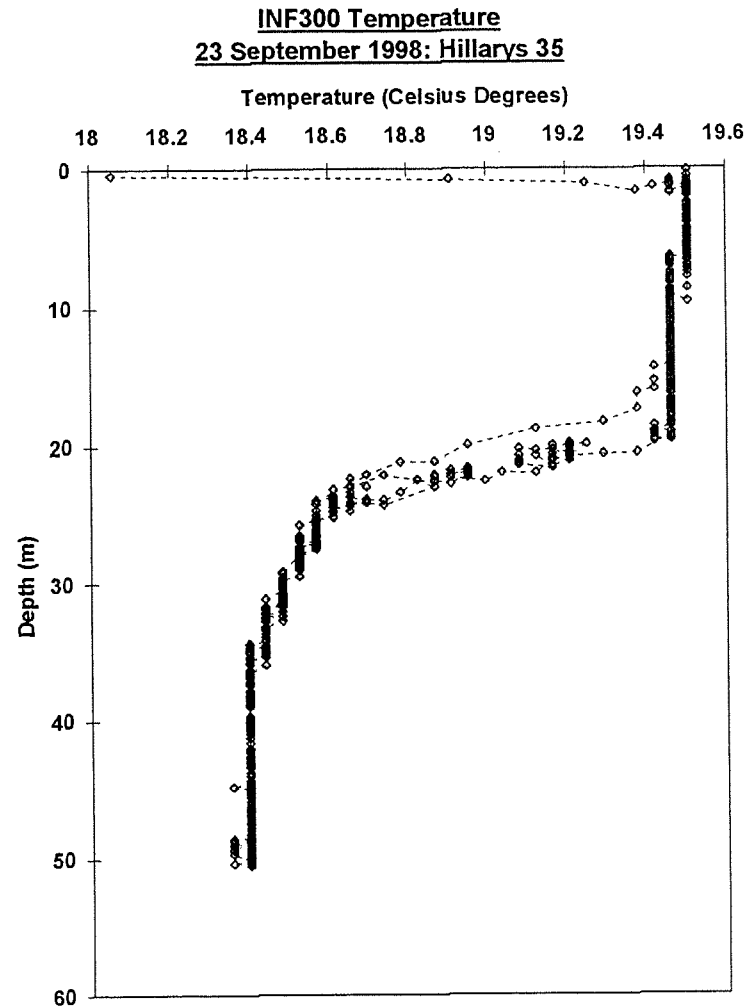
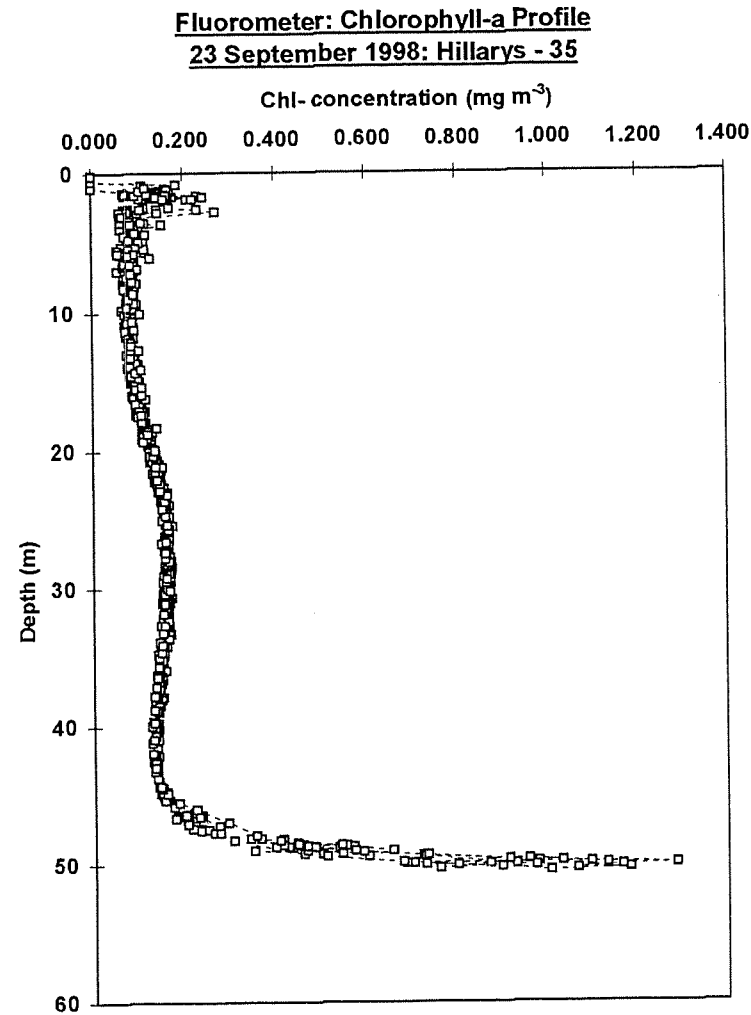


Figure 5.2 (a - left, b - right) Chlorophyll profile (a) and temperature profile (b) measured using the Biospherical INF300 instrument. The reason for the increase in chlorophyll concentration at 50 m depth, the approximate depth of the water at this measurement station, is unclear. The increase may be due to reflectance from sea grass, a chlorophyll maximum near the sea floor, or possibly instrument tilt. The temperature profile shows a distinct thermocline at about 20 m depth.

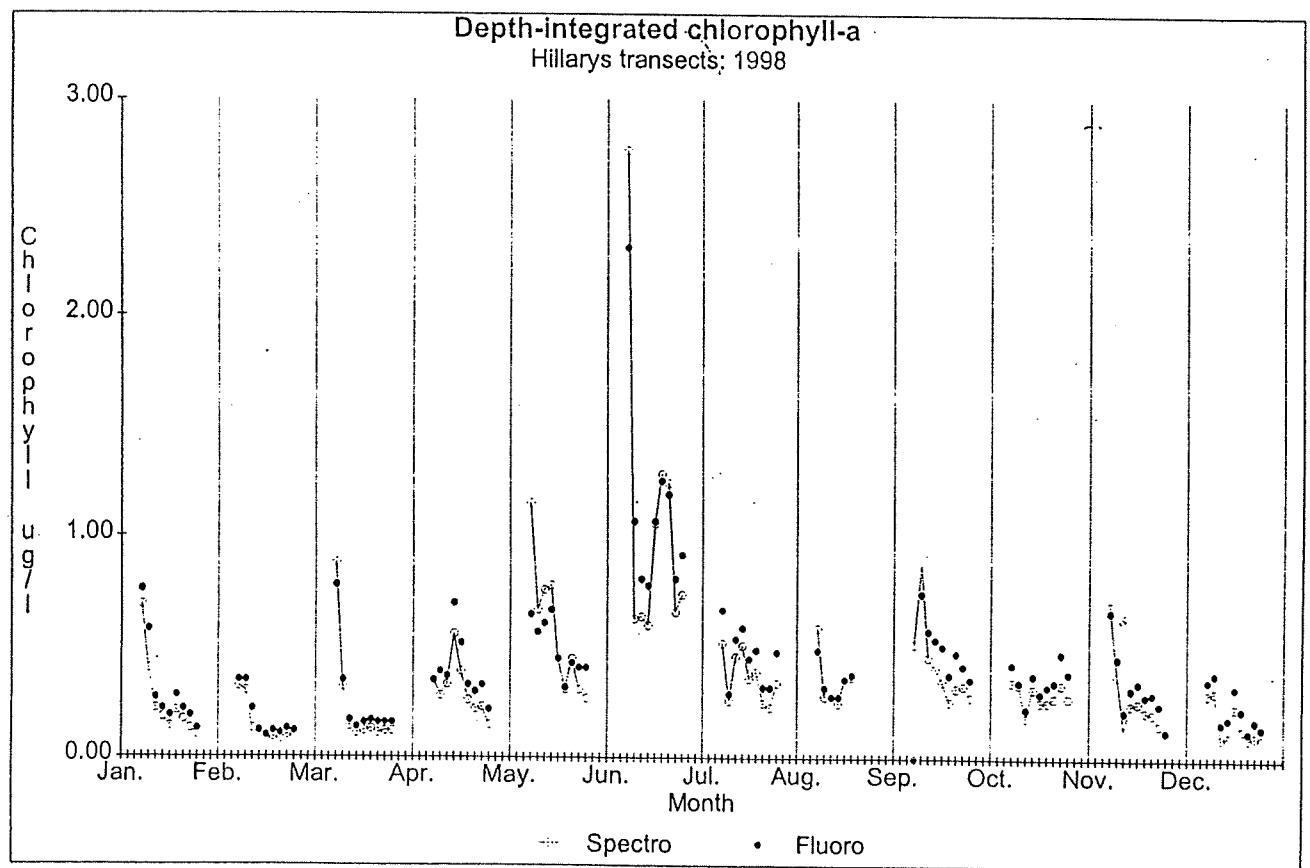
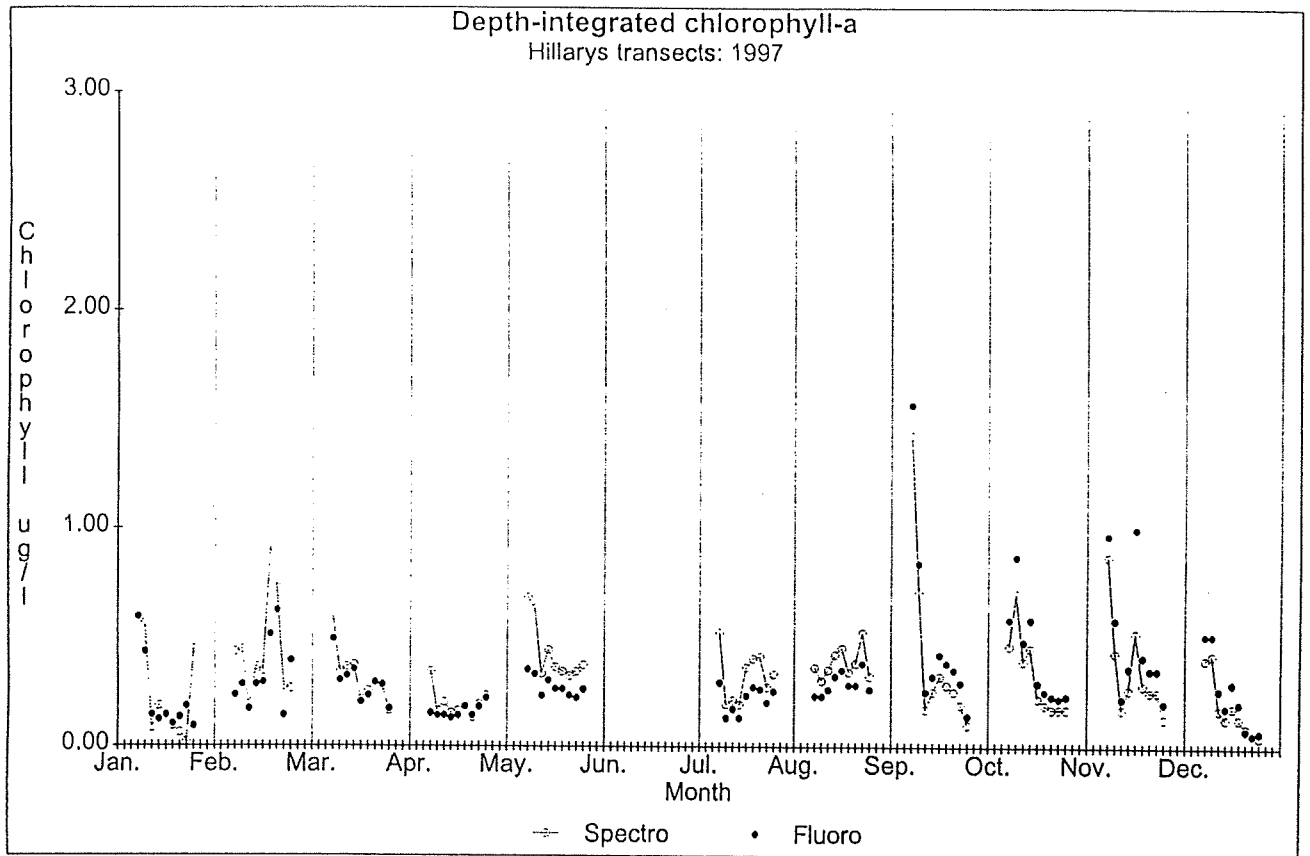


Figure 5.3: Cross-shelf depth-integrated chlorophyll transects for (a - top) 1997 and (b - bottom) 1998, derived from the spectrophotometer (joined open circles) and the fluorometer (closed circles). Each segment represents a monthly transect, and the stations are along the segment with H0 (inshore) on the left and H40 (offshore) on the right.

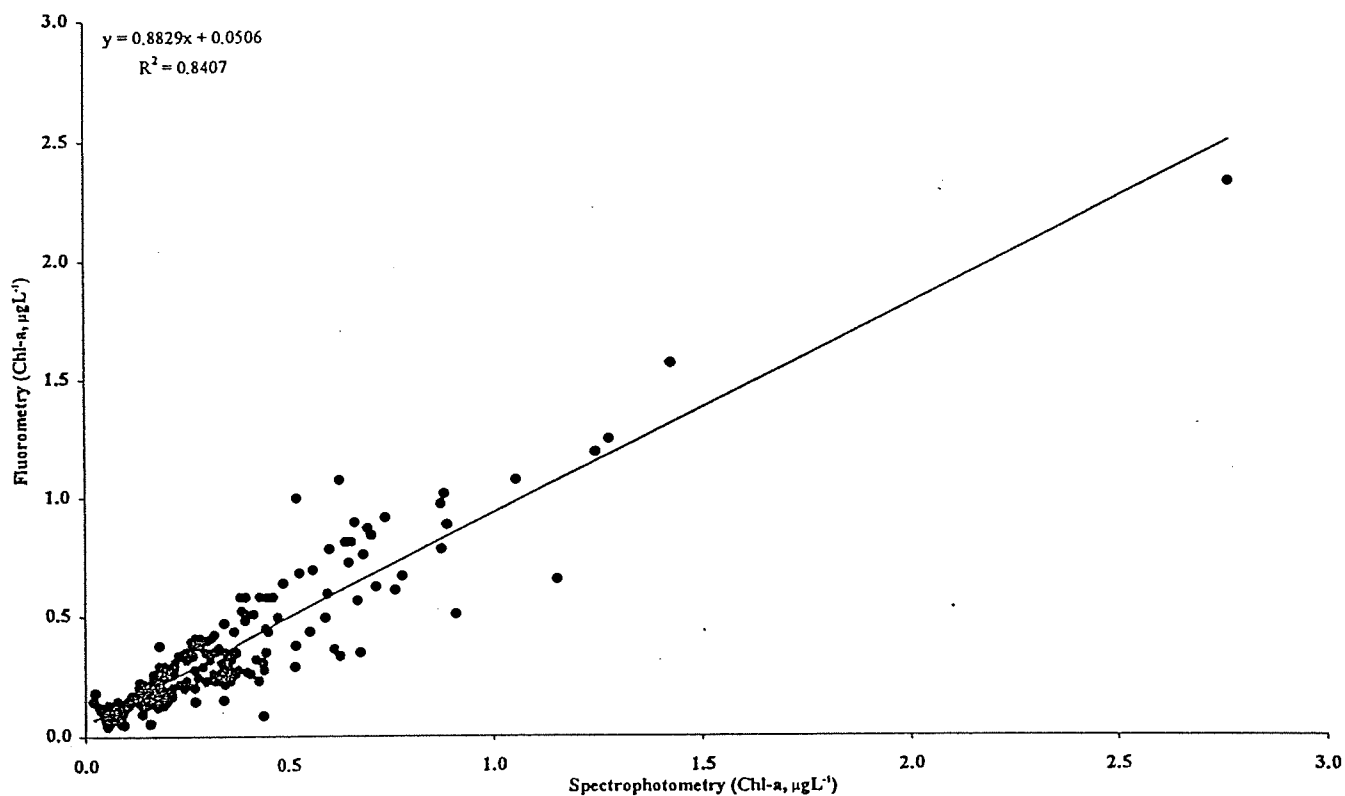


Figure 5.4: Scatter-plot of chlorophyll concentrations measured by fluorometer against those from the spectrophotometer from the Hillarys transects between October 1996 and June 1998. Reproduced from Hellereen and Pearce (2000).

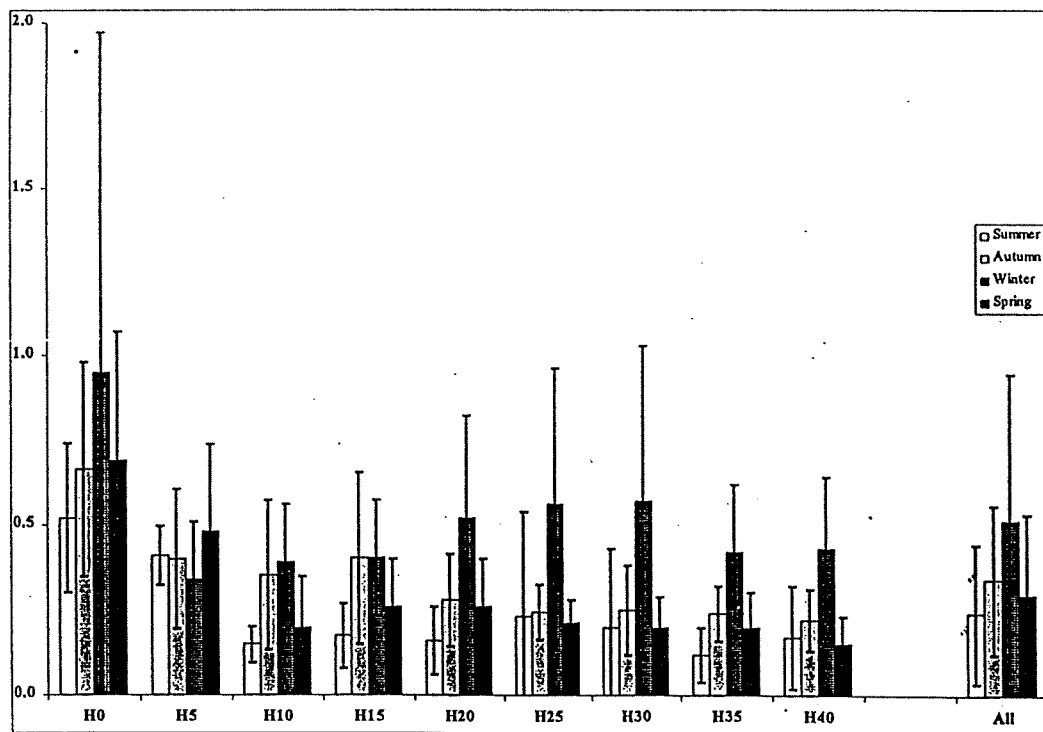
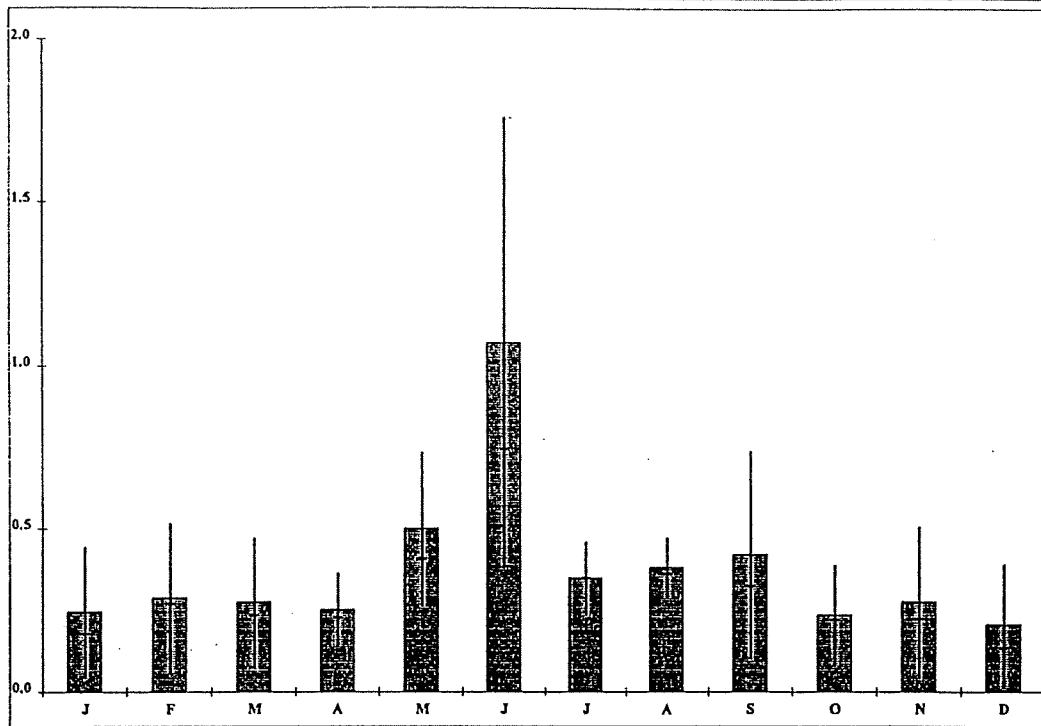
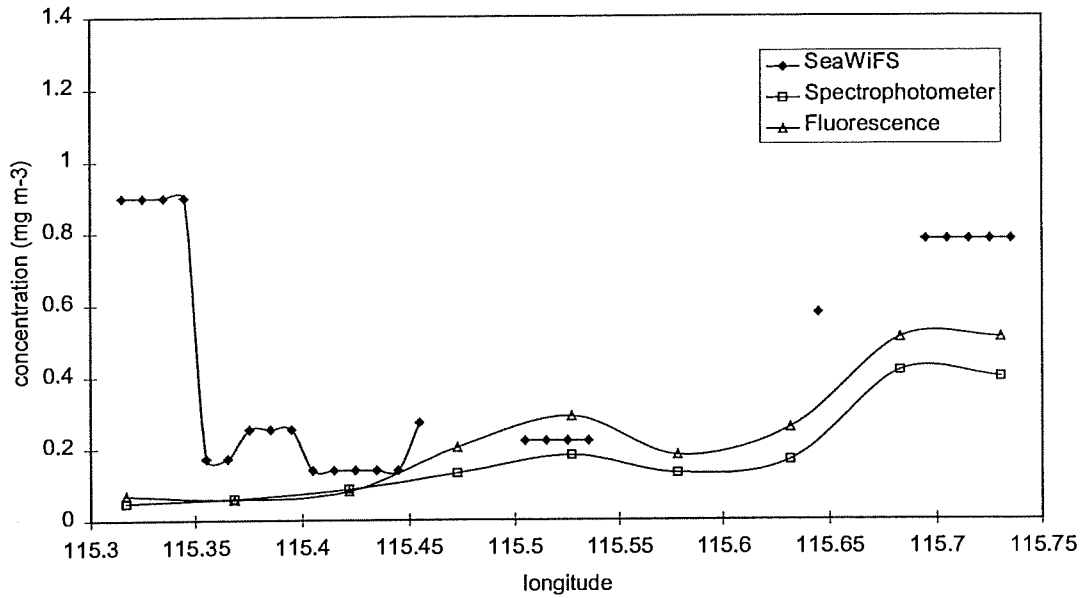


Figure 5.5: (a - top) Monthly mean chlorophyll concentrations, with standard deviation bars; averaged across all 9 stations H0 to H40 along the Hillarys transects between October 1996 and June 1998. (b - bottom) Seasonally-averaged chlorophyll concentrations (with standard deviation bars) at each station along the Hillarys transect, between October 1996 and June 1998. The seasons are in sequence summer (December to February), autumn (March to May), winter (June to August) and spring (September to November). Reproduced from Hellen and Pearce (2000).

Hillarys Transect 16th December 1997
Chlorophyll data



Hillarys Transect 19th January 1998
Chlorophyll data

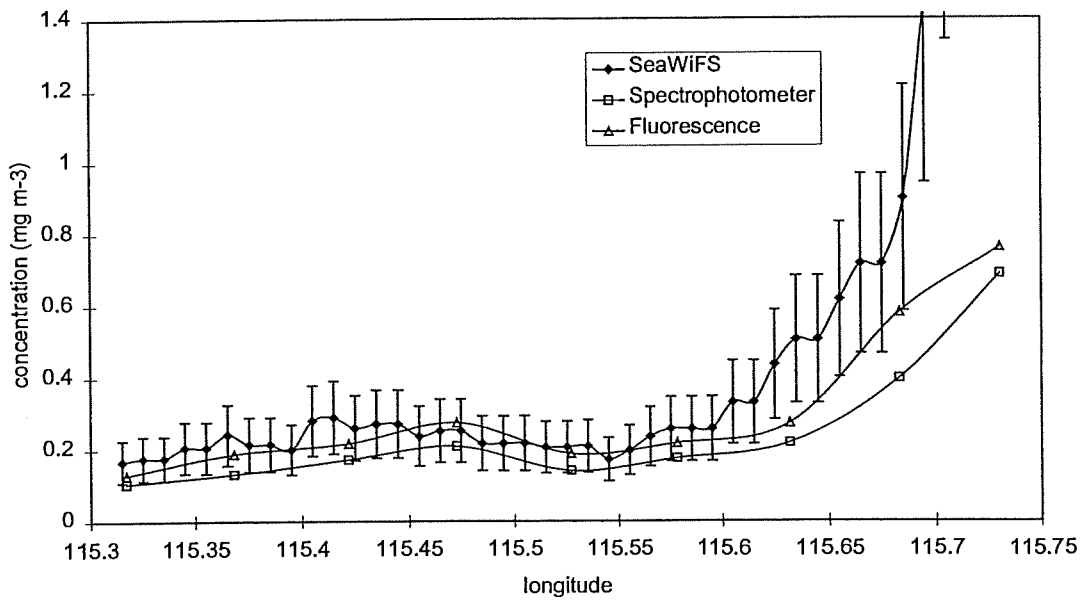
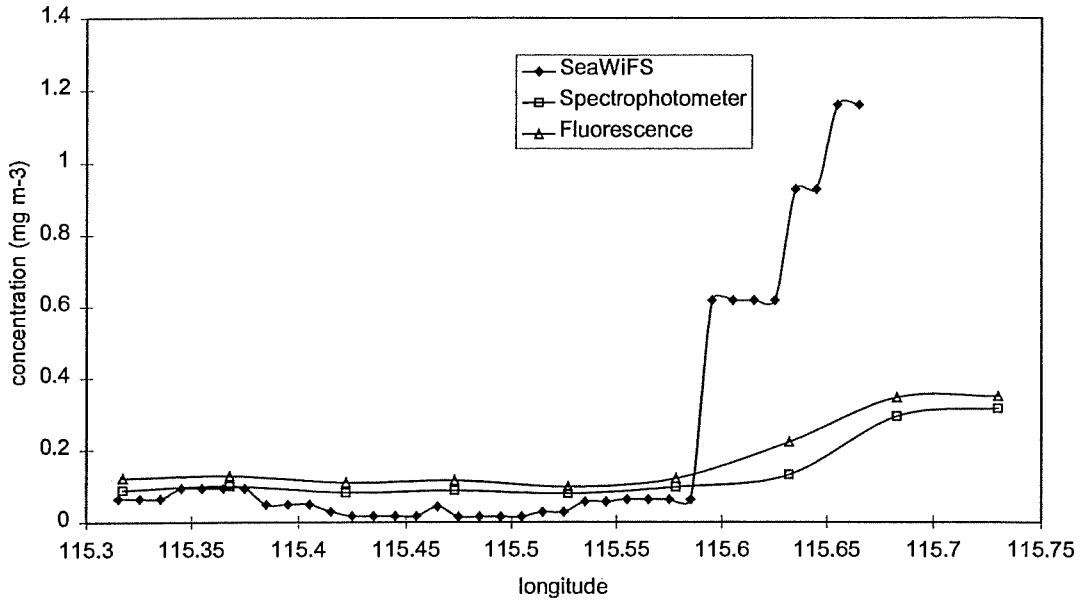


Figure 5.6 (a - top, b - bottom) Chlorophyll data obtained by in-situ sampling and subsequent laboratory procedures (Spectrophotometer and Fluorescence), and chlorophyll values derived from SeaWiFS data. Where error bars are shown this indicates the SeaWiFS quality control flags were zero for at least some portion of the pass. See Section 9 and Table 9.1 for information on the quality control flags. The error bars show the $\pm 35\%$ accuracy specified for SeaWiFS open ocean chlorophyll data.

Hillarys Transect 16th February 1998
Chlorophyll data



Hillarys Transect 16th February 1998
Chlorophyll data

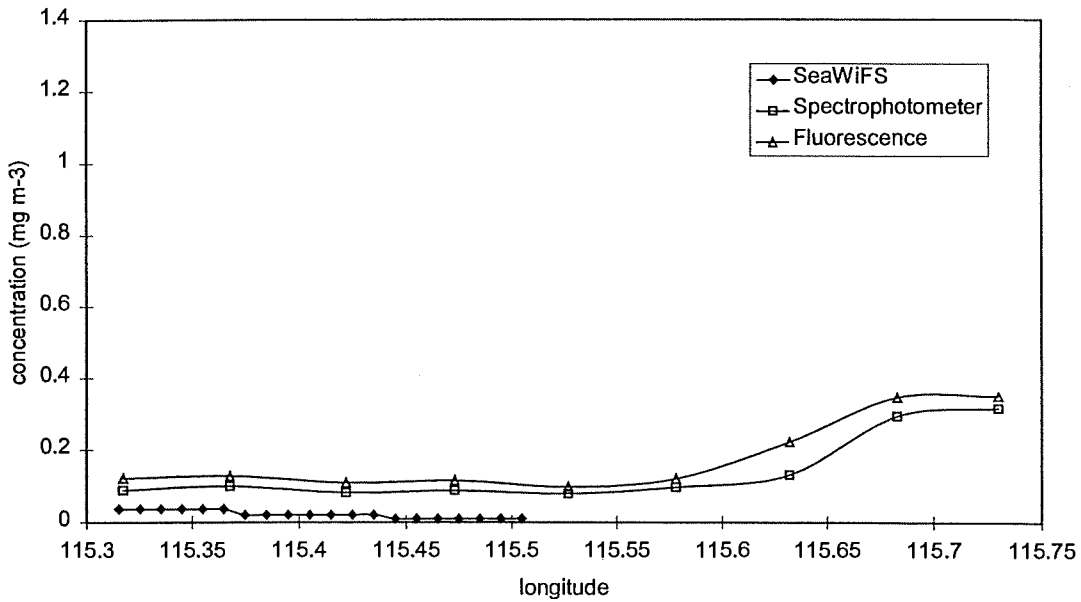
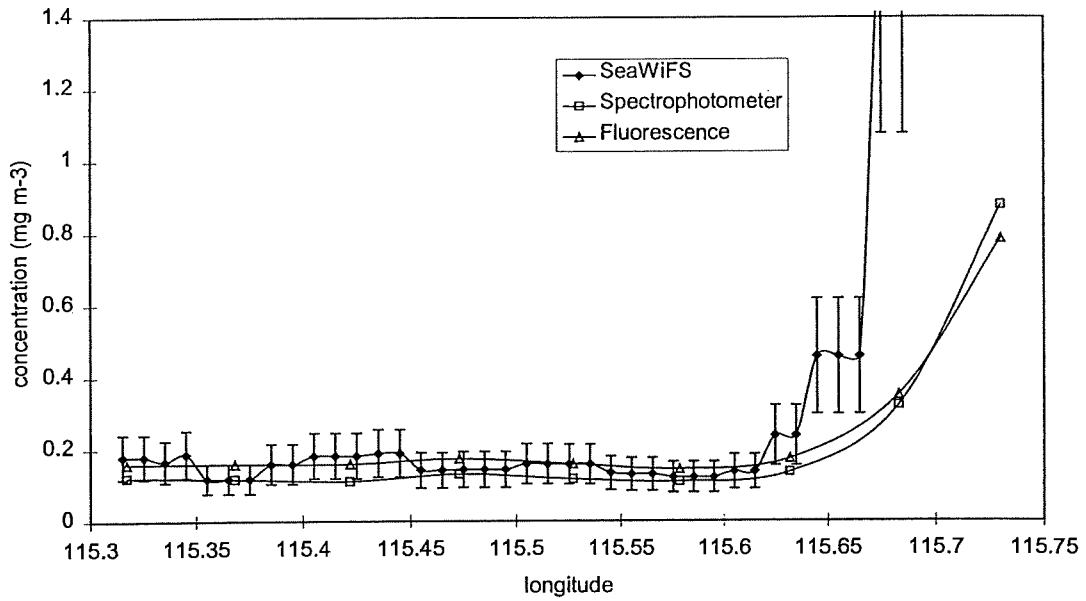


Figure 5.7 (a - top, b - bottom) Chlorophyll data obtained by in-situ sampling and subsequent laboratory procedures (Spectrophotometer and Fluorescence), and chlorophyll values derived from SeaWiFS data.

Hillarys Transect 17th March 1998
Chlorophyll data



Hillarys Transect 21st April 1998
Chlorophyll data

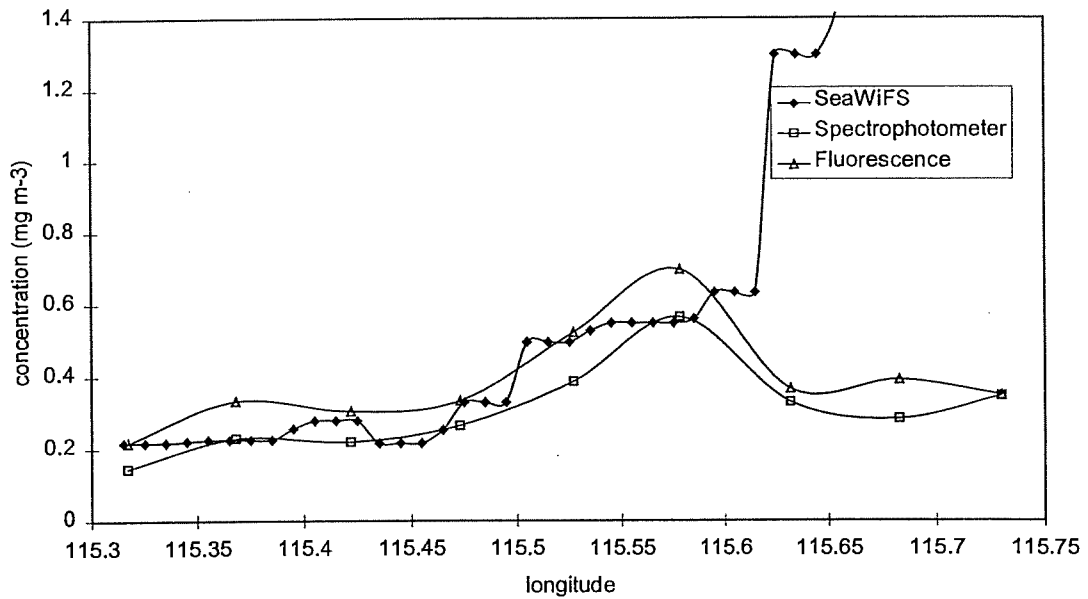
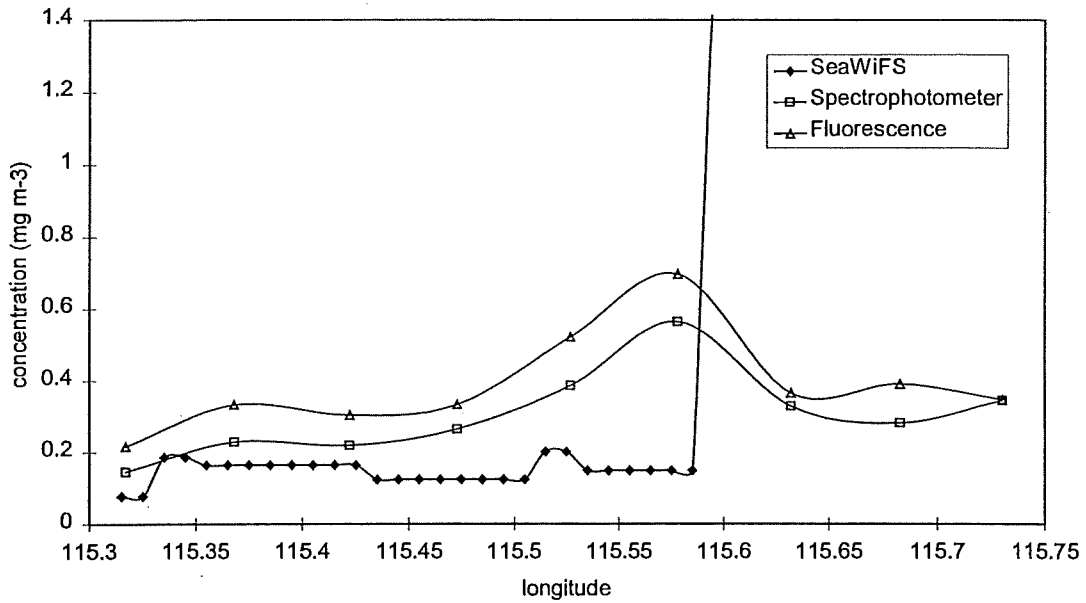


Figure 5.8 (a - top, b - bottom) Chlorophyll data obtained by in-situ sampling and subsequent laboratory procedures (Spectrophotometer and Fluorescence) , and chlorophyll values derived from SeaWiFS data. Where error bars are shown this indicates the SeaWiFS quality control flags were zero for at least some portion of the pass. See Section 9 and Table 9.1 for information on the quality control flags. The error bars show the $\pm 35\%$ accuracy specified for SeaWiFS open ocean chlorophyll data.

Hillarys Transect 21st April 1998
Chlorophyll data



Hillarys Transect 19th May 1998
Chlorophyll data

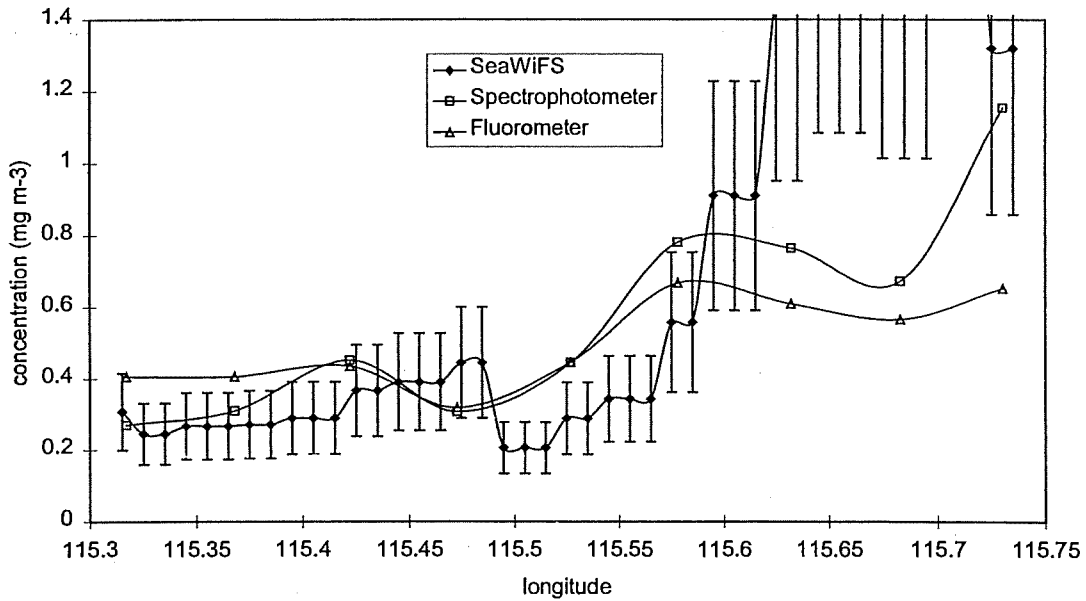


Figure 5.9 (a - top, b - bottom) Chlorophyll data obtained by in-situ sampling and subsequent laboratory procedures (Spectrophotometer and Fluorescence), and chlorophyll values derived from SeaWiFS data. Where error bars are shown this indicates the SeaWiFS quality control flags were zero for at least some portion of the pass. See Section 9 and Table 9.1 for information on the quality control flags. The error bars show the $\pm 35\%$ accuracy specified for SeaWiFS open ocean chlorophyll data.

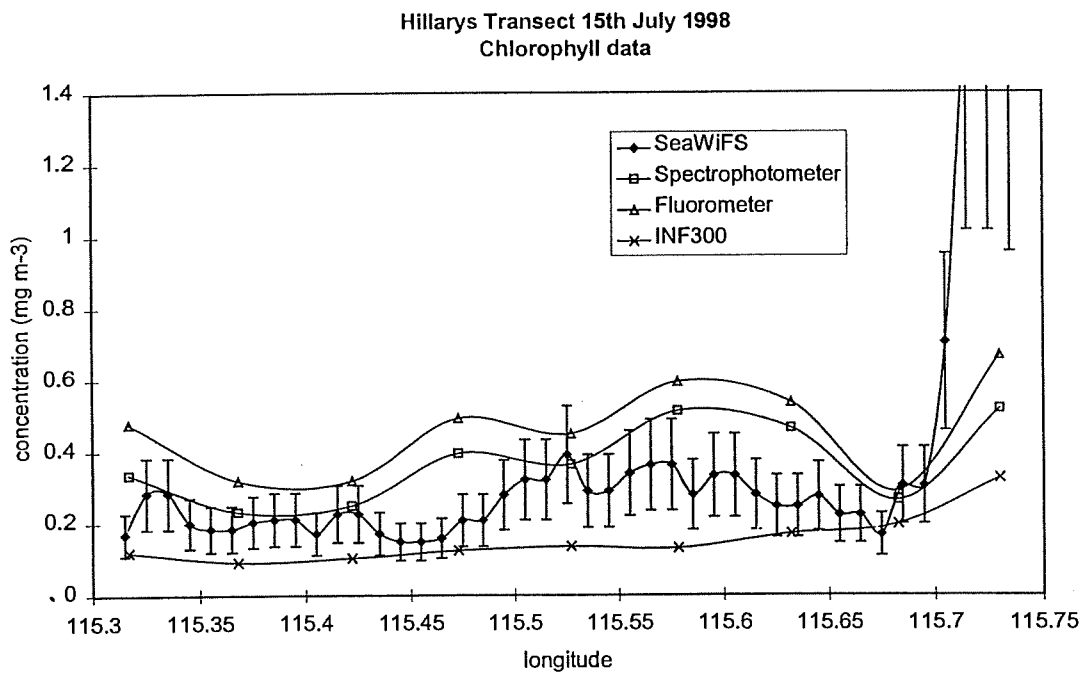
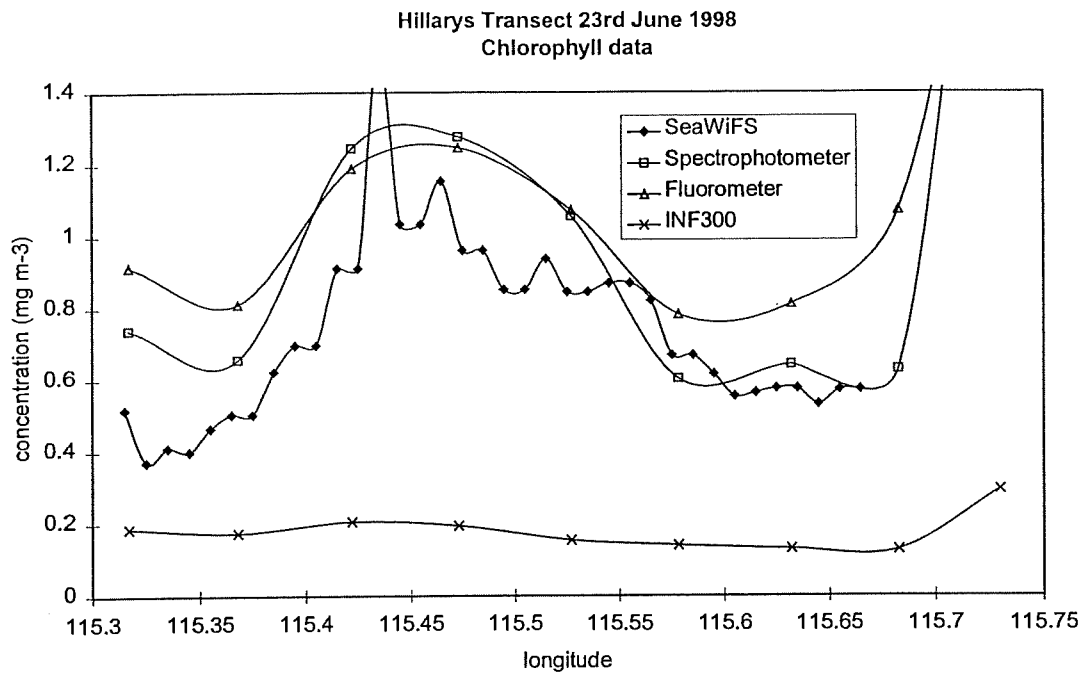
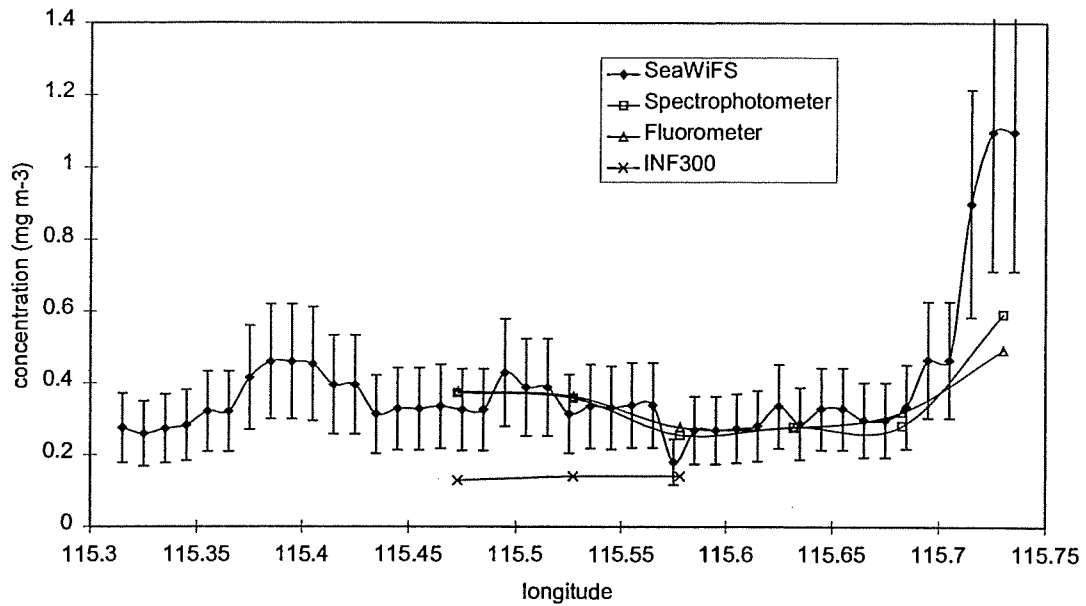


Figure 5.10 (a - top, b - bottom) Chlorophyll data obtained by in-situ sampling and subsequent laboratory procedures (Spectrophotometer and Fluorescence), in-situ chlorophyll fluorescence vertical profile measurements (INF300) and chlorophyll values derived from SeaWiFS data. Where error bars are shown this indicates the SeaWiFS quality control flags were zero for at least some portion of the pass. See Section 9 and Table 9.1 for information on the quality control flags. The error bars show the $\pm 35\%$ accuracy specified for SeaWiFS open ocean chlorophyll data.

Hillarys Transect 26th August 1998
Chlorophyll data



Hillarys Transect 23rd September 1998
Chlorophyll data

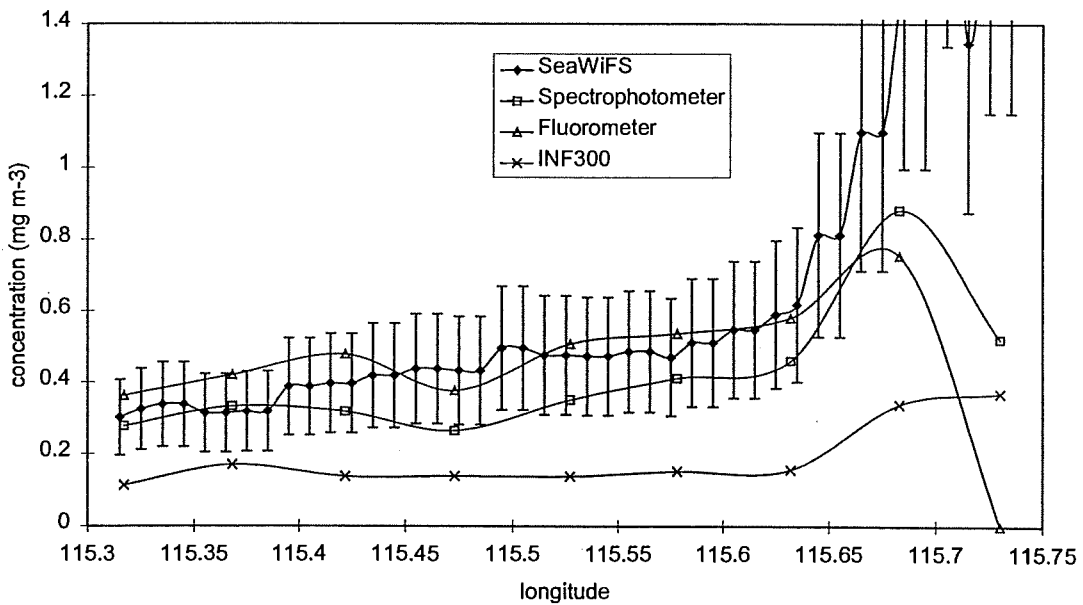
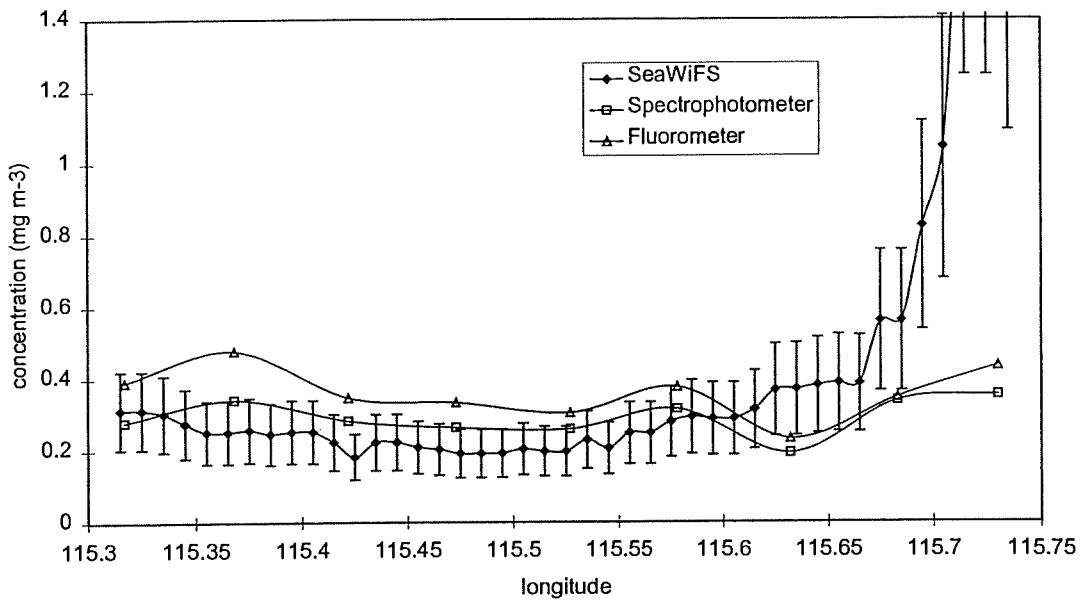


Figure 5.11 (a - top, b - bottom) Chlorophyll data obtained by in-situ sampling and subsequent laboratory procedures (Spectrophotometer and Fluorescence) , in-situ chlorophyll fluorescence vertical profile measurements (INF300) and chlorophyll values derived from SeaWiFS data. Where error bars are shown this indicates the SeaWiFS quality control flags were zero for at least some portion of the pass. See Section 9 and Table 9.1 for information on the quality control flags. The error bars show the $\pm 35\%$ accuracy specified for SeaWiFS open ocean chlorophyll data.

Hillarys Transect 20th October 1998
Chlorophyll data



Hillarys Transect 10th November 1998
Chlorophyll data

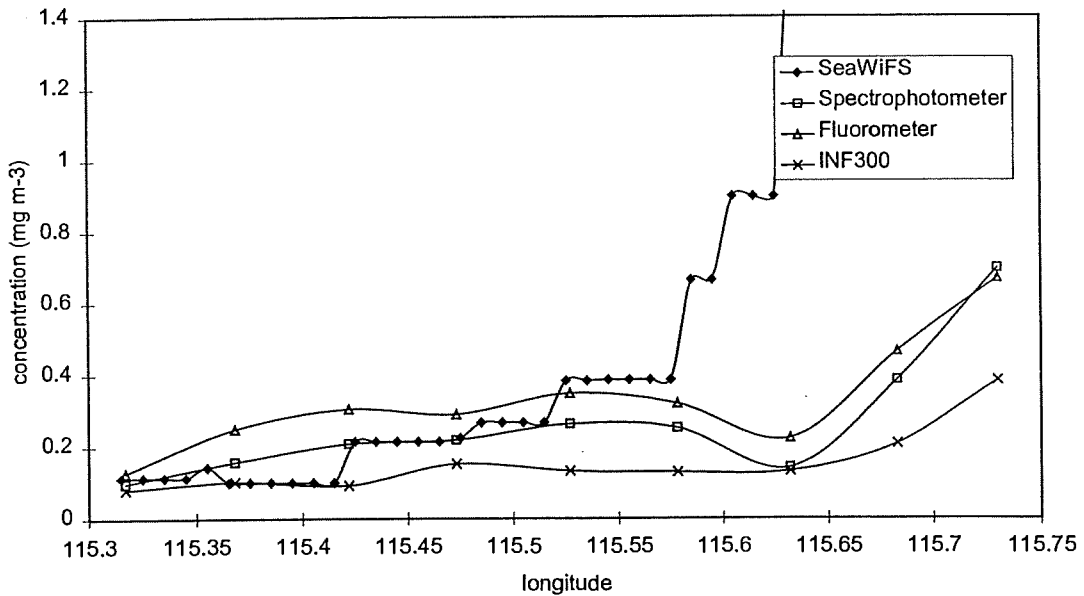
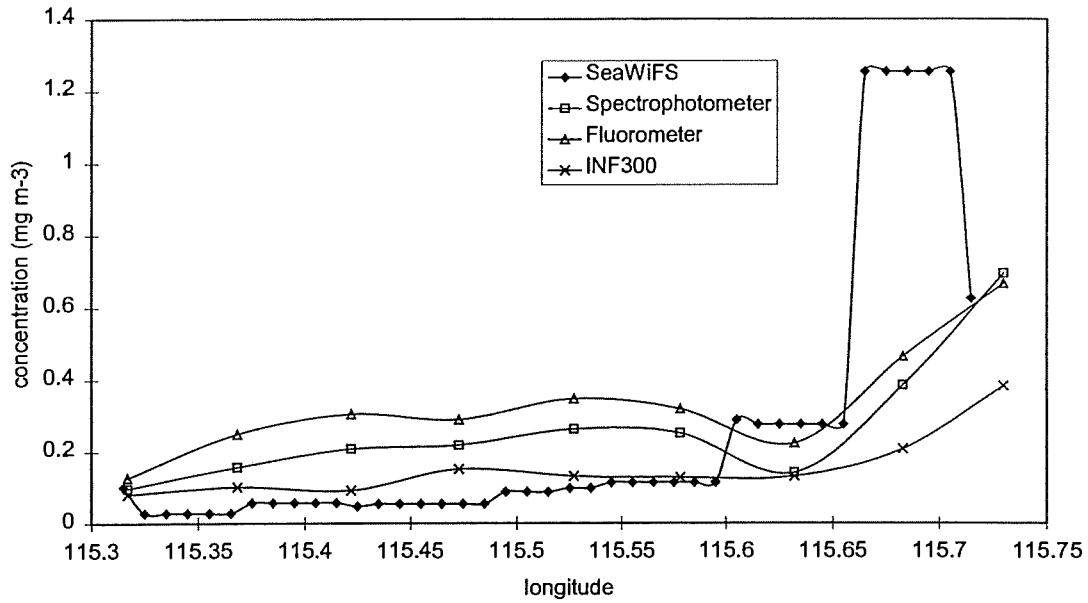


Figure 5.12 (a - top, b - bottom) Chlorophyll data obtained by in-situ sampling and subsequent laboratory procedures (Spectrophotometer and Fluorescence), in-situ chlorophyll fluorescence vertical profile measurements (INF300) and chlorophyll values derived from SeaWiFS data. Where error bars are shown this indicates the SeaWiFS quality control flags were zero for at least some portion of the pass. See Section 9 and Table 9.1 for information on the quality control flags. The error bars show the $\pm 35\%$ accuracy specified for SeaWiFS open ocean chlorophyll data.

Hillarys Transect 10th November 1998
Chlorophyll data



Hillarys Transect 12th December 1998
Chlorophyll data

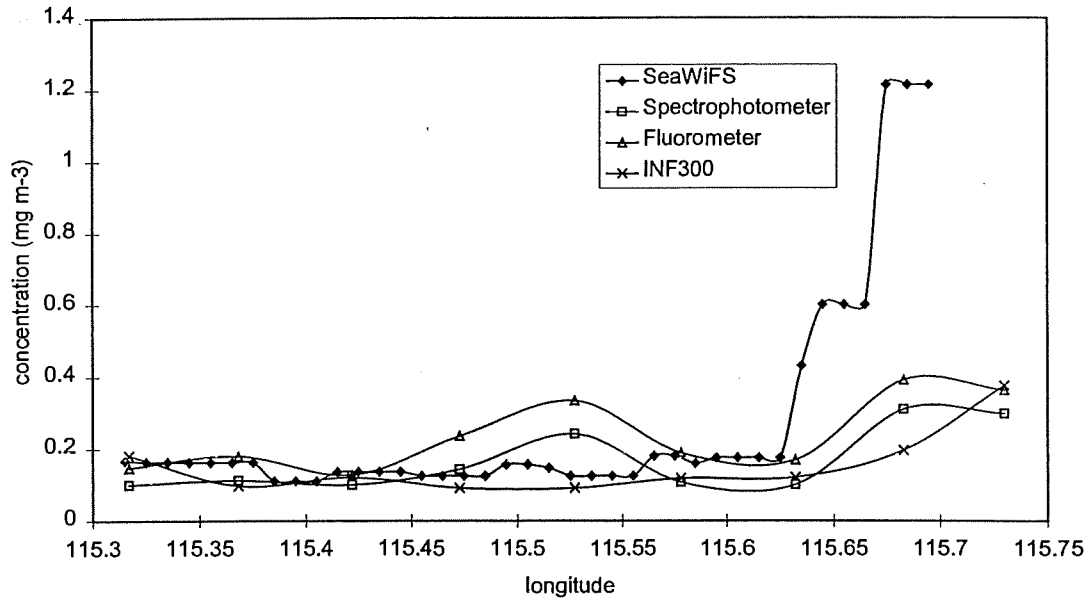


Figure 5.13 (a - top, b - bottom) Chlorophyll data obtained by in-situ sampling and subsequent laboratory procedures (Spectrophotometer and Fluorescence), in-situ chlorophyll fluorescence vertical profile measurements (INF300) and chlorophyll values derived from SeaWiFS data. Where error bars are shown this indicates the SeaWiFS quality control flags were zero for at least some portion of the pass. See Section 9 and Table 9.1 for information on the quality control flags. The error bars show the $\pm 35\%$ accuracy specified for SeaWiFS open ocean chlorophyll data.

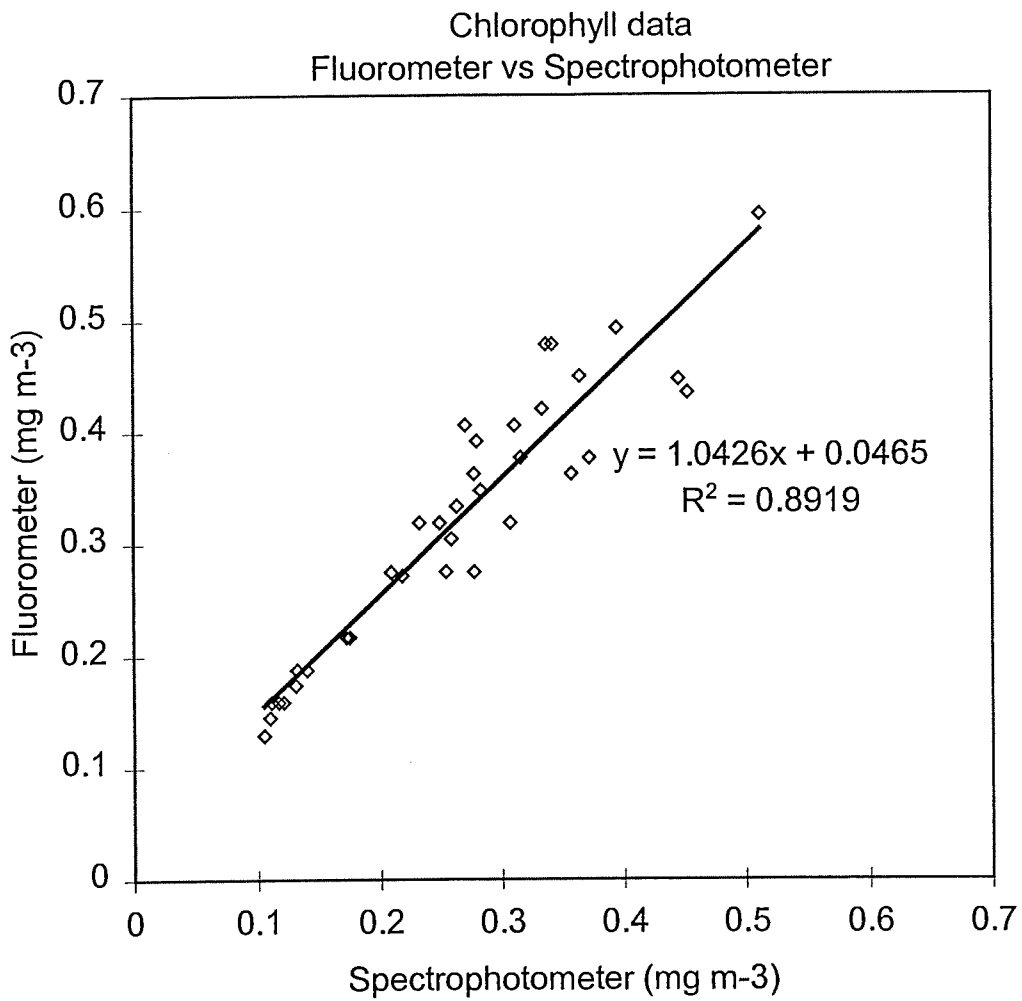


Figure 5.14 Comparison between in-situ chlorophyll data derived by fluorometric measurements and spectrophotometric measurements. These in-situ data correspond to dates and station locations where the concurrent SeaWiFS chlorophyll data had Level 2 processing flags of zero value. See section 9 and tables 9.1 and 9.2 therein.

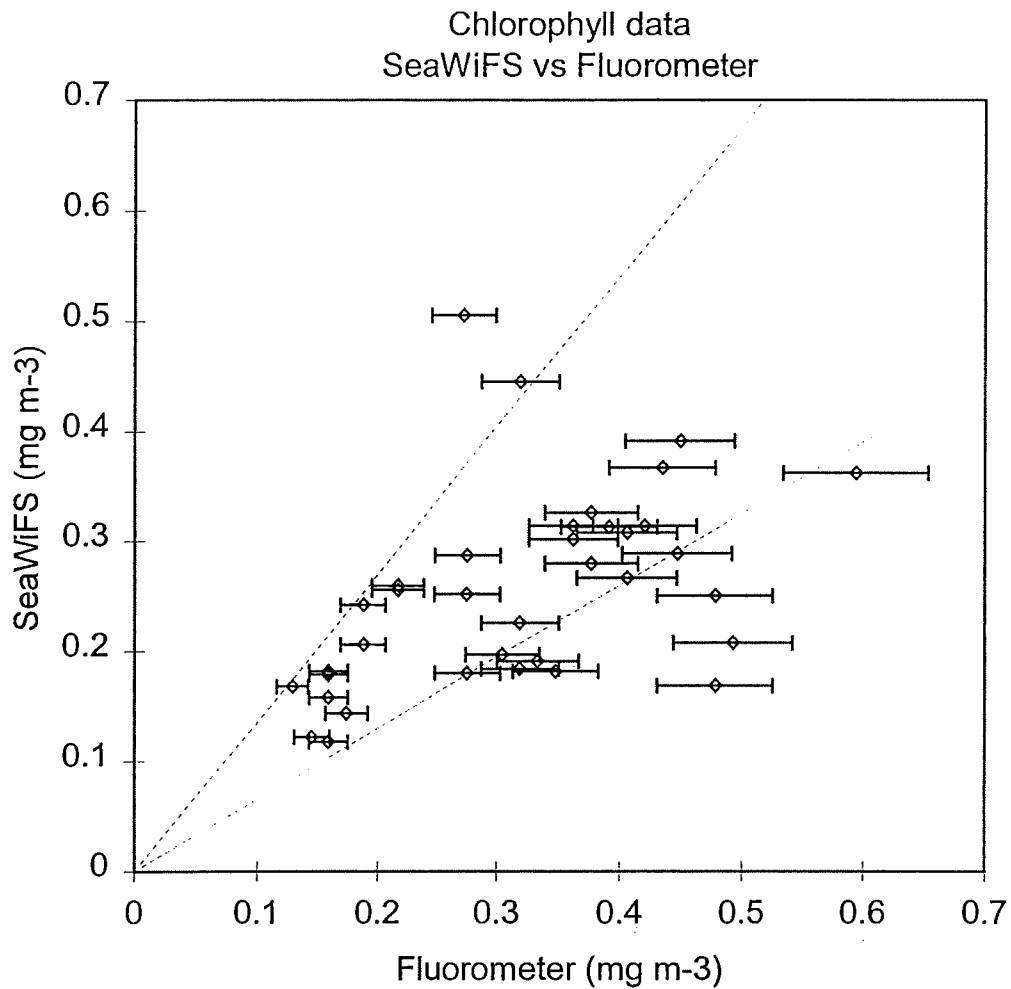


Figure 5.15 Comparison between SeaWiFS chlorophyll data and in-situ chlorophyll concentrations derived by fluorometric measurements. These data correspond to dates and station locations where the SeaWiFS chlorophyll data had Level 2 processing flags of zero value. See section 9 and tables 9.1 and 9.2 therein. The dashed lines indicate the NASA specified $\pm 35\%$ accuracy for the remotely sensed chlorophyll product. The error bars on data points indicate the estimated $\pm 10\%$ uncertainty on in-situ chlorophyll measurements.

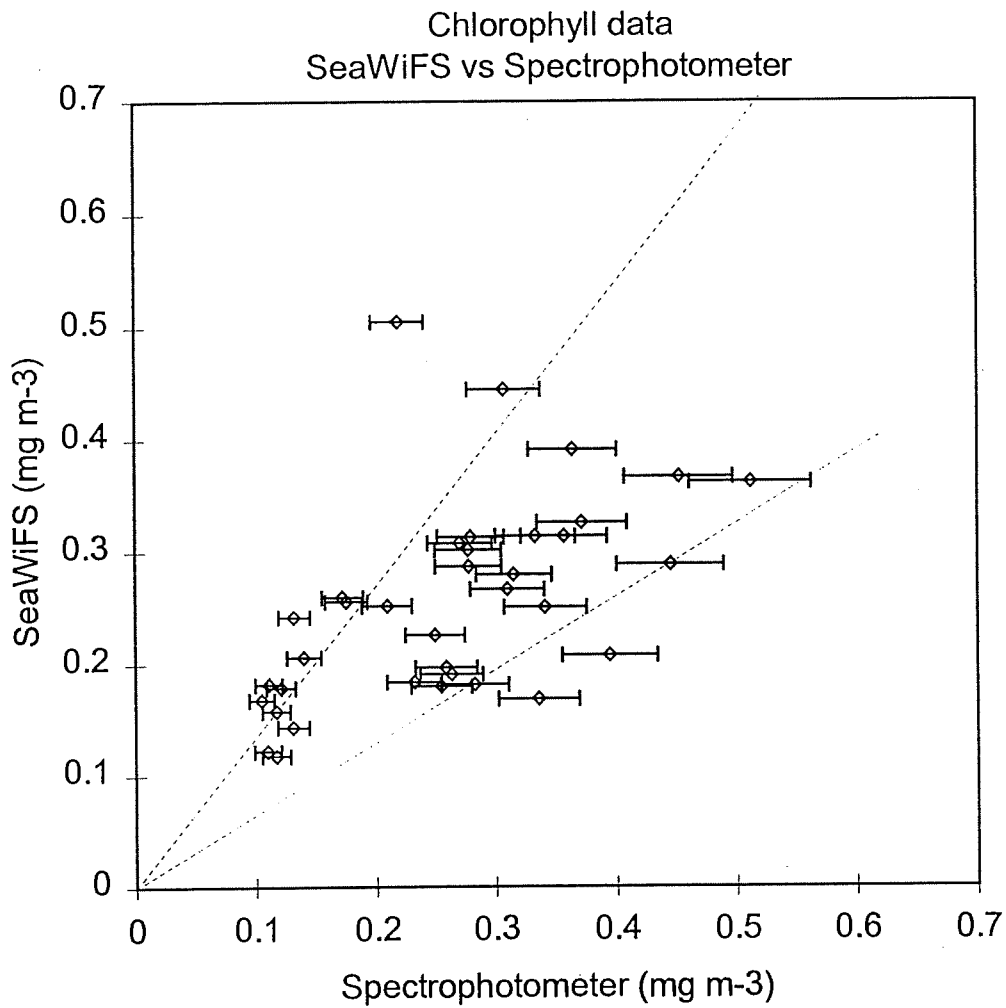


Figure 5.16 Comparison between SeaWiFS chlorophyll data and in-situ chlorophyll concentrations derived by spectrophotometric measurements. These data correspond to dates and station locations where the SeaWiFS chlorophyll data had Level 2 processing flags of zero value. See section 9 and tables 9.1 and 9.2 therein. The dashed lines indicate the NASA specified $\pm 35\%$ accuracy for the remotely sensed chlorophyll product. The error bars on data points indicate the estimated $\pm 10\%$ uncertainty on in-situ chlorophyll measurements.

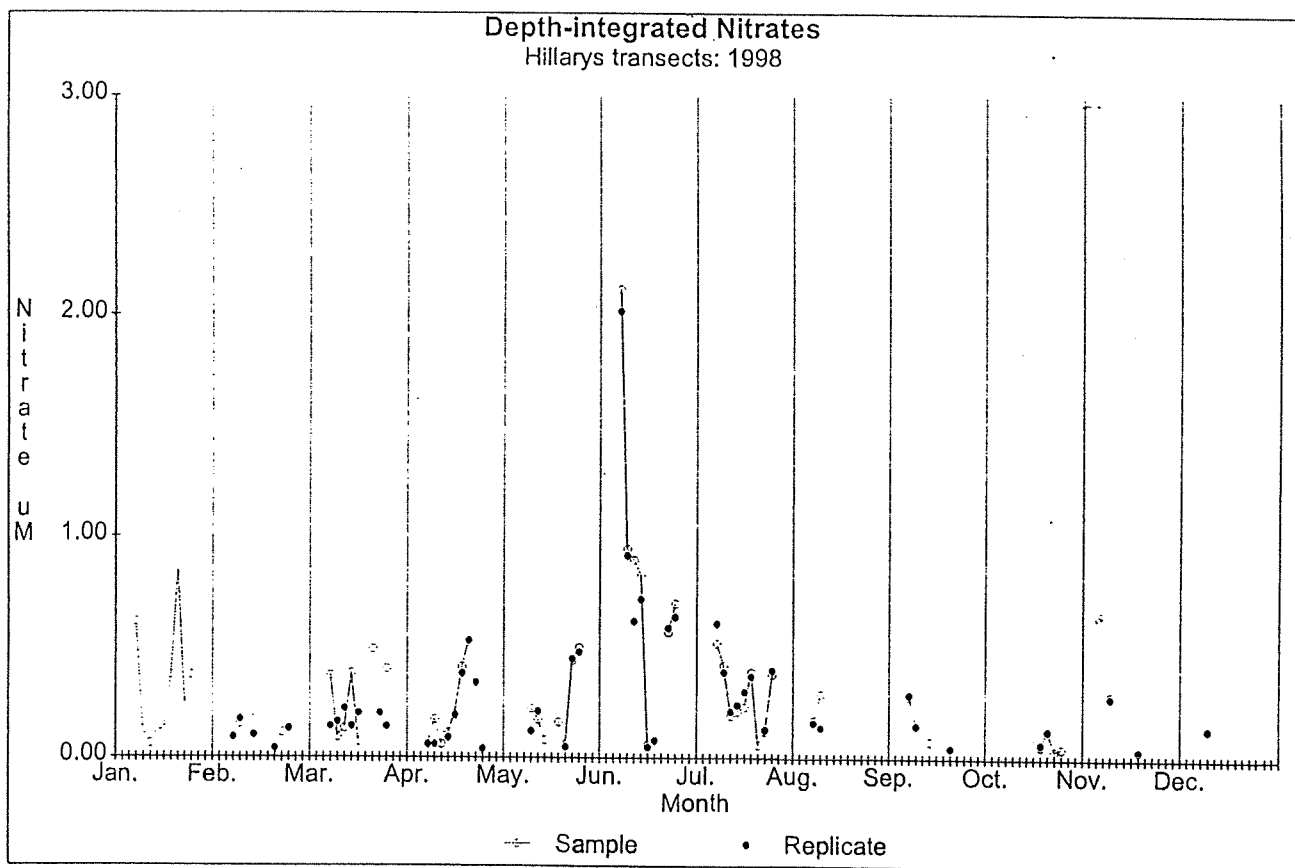
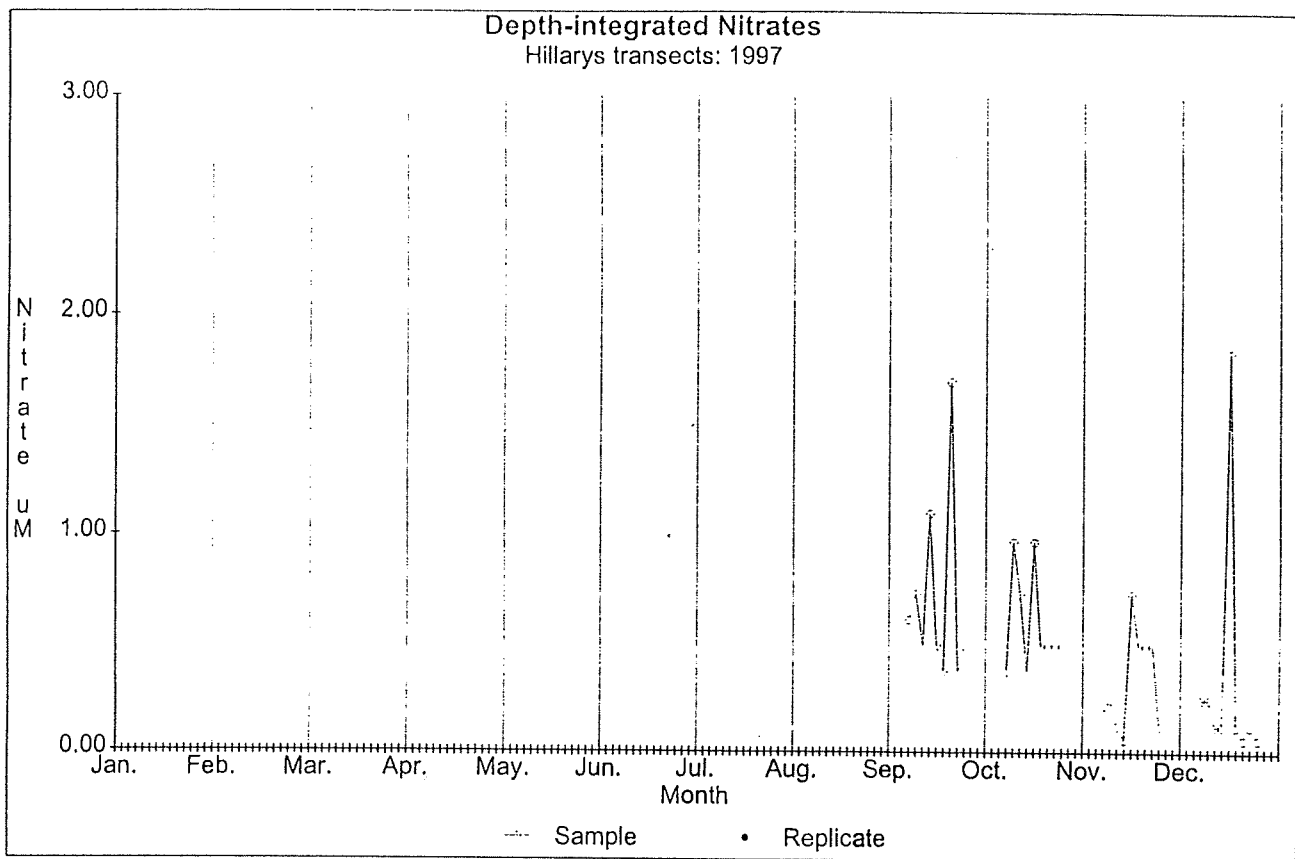


Figure 5.17: Cross-shelf depth-integrated nitrate transects for (a - top) 1997 and (b - bottom) 1998. Each segment represents a monthly transect, and the stations are along the segment with H0 (inshore) on the left and H40 (offshore) on the right. Samples prior to September 1997 were unfortunately lost. Filled circles are replicate samples.

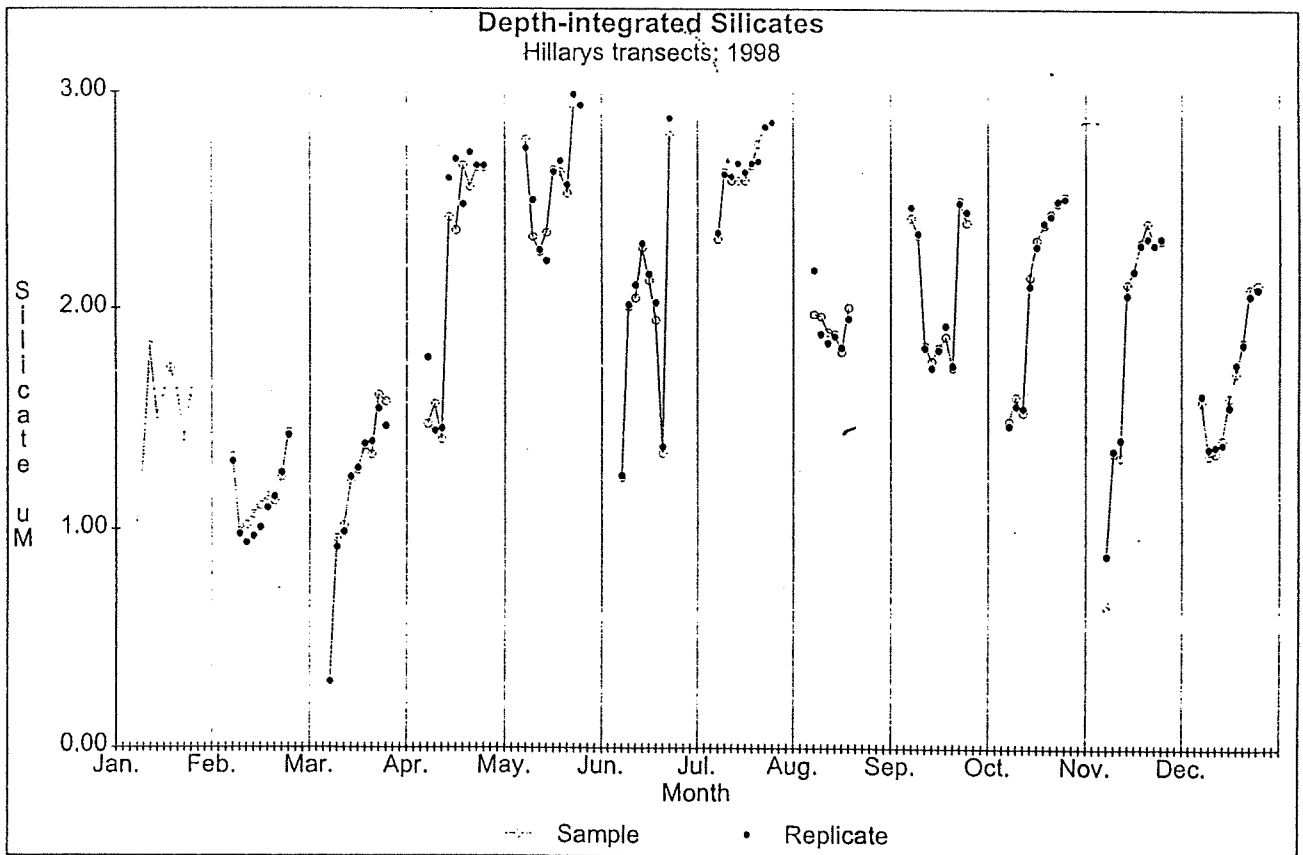
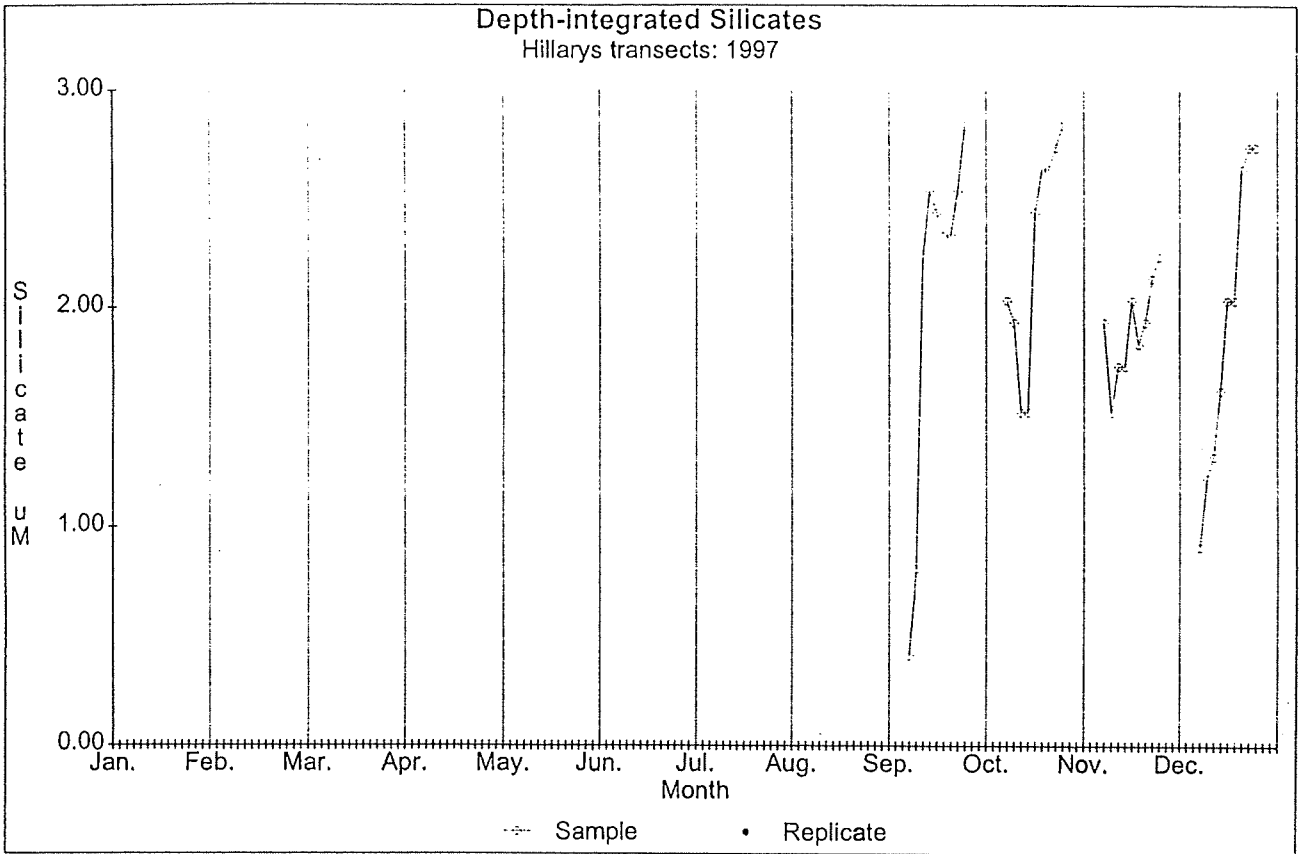


Figure 5.18: Cross-shelf depth-integrated silicate transects for (a - top) 1997 and (b - bottom) 1998. Each segment represents a monthly transect, and the stations are along the segment with H0 (inshore) on the left and H40 (offshore) on the right. Samples prior to September 1997 were unfortunately lost. Filled circles are replicate samples.

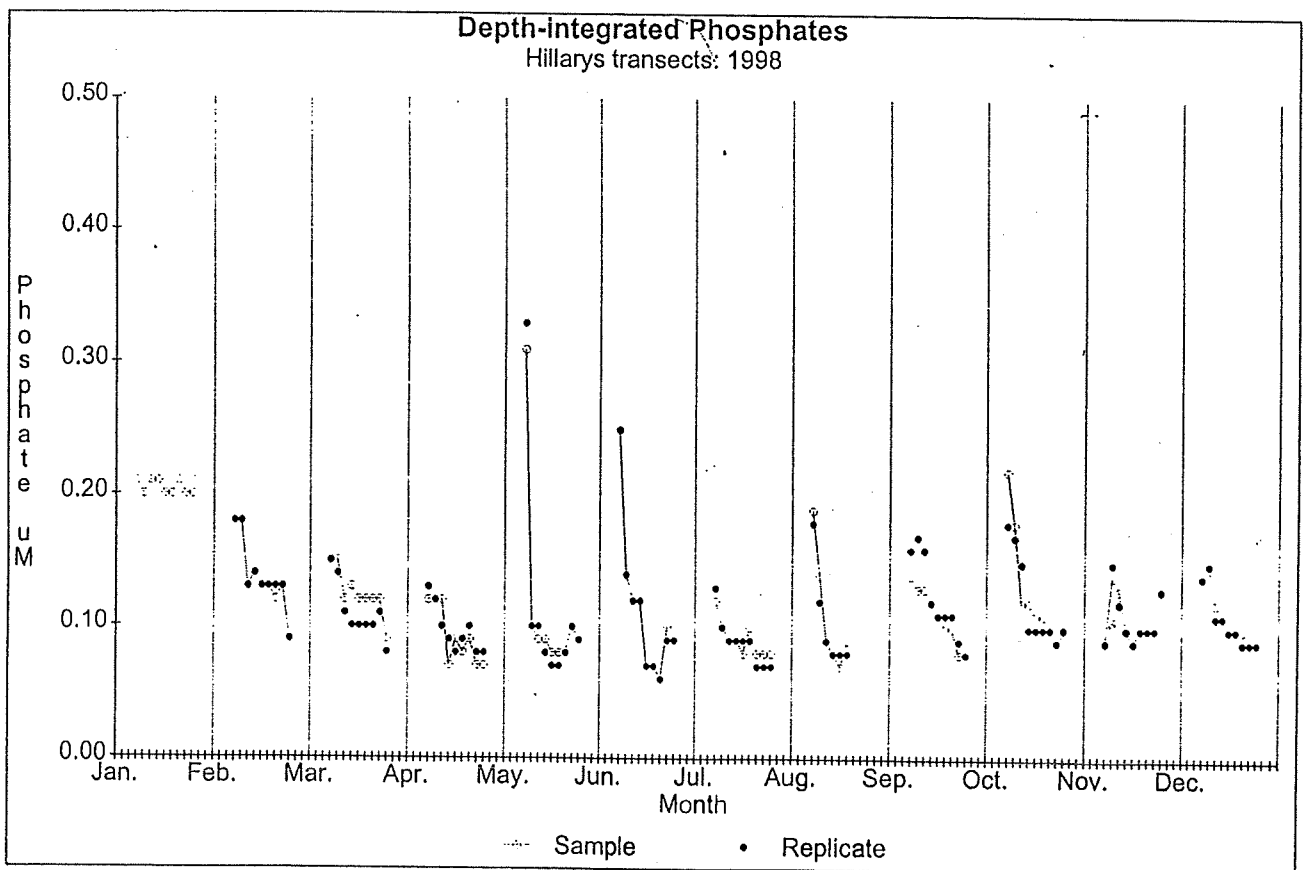
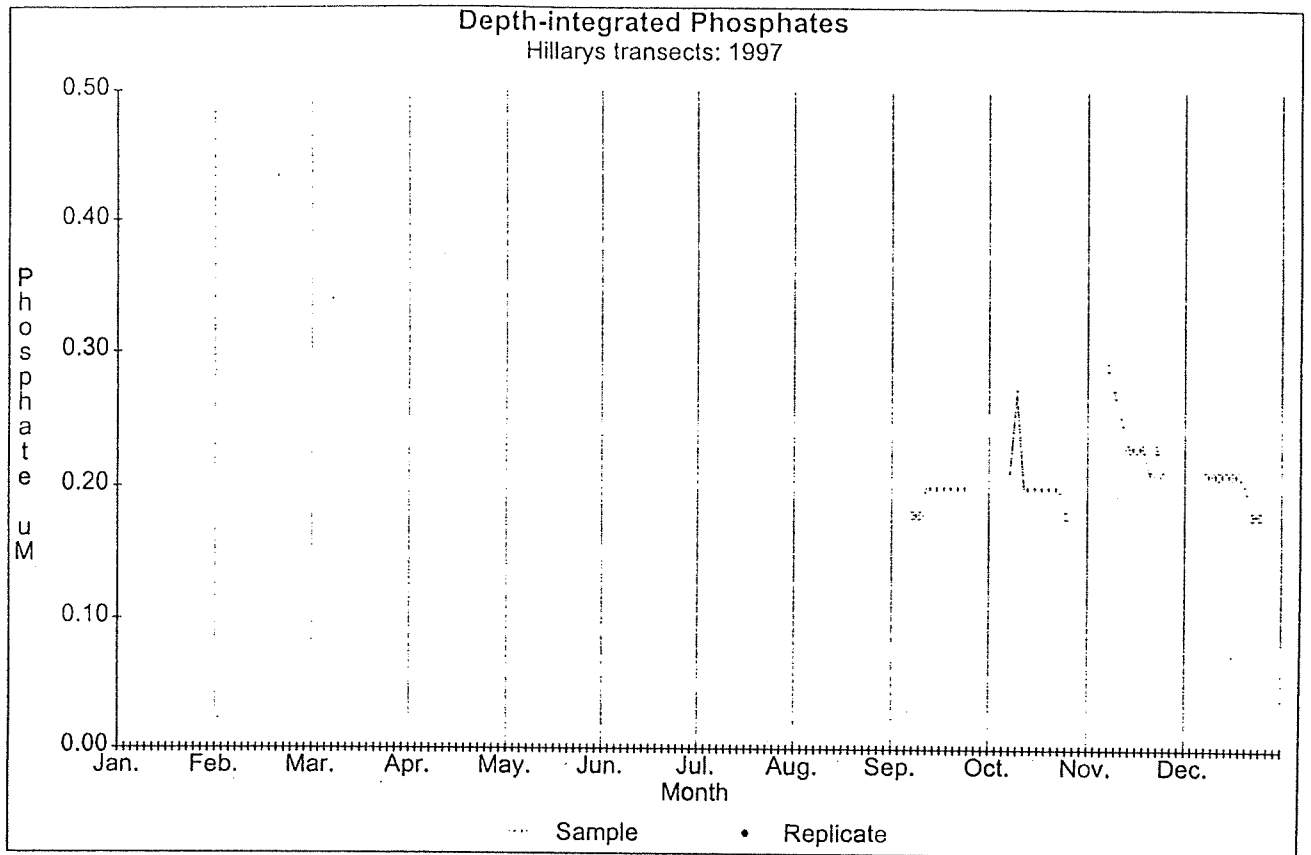


Figure 5.19: Cross-shelf depth-integrated phosphate transects for (a - top) 1997 and (b - bottom) 1998. Each segment represents a monthly transect, and the stations are along the segment with H0 (inshore) on the left and H40 (offshore) on the right. Samples prior to September 1997 were unfortunately lost. Filled circles are replicate samples.

Section 6: Light (Peter Fearn and Mervyn Lynch)

6.1 Instrument Deployment Methods and Data

Secchi Disk - Water transparency

Water column transparency, or water column turbidity, determines the total visible radiation at depth in the water column. The amount of photosynthetically active radiation (PAR) is important in studies of bioproductivity. The water clarity is also of importance for aesthetic reasons. Suspended sediments, which enhance turbidity, may settle onto seagrass or coral. The Secchi disc (in this case a 31 cm diameter steel plate painted with alternate black and white quadrants) is a simple device for measuring water clarity. The Secchi depth is that depth when, according to an observer(s), the disk is no longer visible from above the water's surface.

Accepted instructions for measuring Secchi depth direct the user to lower the Secchi disk into the water to a depth where it is no longer visible, note this depth, then raise the disk to a depth where it becomes visible. The average of this depth and the previously noted depth is then recorded as the Secchi depth.

The effect of the surface is not meant to be an influencing factor in determining the Secchi depth. However, due to surface roughness and reflectance variations, typically the most difficult aspect for the operator is observing the disk through the water's surface. For this reason operators were instructed to lower the disk through the shadow of the side of the boat if this was possible. This decreased the glitter from the water's surface. It was found that refraction effects due to surface waves caused the image of the disk to "break up". Loss of visibility of the disk is not meant to be due to surface effects. For this reason operators were instructed to lower and raise the disk a number of times at a depth where it would become clearly visible on rising slightly, and not visible on lowering slightly. At the shallowest stations, the disc was sometimes still visible on the seabed.

The attenuation of light through the water column is due to the optical properties of the water and its constituents. If one considers the main optical constituent to be phytoplankton, then one may determine a maximum possible chlorophyll concentration using the Secchi depth. (Megard and Berman 1989.)

Li-cor - Light profiles

Measurements of PAR are of relevance to studies of bioproductivity, and as a measure of water clarity. As the PAR is transmitted down through the water column the spectral extent, from 400 nm to 700 nm is diminished as highly absorbed wavelengths are attenuated. One may expect the vertical attenuation of PAR, especially at greater water depths, to be correlated to some extent with the spectral attenuation coefficient for 490 nm light derived from SeaWiFS data.

Subsurface light profiles were obtained using a 4-PI Li-cor model LI-250 Lightmeter #LMA-103, with a spherical sensor SPQA0266. The Li-cor PAR sensor measures the total available scalar irradiance across the full width of the visible spectrum.

An initial reading was taken in air (above the water surface). The surface measurement was made by holding the instrument on the side of the boat, as high as possible so as to "see" as

much clear sky as possible. The instrument was then suspended on the sunny side of the boat at successive depths. During the start of the transect program these depths included 1 m intervals down to 6 m then at 2 m intervals down to a maximum of 18 m (the maximum length of the cable). Following upgrading of the instrument, including increasing cable length, the depth intervals were at 1 m from 1 m down to 10 m, then at 5 m intervals from 10 down to 45 m. The readings were noted manually. Once the instrument had reached its maximum depth it was raised quickly to the surface.

6.2 Results and Discussion

The attenuation coefficient of scalar PAR may be calculated using the Li-cor measurements. **Figure 6.1(a)** shows the natural log of the 'raw' Li-cor data for all stations on the 14th October 1997. Often the near surface measurements are affected greatly by surface effects. For all Li-cor data processing the top 6 m was discarded, unless the water was too shallow, in which case the top 6 m of measurements were included in calculations. Straight lines were fit to the logarithmic data curves below 6 m depth, as shown in **Figure 6.1(b)**, and the intercepts of these curves were used to extrapolate back to the surface to estimate the surface irradiance for the narrow band of light at the surface corresponding to the spectral band at depth. The goodness of fit of the straight lines to the profile data provides an estimate of the quality of the data. **Figure 6.2(a)** shows the percentage of surface irradiance with depth for all stations for the 14th October 1997. One must realize that the broad spectrum of irradiance (400-700 nm) near the surface is soon diminished in spectral extent as depth increases. The attenuation coefficient near the surface will tend to be very high as highly attenuated wavelengths are absorbed. The more penetrating wavelengths will not be attenuated as rapidly, hence the attenuation coefficient will tend to decrease with depth. One may calculate the attenuation of light at some depth, over a finite depth interval, or calculate the attenuation of light relative to some surface level. For this report the attenuation of PAR has been calculated relative to the surface value estimated by extrapolation of the data at depths greater than 6 m back to the surface (as in **Figure 6.1(a)**). **Figure 6.2(b)** shows the attenuation of PAR at all stations for 14th October 1997 from depths greater than 6 m measured relative to the surface extrapolated irradiance value. The shallower stations, H0 H5 and H15, have higher attenuation coefficients than the deeper stations. The shallower stations may be influenced by close proximity to shore and associated sediment or nutrient runoff, or by mixing of bottom sediments into the water column. **Figures 6.3(a) to 6.10(b)** show all the Li-cor measured attenuation coefficients averaged over depths from 6 m downwards (filled triangles), compared to the SeaWiFS measured K490 (filled diamonds joined by solid curve). Some plots also show the Secchi depth (empty squares), plotted along the right hand axis.

All data corresponding to dates and stations where SEADAS quality control flags were equal to zero were extracted from the data base and analyzed. **Figure 6.11** shows the SeaWiFS K490 data and the Li-cor Kpar data compared. The dashed lines on **Figures 6.11** indicate limits of 35% of the SeaWiFS K490 values (although the SeaWiFS Technical Memo. series does not

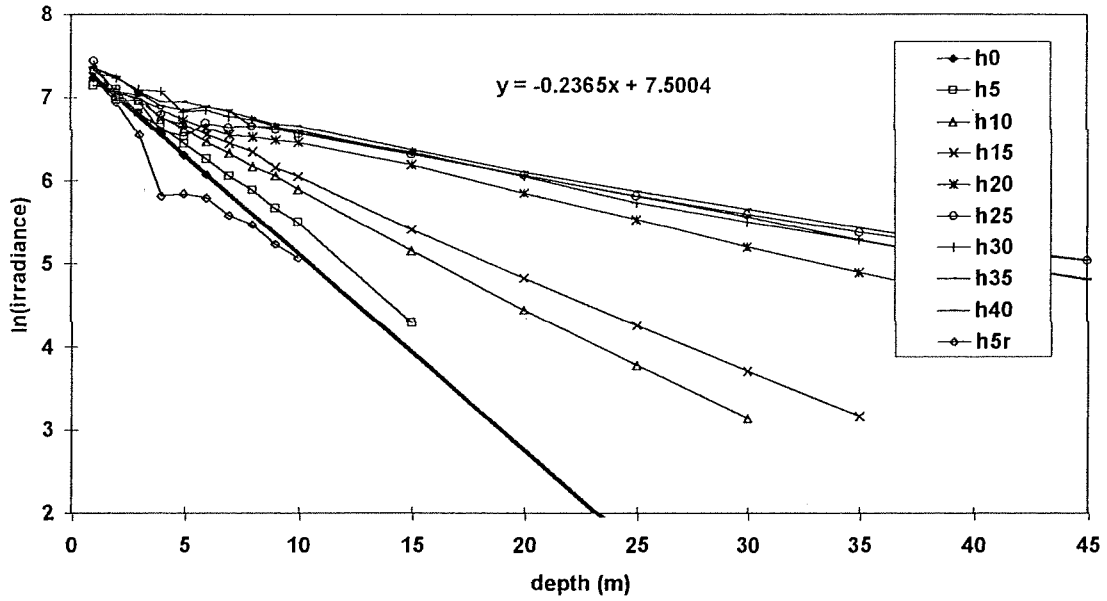
specify suggested uncertainty limits for the K490 product). Data points falling outside these lines may be considered to not support the ground truthing exercise. Most of the in-situ measured attenuation coefficients fall within the 35% limits, a pleasing result considering we are comparing attenuation coefficients of different spectral nature.

6.3 Conclusions

SeaWiFS Ocean Optics Protocols (Mueller and Austin 1995) advise that optical profiling instruments be deployed roughly from 3m to 15m (based on attenuation coefficients measured in this project) from a ship in an attempt to avoid ship shadow effects. They also suggest that deploying instruments from the stern of large research vessels may also help diminish ship shading effects. For this series of optical measurements deployment at distance from the research vessel was not possible. The guidelines do refer to large ocean going research vessels. The research vessel used in this series of measurements was small in size. Ship shadow effects have been avoided as much as possible by deploying instruments on the sunlit side of the boat. The good agreement between the satellite measured K490 and the Kpar values is very encouraging.

As suggested in the previous section on chlorophyll in-situ measurements and satellite derived measurements, the in-situ readings and satellite derived values do tend to agree, at least in the general trends indicated. The best comparisons between K-490 and the K-par tend to be for the transect dates when SeaWiFS quality control flags were equal to 0. For most of the stations beyond H15 the in-situ K-par measurements were well within 35% uncertainty associated with the K-490 satellite derived values. This good agreement suggests that satellite derived attenuation coefficients may be used, with reasonable confidence, to augment in-situ sampling, and also to support large spatial scale water quality studies. The satellite derived products help provide a regional overview, highlighting meso-scale structures and possible relationships between different water types.

LICOR - ln(Irradiance)
14th October 1997



Extrapolation of E back to surface (14/10/97)
(discard first 6 m)

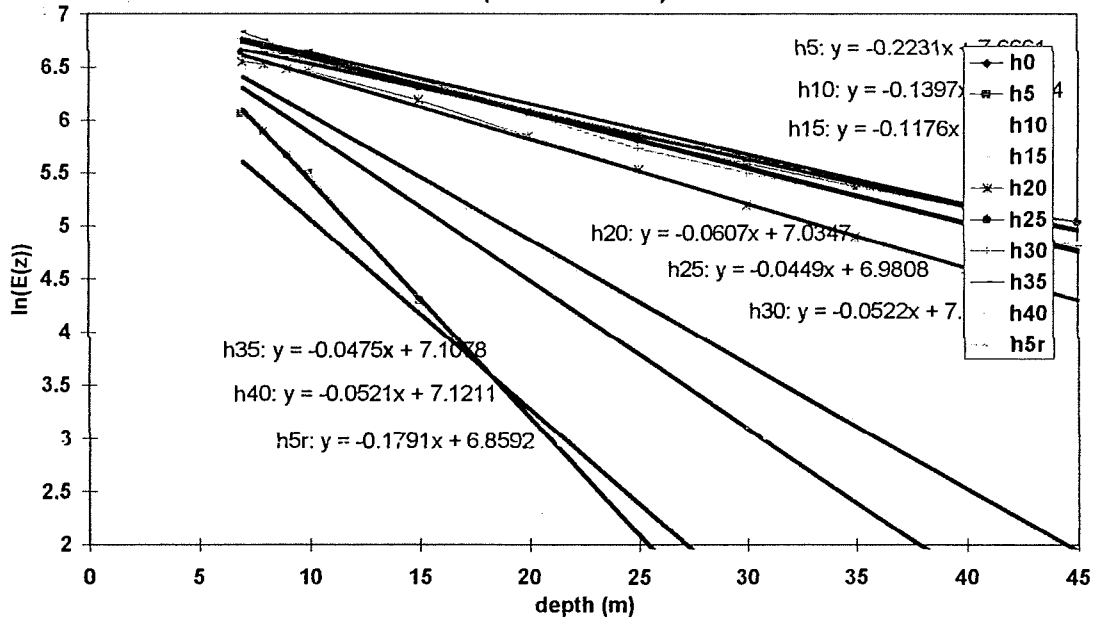


Figure 6.1 (a - top, b - bottom) Li-cor PAR (Photosynthetically Active Radiation) sensor data. Typically about the top 6 m of measurements are surface affected. When trendlines are fitted to the PAR profile data the top 6 m of data are removed, as shown in the lower figure. When the water is shallow however, as it is at station H0, then the complete profile is used to extrapolate (upper figure).

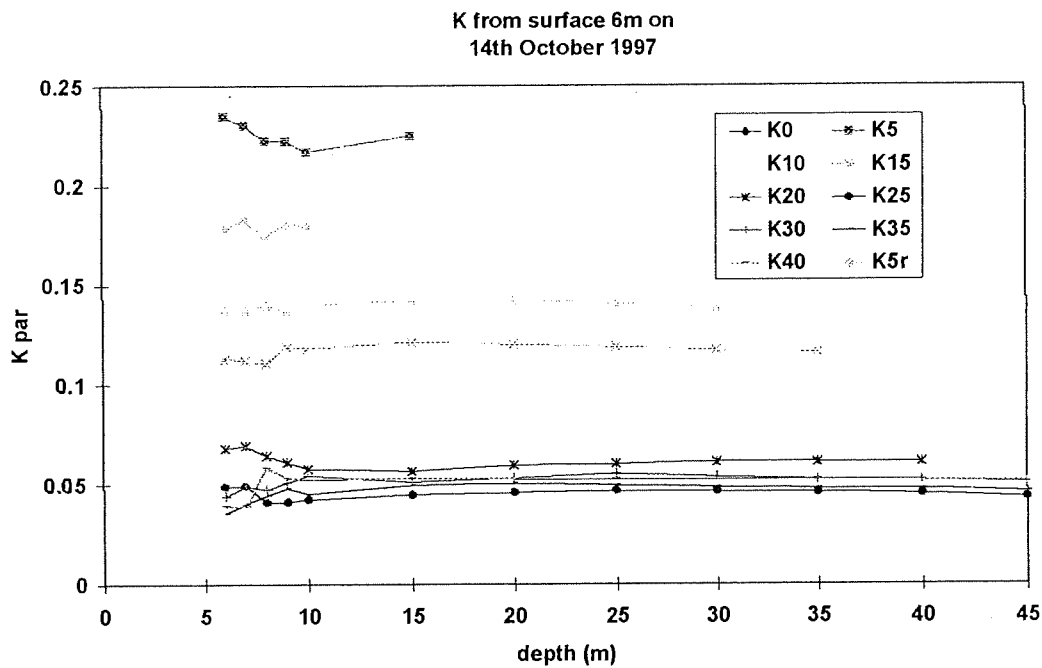
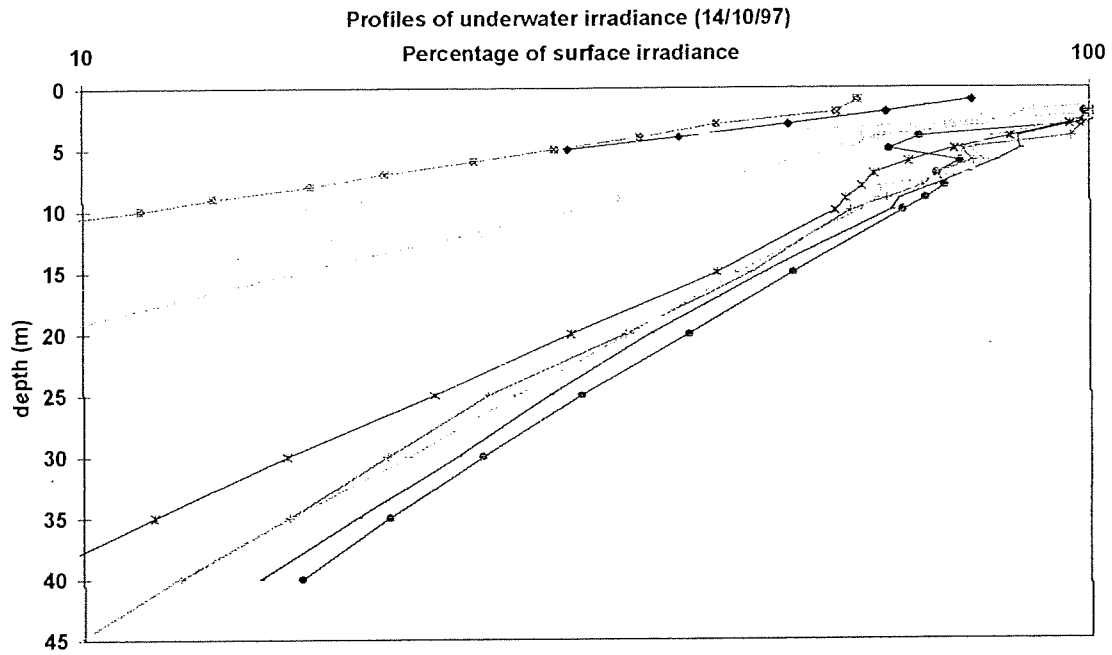
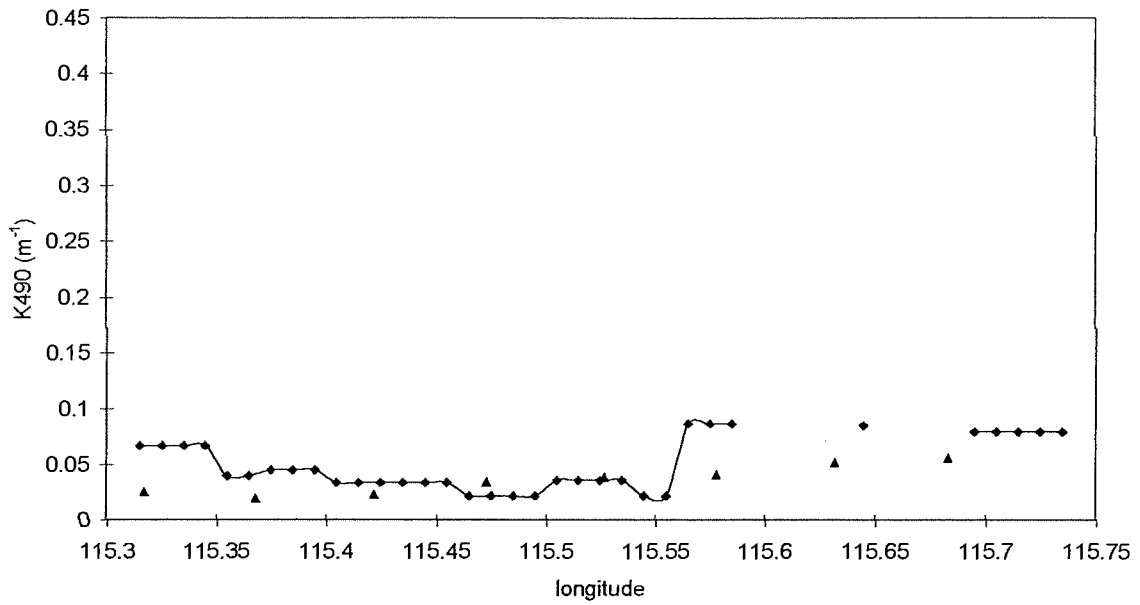


Figure 6.2 (a - upper, b - lower) Having determined the (sub)surface irradiance by extrapolation of PAR profile data, one may calculate the percentage of irradiance at depth as a percentage of the surface value (upper figure). The attenuation coefficient (K_{par}) may be calculated relative to the surface value, an indication of the average attenuation from the surface down to the specified depth. The average attenuation coefficient relative to the surface is shown in the lower figure. Note that data for the top 6 m has been discarded. Clearly the shallower water displays higher attenuation and deeper water displays lower attenuation.

Hillarys transect K490
16th December 1997



Hillarys transect K490
19th January 1998

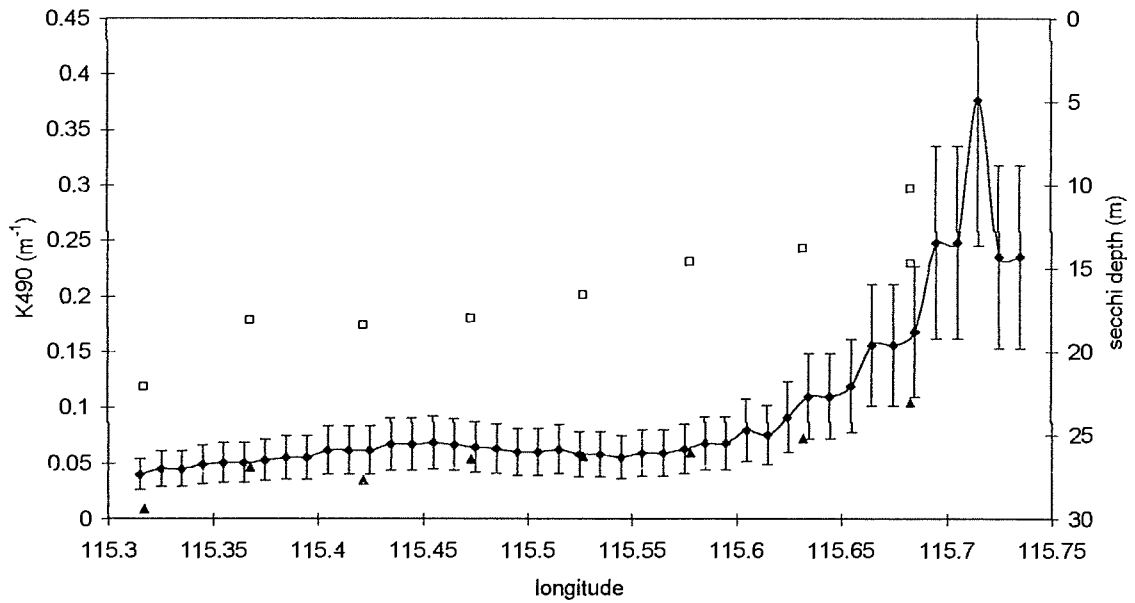


Figure 6.3 (a - top, b - bottom) Attenuation coefficient data obtained by in-situ measurement of PAR profiles (filled triangles) and K490 (attenuation coefficient at 490 nm) values derived from SeaWiFS data (filled diamonds and curve). Where error bars are shown this indicates the SeaWiFS quality control flags were zero for at least some portion of the pass. See Section 9 and Table 9.1 for information on the quality control flags. The error bars show $\pm 35\%$ accuracy for the SeaWiFS K490 product. The right hand axis (if present) is the scale for the Secchi depth (empty squares).

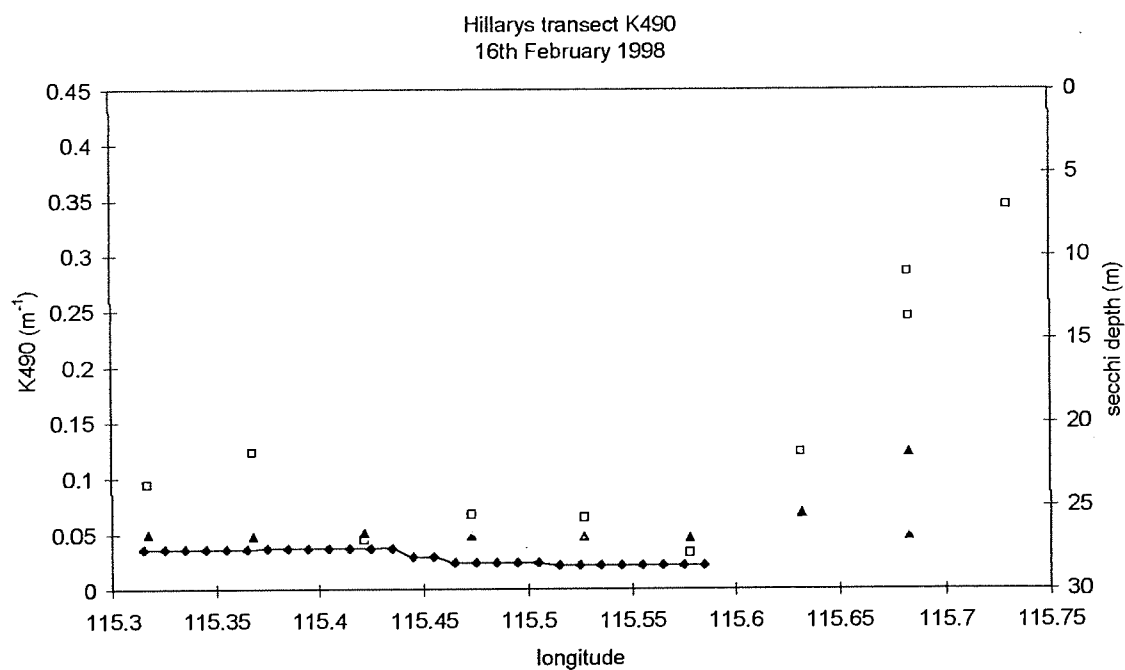
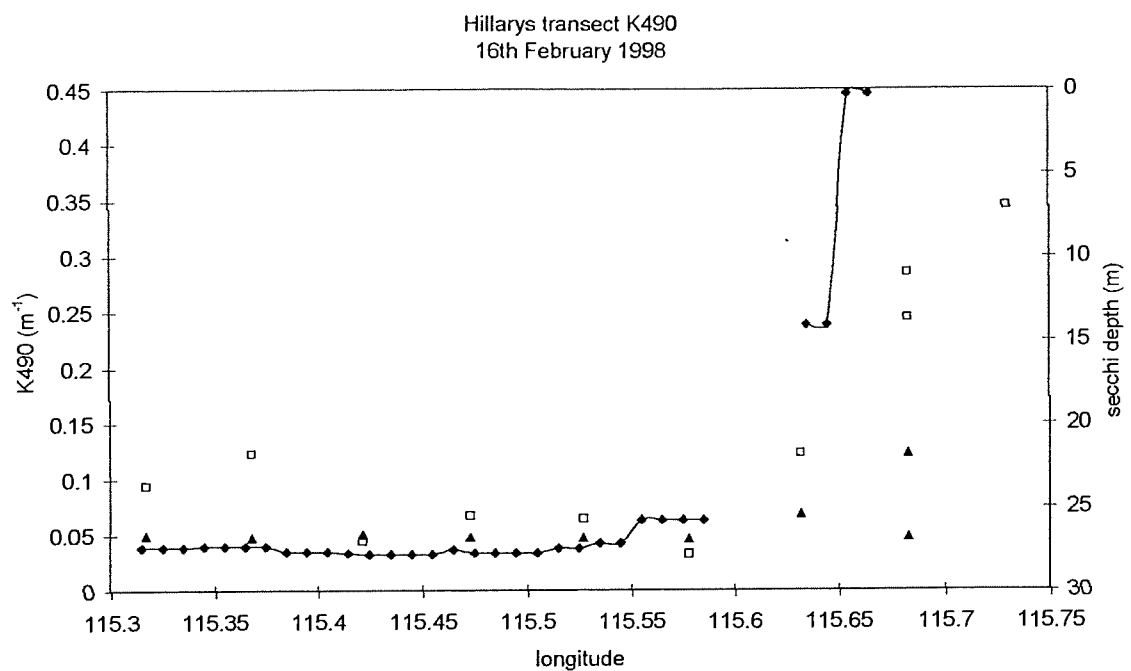


Figure 6.4 (a - top, b - bottom) Attenuation coefficient data obtained by in-situ measurement of PAR profiles (filled triangles) and K_{490} (attenuation coefficient at 490 nm) values derived from SeaWiFS data (filled diamonds and curve). The right hand axis is the scale for the Secchi depth (empty squares).

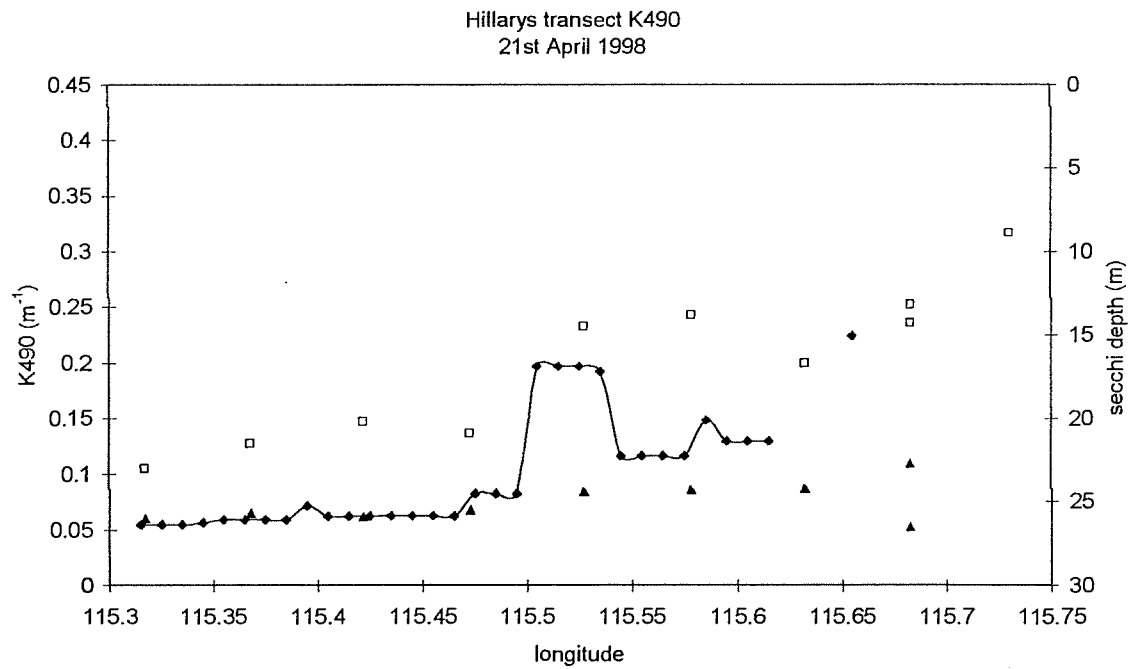
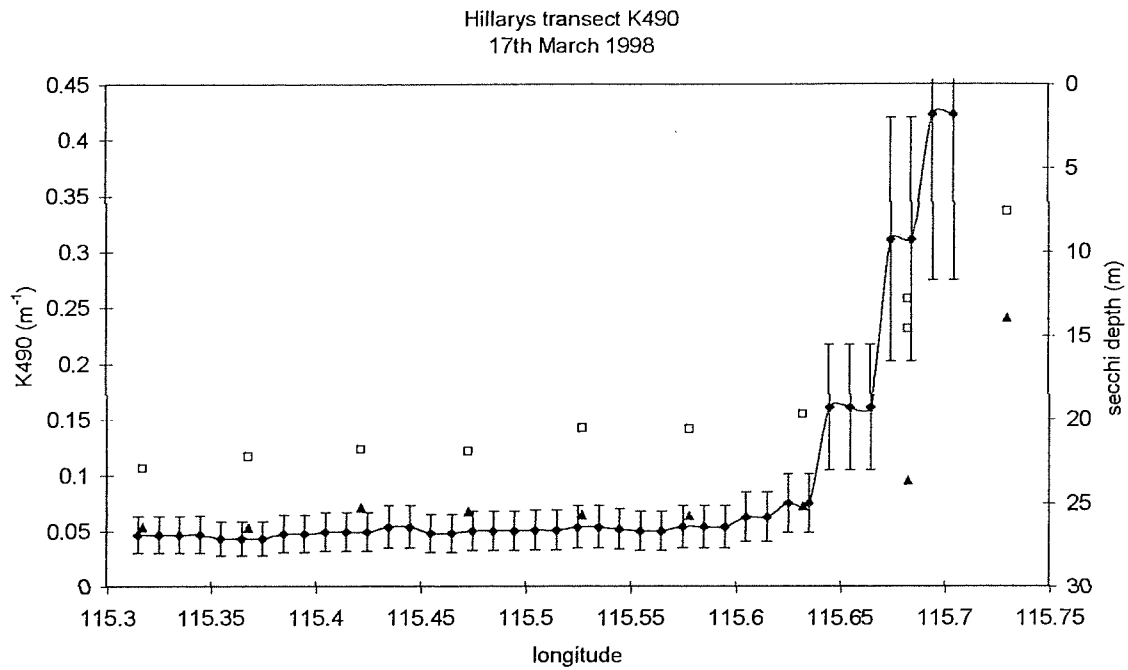


Figure 6.5 (a - top, b - bottom) Attenuation coefficient data obtained by in-situ measurement of PAR profiles (filled triangles) and K490 (attenuation coefficient at 490 nm) values derived from SeaWiFS data (filled diamonds and curve). Where error bars are shown this indicates the SeaWiFS quality control flags were zero for at least some portion of the pass. See Section 9 and Table 9.1 for information on the quality control flags. The error bars show $\pm 35\%$ accuracy for the SeaWiFS K490 product. The right hand axis is the scale for the Secchi depth (empty squares).

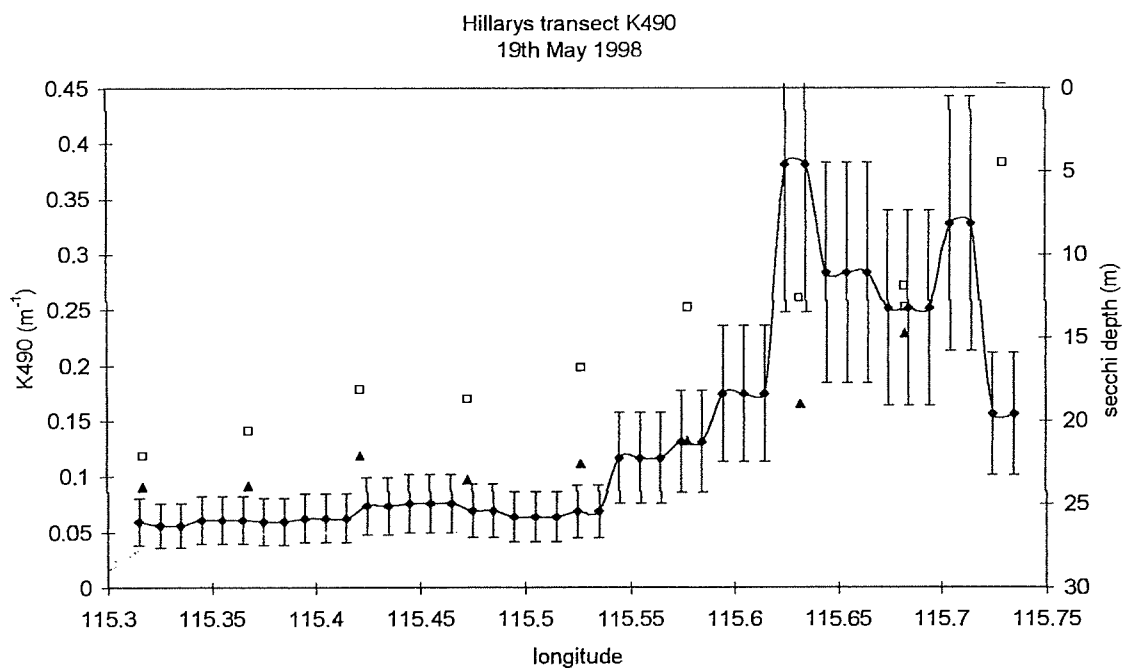
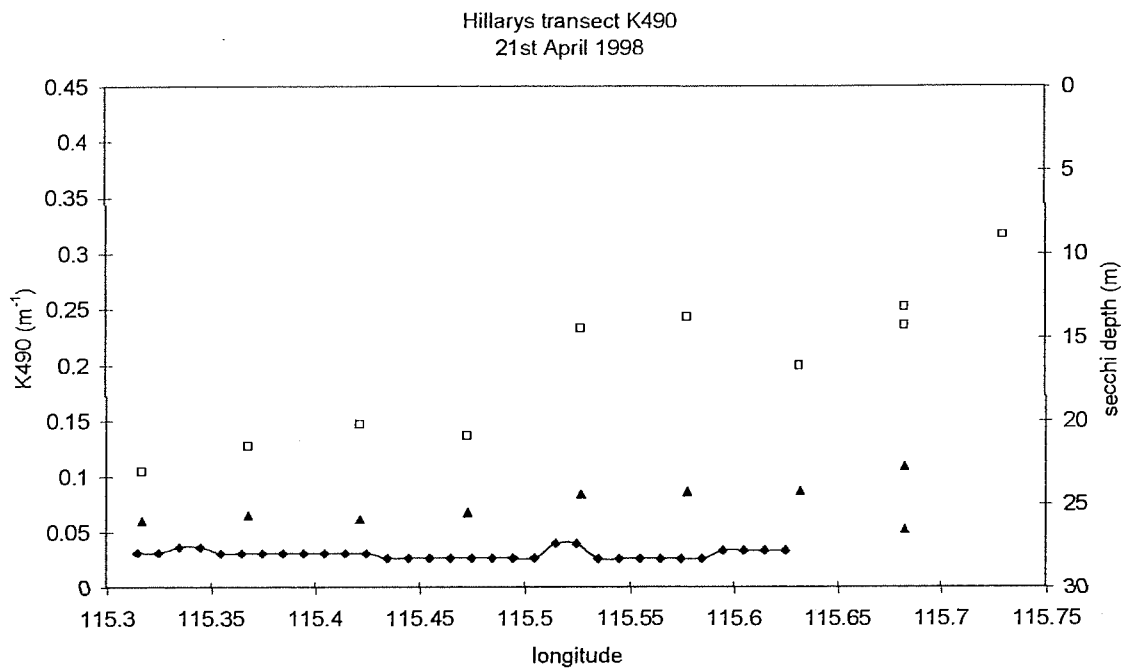


Figure 6.6 (a - top, b - bottom) Attenuation coefficient data obtained by in-situ measurement of PAR profiles (filled triangles) and K490 (attenuation coefficient at 490 nm) values derived from SeaWiFS data (filled diamonds and curve). Where error bars are shown this indicates the SeaWiFS quality control flags were zero for at least some portion of the pass. See Section 9 and Table 9.1 for information on the quality control flags. The error bars show $\pm 35\%$ accuracy for the SeaWiFS K490 product. The right hand axis is the scale for the Secchi depth (empty squares).

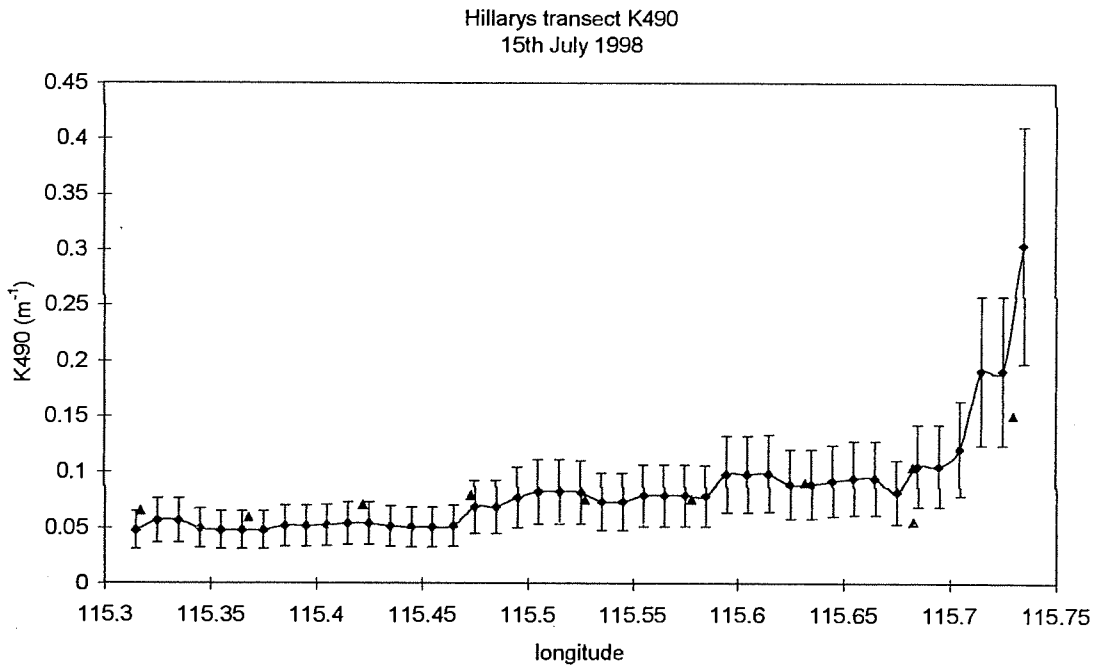
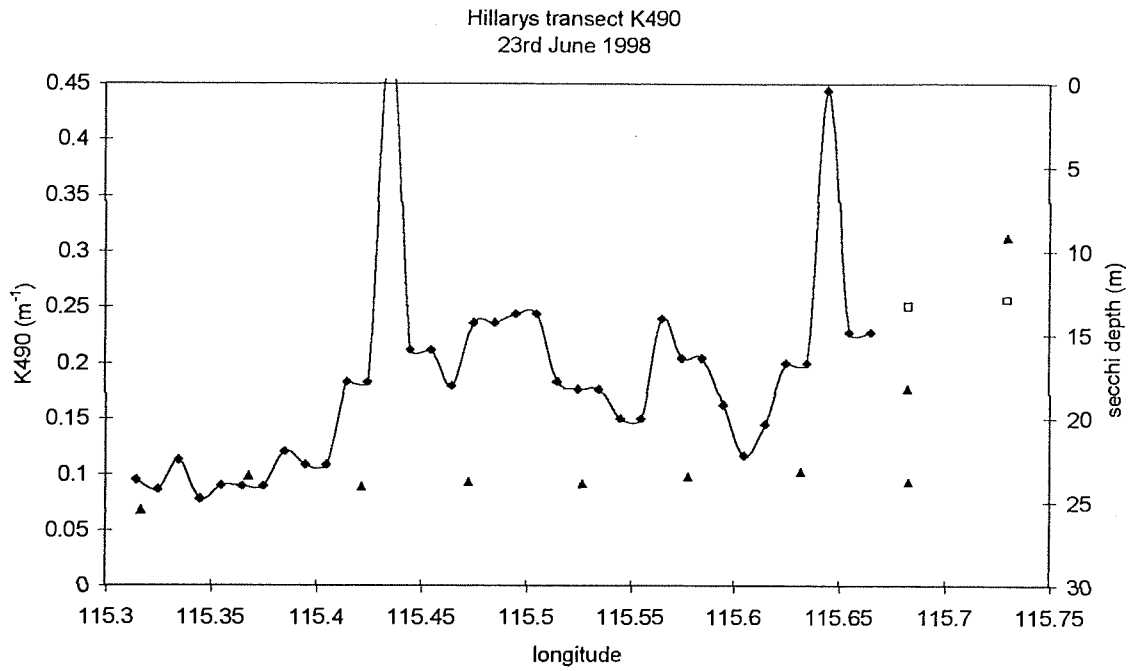


Figure 6.7 (a - top, b - bottom) Attenuation coefficient data obtained by in-situ measurement of PAR profiles (filled triangles) and K490 (attenuation coefficient at 490 nm) values derived from SeaWiFS data (filled diamonds and curve). Where error bars are shown this indicates the SeaWiFS quality control flags were zero for at least some portion of the pass. See Section 9 and Table 9.1 for information on the quality control flags. The error bars show $\pm 35\%$ accuracy for the SeaWiFS K490 product. The right hand axis (if present) is the scale for the Secchi depth (empty squares).

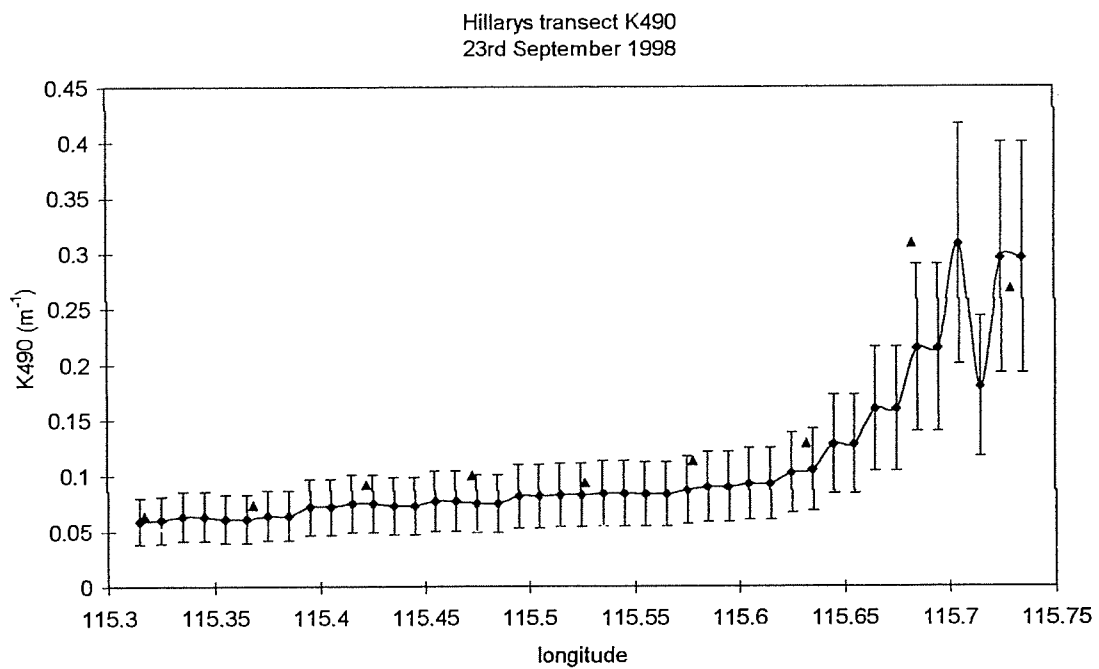
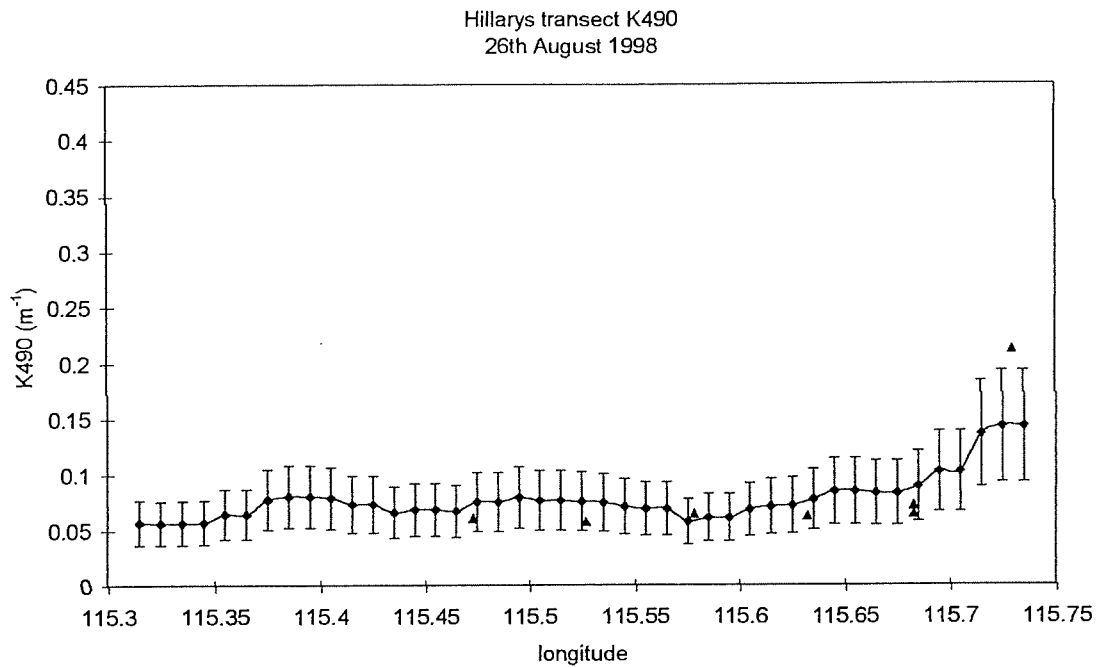


Figure 6.8 (a - top, b - bottom) Attenuation coefficient data obtained by in-situ measurement of PAR profiles (filled triangles) and K490 (attenuation coefficient at 490 nm) values derived from SeaWiFS data (filled diamonds and curve). Where error bars are shown this indicates the SeaWiFS quality control flags were zero for at least some portion of the pass. See Section 9 and Table 9.1 for information on the quality control flags. The error bars show $\pm 35\%$ accuracy for the SeaWiFS K490 product.

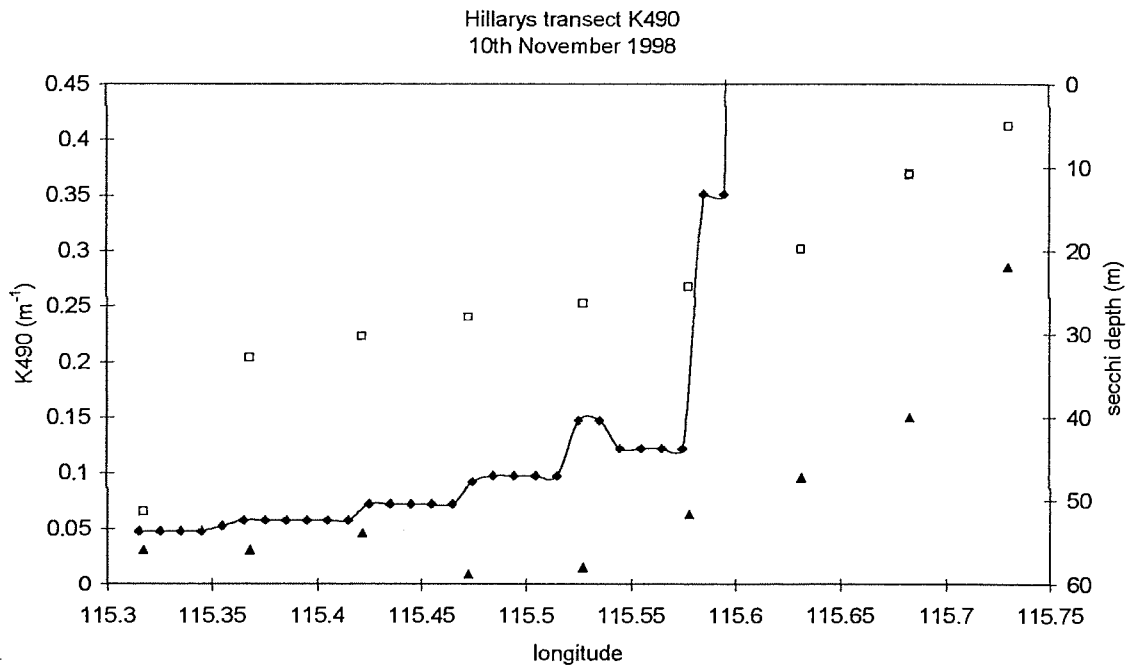
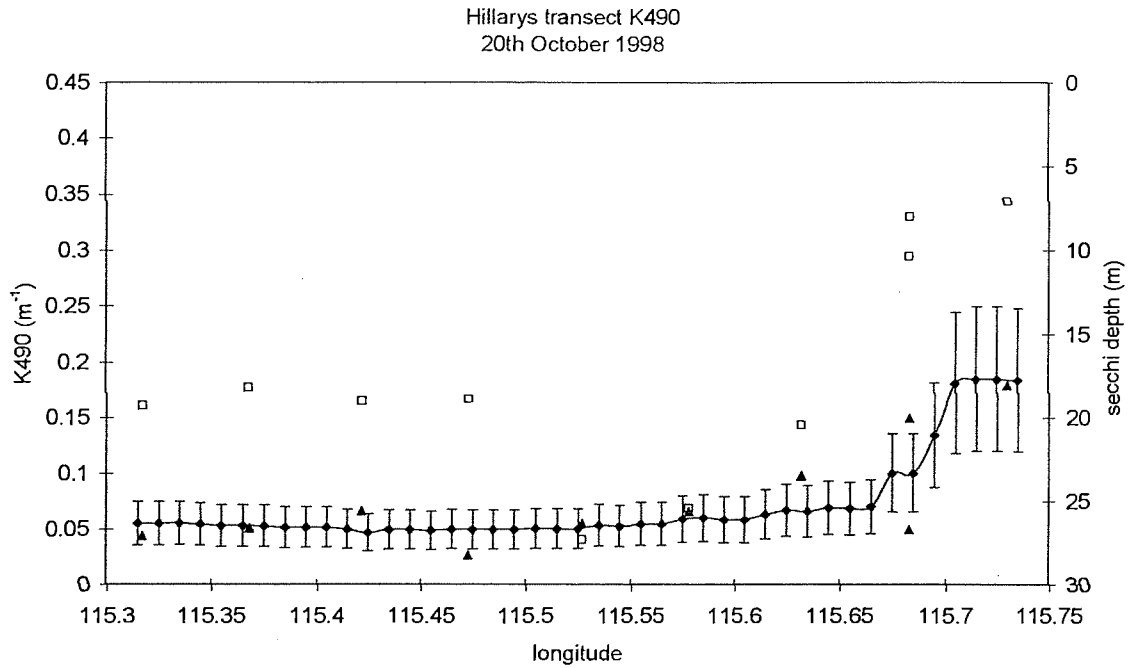


Figure 6.9 (a - top, b - bottom) Attenuation coefficient data obtained by in-situ measurement of PAR profiles (filled triangles) and K490 (attenuation coefficient at 490 nm) values derived from SeaWiFS data (filled diamonds and curve). Where error bars are shown this indicates the SeaWiFS quality control flags were zero for at least some portion of the pass. See Section 9 and Table 9.1 for information on the quality control flags. The error bars show $\pm 35\%$ accuracy for the SeaWiFS K490 product. The right hand axis is the scale for the Secchi depth (empty squares).

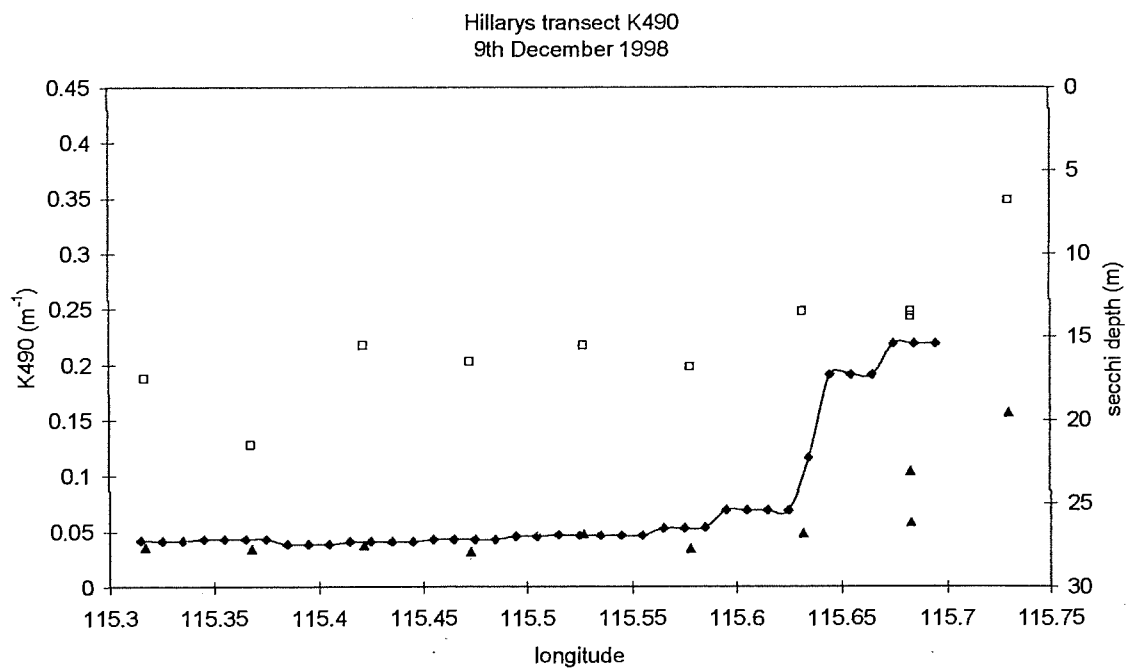
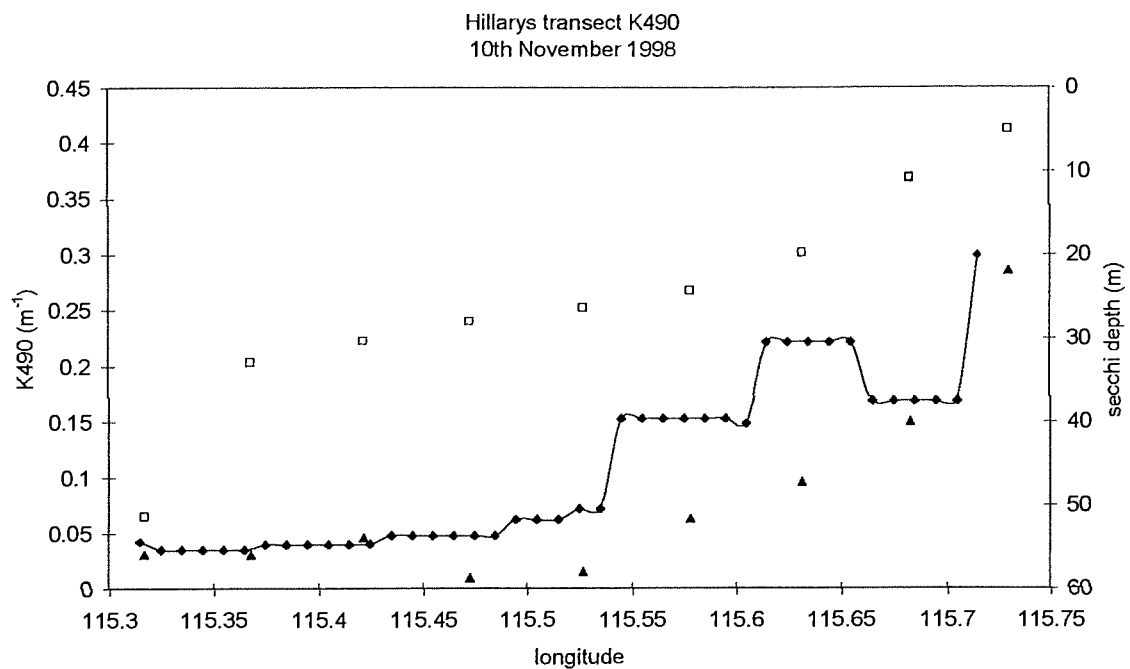


Figure 6.10 (a - top, b - bottom) Attenuation coefficient data obtained by in-situ measurement of PAR profiles (filled triangles) and K490 (attenuation coefficient at 490 nm) values derived from SeaWiFS data (filled diamonds and curve). The right hand axis is the scale for the Secchi depth (empty squares).

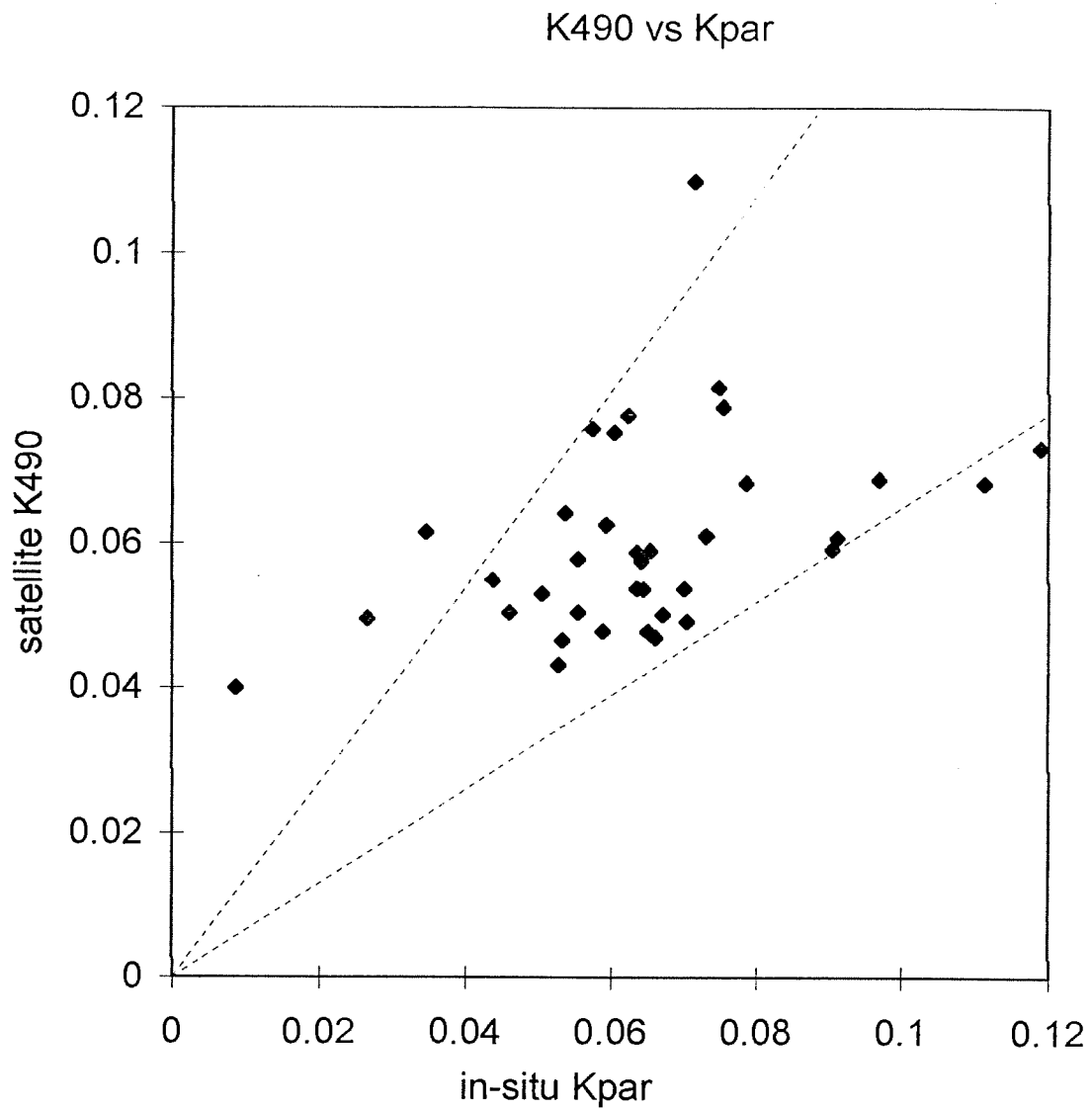


Figure 6.11 Comparison between SeaWiFS K490 data and Kpar measurements derived from in-situ PAR profile measurements using the Li-cor PAR sensor. These data correspond to dates and station locations where the SeaWiFS K490 data had Level 2 processing flags of zero value. See section 9 and tables 9.1 and 9.2 therein. The dashed lines indicate a $\pm 35\%$ accuracy for the remotely sensed K490 product.

Section 7: Meteorology (Alan Pearce)

To provide some background meteorological information for the transects, some simple measurements were made of wind and air temperature at each station. While not highly accurate, they provide a convenient record of weather conditions to help explain some of the anomalies in the SST and ocean colour data. The results are therefore not presented here.

Wind

Wind speed was measured on each station using a hand-held Watski anemometer by visually noting the range of speeds (knots) over five 10-second periods about a minute apart, by an observer standing on the bridge of the boat; the height above the sea surface was about 5 m. Wind direction was noted by using a compass monocular to read the direction from which the wind was blowing. These observations were generally made by the boat crew.

The mean wind speed for the station was computed from the 10 readings and converted to m/s. There was some indication that the observed wind speed depends on the angle the anemometer was held to the wind, so some calibration is clearly required. There may on occasion have been some obstruction from the vessel's superstructure but this was minimised where possible.

Hourly measurements of wind and air temperature (*inter alia*) are made by the National Tidal Facility Seaframe weather station at Hillarys Marina, while 1/2-hourly data are also available from the Automatic Weather Station (AWS) operated by the Bureau of Meteorology on Rottnest Island. 10-minute winds have also been obtained from an anemometer on top of the 70 m high Fremantle Port Authority (FPA) building in Fremantle. The data have not yet been analysed in full, but are available to complement the on-board wind observations.

Air temperature

Wet- and dry-bulb thermometer readings were taken from the bow of the boat using a Zeal psychrometer, and the relative humidity was derived from a table of wet-bulb depression vs. dry-bulb. Air temperatures have also been obtained from the Seaframe facility at Hillarys marina, the AWS at Rottnest Island and the FPA.

Section 8: AVHRR imagery (Alan Pearce)

Advanced Very High Resolution Radiometer (AVHRR) satellite imagery has been received in Perth since 1981, and NOAA-14 images for each Hillarys transect have been obtained from the Western Australian Satellite Technology and Applications Consortium (WASTAC). These images are used here both to show the gross surface thermal structure across the continental shelf off Perth (including the warm Leeuwin Current offshore) and for comparison of the satellite-derived sea-surface temperatures (SSTs) against *in situ* measurements from the Hillarys transect data.

8.1 Data and Methods

Satellite image processing

Full-resolution NOAA-14 AVHRR images for the southwestern region of Western Australia (covering the latitude range 30° to 35°S) were obtained from the Western Australian Satellite Technology and Applications Consortium (WASTAC) and the Remote Sensing Services Section of the WA Department of Land Administration (DOLA) for each transect day. These were in mNOAA format, the image processing package which has been used for displaying the images in this phase of the project. The standard mNOAA area-7 image covers the transect area. These images were displayed and enhanced to show thermal structures associated with the Leeuwin Current and coastal waters in the vicinity of the transect.

For quantitative analysis:

- 1) a 102 line by 87 pixel block covering the area 31.5° to 32.5°S, 114.9° to 115.9°E was extracted from each image, containing the raw counts in AVHRR bands 1 and 2, the brightness temperatures T4 and T5, and the McMillin and Crosby (1984) and Non-Linear SST (NLSST) sea-surface temperatures. In an earlier study examining a variety of SST algorithms, Pearce *et al.* (1989) found the McMillin and Crosby SST algorithm to be the most appropriate for Perth coastal waters, but the more recent NLSST takes into account scan-angle effects which may be important near the edges of the swath.
- 2) The position of Rottnest Island was identified using the AVHRR band 2, and the latitude of the Hillarys transect was then found by moving up 19 lines from the south-western corner of the Island; this manual procedure was to minimise geolocation errors in latitude.
- 3) The transect line as well as the adjacent line on each side were extracted for band 2 (to show land and clouds), the McMillin & Crosby SST and the NLSST. The presence of cloud was assessed by examining the variability in the 3*3 arrays in band 2.
- 4) To compensate for longitudinal geolocation (east-west) errors, the transects were manually adjusted so that they all matched at the coast. The estimated positional accuracy is therefore +-1 pixel.
- 5) The running means of 3*3 pixel arrays were computed along the three extracted bands to reduce small-scale variability. For the inshore station H0, which was just off Hillarys Marina, the

average was taken of the 3 pixels immediately adjacent to the coast instead of the 9-pixel block which would have included land.

6) Transect charts were plotted to show the comparison between the two SST algorithms and the in situ (bucket) temperatures, as well as the cross-shelf variability.

Table 8.1: List of ascending (daytime) NOAA-AVHRR orbits processed for the Hillarys transects. The maximum elevation of the satellite pass is shown as an indicator of the scan-angles involved. When the pass was cloudy, a clear image for an adjacent day was selected (flagged * here).

Date	(DayNo)	Sat/Orbit	(WAST)	MaxElev	Notes
7 Oct 1996*	(96281)	N14/09125	(1421)	66°E	(adjacent day)
8 Oct 1996	(96282)	N14/09139	(1410)	53°E	cloudy
11 Nov 1996	(96316)	N14/09619	(1442)	73°W	
10 Dec 1996	(96345)	N14/10028	(1428)	75°E	
13 Jan 1997	(97013)	N14/10508	(1459)	57°W	
16 Feb 1997*	(97047)	N14/10988	(1530)	30°W	(adjacent day)
17 Feb 1997	(97048)	N14/11002	(1519)	38°W	cloudy
19 Mar 1997	(97078)	N14/11425	(1452)	73°W	
21 Apr 1997	(97111)	N14/11891	(1534)	30°W	cloudy
23 Apr 1997*	(97109)	N14/11919	(1512)	48°W	(adjacent day)
21 May 1997	(97141)	N14/12314	(1507)	56°W	
16 Jun 1997	(97167)	N14/12681	(1525)	39°W	
21 Jul 1997	(97202)	N14/13174	(1403)	31°E	
21 Jul 1997	(97202)	N14/13175	(1543)	28°W	
20 Aug 1997	(97232)	N14/13598	(1516)	51°W	
17 Sep 1997	(97260)	N14/13993	(1511)	63°W	
14 Oct 1997	(97287)	N14/14374	(1516)	56°W	
18 Nov 1997	(97322)	N14/14868	(1534)	41°W	
15 Dec 1997	(97349)	N14/15249	(1539)	39°W	
19 Jan 1998	(98019)	N14/15742	(1415)	30°E	
19 Jan 1998	(98019)	N14/15743	(1556)	29°W	
16 Feb 1998	(98047)	N14/16137	(1409)	25°E	
16 Feb 1998	(98047)	N14/16138	(1549)	34°W	
17 Mar 1998	(98076)	N14/16547	(1531)	53°W	
21 Apr 1998	(98111)	N14/17041	(1557)	32°W	
17 May 1998*	(97137)	N14/17408	(1602)	31°W	(adjacent day)
19 May 1998	(98139)	N14/17436	(1540)	51°W	cloudy
23 Jun 1998	(98174)	N14/17930	(1555)	38°W	
15 Jul 1998	(98196)	N14/18240	(1512)	79°E	
25 Aug 1998*	(98257)	N14/18819	(1602)	38°W	(adjacent day)
26 Aug 1998	(98258)	N14/18833	(1550)	48°W	cloudy
23 Sep 1998	(98266)	N14/19228	(1541)	63°W	
20 Oct 1998	(98293)	N14/19609	(1543)	62°W	
9 Nov 1998*	(98313)	N14/19891	(1522)	75°E	(adjacent day)
10 Nov 1998	(98314)	N14/19905	(1511)	59°E	cloudy
9 Dec 1998	(98343)	N14/20314	(1450)	59°E	

Cloud prevented acquisition of useful AVHRR images on 6 of the transect days; adjacent days were processed (if clear) to show regional features of the Leeuwin Current at the time but

these were not used in the SST validation analysis. On 3 occasions (July 1997 and January and February 1998), the satellite orbits were such that two successive AVHRR passes overlapped the area, enabling a comparison of the SST accuracy from near the edges of the passes, one (the eastern pass) with a largely land air mass and the other (western) entirely over water.

8.2 Results and Discussion

Satellite images

The satellite images clearly show the seasonal change across the continental shelf. As described in **Section 3**, the Leeuwin Current (depicted as red in **Figure 8.1a**) is present along the outer shelf during the winter months. At the same time, the coastal nearshore waters have cooled (shown as blue) so there is a strong temperature gradient from the coast out into the Leeuwin Current. In summer, on the other hand, the shallow nearshore waters have warmed (**Figure 8.1b**, orange/yellow strip along the coast) and the Capes Current is transporting cool water northward (blue); offshore the weak Leeuwin Current (red/yellow) is now patchy and ill-defined. Cross-shelf temperature gradients are correspondingly weak.

On occasion, tongues of warm Leeuwin Current water penetrate across the continental shelf towards the coast (**Figure 8.2a**), representing active cross-shelf exchange with the coastal region and having important implications for the transport of larvae to/from the inshore waters. As found previously using satellite-tracked drifting buoys (Cresswell 1980), large eddies peeling offshore from the main current are also a feature of many images (**Figure 8.2b**) and illustrate the complex nature of the surface currents along the Western Australian coast.

Transect plots

Plots of the McMillin-Crosby and NLSST full-resolution SSTs and the Hillarys bucket temperatures have been generated for each of the cloud-free transects. As pointed out above, on 3 occasions the Hillarys area was at the edge of two overlapping swaths from adjacent orbits about 100 minutes apart, in which cases both transects have been plotted for comparison.

Generally, the cross-shelf surface structure was faithfully followed by the satellite data, allowing for the time difference between the transect measurements (0900 to about 1230) and the satellite overpass (1400 to 1600 -- **Table 8.1**). Sometimes the fit was remarkable (e.g. **Figures 8.3h, j and l**) indicating that the satellite temperatures were reliable right up to the coast itself. The inshore cooling in winter was very evident (**Figure 8.3 a, i, j, l, t, u, w**) as was the warming along the coast in summer (with the cooler Capes Current mid-shelf: **Figure 8.3 e, o, p**). Usually the temperature continued to rise into the Leeuwin Current along the outer shelf, although on occasion the Current was particularly narrow and well-defined on the shelf (**Figure 8.3 i and w**, confirmed by the satellite images, not included here, which also reveal that in both cases there was another filament of the Leeuwin Current further offshore). In most cases, the repeat station at H5 in the early afternoon encountered slightly warmer conditions than in the morning, and these tended to agree better with the satellite temperatures and so reflected the gradual warming of the near-

coastal water during the day. In August and November 1997 and perhaps July 1998 (**Figures 8.3j, n and u**) this was not the case.

The repeated station at H5 allowed some estimate of water temperature changes over the 4 hours between the outward (about 0930 hrs) and inward (about 1330) segments. The temperature difference varied from 0.3° cooling to about 1°C warming (usually in summer). The SDL vertical temperature profiles indicate that on the occasions when the temperature rise at H5 was over 0.6°C, most of this was direct warming in the top 2 or 3 m of water, and sometimes despite 10 to 20 knots of wind blowing. Hourly temperatures from a self-recording temperature logger moored at mid-depth in about 6 m of water in Marmion Lagoon enabled independent estimates to be made of the temperature change during the 5 hours or so between the inshore transect stations and the AVHRR overpass (about 3pm). The temperature logger data were available for irregular periods between the first transect in October 1996 and March 1998 (Pearce and Pether, in prep.). The maximum temperature rise during the 5-hour period varied between 0° and 0.4°C, the latter (as would be expected) during the summer months. These measurements indicate that surface warming between the time of the station measurements and that of the satellite overpass can be up to a degree.

On those 3 occasions when there were two overlapping AVHRR passes on the same afternoon, the two profiles generally agreed very well (albeit with the anticipated subtle changes in the smaller-scale structure) despite the large zenith (scan) angles from the satellite -- note the large satellite elevations in **Table 8.1**. In July 1997 (**Figure 8.3k**) there was a slight cooling over the inner shelf between the two overpasses, and in January 1998 (**Figure 8.3p**) there was small warming over mid-transect. The situation in February 1998 (**Figure 8.3q**) was interesting in that the NLSST remained almost constant between the two overpasses, whereas the McMillin-Crosby SST was initially 1°C cooler than the NLSST (but fitted the *in situ* temperature better) but by the next overpass the McMillin-Crosby SST had risen to within 0.3°C of the NLSST.

The only major disagreement between the transect surface temperatures and the AVHRR was in November 1996 (**Figures 8.3c and d**), when there were difficulties with both the *in situ* and satellite temperatures: On the day of the transect (11th November) the AVHRR SSTs were way too high and did not match the cross-shelf structure indicated by the bucket measurements, whereas on the previous day the satellite temperatures were about 4°C cooler and matched the surface measurements near the coast. On this occasion neither the underway temperatures nor the SDL showed the elevated bucket temperatures at the outer end of the transect. The transect day was very calm (although cloudy) with winds of only about 1 m/s when the boat was along the outer transect, so there must have been some surface heating which affected the bucket but not the YSI or SDL measurements -- for future work, higher precision near-surface sampling techniques should be used to more adequately resolve vertical stratification in the upper metre of ocean under calm conditions.

The 3° to 4°C temperature difference between the surface and satellite measurements and the difference in the AVHRR SSTs between the 10th and 11th (**Figures 8.3c and d**) indicate that the satellite measurements on the transect day were in error. The colour satellite image for that day indicates that there was in fact patchy cloud offshore of the transect even though this did not show up in the Band 2 data over the transect itself. The T4-T5 difference on the 11th (1.5° to 2.5°C) was *much* higher than on the 10th (<0.5°C), resulting in a very large SST correction and pushing the derived SSTs well above the *in situ* temperatures. Examination of the thermal calibration data (see Pearce *et al.* 1989 for details of the procedure) indicates that the gradients, intercepts and target temperatures for the 10th and 11th were very similar, but the atmospheric water vapour loading (courtesy of the Bureau of Meteorology) was much higher on the 11th, so water vapour/cloud was almost certainly responsible for the erroneous satellite SSTs on that day. Clearly, more sophisticated cloud-screening techniques than used here will be required for future work.

Satellite-surface scatterplots

The general comparison between the satellite-derived SSTs and the bucket temperatures (**Figure 8.4**) shows reasonably good agreement from both algorithms. The basic statistics, with a sample size of 207 samples, are:

Algorithm	Corr.	Bias (°C)	RMS Diff. (°C)
McMillin-Crosby	0.945	0.19	0.58
NLSST	0.949	0.36	0.64

The results for McMillin-Crosby are similar to those found by Pearce *et al.* (1989) in an earlier study from a much smaller dataset off Perth using NOAA-7 and NOAA-9 data, with a bias of less than 0.2°C (absolute value) and RMS difference 0.6°C. Interestingly, the NLSST results are not as good as the simple algorithm. The histograms (**Figure 8.5**) indicate that about 65% of the McMillin-Crosby SSTs fall within $\pm 0.5^\circ\text{C}$ of the *in situ* temperatures and 88% within $\pm 1^\circ\text{C}$, while the corresponding statistics for the NLSST are 62% and 86% respectively.

8.3 Conclusions

Using established algorithms, satellite-derived SSTs compare favourably with surface measurements despite the differences in area sampled, time-of-day, depth layer sampled and sensor type. Some two-thirds of the satellite observations fall within 0.5°C of the surface (bulk) temperatures. On the other hand, differences of over 2°C and even exceeding 5°C can exist on occasion, apparently due to undetected cloud (perhaps high and thin cirrus) so more reliable means of screening cloud from the images is required.

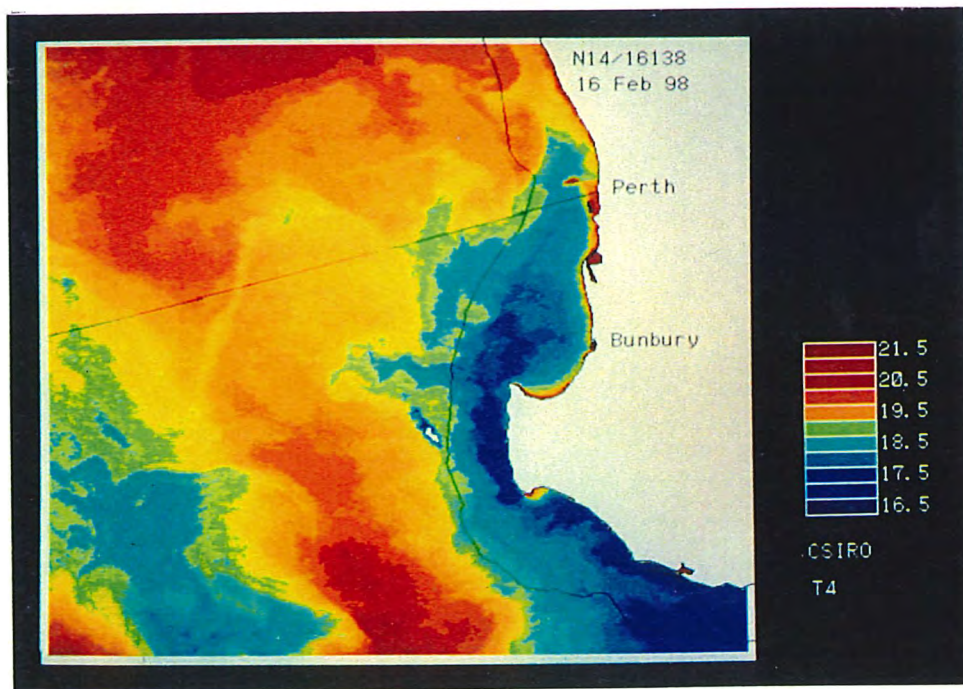
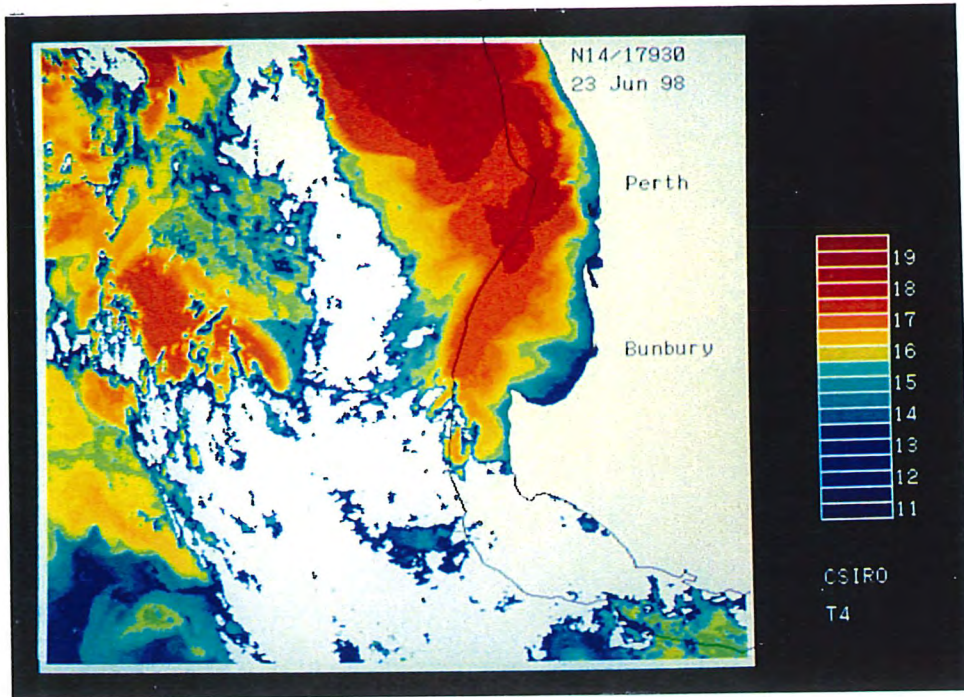


Figure 8.1: NOAA-AVHRR satellite images showing the sea-surface temperature off the southwestern coast in (upper) June 1998 (representing winter conditions) and (lower) February 1998 (summer). The warmest water is depicted as red, cooling through yellow and green to the coolest water in blue; the temperatures are the brightness temperatures in AVHRR band 4, and have not been corrected for atmospheric absorption. Patchy white areas offshore are clouds. The black contour marks the position of the 200 m isobath, approximately delineating the edge of the continental shelf.

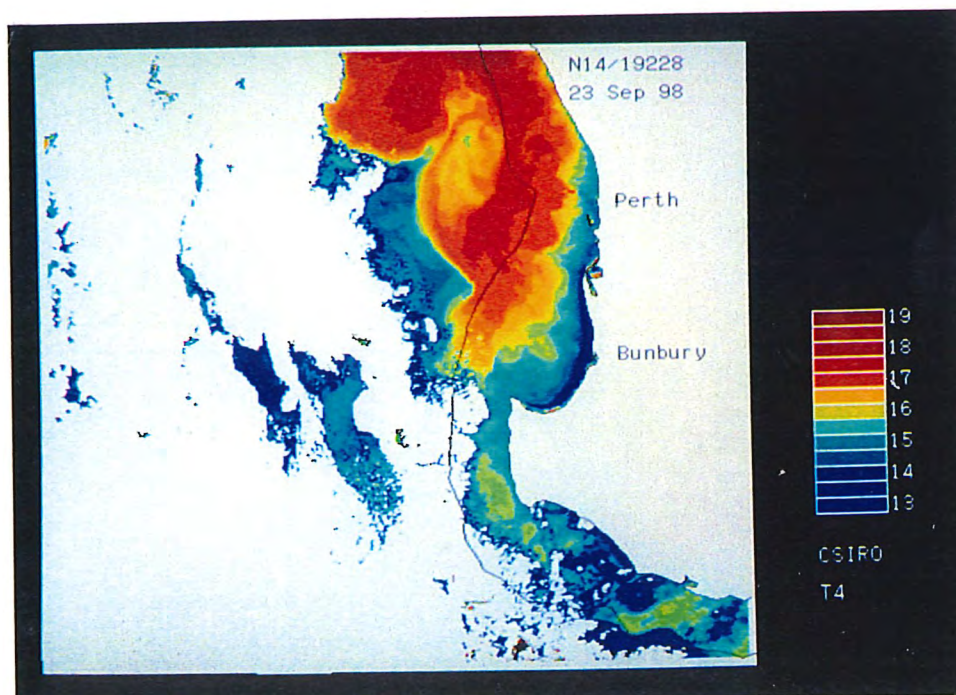
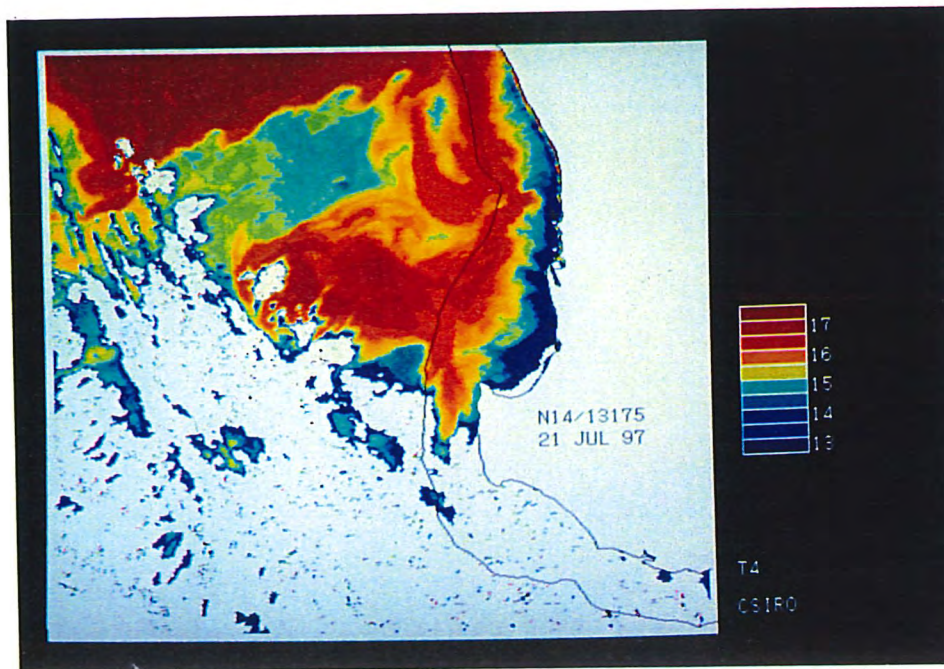
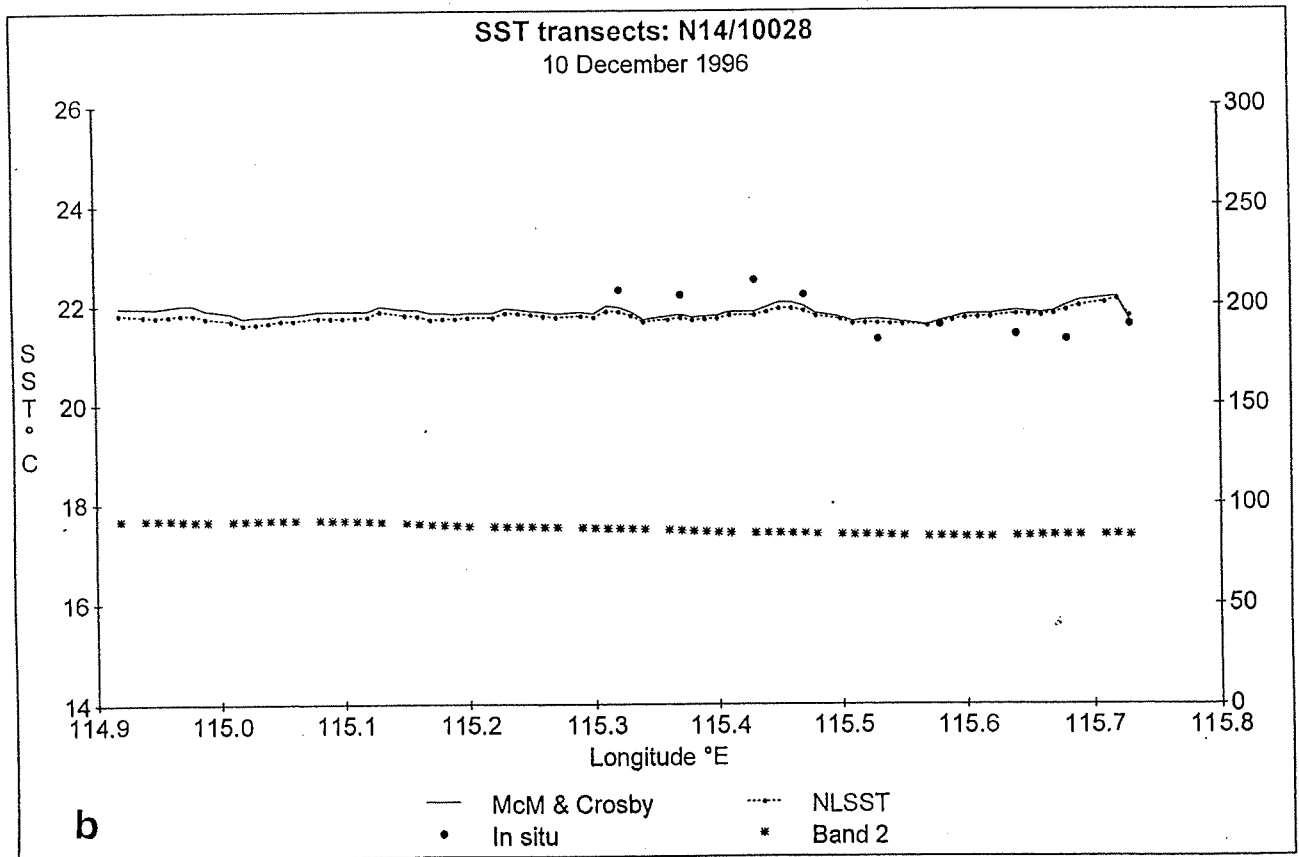
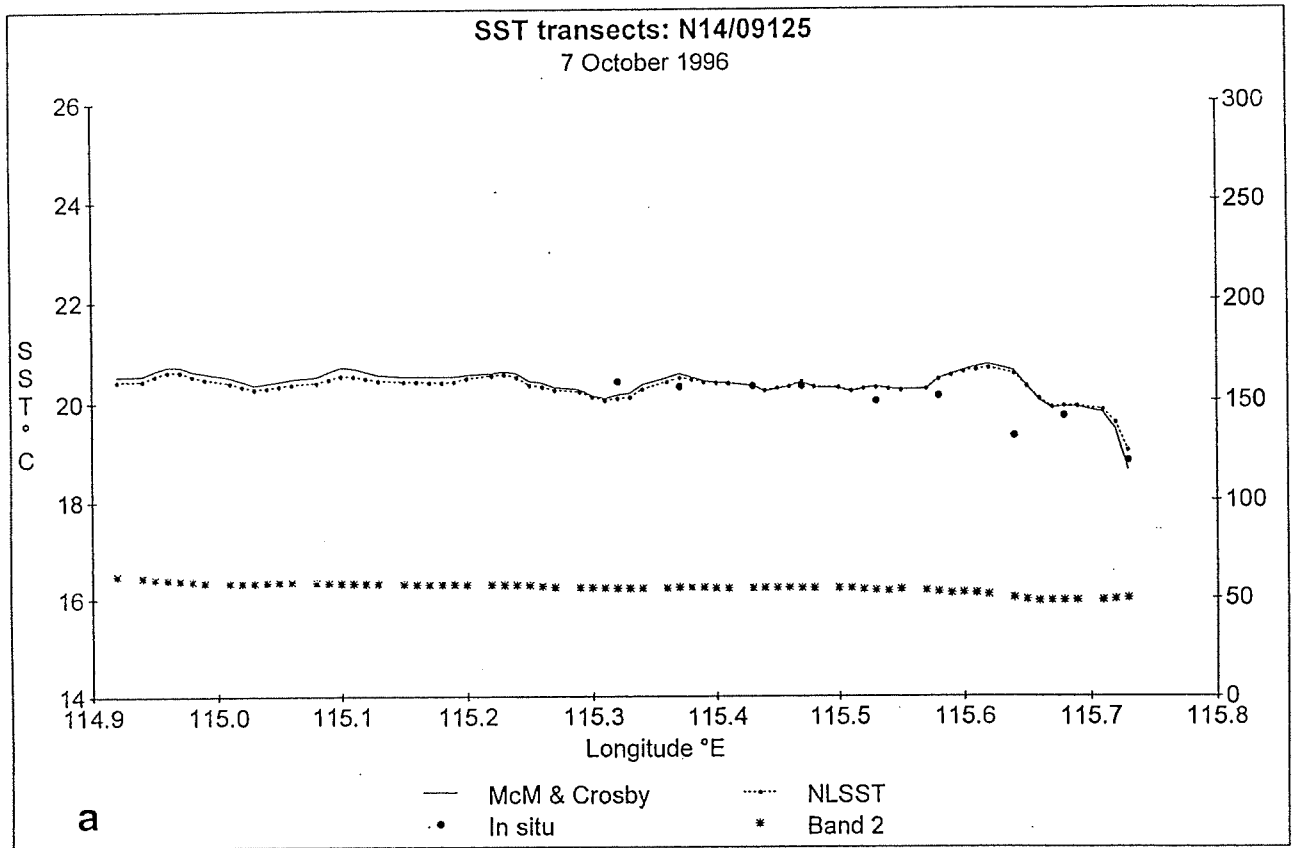
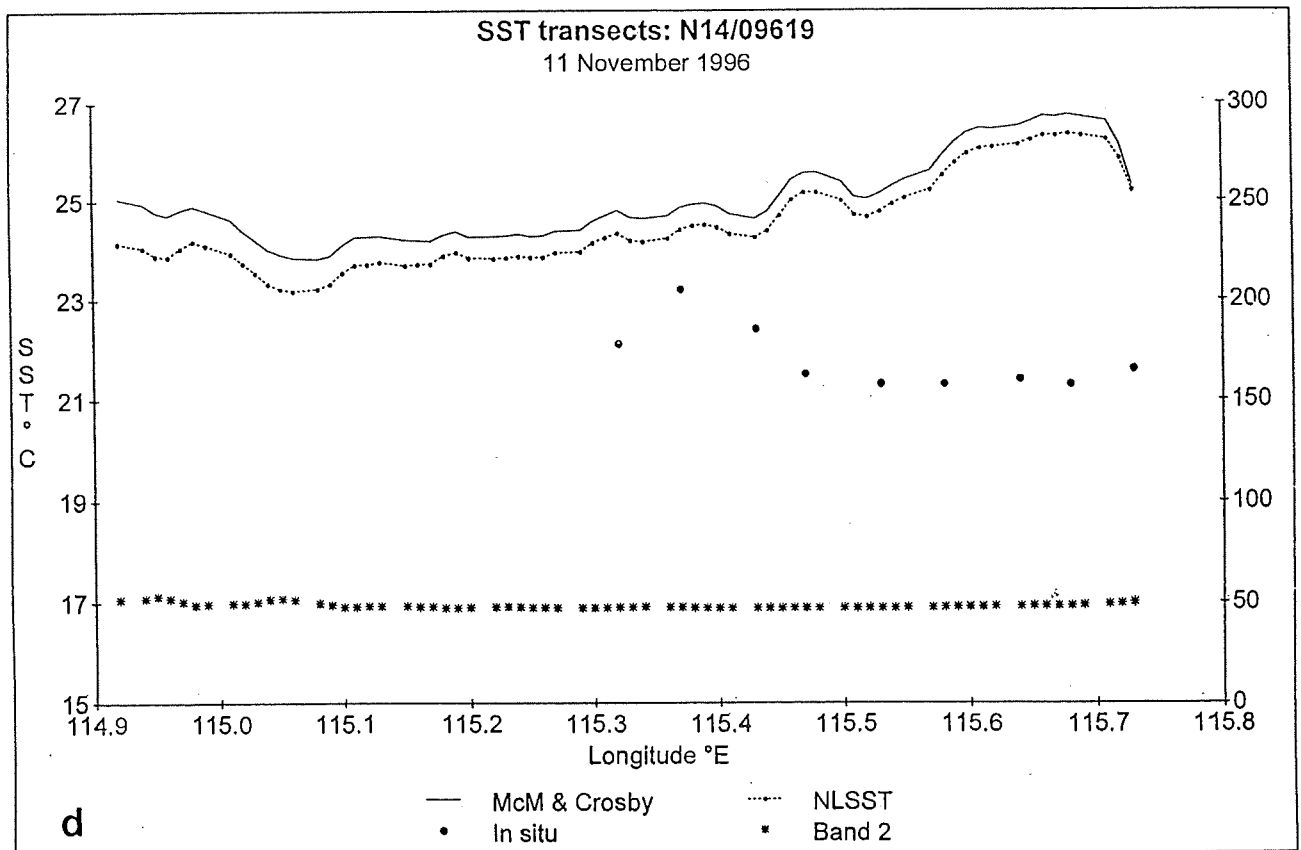
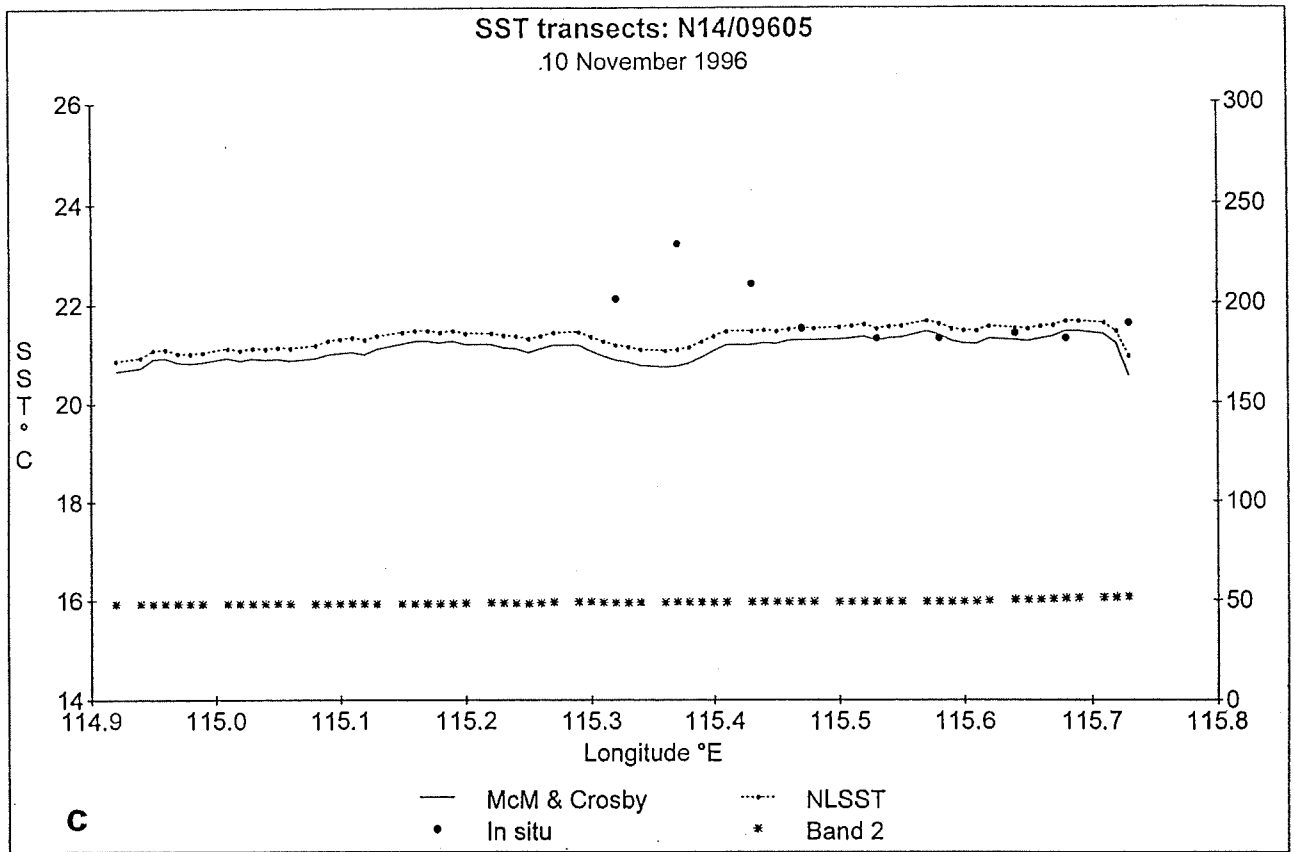
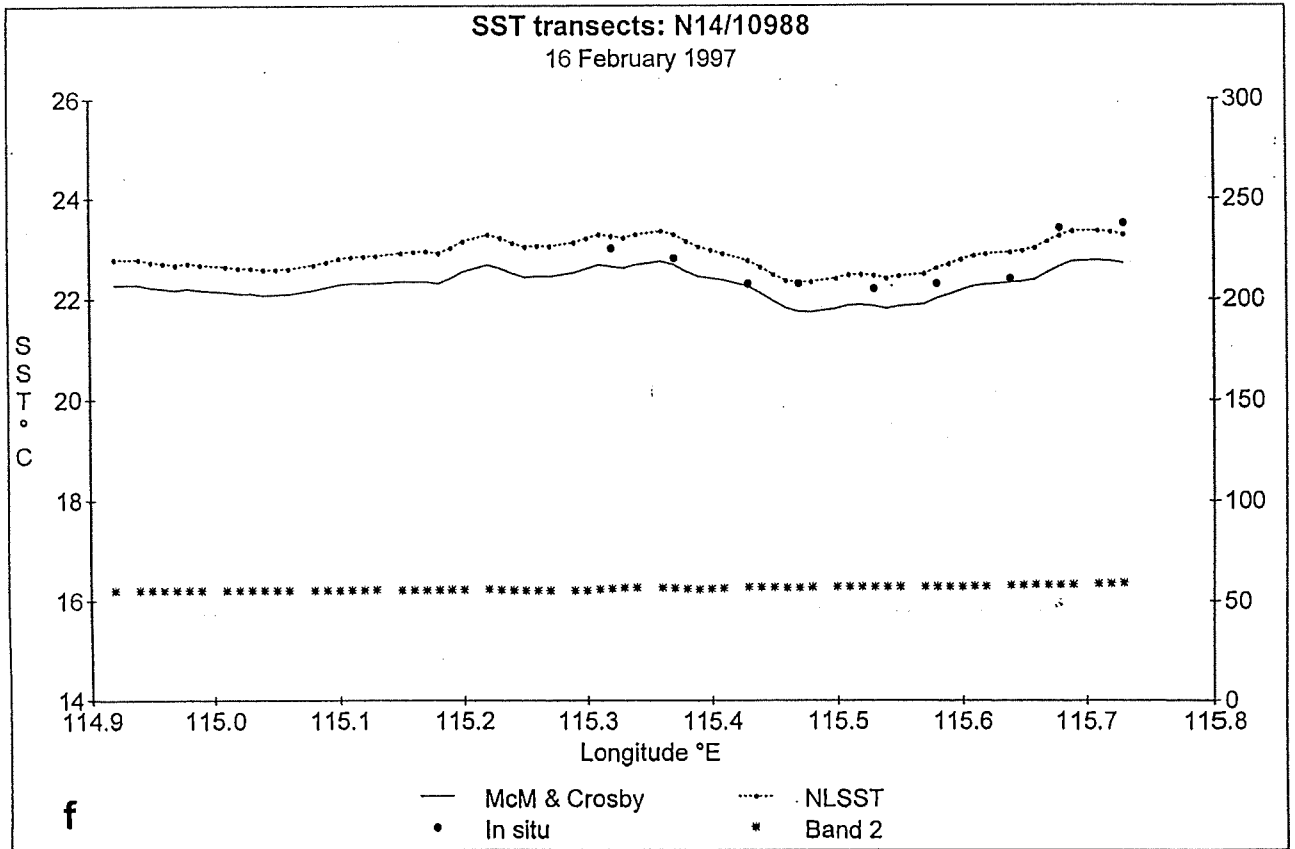
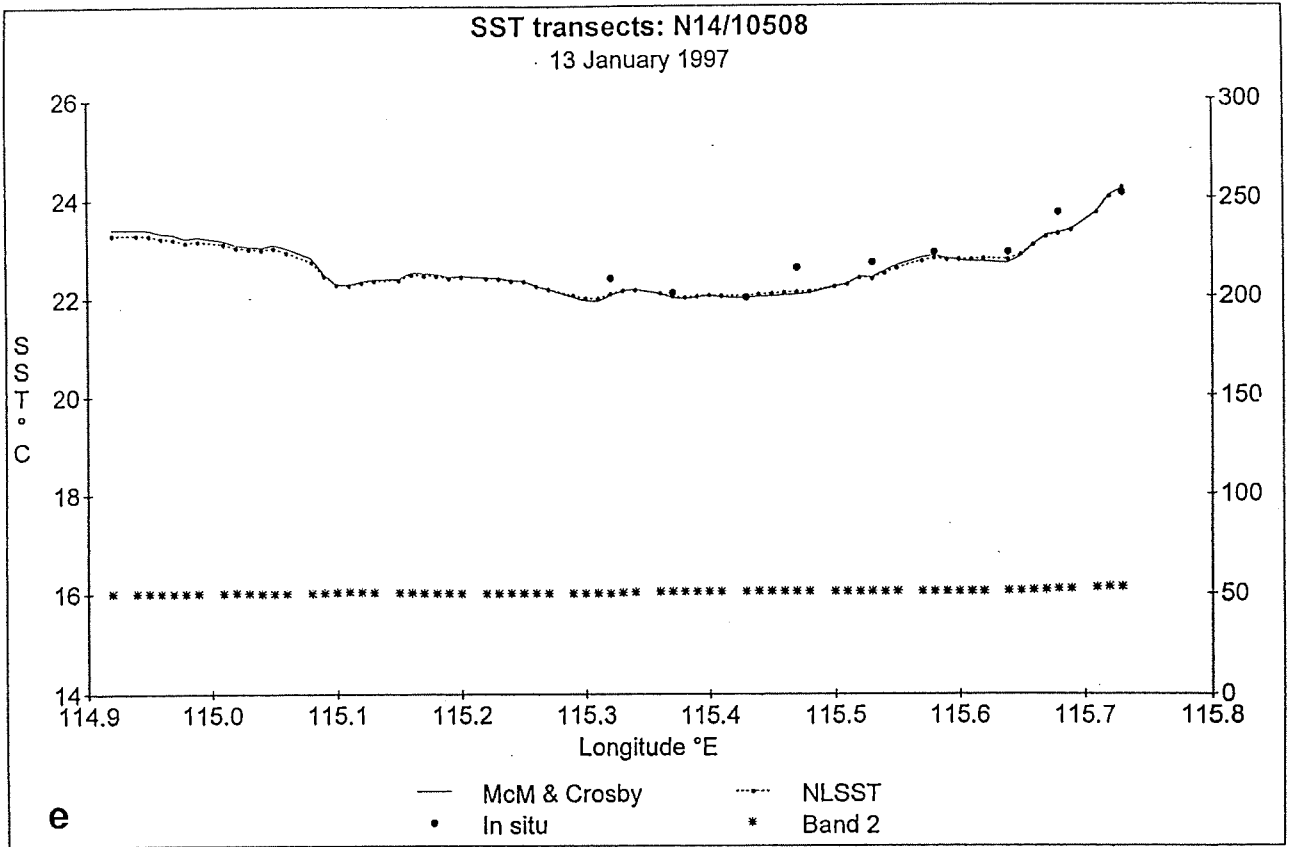


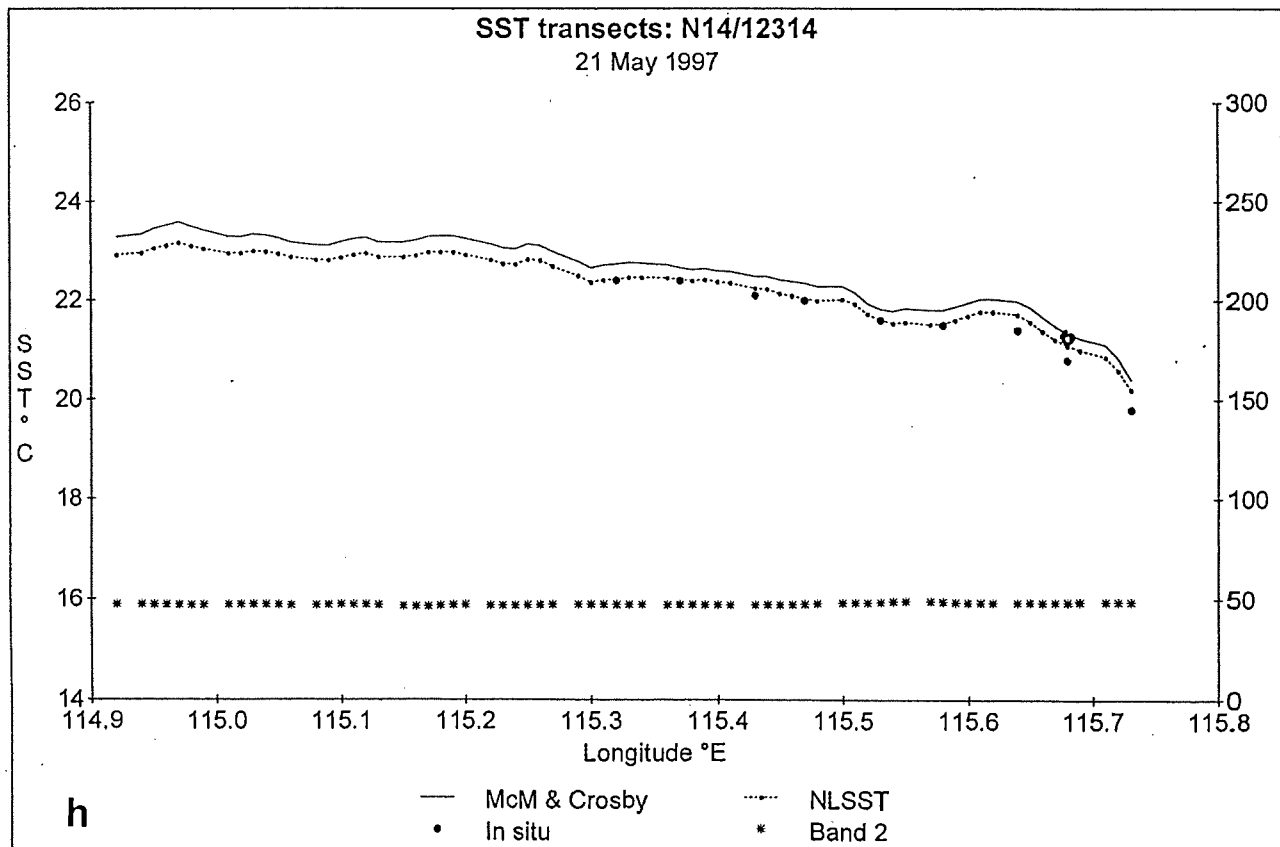
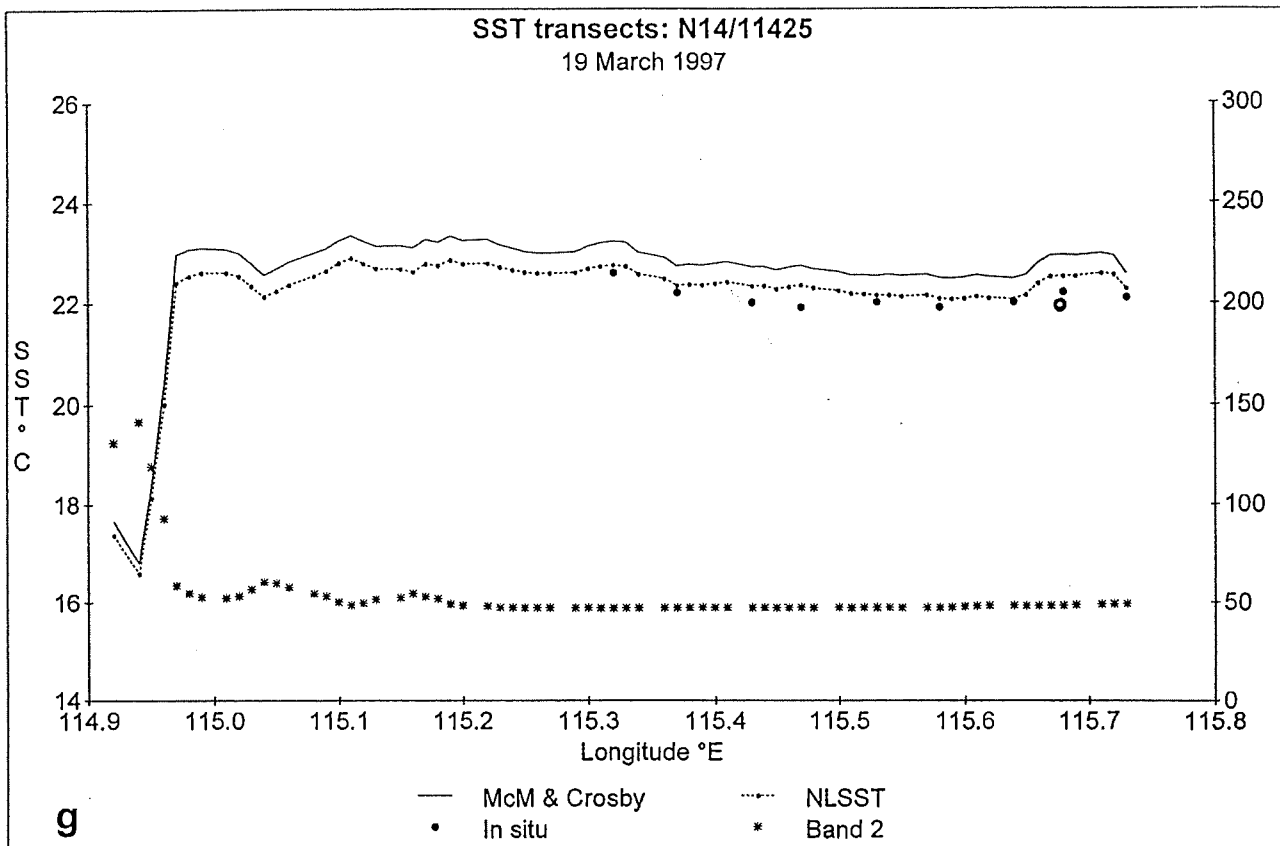
Figure 8.2: NOAA-AVHRR satellite images showing the sea-surface temperature off the southwestern coast in (upper) July 1997, showing the movement of Leeuwin Current onto the shelf, and (lower) September 1998, with a clockwise eddy carrying a filament of warm water northwards offshore of the Leeuwin Current. Other details are as in **Figure 8.1**.

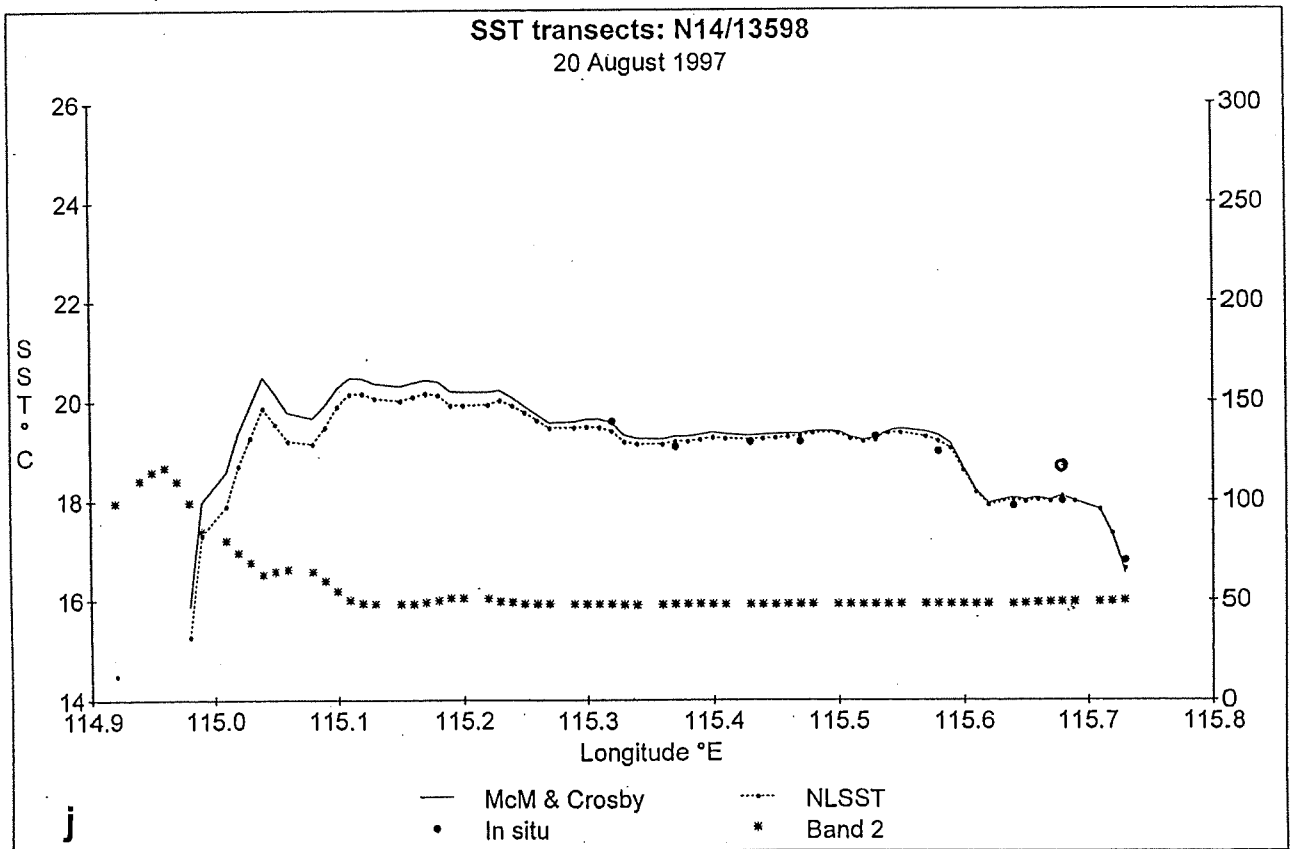
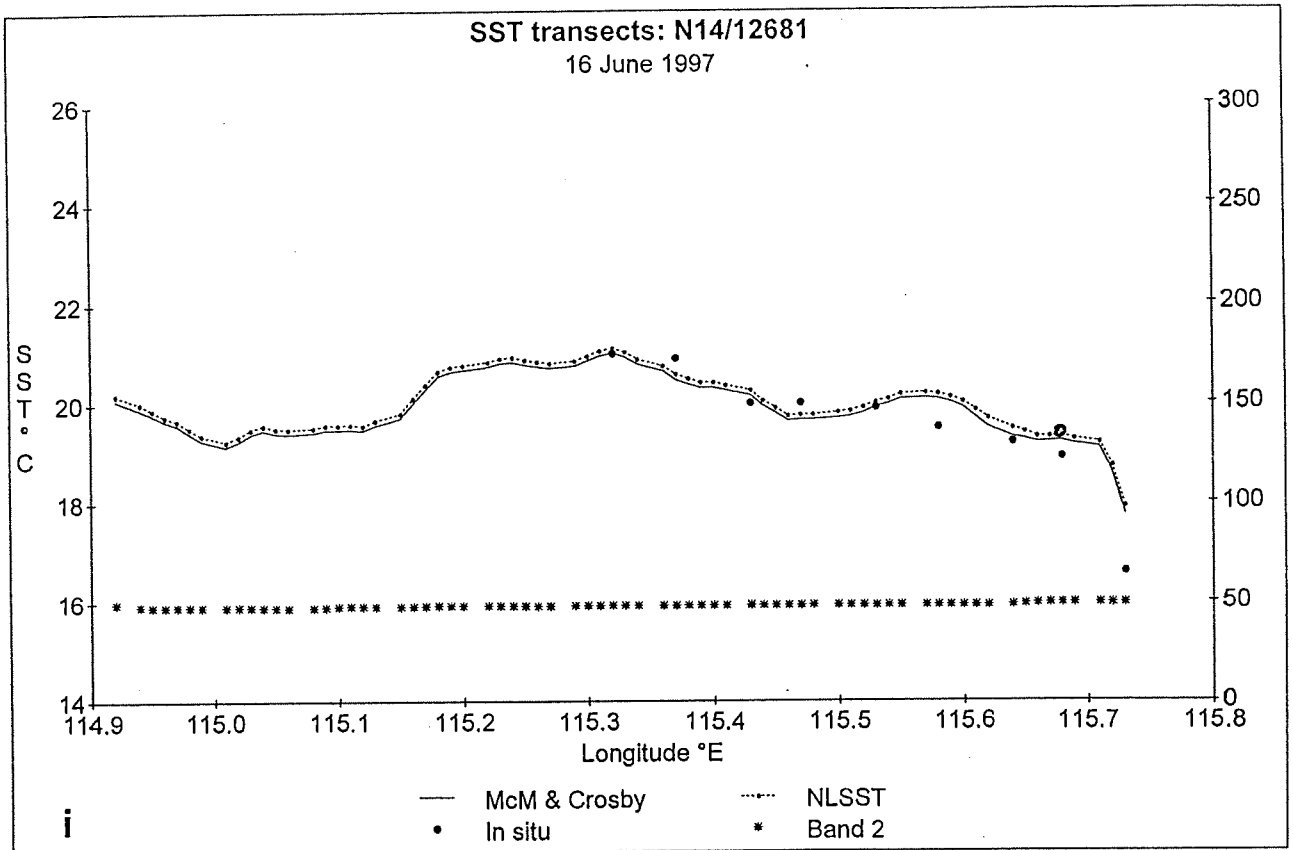
Figure 8.3 (a to x): Sea-surface temperature transects from the Hillarys surveys between October 1996 and December 1998. Each transect plot shows the satellite-derived SSTs from the McMillin and Crosby algorithm (solid line) and the NLSST (dotted), with the on-station bucket temperatures (filled circles) and the raw counts in the near-infrared AVHRR channel 2 (asterisks). The apparent small periodic gaps in the channel 2 data are because the pixel size of 1.1 km is not identical to 0.01° longitude. The plots are not strictly in sequence so that repeat images on the same day (k, p, q) can be paired, and the satellite SSTs for 10th November 1996 (c) have been included because of the extremely poor fit on the transect day 11th November (d) -- see **Figure 8.4**. The presence of cloud is indicated by a rise in Channel 2 (asterisks) and a commensurate fall in the SST, e.g. in (g) and (j). The thicker open circles at the second station from the coast represent the repeat bucket samples at H5, taken at about 1330 each day, initiated from March 1997.

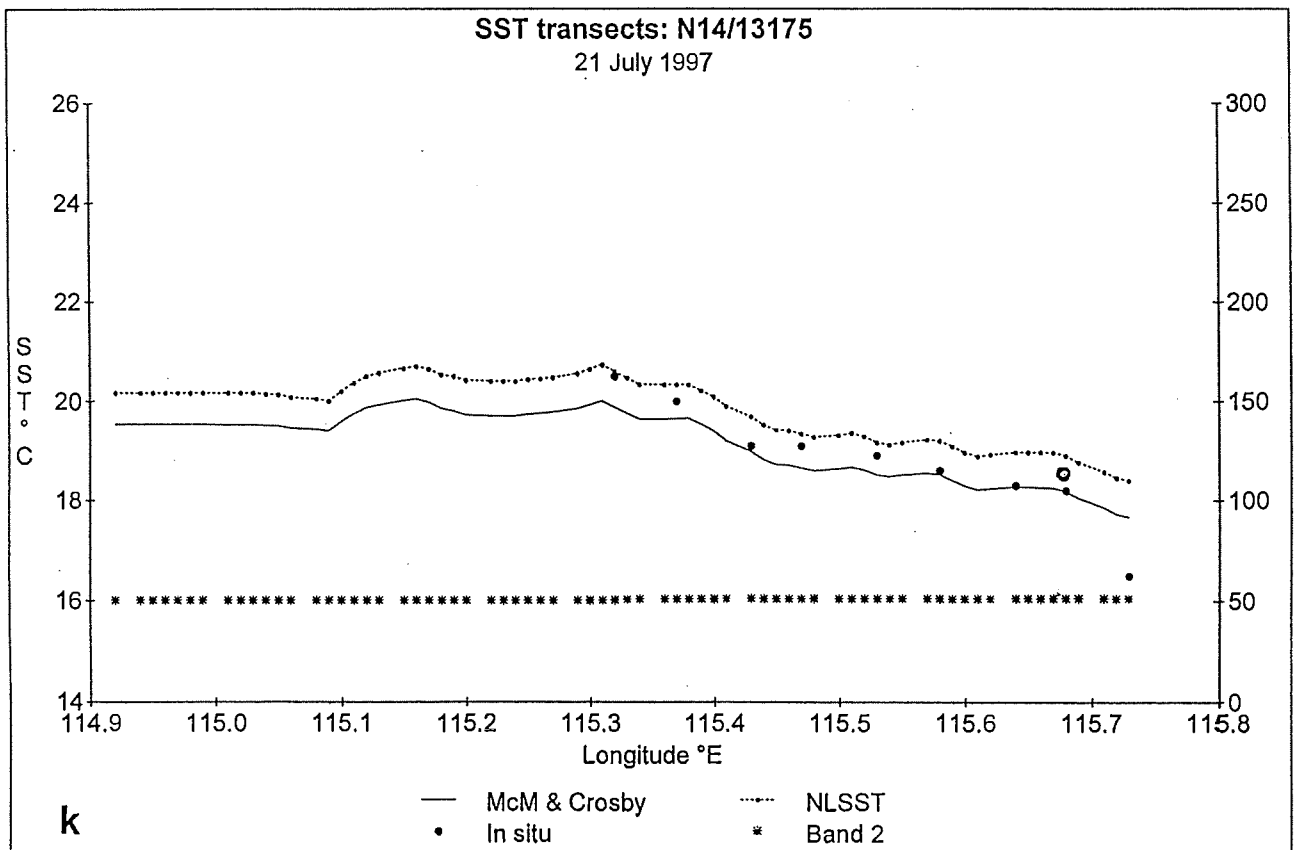
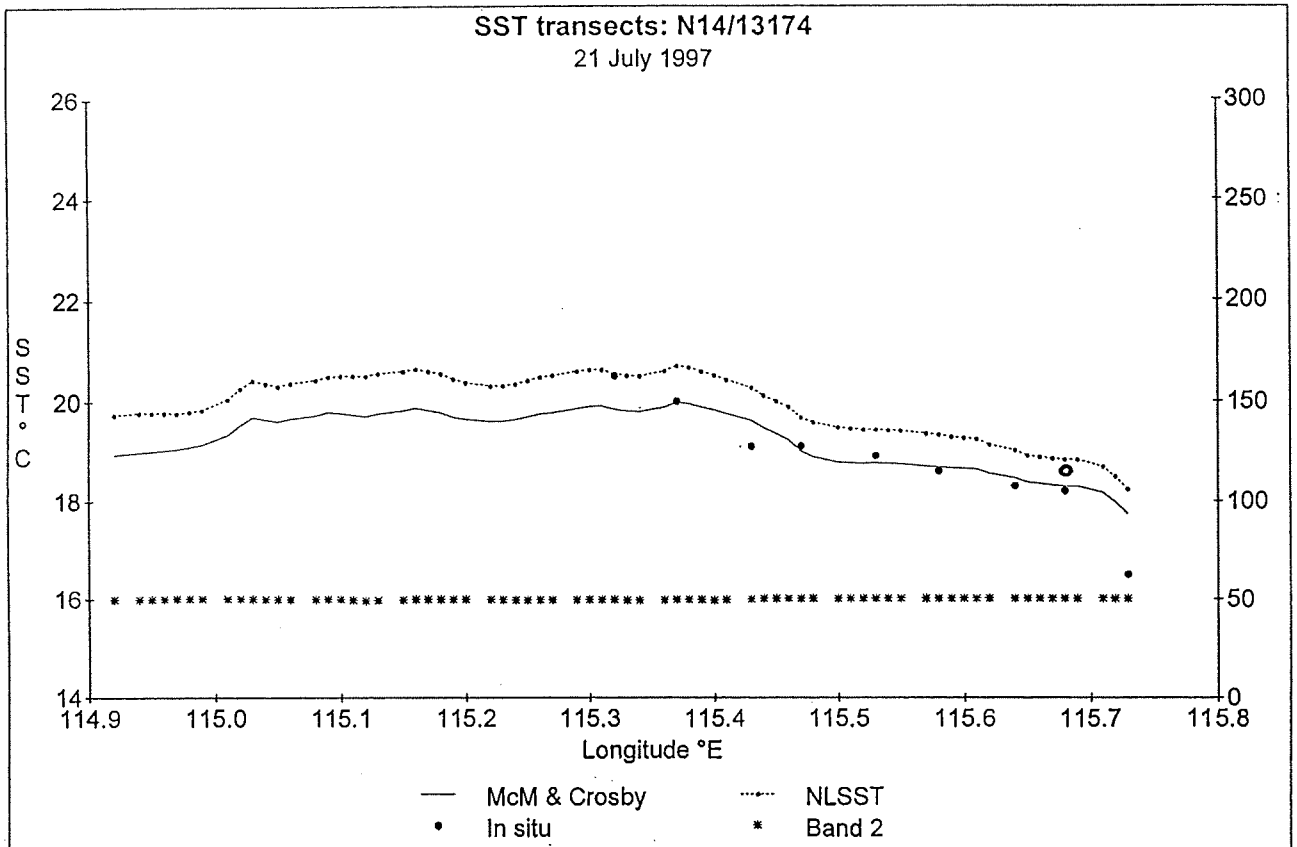


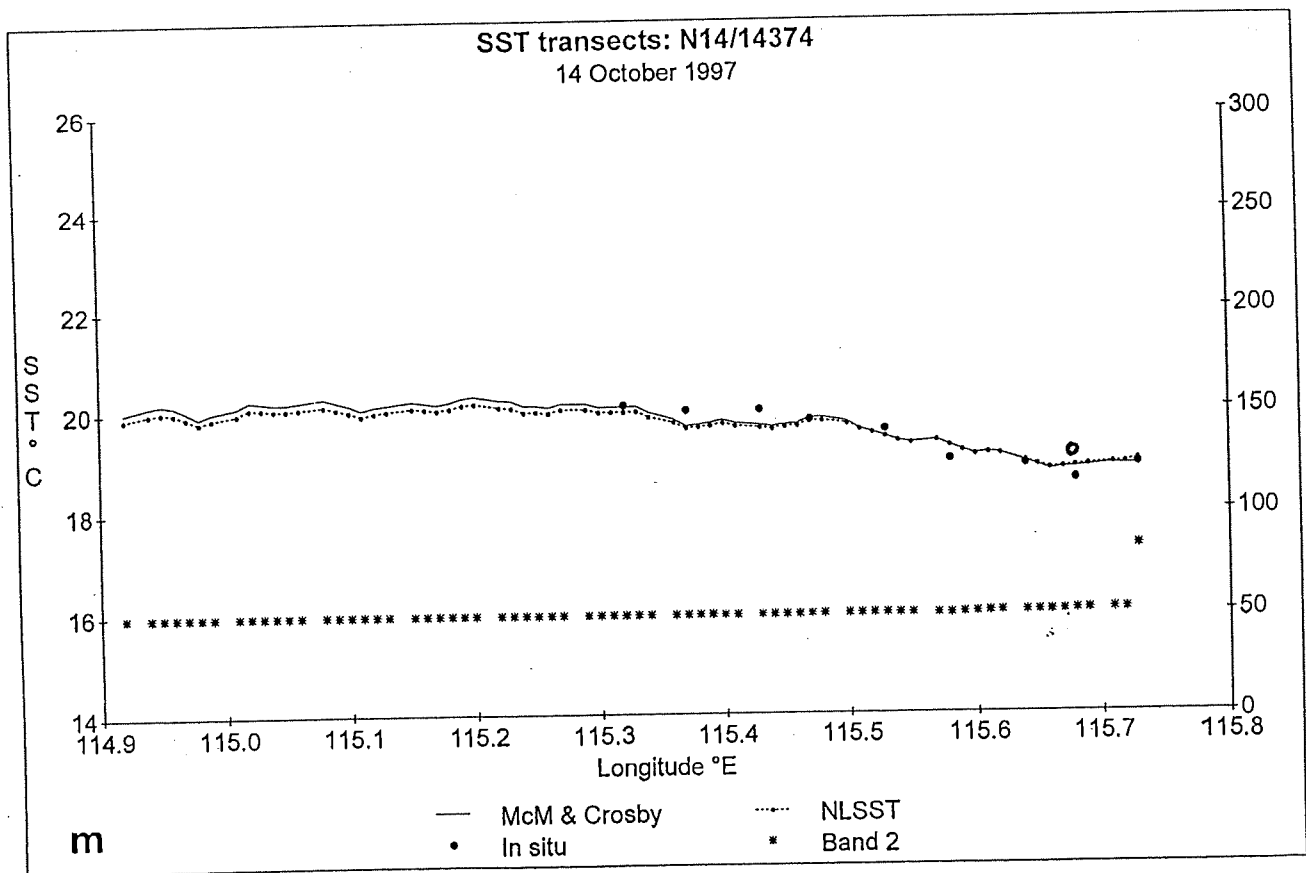
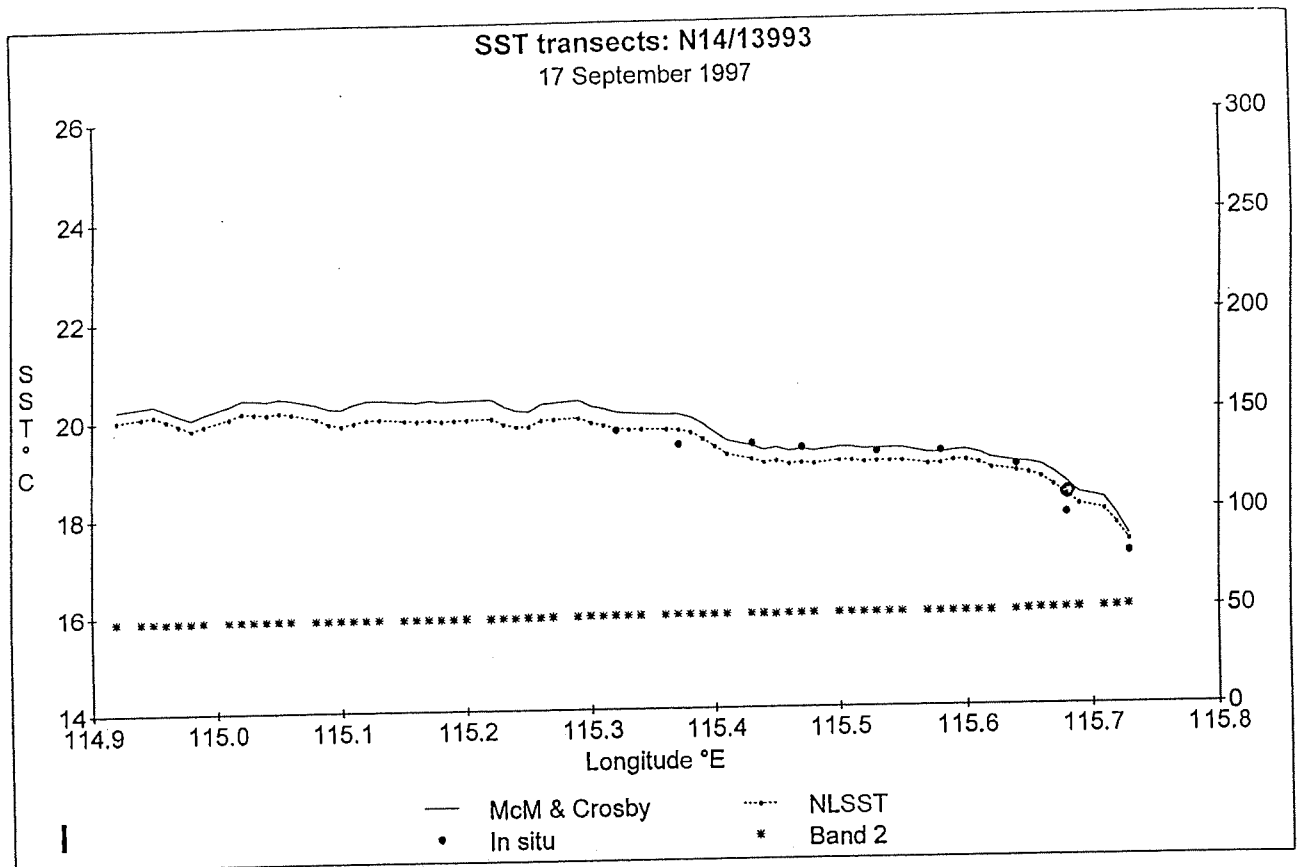


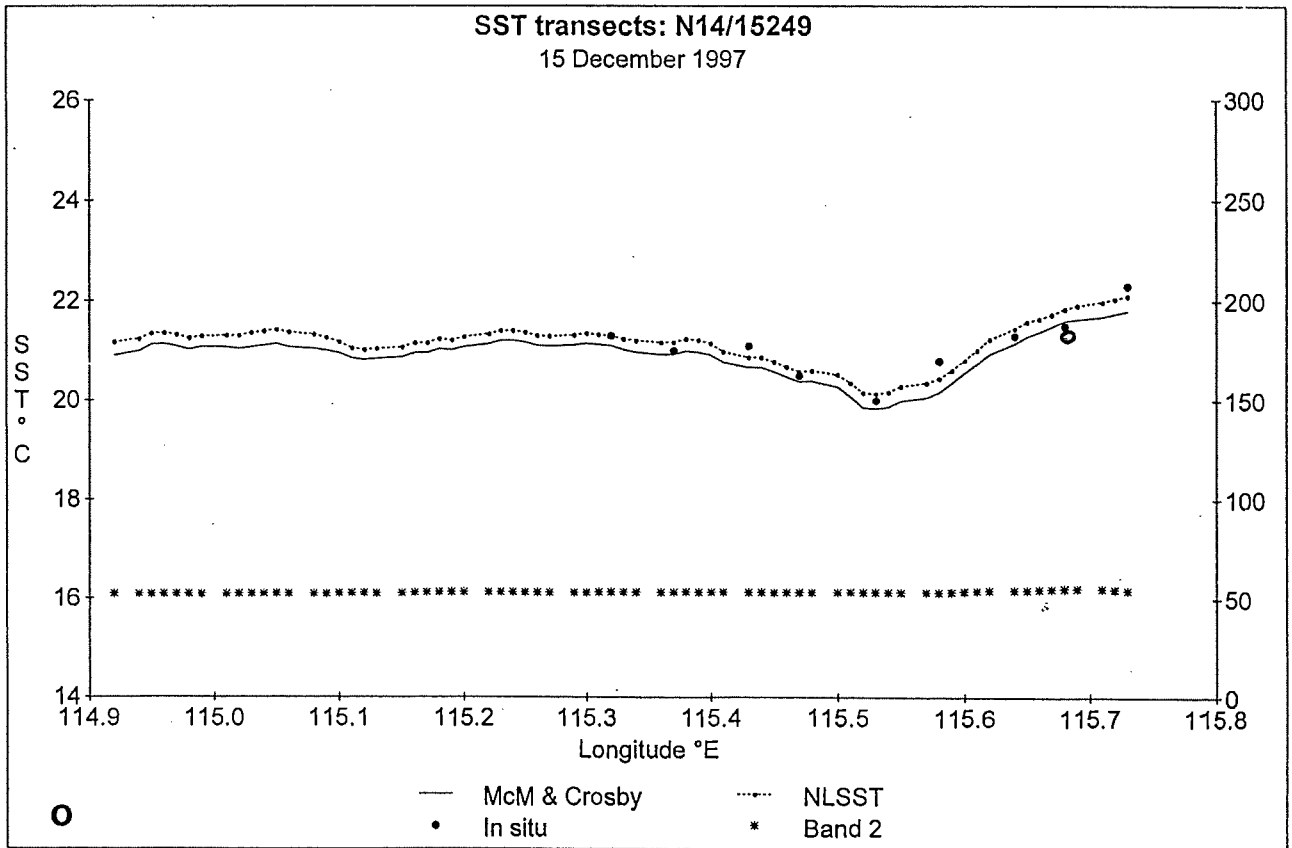
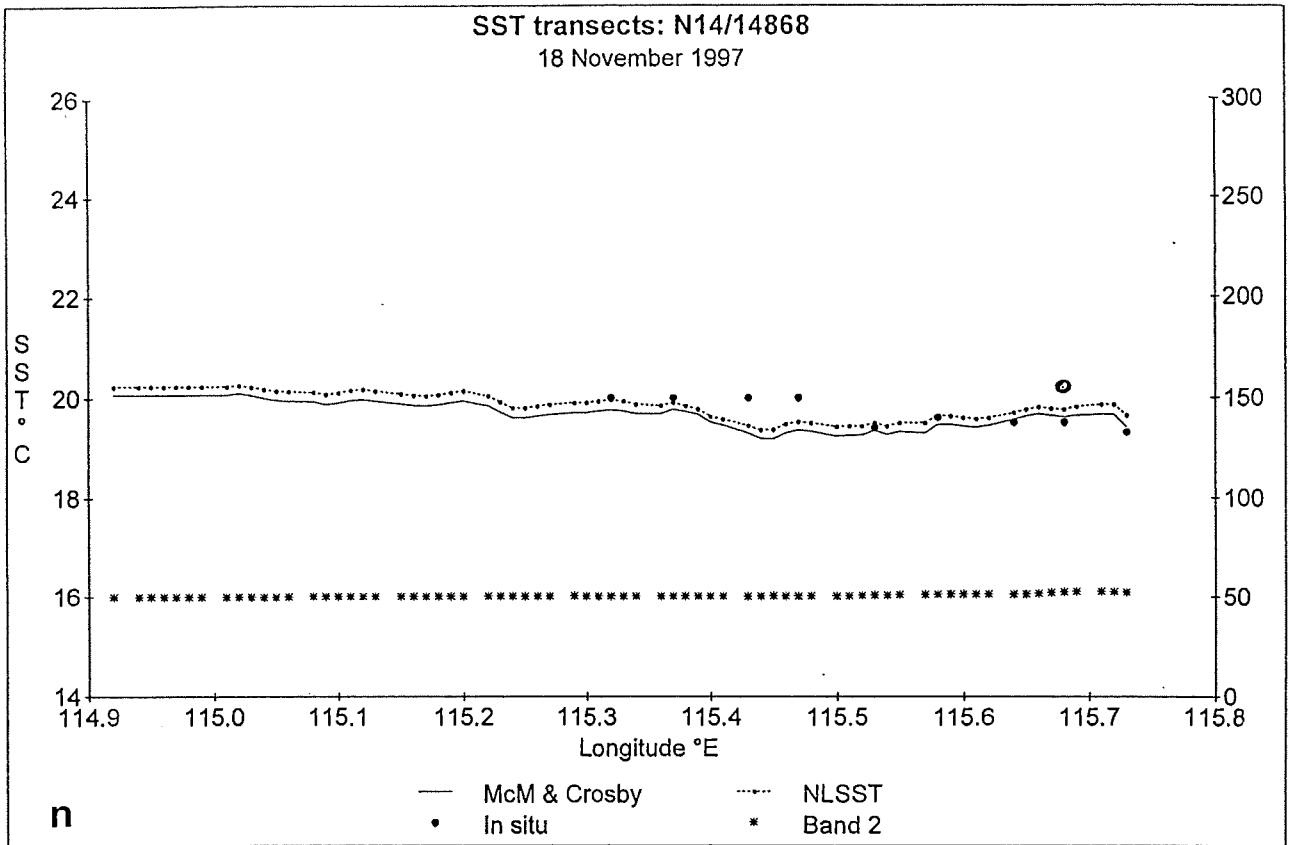


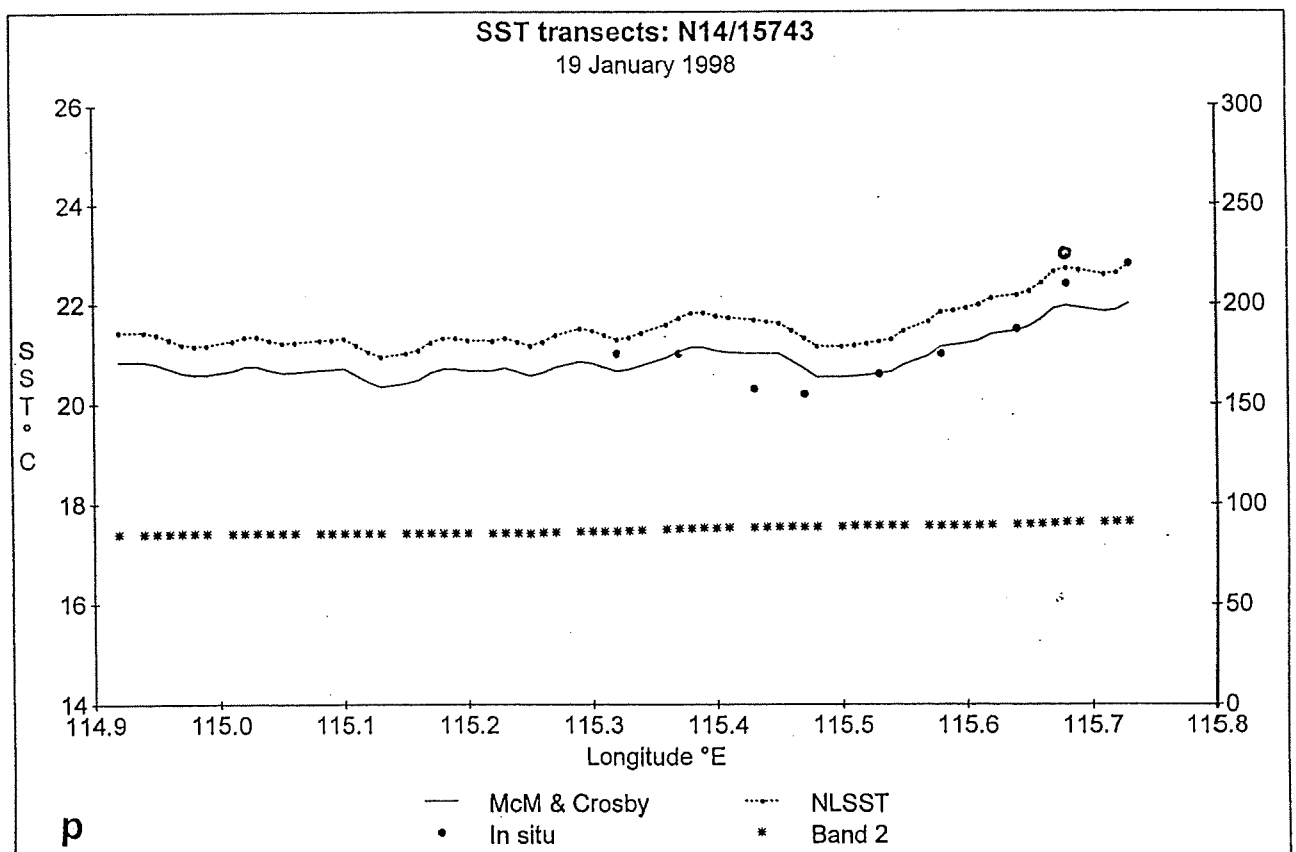
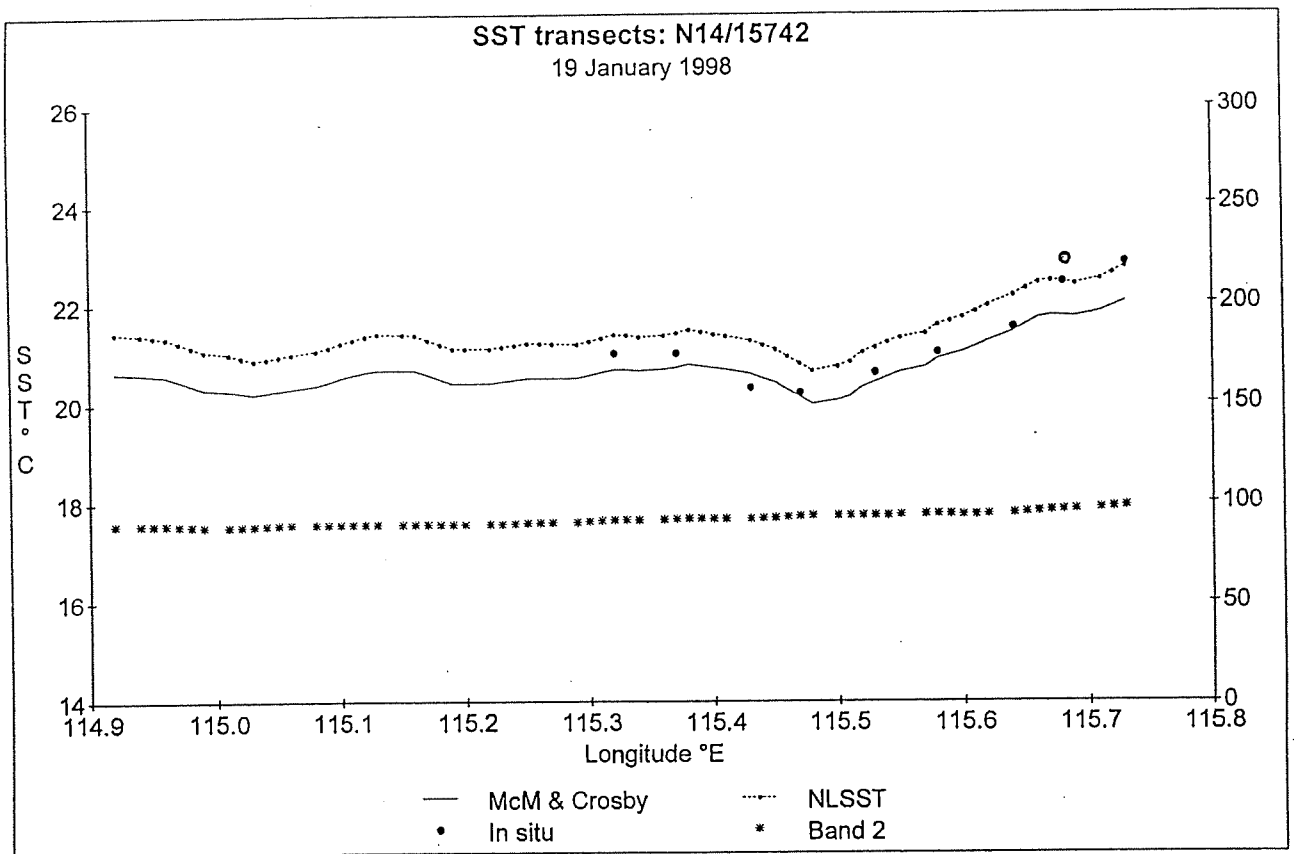


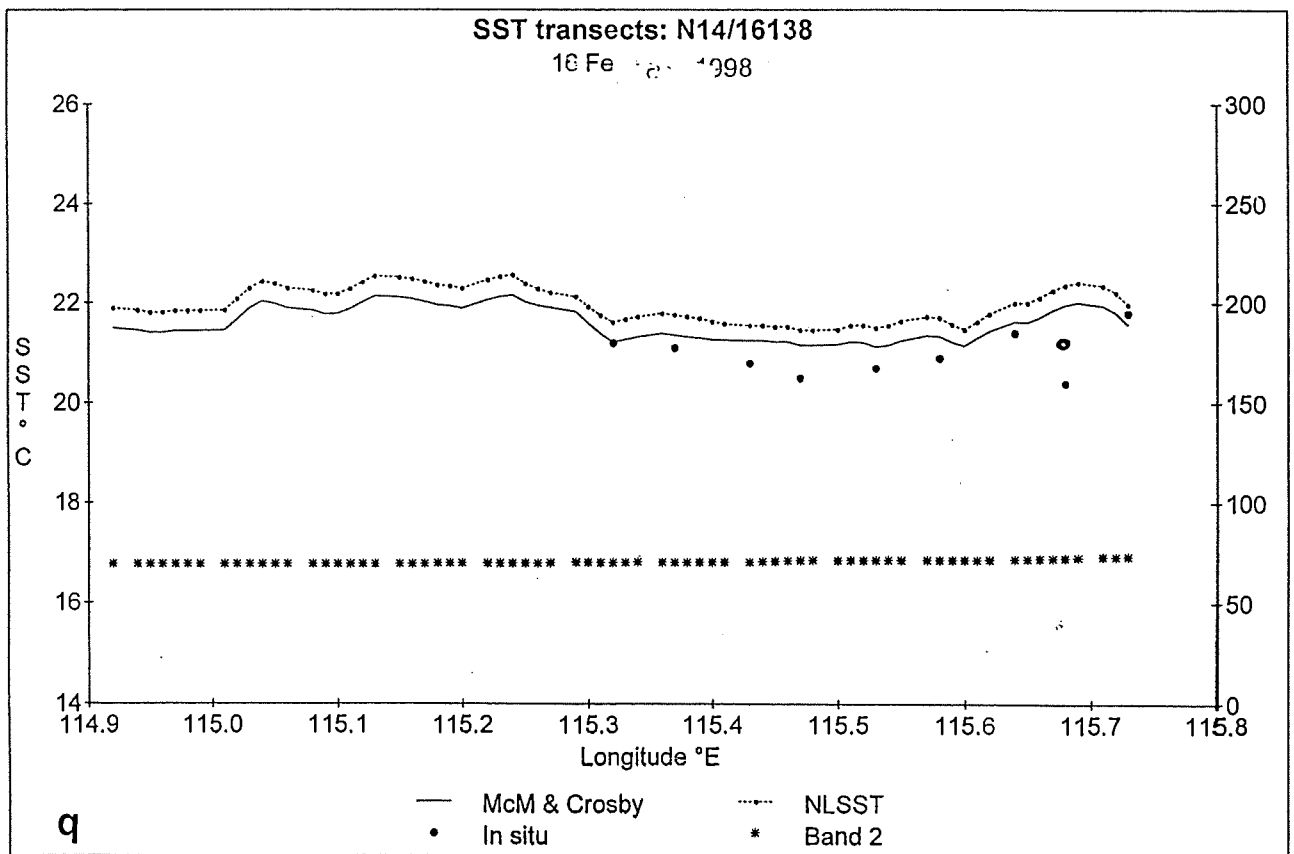
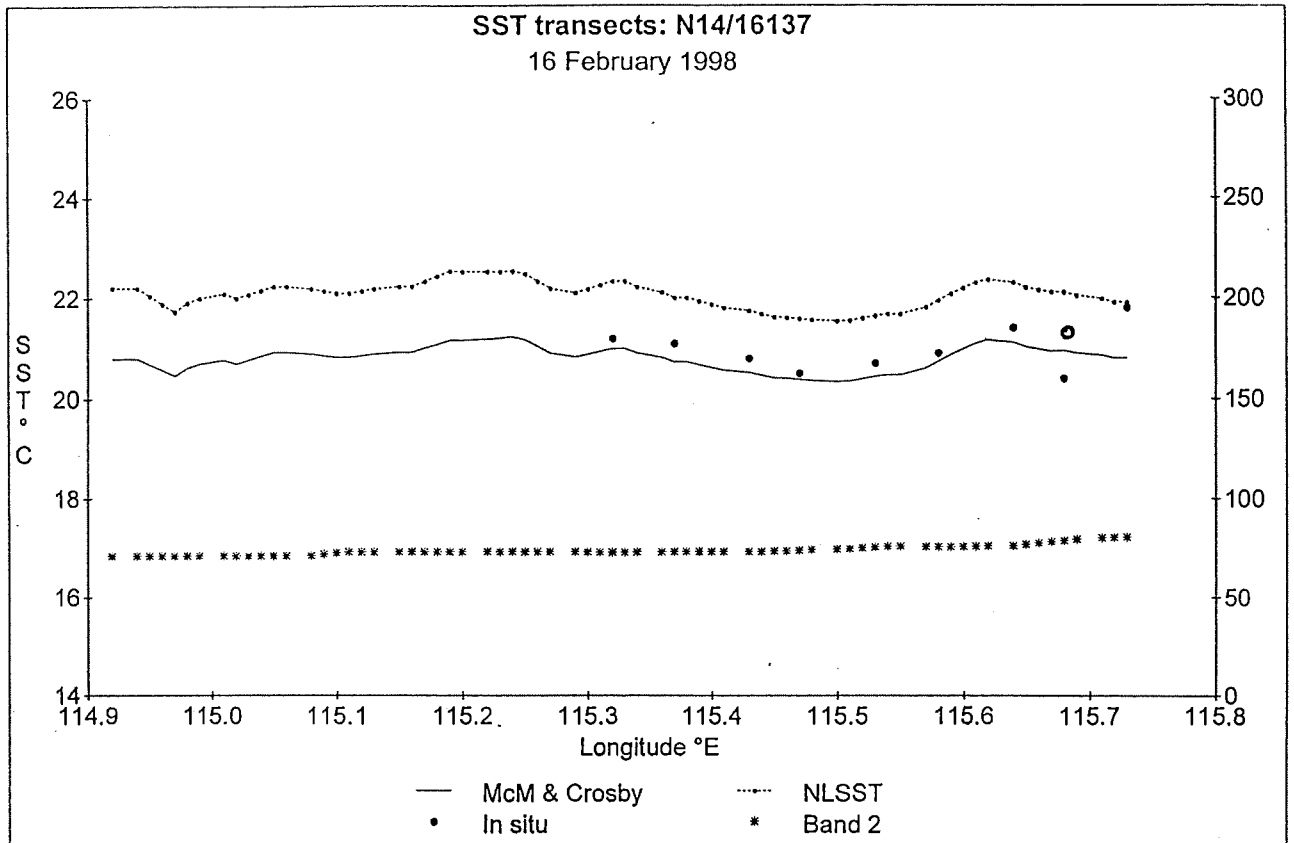


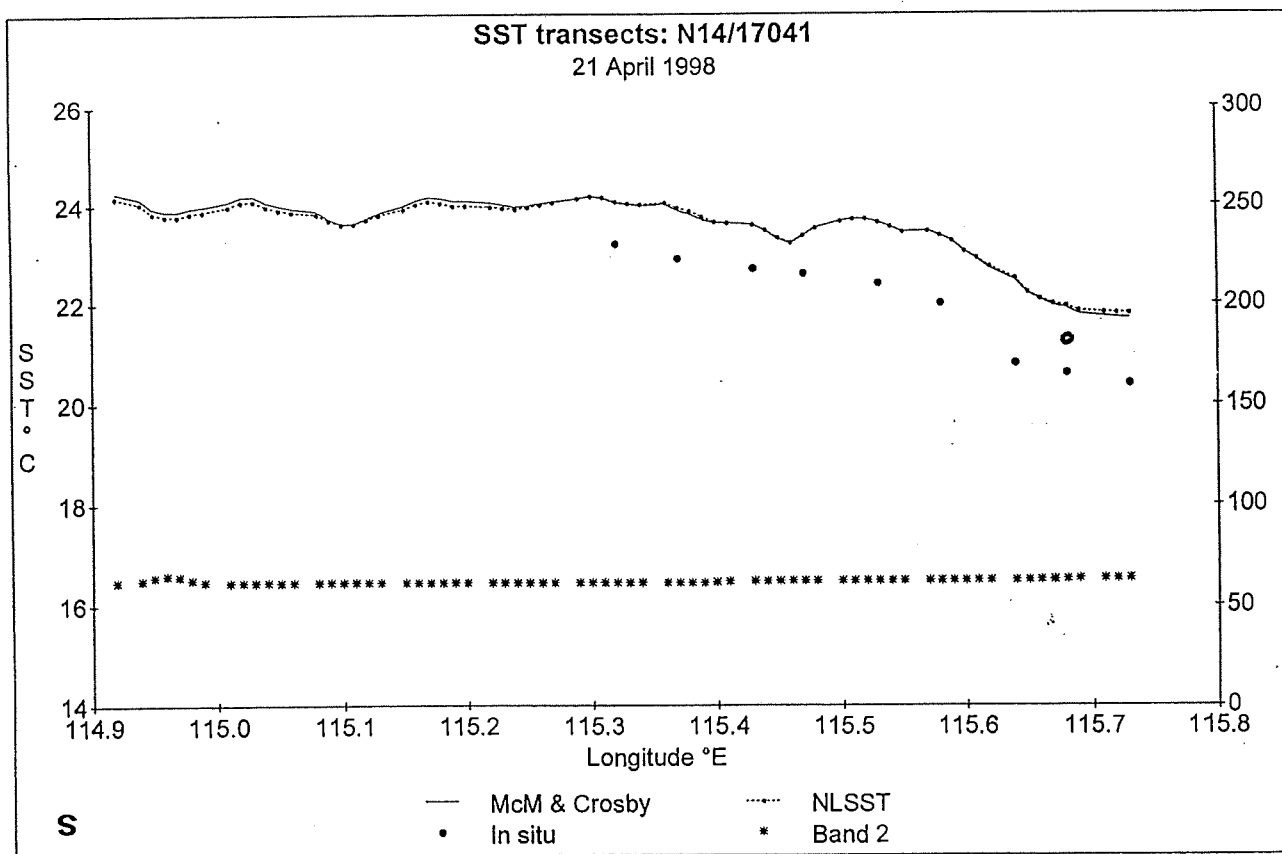
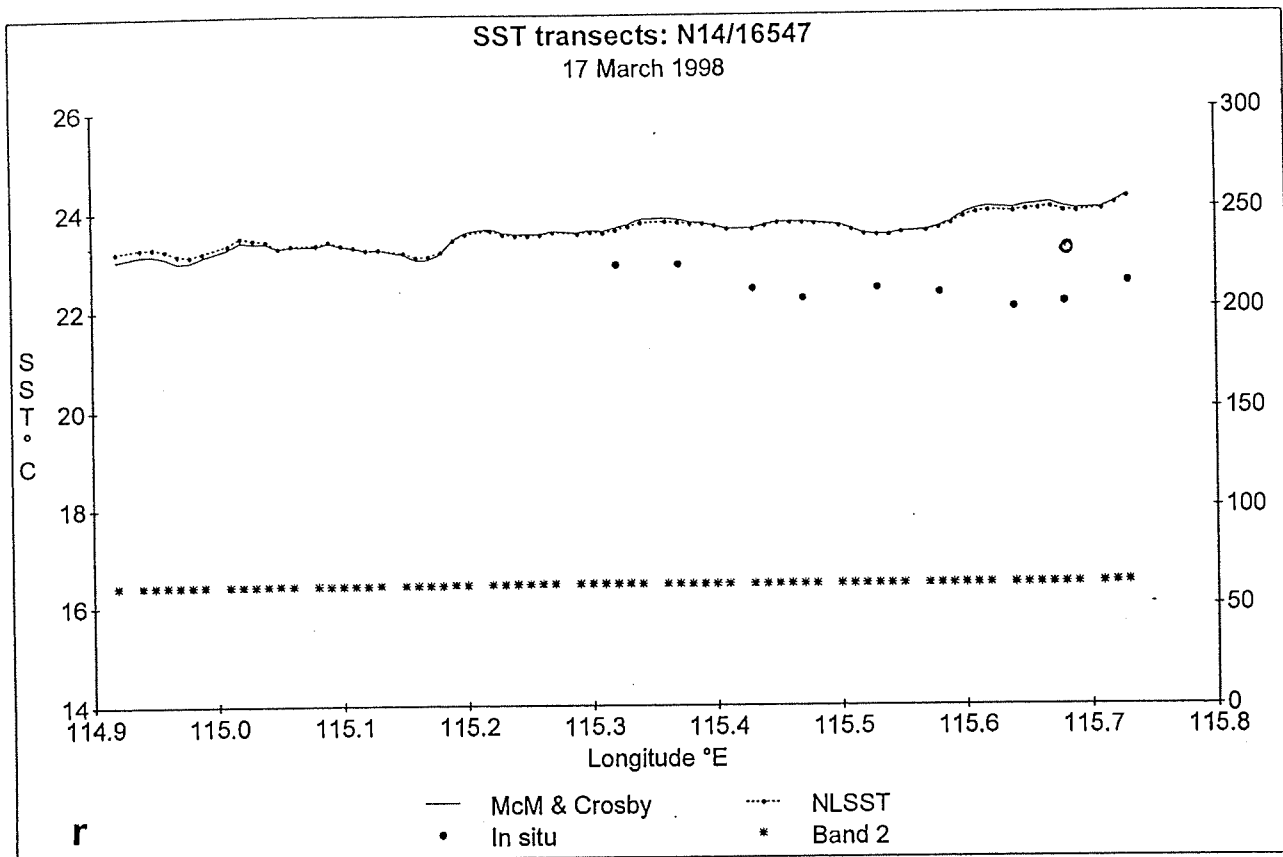


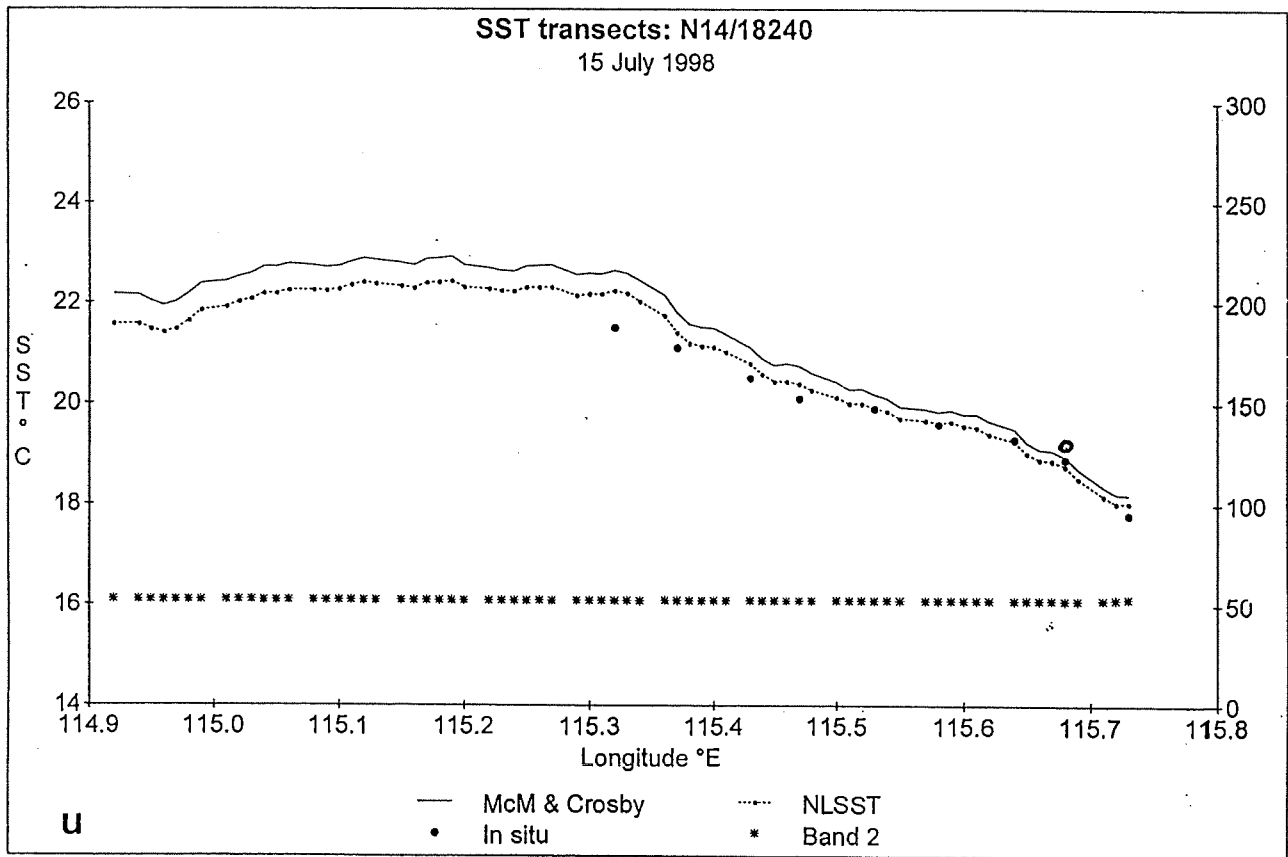
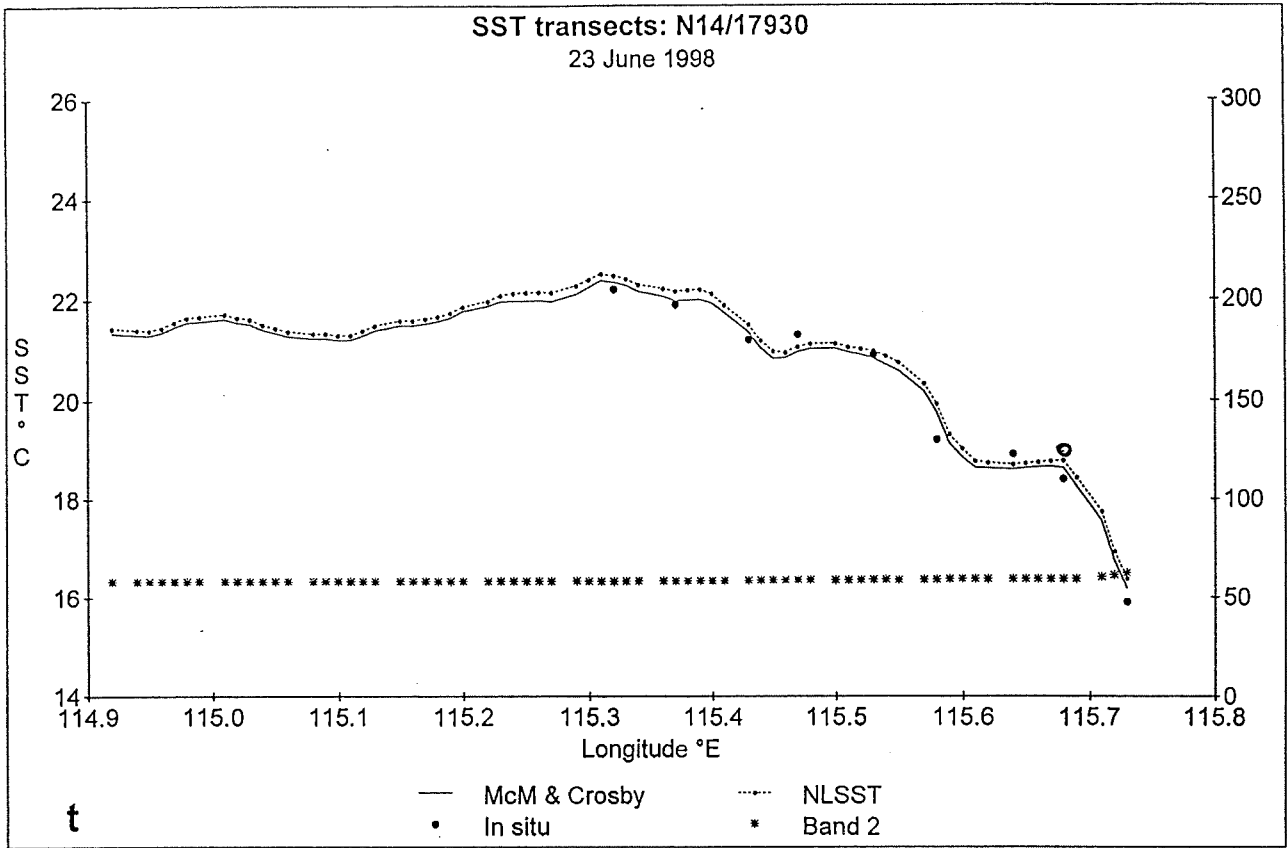


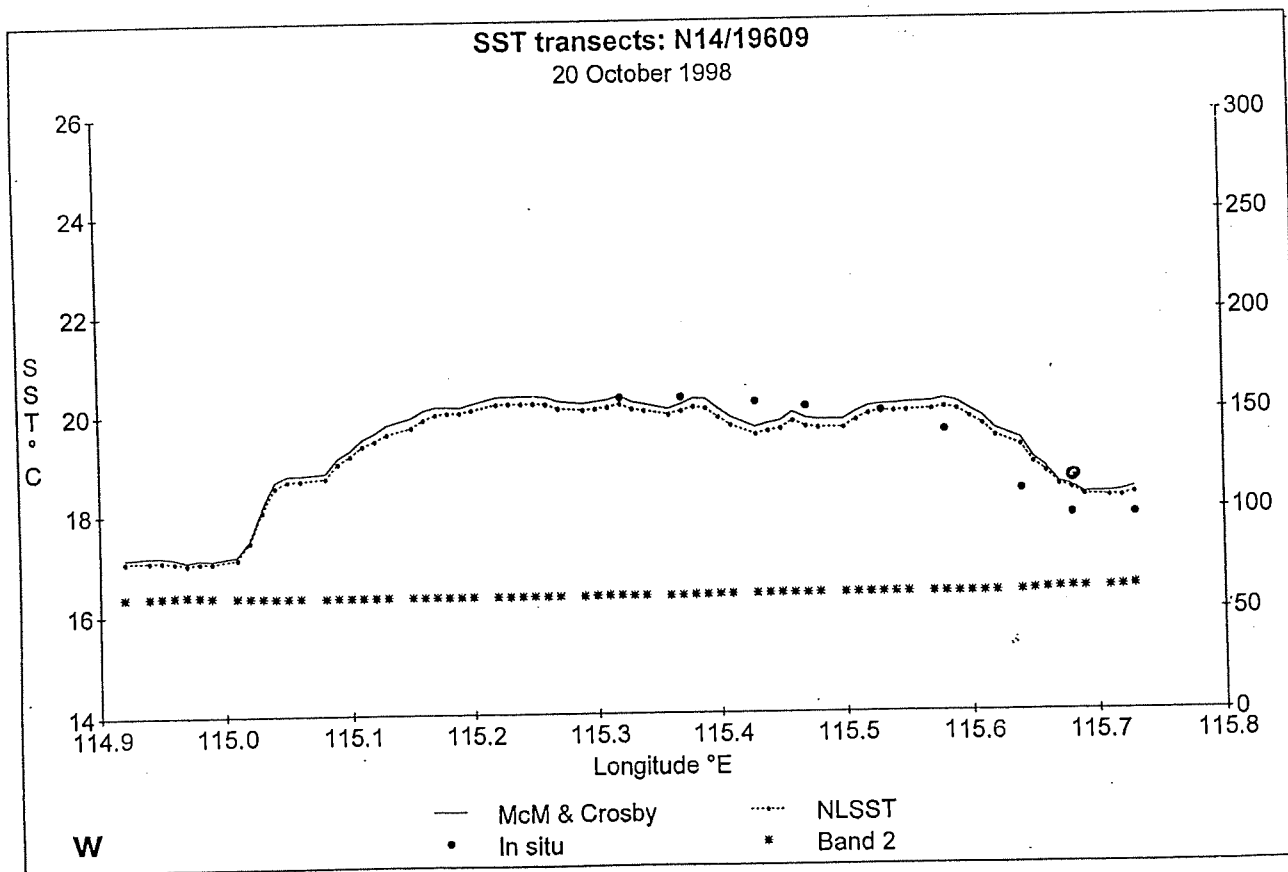
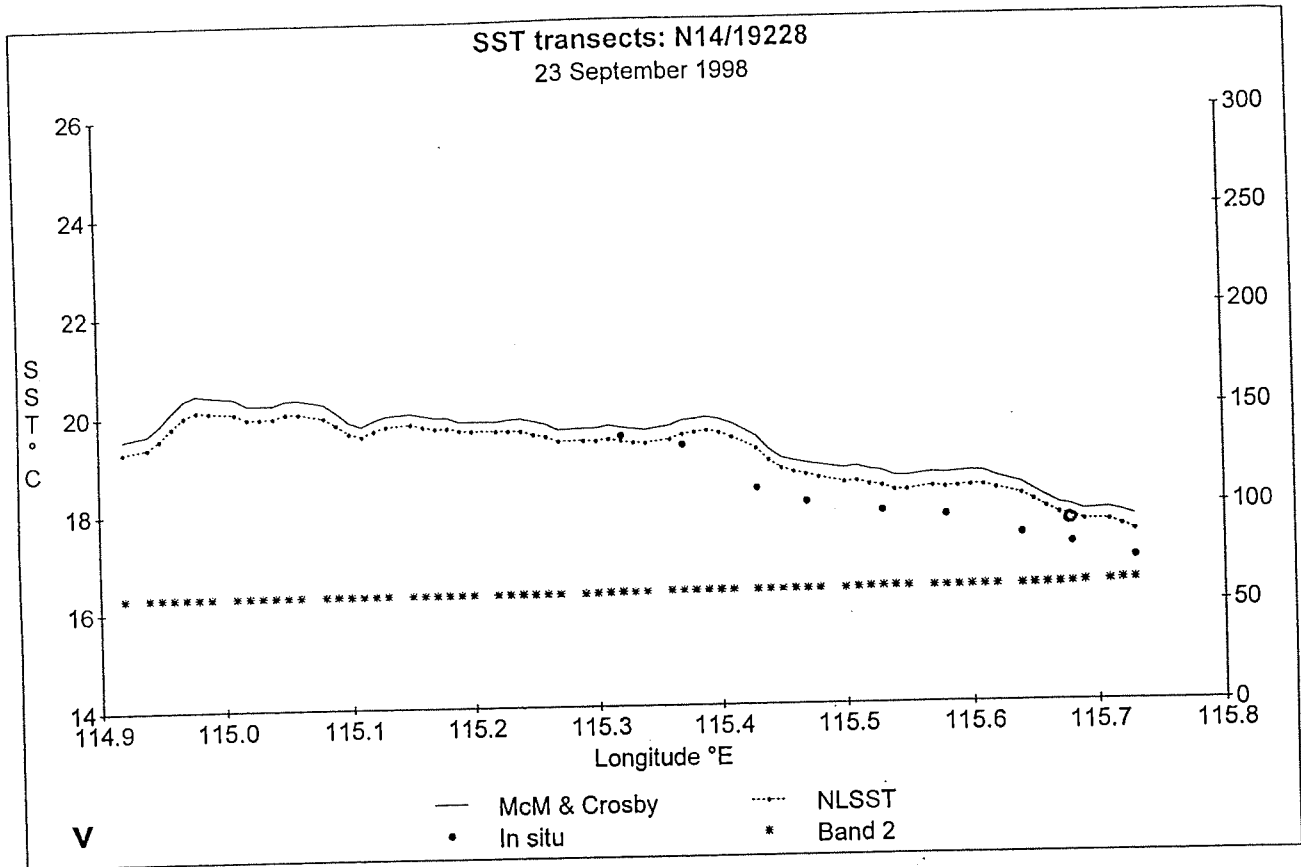


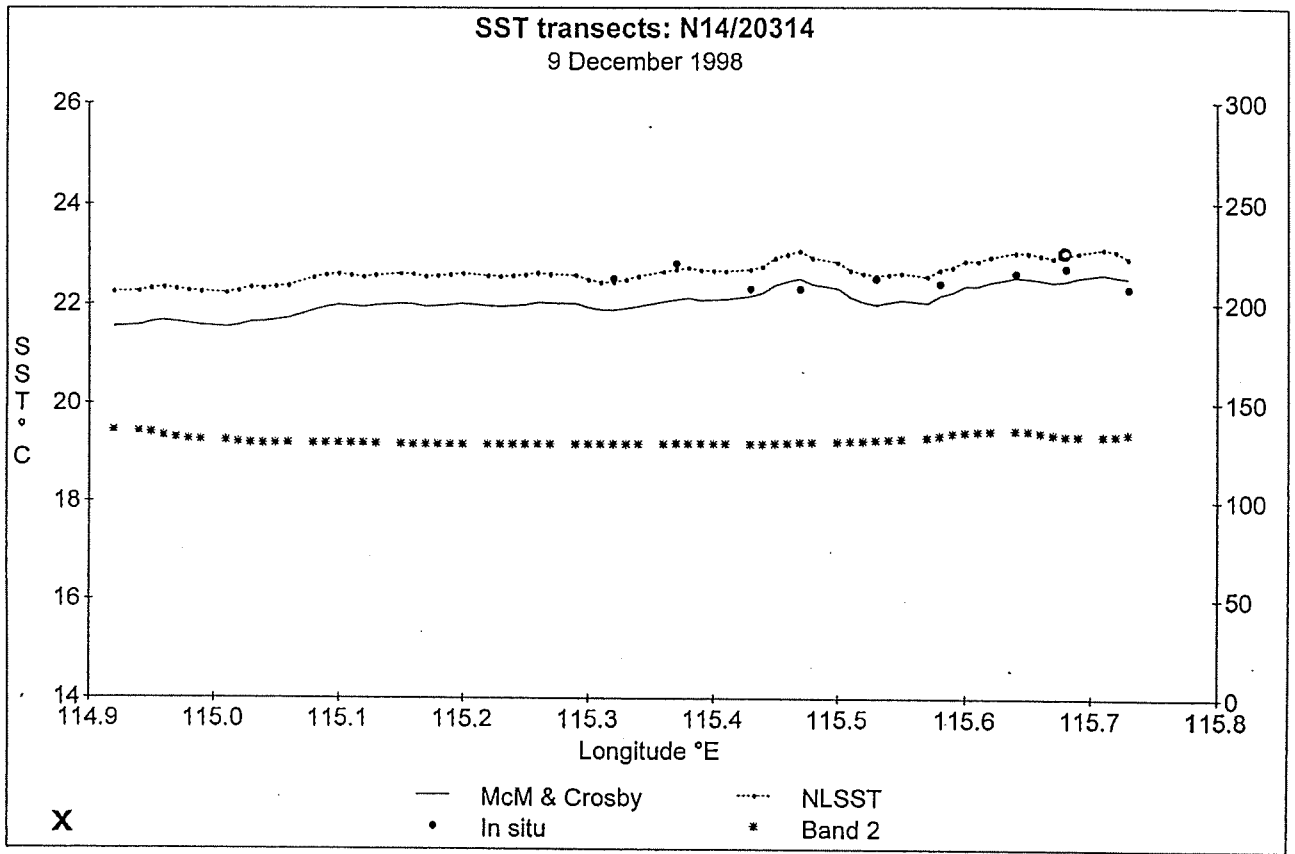












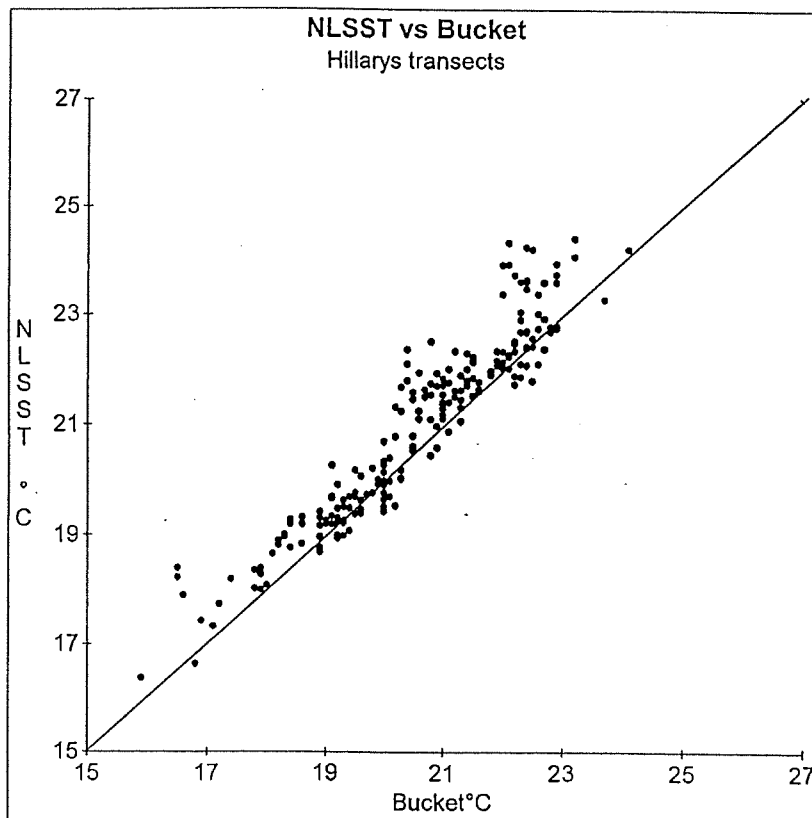
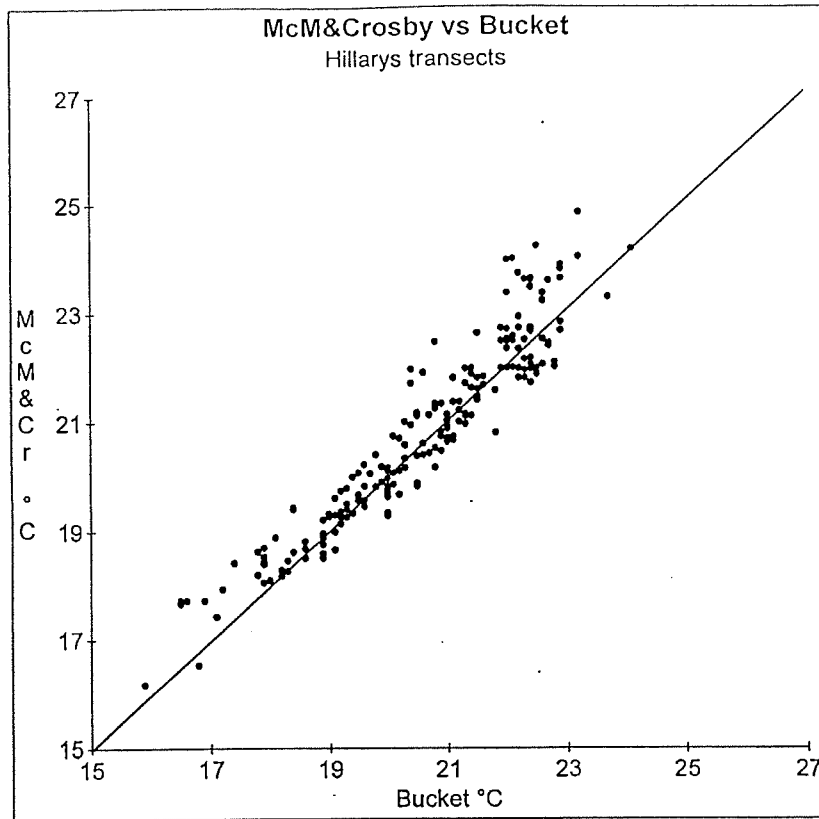


Figure 8.4: Scatterplots of AVHRR-derived SSTs against the bucket measurements for the (a) McMillin-Crosby and (b) NLSST algorithms. The solid line is the ideal line of perfect fit.

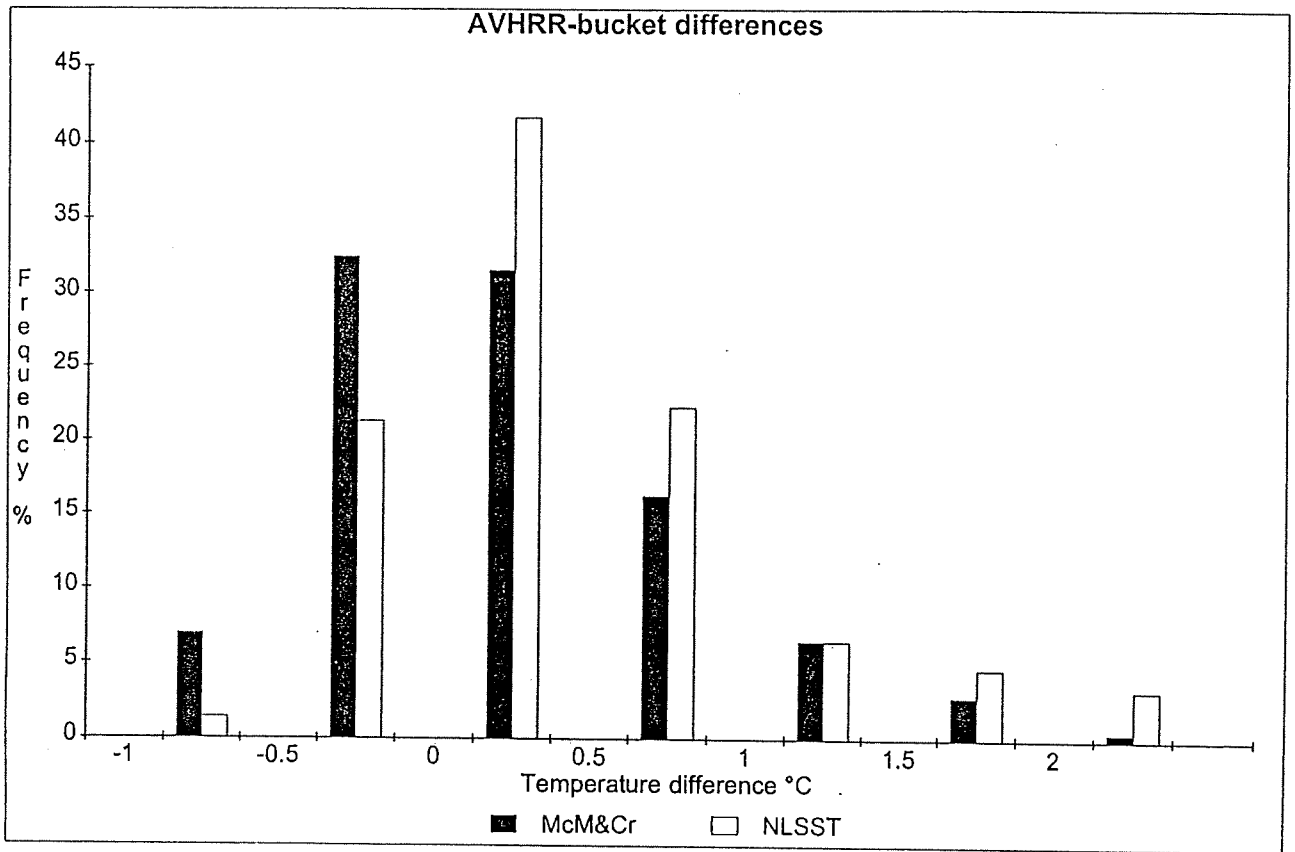


Figure 8.5: Histograms of the temperatures differences between the AVHRR and bucket temperatures, with the McMillin-Crosby algorithm shown with solid bars and the NLSST with clear bars. The high differences from the 11th November transect are not included on this Figure.

Section 9: SeaWiFS imagery (Peter Fearn, Jim Davies, Mervyn Lynch and Helen Chedzey)

9.1 Instrument Deployment and Data

Remote sensing relies on the sunlight backscattered from the ocean to convey information about optically active marine constituents. Differences in the spectral absorption and scattering properties of various oceanic constituents may allow us to infer the concentration of these constituents from space. Satellite borne ocean colour sensors measure light from the ocean in a number of spectral bands. The spectral positions of these bands are chosen to be most sensitive to changes in the colour of the ocean due to changes in concentration of pigments such as chlorophyll. At the same time, the spectral position must be chosen to minimize the effects of the atmosphere.

August 1997 marked the revival of the production of visible channel imagery of the ocean with the launch of the SeaWiFS (Sea-viewing Wide Field-of-view Sensor). This polar orbiting instrument has six 20 nm wide channels and two 40 nm wide channels in the wavelength range 400 to 900 nm. It provides 1 km resolution global coverage ocean colour measurements every 1 to 2 days.

SeaWiFS data was downloaded by the Western Australian Satellite Technology and Applications Consortium (WASTAC) and processed using SEADAS, the standard SeaWiFS data processing software. Scientists in Western Australia began utilizing the SeaWiFS data in 1998, with preliminary analyses comparing in-situ chlorophyll measurements to SeaWiFS derived chlorophyll concentration (Chedzey 1998).

Previous sections of this report present chlorophyll data and attenuation coefficient (K 490) data as measured by the SeaWiFS sensor, and compares the remotely sensed data to *in situ* data. This section of the report displays a sample of the SeaWiFS chlorophyll images. Each image has been extracted from a full level 2 pass. The extracted region, extending from 31.25° to 32.75°S, and from 114.0° to 116.0°E, is remapped to a mercator projection with 200 lines and 200 pixels within the study region. This remapping produces close to 40 samples along the length of the 40 km Hillarys transect.

9.2 Results and Discussion

Due to licensing agreements, SeaWiFS imagery is not able to be distributed freely to non-approved groups or individuals. Data derived from imagery is however able to be reported. **Sections 5 and 6** utilize SeaWiFS ocean colour data. Comparisons are made with various *in situ* measurements.

During the SEADAS processing to level 2 data (including chlorophyll concentration and K-490) sixteen different parameters are checked to determine data quality. If these various parameters fall outside certain bounds then pixels may be flagged as suspect in terms of data quality. **Table 9.1** shows the flag values at each of the longitude locations for each transect date.

Table 9.2 shows the sixteen different bits which may be set to indicate each of the quality control flags. Table 9.3 shows the bits set corresponding to all the quality flags shown in Table 9.1.

Figures 9.1 to 9.9 show samples of SeaWiFS chlorophyll images obtained on the same dates as some of the sampling cruises. In terms of the colour scale used to display the chlorophyll data, red colours indicate high concentrations of chlorophyll, blue medium concentrations, and green low concentrations. The transect location is indicated by the red line running perpendicular to the coast, just above the middle of each image.

Clearly the chlorophyll concentration decreases as distance from the coast increases. It would appear that, over the region being studied, the mean chlorophyll concentration increases towards the middle of the year, and decreases towards the end of the year. The offshore waters, beyond about 40 km, tend to be relatively featureless, in terms of chlorophyll concentration variations, during the summer months. During the winter months, when the concentrations are slightly elevated, there are some features evident, but most of the variations still tends to be closer to the shore. The speckled and black regions in the lower left corners of Figures 9.5 and 9.6 indicate the presence of cloud.

9.3 Conclusions

The nature of ship based water sampling, or any form of *in situ* work for that matter, produces point measurements at a spatial resolution dependent upon the number and location of stations sampled. Where this provides the most accurate point measurements, an overview may only be provided by remote sensing techniques. Influences of surrounding waters, temporal patterns over periods of days, weeks, months or even years may be provided by use of remote sensing. The *in situ* sampling has supported the validity of the SeaWiFS data products. This bodes well for the future of remote sensing and its application to future work involving monitoring of oceanic and coastal waters.

Lon	16/12/98	19/1/98	16/2/98a	16/2/98b	17/3/98	21/4/98a	21/4/98b	19/5/98	23/6/98	15/7/98	26/8/98	23/9/98	20/10/98	10/11/98b	9/12/98
115.315	11056	0	32	16432	0	32	304	0	0	0	0	0	0	16432	32
115.325	11056	0	32	16432	0	32	304	0	0	0	0	0	0	16432	32
115.335	11056	0	32	16432	0	32	305	0	128	0	0	0	0	16432	32
115.345	11056	0	32	16432	0	32	305	0	0	0	0	0	0	16432	32
115.355	11056	0	32	16432	0	32	48	0	0	0	0	0	0	16432	32
115.365	11056	0	32	16432	0	32	48	0	0	0	0	0	0	16432	32
115.375	11056	0	32	16560	0	32	48	0	0	0	0	0	0	16432	32
115.385	11056	0	16416	16560	0	32	48	0	128	0	0	0	0	16432	32
115.395	11056	0	16416	16560	0	32	48	0	0	0	0	2048	0	16432	32
115.405	9008	0	16416	16560	0	32	48	0	0	0	0	2048	0	16432	32
115.415	9008	0	16416	16560	0	32	48	0	128	0	0	2048	0	16432	32
115.425	9008	0	16416	16560	0	32	48	0	128	0	0	2048	0	16432	32
115.435	9008	0	16416	16560	0	32	16432	0	128	0	0	2048	0	16560	32
115.445	9008	0	16416	16432	0	32	16432	0	128	0	0	2048	0	16560	32
115.455	9008	0	16416	16432	0	32	16432	0	128	0	0	2048	0	16560	32
115.465	-7248	0	32	16432	0	32	16432	0	128	0	0	2048	0	16560	32
115.475	-7248	0	16416	16432	0	32	16432	0	128	0	0	2048	0	16560	32
115.485	-7248	0	16416	16432	0	32	16432	0	128	0	0	2048	0	16560	32
115.495	-7248	0	16416	16432	0	32	16432	0	128	0	0	2048	0	16560	32
115.505	9008	0	16416	16432	0	160	16432	0	128	0	0	2048	0	16560	32
115.515	9008	0	16416	-15952	0	160	16688	0	128	0	0	2048	0	16560	32
115	9008	0	16416	-15952	0	160	16688	0	128	0	0	2048	0	16560	32
115.525	9008	0	32	-15952	0	160	16816	0	128	0	0	2048	0	16560	32
115.545	-15439	0	32	-15952	0	32	16816	128	128	0	0	2048	0	16560	32
115.555	-15439	0	16544	-15952	0	32	16816	128	128	0	0	2048	0	16560	32
115.565	2865	0	16544	-15952	0	32	16816	128	128	0	0	2048	0	16560	32
115.575	2865	0	16544	-15952	0	32	16816	128	128	0	0	2048	0	16560	32
115.585	2865	0	16544	-15952	0	480	16816	128	128	128	64	2112	0	16560	32
115.595	-7184	64	416	-15887	0	416	497	128	192	192	64	2112	64	16560	224
115.605	-7184	64	416	-15887	0	416	497	128	192	192	64	2112	64	496	224
115.615	-7184	64	416	-15887	0	416	497	128	128	128	64	2112	64	432	224
115.625	-7184	64	416	-15887	64	480	497	192	128	128	0	2112	64	432	224
115.635	-7184	0	480	-15887	64	480	-15951	192	128	128	0	2048	64	432	480
115.645	11120	0	480	-15887	192	480	-15951	192	128	128	0	2048	2048	432	416
115.655	-7248	0	416	-15887	192	417	-15951	192	192	192	0	2048	2048	432	416
115.665	-7248	64	416	-15887	192	480	-15951	192	192	192	64	3136	2048	2417	416
115.675	-7248	64	-15375	-15887	2496	480	-15887	448	-16191	192	64	3136	2112	2417	480
115.685	-7248	192	-15375	-15887	2496	480	-15887	448	-16191	192	192	2368	2112	2417	480
115.695	11120	2496	-15375	-15887	2496	480	-15887	448	-16191	192	64	2368	3136	2417	480
115.705	11120	2496	-15375	-15887	2496	-15375	-15887	2496	-15935	449	64	2368	2112	2417	818
115.715	11120	10560	-15375	-15887	-15407	-15375	-15887	2496	-15935	3393	3392	2368	3392	496	818
115.725	11120	11072	-15375	-15887	-15407	-15375	-15887	3392	2496	3393	3392	11072	3392	818	818
115.735	11120	11072	-15375	-15887	-15407	818	-15375	3392	770	2496	3392	11072	3392	818	818

Table 9.1: SEADAS level 2 quality control flags. The Hillarys transect is run at -31.829 degrees latitude. The table above lists the level 2 quality control flags associated with each SeaWiFS image pixel at the indicated longitudes. See table 9.2 for explanation of the flag values. Rows with longitude values corresponding to Hillarys transect sampling stations are displayed in bold text. The eastern most station (H0) is at 115.73 degrees longitude so the bottom two rows (± 0.005 degrees) are both displayed in bold text.

Bit Set = 1	Condition Indicated	Algorithm Name
1	atmospheric correction algorithm failure	EPSILON1
2	land	LAND1
3	missing ancillary data	ANCIL1
4	Sun glint	SUNGLINT1
5	total radiance greater than knee value	HIGHT1
6	large spacecraft zenith angle	SATZEN1
7	shallow water	COASTZ1
8	negative water-leaving radiance	NEGLW1
9	stray light	STRAYLIGHT1
10	cloud and ice	CLDICE1
11	coccolithophores	COCCOLITH1
12	turbid, case-2 water	TURBIDW1
13	large solar zenith angle	SOLZEN1
14	high aerosol concentration	HIGHTAU1
15	low water-leaving radiance at 555 nm	LOWLW1
16	chlorophyll algorithm failure	CHLOR1

Table 9.2: SEADAS level 2 processing quality control flags.

flag	bit values	flag	bit values
-16191	1100000011000001	449	0000000111000001
-15952	1100000110110000	480	0000000111100000
-15951	1100000110110001	496	0000000111110000
-15935	1100000111000001	497	0000000111110001
-15887	1100000111110001	770	0000001100000010
-15439	1100001110110001	818	0000001100110010
-15407	1100001111010001	2048	0000100000000000
-15375	1100001111110001	2112	0000100001000000
-7248	1110001110110000	2368	0000100101000000
-7184	1110001111110000	2417	0000100101110001
0	0000000000000000	2496	0000100111000000
32	0000000000100000	2865	0000101100110001
48	0000000000110000	3136	0000110001000000
64	0000000001000000	3392	0000110101000000
128	0000000010000000	3393	0000110101000001
160	0000000010100000	9008	0010001100110000
192	0000000011000000	11056	0010101100110000
224	0000000011100000	11072	0010101101000000
304	0000000100110000	11120	0010101101110000
305	0000000100110001	16432	0100000000110000
416	0000000110100000	16560	0100000010110000
417	0000000110100001	16688	01000000100110000
432	0000000110110000	16816	01000000110110000
448	0000000111000000		

Table 9.3: SEADAS level 2 quality control flags and bit values. For example, flag value 16816 (the last entry in the table) corresponds to bits 5, 6, 8, 9 and 15 being set. Table 9.2 shows these bits as indicating flags HIGHLT1, SATZEN1, NEGLW1, STRAYLIGHT1 and LOWLW1 being set.

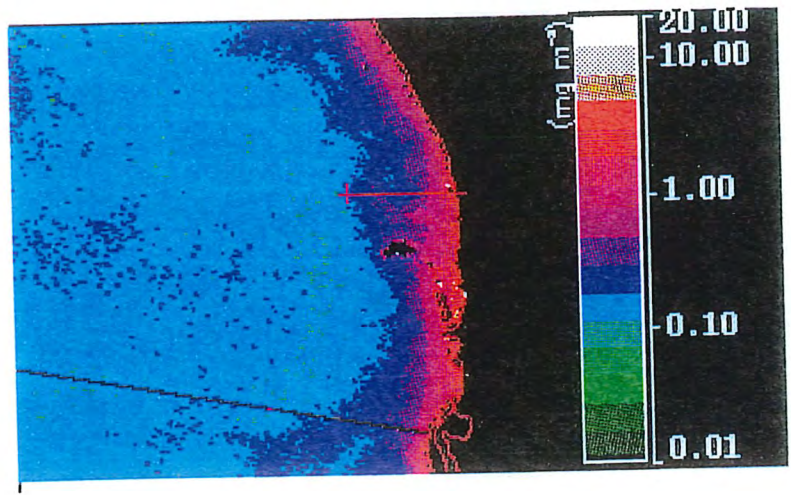


Figure 9.1 SeaWiFS chlorophyll image, 19th January 1998.

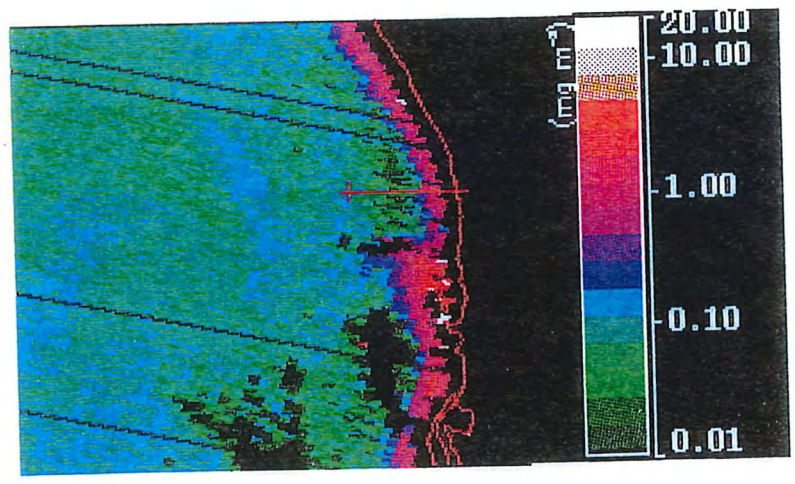


Figure 9.2 SeaWiFS chlorophyll image, 16th February 1998.

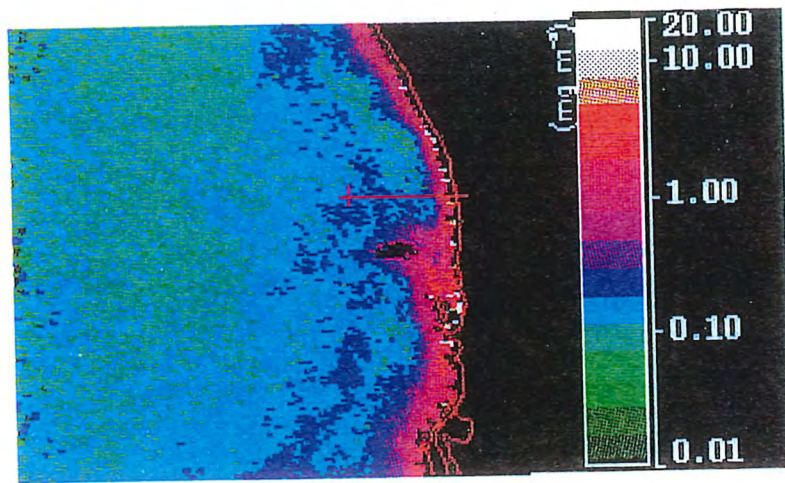


Figure 9.3 SeaWiFS chlorophyll image, 17th March 1998.

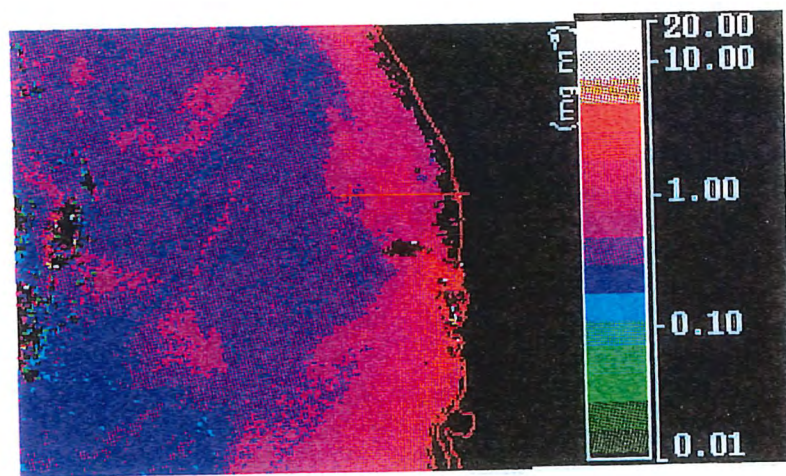


Figure 9.4 SeaWiFS chlorophyll image, 23rd June 1998.

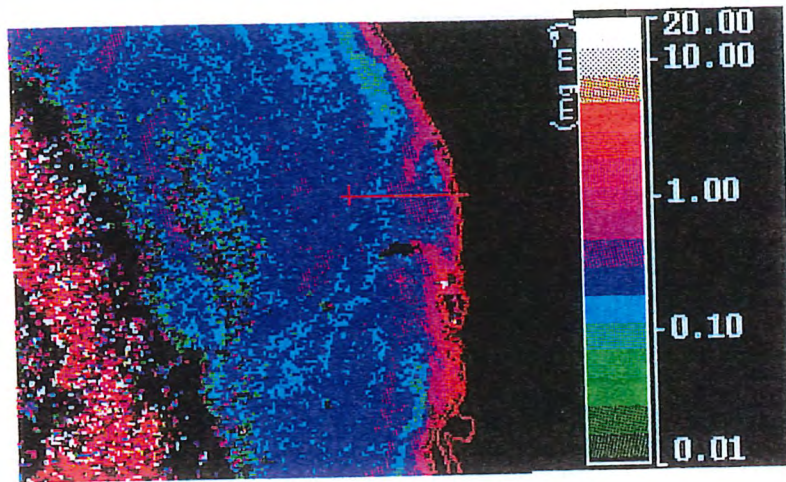


Figure 9.5 SeaWiFS chlorophyll image, 15th July 1998.

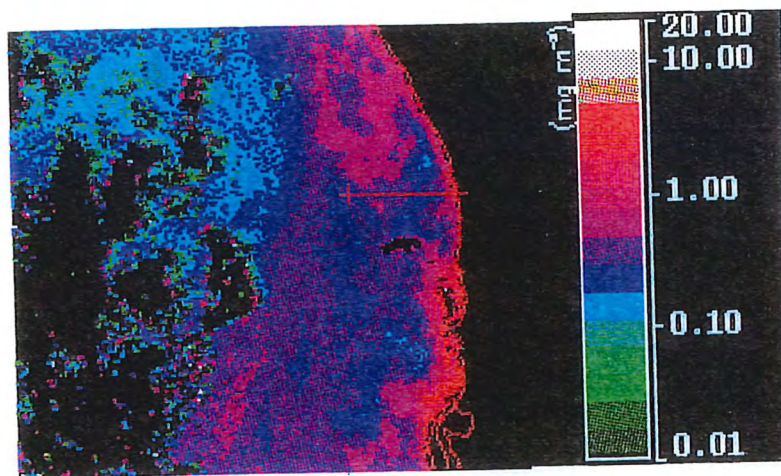


Figure 9.6 SeaWiFS chlorophyll image, 26th August 1998.

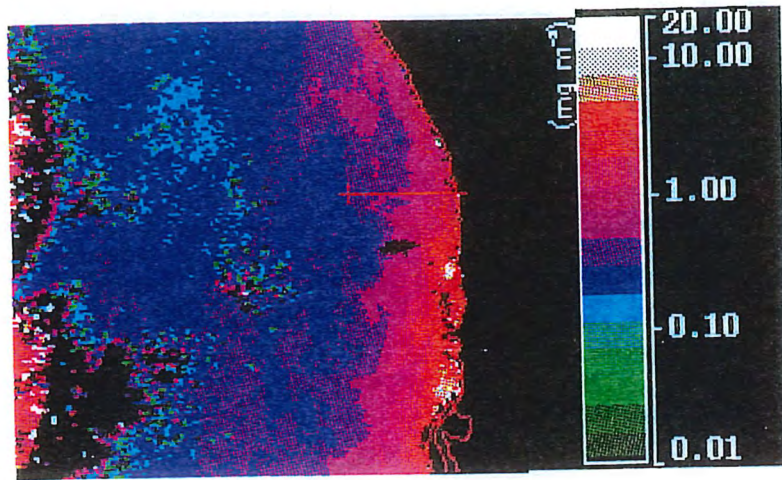


Figure 9.7 SeaWiFS chlorophyll image, 23rd September 1998.

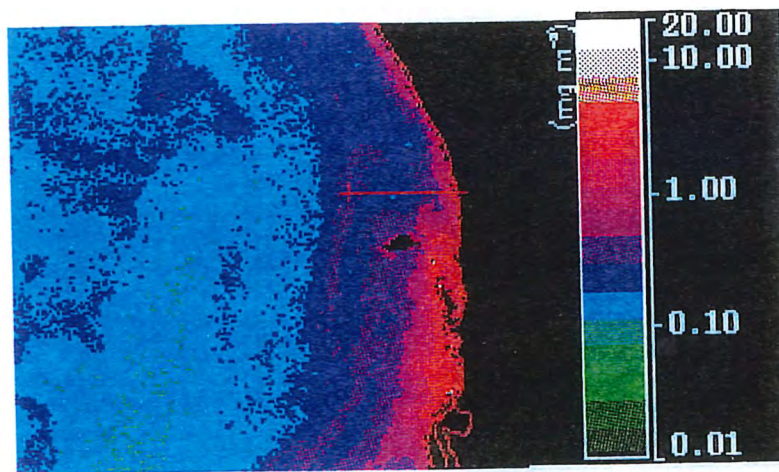


Figure 9.8 SeaWiFS chlorophyll image, 20th October 1998.

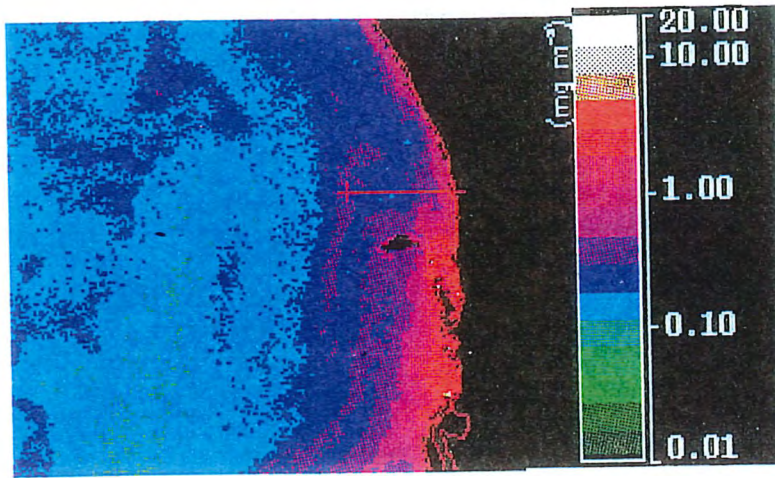


Figure 9.9 SeaWiFS chlorophyll image, 9th December 1998.

Section 10: Phytoplankton (Wilma Vincent, Peter Fearn and Stuart Hellen)

Marine phytoplankton absorb energy from the sun and store it as chemical energy. Phytoplankton thus form the start of the marine food chain. Distribution and seasonal variations of phytoplankton loads may influence location and abundance of fish stocks. Phytoplankton samples were collected for inter-comparisons with the zooplankton samples and chlorophyll measurements, as well as to provide ground-truthing to fine-tune the interpretation of the satellite data.

Because of the difficulty of finding an available experienced phytoplankton taxonomist and the laborious analysis procedures, these samples have not been analysed in any detail and approaches are being made to some universities for possible student projects. A full analysis should include (1) total species list, (2) community composition (% abundance per species), (3) phytoplankton density (cells/litre) and (4) the relative proportions of diatoms, dinoflagellates and silicaflagellates.

10.1 Data and Methods

Because of the low phytoplankton concentrations in our coastal waters, a variety of sampling methods were tried during the 27 surveys before a useful and reliable sampling technique could be standardised. For the first trip in October 1996, vertically-integrated phytoplankton samples were collected from the upper 18 m of the water column (7.5 m at H0) using the pump-sampling system described above in **Section 3**. The hose was lowered and raised a number of times until a total of 20 litres had passed through a 20 µm phytoplankton net suspended in a 20 litre bucket. This integrated water sample was concentrated in the net to a volume of around 30 ml and then transferred to a plastic vial and preserved with the addition of a few ml of Lugol's Iodine Solution.

As the pumping system proved to be too slow, taking about 5 min to provide 20 litres and therefore hindering other operations, a 60 litre surface bucket sample was taken at each site instead of the integrated sample during the following survey in November. Subsequent phytoplankton samples during the first year were collected via vertical or oblique hauls using a 20µm mesh net pulled slowly from about 18 m depth, or near the seabed in shallower water; the net diameter was 400mm and the length 1200mm. The sample was concentrated to around 30 ml and stored on ice before fixation with Lugol's solution.

The availability of a more efficient pump meant that from the beginning of the second year integrated samples could be taken. This was done by slowly raising and lowering a weighted flexible tube attached to a wet/dry pump through a maximum of 10 m depth. 20 litres of the integrated sample was then passed through a 5µm net and concentrated to around 30 ml as before. Two pulled samples were also taken with the 20µm net (at stations H10 and H20) to provide comparability with the previous data.

As from July 1997, a 5µm net was used for the first time at stations H0, H20, H40, and from September of that year the 5µm net was used at all stations and the 20µm net at H5, H25 and H40.

H40. For the whole of 1998, the 5µm net was pulled and a 20 litre integrated water samples was taken at all stations, and the 20 micron net was used only at stations H10 & H30.

All samples were counted using nanoplankton counters, and counting 5 transects, or 100 each of the most numerous species, at 400x magnification.

10.2 Results and Discussion

The relationship of phytoplankton abundance to the satellite and fluorescence data will be influenced by several factors. The relatively coarse scale of resolution of the satellite image gives an average, whereas the various samples taken from the boat would tend to show variations from this. Patchiness of plankton, both vertically and horizontally, is a well known phenomenon related to biological characteristics, wind and wave effects, and other variations in the marine environment (Stavn 1971). In this study there is a difference in levels/depths from which the phytoplankton and fluorescence samples were taken, and the depth to which the satellite sensor detects. Also, the use of nets to concentrate the phytoplankton leads to a probable loss of the picoplankton, which at times may be a major contributor of chlorophyll, although this will be assessed when the data from the settled samples are processed. At this stage, only a few of the phytoplankton samples have been processed in lab, so that general trends only can be reported.

The major groups of phytoplankton found in this study were the Bacillariophyta (diatoms), Dinophyta (dinoflagellates) and Cyanobacteria. The assemblages in the inshore waters were heavily dominated by the Bacillariophyta (**Figures 10.1 and 10.2**), with dinoflagellates often forming a significant proportion, and total counts above 250 cells/ml were recorded in spring blooms. Cell counts fell significantly with distance offshore, being below 10 cells/ml across the outer-shelf stations. However, during a *Trichodesmium* bloom, offshore cell numbers were around 1000 cell/ml. Offshore, the assemblages may be dominated by diatoms, dinophytes or cyanobacteria. The greater biomass of the inshore samples was probably the result of nutrient inputs from groundwater outflows (Johannes and Hearn 1985), and possibly also the result of higher light availability in the water column due to the shallow sandy bottom. The higher inshore biomass occurred in both summer and winter, and does not appear to correlate with inshore-offshore differences in water temperature.

The diatom assemblages were very diverse, although usually dominated by few taxa. The major component of the biomass was usually composed of either several species of *Chaetoceros*, or *Leptocylindris danica* or *Rhizosolenia stolterfothii*, the succession loosely following that described in a nearby embayment by Hellenen and John (1997). *Hemiaulus sp.* were also common, and a short dominance of *Melosira moniliformis* was seen in spring. The dinoflagellate populations were dominated by *Ceratium furca*, with a reasonable diversity of other taxa present in low numbers. Diversity in the Cyanobacteria was poor, with the most frequent being *Trichodesmium sp.*, which forms extensive offshore blooms in the summer, heaviest late in the season. This species has proved difficult to identify further. Other taxa were briefly prominent,

these being the silicoflagellate *Dictyocha fibula* in spring, and a brief periphytic chrysophyte abundance.

10.3 Conclusions

Currently, sensors are collecting global ocean colour and temperature data related to the state of the ocean environment to a spatial resolution of 1 km. We are entering an era where satellite remote sensing capabilities will provide data to spatial resolution of tens of metres, enabling research to be undertaken near river outfalls and within estuarine, river and lake waters. Local sampling provides validation data, and information not detectable from space such as species and population information. However, *in situ* point measurements may not provide enough information to gain a complete understanding of the factors influencing change in the region of interest. This may only be accomplished by remotely sensed data covering not only the local region, but surrounding regions which may influence environmental conditions locally. Combining local measurements and analysis with remotely sensed data can only enhance our understanding of the diverse and complex ecological systems of the aquatic environment (Pearce and Pattiaratchi 1997).

Monitoring of water quality (or factors indicating water quality) must include analysis of large volumes of both temporal and spatial data, possibly from different sources, and the development of new products for interpreting remotely sensed images for coastal managers.

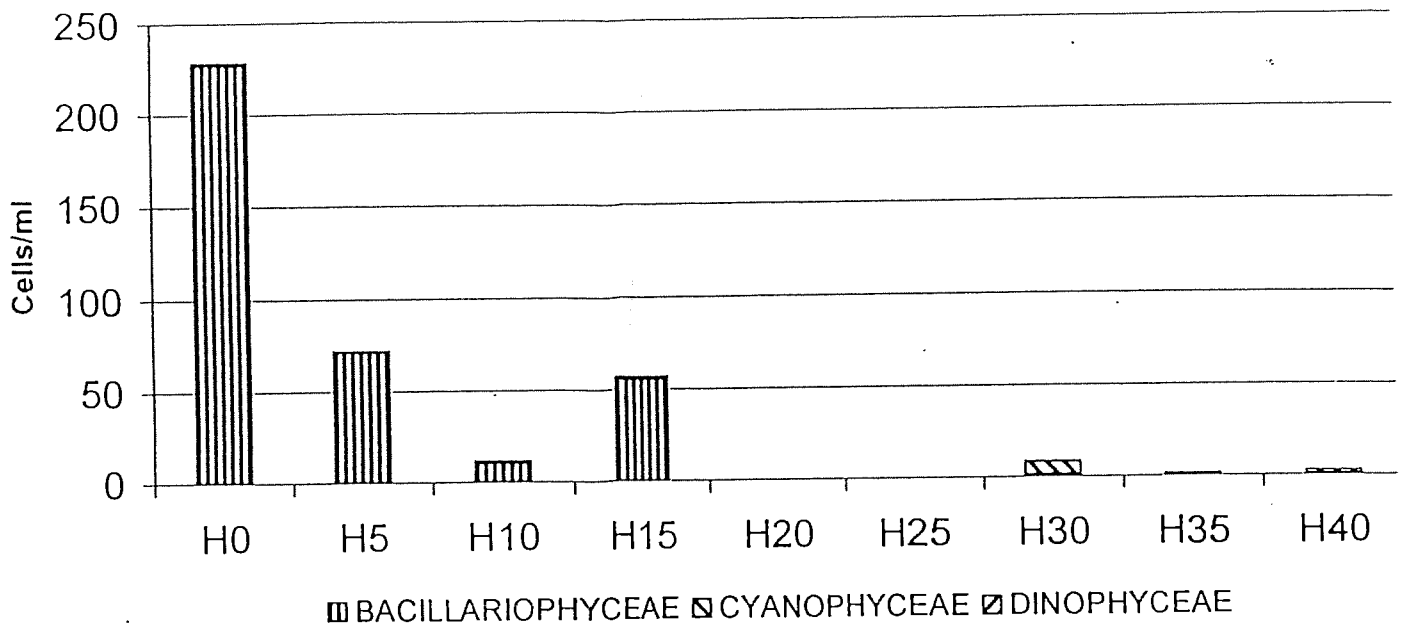


Figure 10.1: Phytoplankton abundances in cells/ml for the Hillarys transect on 11 November 1996. Note there are no data for sites H20 and H25.

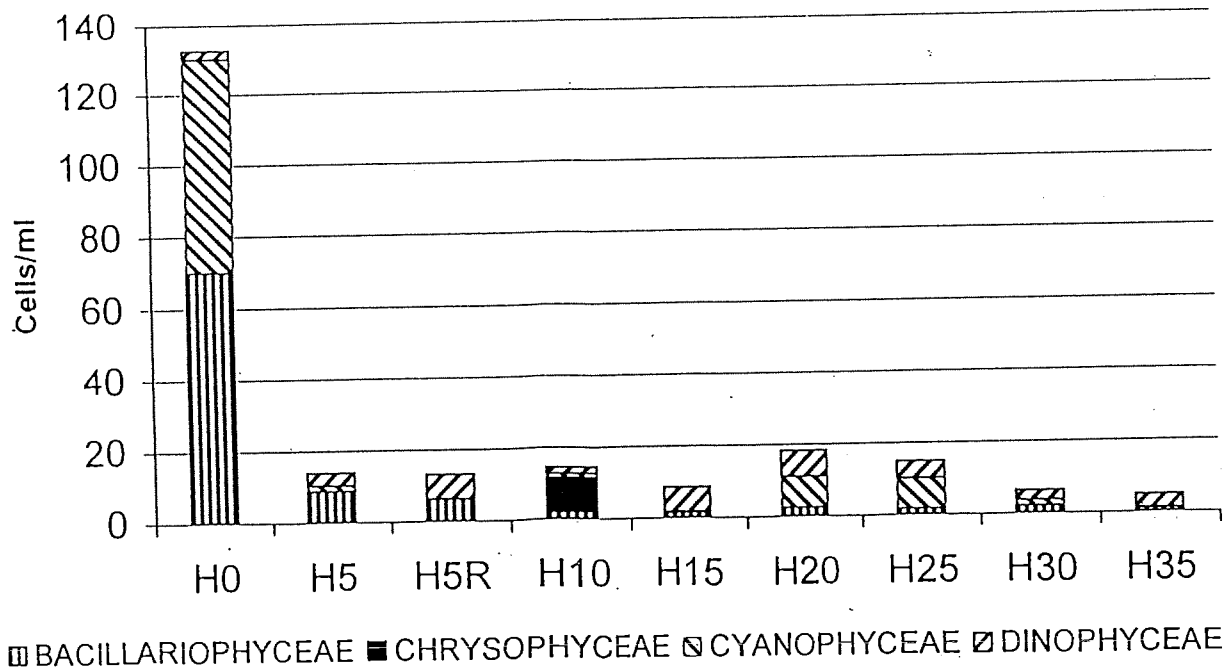


Figure 10.2: Phytoplankton abundances in cells/ml for the Hillarys transect on 17 March 1998. The Cyanophyceae in H20 and H25 is *Trichodesmium* sp. Chrysophytes were periphyton attached to Diatom. Cryptophytes are in H5.

Section 11: Zooplankton (Dan Gaughan)

As in the phytoplankton sampling, some experimentation was required before a consistent zooplankton sampling technique could be devised; the problem was largely because the chartered vessel had no winch with which to pull nets. Similarly, the zooplankton samples have not yet been fully analysed; nevertheless, we believe that they will provide valuable information on seasonal and cross-shelf processes operating near the lower end of the food chain.

Because pilchards (*Sardinops sagax*) in south-west WA primarily feed on micro-crustaceans such as copepods and cladocerans (Gaughan & Potter, 1994) and also periodically concentrate on megazooplankton such as euphausiids (Gaughan, pers. obs.) factors affecting zooplankton are thus likely to also help explain, for example, seasonal changes in cross-shelf distribution of the pilchard stock. The world's major stocks of *S. sagax* (i.e. those occurring in eastern boundary upwelling systems) generally have feeding relationships similar to those for pilchards from Western Australia (e.g. Cole & McGlade, 1998). Knowledge of the lower end of the food chain and its relationship to the environment may provide some insights into the lower west coast pilchard stock using current hypotheses (e.g. Bakun, 1996) developed from the more substantial volumes of work undertaken on this same species overseas. A better understanding of the link between physico-chemical factors, primary production and subsequent secondary production thus has direct benefits for gaining a better understanding of the dynamics of the pilchard (*Sardinops sagax*) stock which occupies the shelf waters along the lower west coast of WA.

Spatial and temporal variations in oceanographic conditions are known to influence the composition and distribution of zooplankton (e.g. Colebrook, 1977) and this has been demonstrated for siphonophores and chaetognaths from shelf waters off southern WA (Gaughan & Fletcher, 1997). However, this latter work was largely descriptive, with variations in seasonal, regional and cross-shelf patterns of abundance and composition being subjectively ascribed to the seasonal changes in strength of the Leeuwin Current as determined by satellite images of SST. The ability to relate the structure of zooplankton communities to the other data sets which were simultaneously collected during this current project (e.g. physical factors, phytoplankton) should permit more objective interpretation(s) of the factors influencing the zooplankton.

Because the need to provide advice for fisheries management is often a major reason that marine studies are undertaken, the opportunity to examine seasonal and cross-shelf patterns in spawning by the pilchard *Sardinops sagax* was also undertaken during the zooplankton study. While monthly plankton samples have previously been used to collect eggs, and thus describe spawning times, of pilchards at Albany on the south coast of WA (Fletcher & Tregonning, 1992) this has not been undertaken on the west coast. While the spawning seasons of pilchards from the Perth metropolitan coast are known from examination of gonadosomatic indices of commercially caught adults (Gaughan, unpublished data), data on cross-shelf variability over an annual cycle at

a distinct location are not available. Such information is considered to be very useful for the interpretation of results obtained from intensive, but temporally limited, ichthyoplankton surveys (e.g. 100s of samples taken along 100s km coastline during 7-10 days) conducted during surveys of spawning biomass of pilchards (i.e. using the daily egg production method) by Fisheries WA.

11.1 Data and Methods

Zooplankton was sampled in each month from October 1996 to December 1998, except for February 1997. All samples were taken with vertical tows which sampled the water column from the surface to 70 m depth or to within 3 m of the bottom in shallower water. In the first two surveys in October and November 1996, samples were taken only at stations H10, H20, H30 and H40. Thereafter, sampling was undertaken at the 8 stations H5 to H40 although in some months station H0 was also sampled. Because of poor sea conditions, some stations were missed in March and August of 1998, and no samples were taken in February 1997.

During the first trip, October 1996, samples were collected with a standard bongo net fitted with 500 μm mesh on one ring and 300 μm mesh on the other. The net was lowered to the required depth and then hauled to the surface by hand. This sampling method was assessed as being inadequate, however, because pulling the relatively large net was very slow and erratic with an obvious 'pumping' action possibly resulting in material being lost through the mouth of the net. Because of this inadequacy and the difference in sampling equipment to subsequent surveys the samples collected on this first cruise will not be used.

In the second and all subsequent surveys, a smaller CalVET net (Smith *et al.* 1985) was employed; this net was also of the bongo design, but both rings had 300 μm mesh and were only 35 cm in diameter. However, hand-hauling this smaller net was also inadequate and samples from this cruise will likewise not be used for quantifying plankton abundance. Between December 1996 and June 1997 a surf-lifesaving reel was used to tow the CalVET nets from the bottom to the surface. While this was a vast improvement over hand-hauling, the condition of the reel deteriorated due to exposure to salt and water and it eventually became inoperable. From July 1997 onwards, the CalVET net was deployed so that it sampled on the way down, with weights added so that the net sampled at approximately 1 m/s; this ensured that the sampling speed was consistent for the duration of each tow and for successive cruises. The mouth of the net closed at the end of the drop, locking the flowmeter impeller, before retrieval to the surface. The net was hand-hauled to the surface using a system of pulleys which considerably simplified the process. At the end of each tow the plankton nets were washed with a deck-hose and the cod-end contents preserved in labelled jars with borax-buffered formalin.

There were insufficient resources (i.e. trained personnel and time) to enable all components of the zooplankton to be quantified. Thirty-five percent of the 188 samples to be used have been partially sorted. Because of the recent work by Gaughan & Fletcher (1997) on siphonophores and chaetognaths in WA and the associated ability to identify members of these groups they have been the first components of the zooplankton samples to be quantified. These

mega-zooplankton are often easier to identify than macro- and meso-zooplankton, noting that identification to the species level will be required and that this can be a time-intensive exercise. In an effort to gain some understanding of variations in other components of the zooplankton, the dominant taxa in each sample were also recorded.

To examine seasonal and cross-shelf patterns in spawning by the pilchard *Sardinops sagax*, the eggs of this species were counted. Pilchard eggs were identified and staged (i.e. developmental stages) using White & Fletcher (1997). Pilchard larvae were also staged as being either yolk-sac, pre-flexion or post flexion and counted.

In an effort to assess the usefulness of the zooplankton data collected during the project, and given the resource limitations, data from only four cruises will be presented in this report. The cruises examined are from June and December of both 1997 and 1998; these were chosen to provide seasonal contrast over two annual cycles.

11.2 Results and Discussion

The choice of which taxa to first investigate has thus far met with both success and a degree of disappointment. Siphonophores were rare. Despite this, a wide variety of siphonophore species are quite easy to identify to the specific level and thus quantifying this component of the zooplankton has been straightforward. Although only 35% of the samples have been sorted there have already been about 20 species identified, including two which are new records (Gaughan, unpublished data) for southern WA waters. However, chaetognaths are intrinsically more difficult to identify to the specific level and thus only four key species were routinely identified, these being *Sagitta enflata*, *S. minima*, *S. regularis* and *Pterosagitta draco*. Other species of chaetognaths encountered besides these four will likely require a concerted effort to identify. The choice of chaetognaths was appropriate as these were typically the most common and abundant species in the samples thus far sorted. A single species of Hydromedusae, *Auglaura hemistoma*, was also quantified since previous experience had shown it to be common and easy to identify.

As with the chaetognaths and siphonophores, the other taxa in the samples include species which are easily identified and others which will probably prove to be more difficult. For example, the calanoid *Temora turbinata* and the cladoceran *Penilia avirostris* are both relatively easy to consistently identify, whereas various species of *Acartia*, a frequently dominant calanoid genus, are notoriously hard to identify.

Because of the need to use relatively small nets on the vessel chartered for the surveys, the amounts of plankton obtained in samples was generally small. This has resulted in particularly low catches rates for taxa, such as siphonophores, which often occur at relatively low concentrations. Because of this situation, data for only a few taxa will be presented in this report. The cross-shelf and seasonal variations of these taxa are shown in **Tables 11.1 and 11.2**.

Table 11.1. Mean densities (no/0.1 m²) of the dominant chaetognath species, one Hydromedusae species and numbers of siphonophore species at stations H5 to H40 across the continental shelf adjacent to Hillarys. Data has been pooled across months.

	Cross-shelf sampling stations							
	H5	H10	H15	H20	H25	H30	H35	H40
<i>Sagitta enflata</i>	4.8	28.0	29.2	18.8	37.8	18.0	14.3	20.2
<i>Sagitta minima</i>	0.0	0.0	0.7	1.3	3.0	4.0	6.0	5.3
<i>Sagitta regularis</i>	0.7	0.3	0.3	1.0	3.0	3.3	2.0	7.7
<i>Pterosagitta draco</i>	0.0	0.5	0.5	1.5	1.7	2.0	8.3	9.2
<i>Auglaura hemistoma</i>	0.3	0.2	1.0	2.5	3.0	5.0	3.7	11.2
Number of siphonophore species	0.7	0.5	0.0	0.0	2.0	2.5	2.6	2.8

Table 11.2. Mean densities (no/0.1 m²) of the dominant chaetognath species, one Hydromedusae species and numbers of siphonophore species in winter and summer of 1997 and 1998. Data has been pooled across stations.

Month	Jun97	Dec97	Jun98	Dec98
<i>Sagitta enflata</i>	29.8	1.5	52.8	3.3
<i>Sagitta minima</i>	2.1	3.9	1.1	8.4
<i>Sagitta regularis</i>	3.7	0.0	3.4	0.0
<i>Pterosagitta draco</i>	3.6	1.6	4.8	1.6
<i>Auglaura hemistoma</i>	5.7	0.5	6.1	1.6
No. siphonophore species	1.4	0.7	3.0	0.1

Sagitta enflata had a relatively even distribution across the shelf, except for quite low numbers at the inner most station (H5). This contrasted the abundances of other species and the diversity of siphonophores which generally increased with distance from shore.

The seasonal patterns for the taxa examined and were remarkably similar to those recorded by Gaughan & Fletcher (1997) for plankton samples taken in 1992/93 on the south coast WA. Thus, *Sagitta enflata*, *S. regularis*, *Pterosagitta draco* and *Auglaura hemistoma* were more abundant in winter, while *S. minima* was more abundant in summer. Diversity of siphonophores on the south coast was likewise higher in winter. The similarities seen to date between zooplankton from the Hillarys transects and those data collected from the south coast of WA in 1992/93 suggest that similarities exist in pelagic processes at these widely separate regions which are both influenced by the Leeuwin Current.

11.3 Conclusions

The spatial and temporal scales of sampling are adequate to detect cross-shelf and seasonal changes in zooplankton composition and abundance. Furthermore, given the opportunistic advent of the zooplankton component of the surveys, the scale of sampling is also at the maximum that could be achieved by staff currently available at Fisheries WA.

Study which attempts to relate the zooplankton data to environmental and biological data will enhance understanding of pelagic processes in shelf waters on the lower west coast of WA and will hopefully continue. The potential that such analyses may provide a reasonable base for developing hypotheses about pelagic processes along other parts of the WA coast which are subjected to the Leeuwin Current is very likely given the similarity, albeit from limited data, between Hillarys and waters between Albany and Esperance. Because the zooplankton were collected simultaneously with other biological and environmental data it should be possible to objectively interpret the results, which will provide a more robust basis for generating hypotheses regarding pelagic ecosystem in south-western Australia than is currently possible.

Section 12: Solarimeter (Jim Davies and Mervyn Lynch)

12.1 Introduction

SeaWiFS observations require corrections to be made for the scattering and absorption effects of the intervening atmosphere in order to accurately determine the water-leaving radiance that is used in ocean chlorophyll abundance algorithms. At wavelengths longer than approximately 700 nm, moderately clear water appears dark (zero water-leaving radiance) due to the intrinsic absorption of water. Under the assumption that SeaWiFS channels at 765 and 865 nm collect photons scattered in the atmosphere only (over ocean water), the SeaWiFS processing algorithms generate the aerosol optical depth at 865 nm and, using the radiances in the 765 and 865 nm channels, generate a factor to allow the aerosol optical depth to be estimated at other wavelengths. Validating the aerosol optical thickness calculated by the SeaWiFS atmospheric correction algorithm is assisted by ground-based measurements. To this end a Yankee Environmental Systems Multi-Filter Rotating Shadowband Radiometer (MFR7) was installed on Rottnest Island (32.00°S, 115.50°E) late in September 1998. This solar photometer configuration employs a whole sky viewing detector and a blackened metal strip that is moved, by stepper motor, to occlude the sun. The direct solar irradiance may be calculated from a combination of sun-blocked and sun-unblocked measurements. A time sequence of direct solar irradiances may then be processed to provide aerosol optical depths in a number of spectral channels.

12.2 Method

The MFR7 has a broadband unfiltered silicon detector channel and six 10 nm (full-width half-maximum) channels at 416.5, 501.2, 615.8, 673.6, 867.6 & 939.5 nm. The instrument is suitable for retrieving total optical depths in these channels and, after corrections for ozone and surface pressure, can deliver an aerosol optical depth for each channel (except the 939.5 nm channel which is contaminated by water vapour). Aerosol optical depths from the MFR7 are based on measurements of atmospheric extinction whereas spaceborne sensors use the angular scattering properties of molecules and aerosols, as well as extinction properties, to arrive at an aerosol optical depth. In both measurement schemes assumptions are made about the albedo of the earth's surface and the angular scattering characteristics of the aerosol particles. However, extinction-only methods are much less sensitive to errors in these assumed values and so a solar photometer derived aerosol optical depth is a reliable ground truth measurement against which a satellite based estimate can be verified.

A "Langley regression" regresses the logarithm of the direct solar irradiance (cutting unit area normal to the solar direction) against the air mass. The air mass is the ratio of the total atmospheric path length in the solar direction to the total vertical atmospheric path length. The slope of a Langley regression is the negative of the total optical depth for any given wavelength. We have used the Langley Analyser software from the Atmospheric Sciences Research Center, Albany, New York to arrive at total optical depths from MFR7 data. Surface pressure fields and ozone thicknesses (from the SeaWiFS ancillary data DAAC) were used to compute molecular and

ozone optical depths. These were then removed from the total optical depth to leave the aerosol optical depths. The SeaWiFS 865 nm aerosol optical depth product can be compared directly with the MFR7 867.6 nm channel aerosol optical depth as a method of validating the SeaWiFS atmospheric correction.

12.3 Results

Aerosol optical depths derived from the Rottneest Island MFR7 are shown in **Figures 12.1 to 12.3** together with the Angstrom coefficient of the aerosol. (The ratio of aerosol optical depths from two spectral channels is set equal to the ratio of the channel wavelengths raised to a negative power that is the Angstrom coefficient). In this work we have used the 867.6 and the 501.2 nm MFR7 channels to quantify the Angstrom coefficient. In general the Angstrom coefficient is large (up to a limiting value of four) for a very fine dust aerosol and small (down to zero or possibly below) for large, salt spray aerosol.

The Hillarys transect during the month of October, 1998 took place on the 20th. However, no MFR7 data was available on this date. On the morning of 10th November, 1998, the 867.6 nm aerosol optical depth was 0.031 ± 0.002 . The Langley regression on which this is based is shown in **Figure 12.4**. Since the algorithm to compute the SeaWiFS 865 nm aerosol optical depth relies upon a zero water leaving radiance at that wavelength, no value is available precisely over the location of the solar photometer. Instead we have taken the SeaWiFS 865 nm aerosol optical depth product from the region $31.9^\circ - 32.1^\circ\text{S}$, $115.2^\circ - 115.4^\circ\text{E}$, immediately to the west of Rottneest Island, i.e. on the open ocean side. The SeaWiFS atmospheric correction algorithm yields 0.044 ± 0.010 as the 865 nm aerosol optical depth (file S1998314044430.L2 processed by SeaDAS 3.0b3).

On the morning of 9th December, 1998, the 867.6 nm aerosol optical depth was 0.036 ± 0.002 . The Langley regression on which this is based is shown in **Figure 12.5**. Once again the SeaWiFS atmospheric correction algorithm yields a higher value for the 865 nm aerosol optical depth of 0.057 ± 0.010 (file S1998343031637.L2).

Clearly there is some discrepancy between aerosol optical depths derived from the SeaWiFS sensor and from the MFR7 solar photometer on the two Hillarys transect days for which we have contemporaneous SeaWiFS and MFR7 data, on both occasions the SeaWiFS atmospheric correction providing optical depths greater than the solar photometer. However, it must be pointed out that the aerosol optical depths are very small so that while the relative deviation may seem large, the absolute error is still very small, of the order 0.02. The relevance of this discrepancy to SeaWiFS estimates of phytoplankton concentration is expected to be small for most viewing geometries.

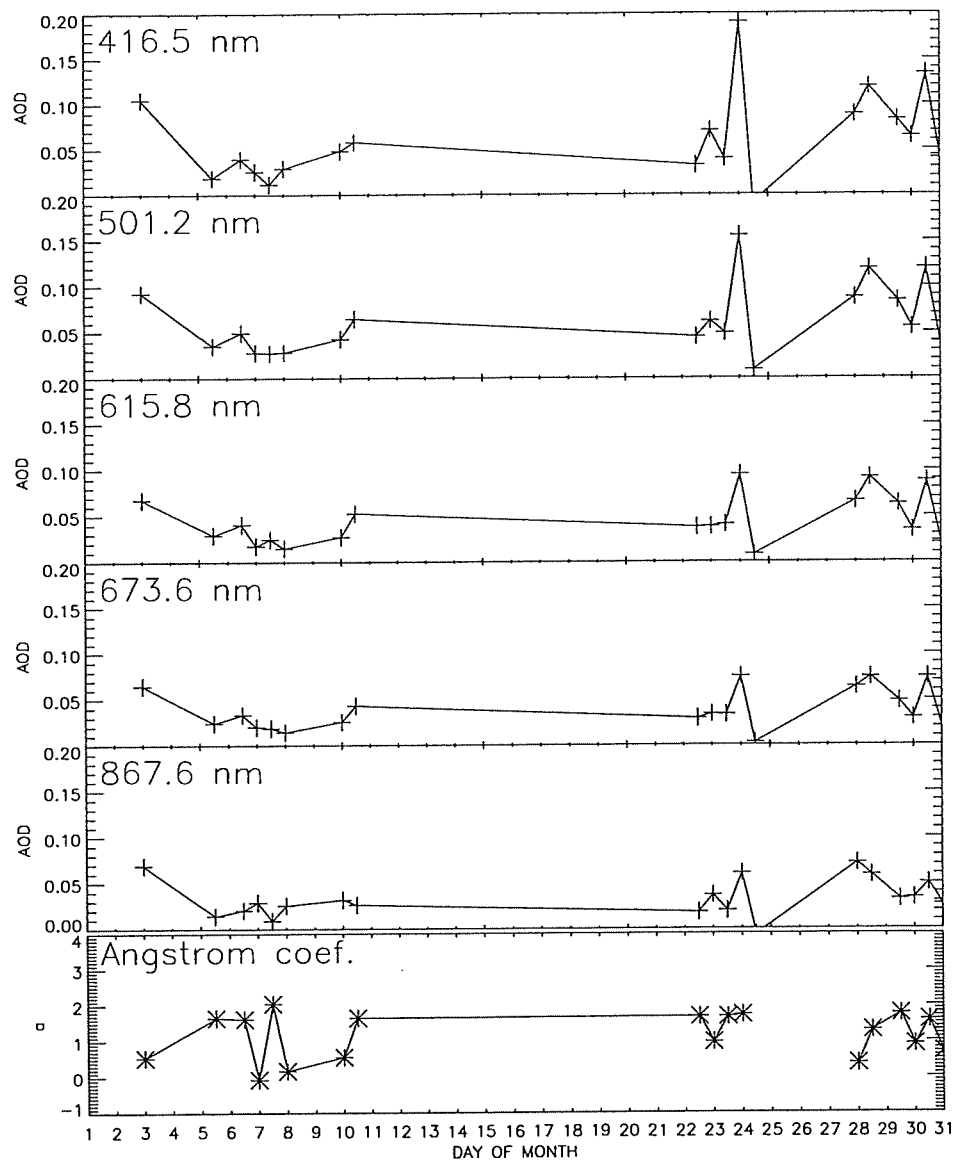


Figure 12.1: MFR7 aerosol optical depths and Angstrom coefficients for October, 1998.

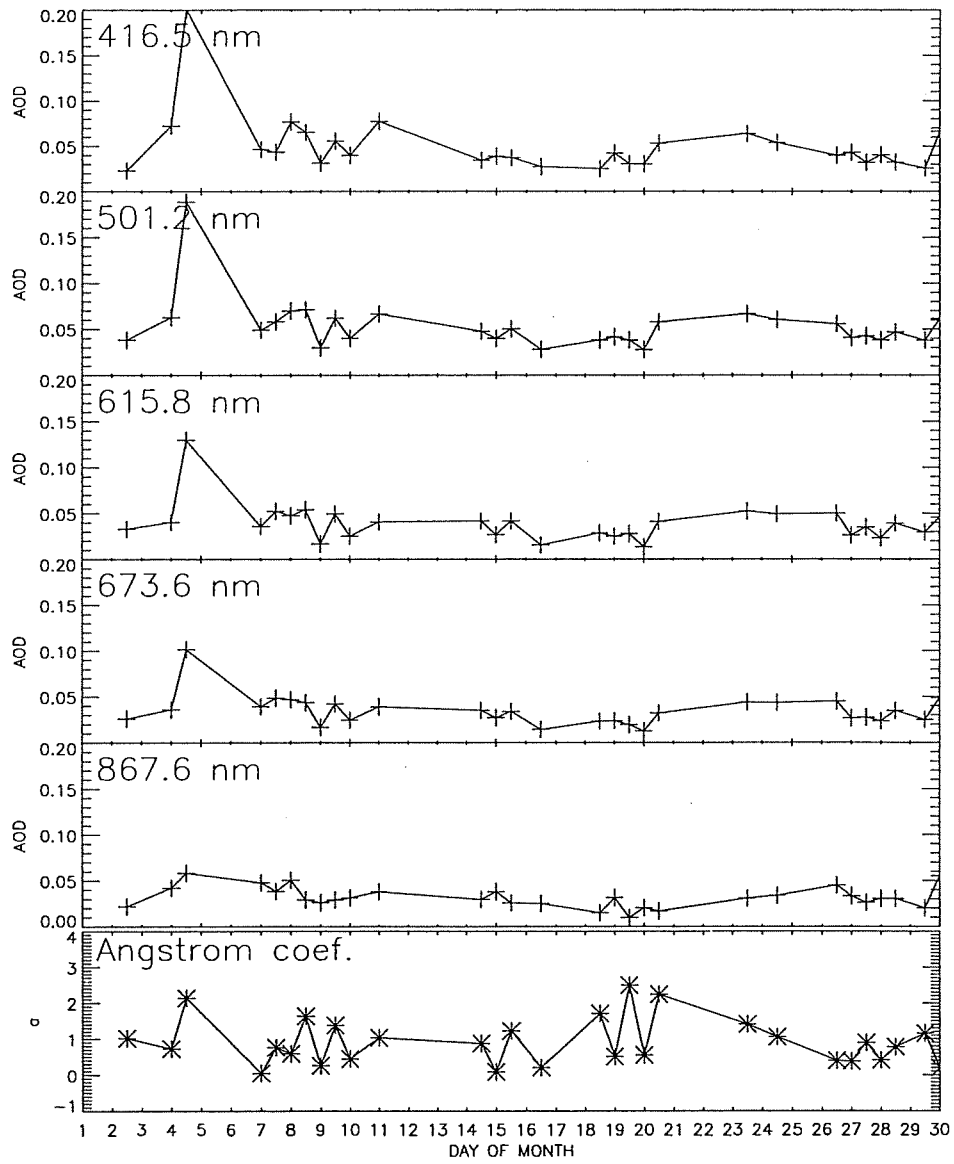


Figure 12.2: MFR7 aerosol optical depths and Angstrom coefficients for November, 1998.

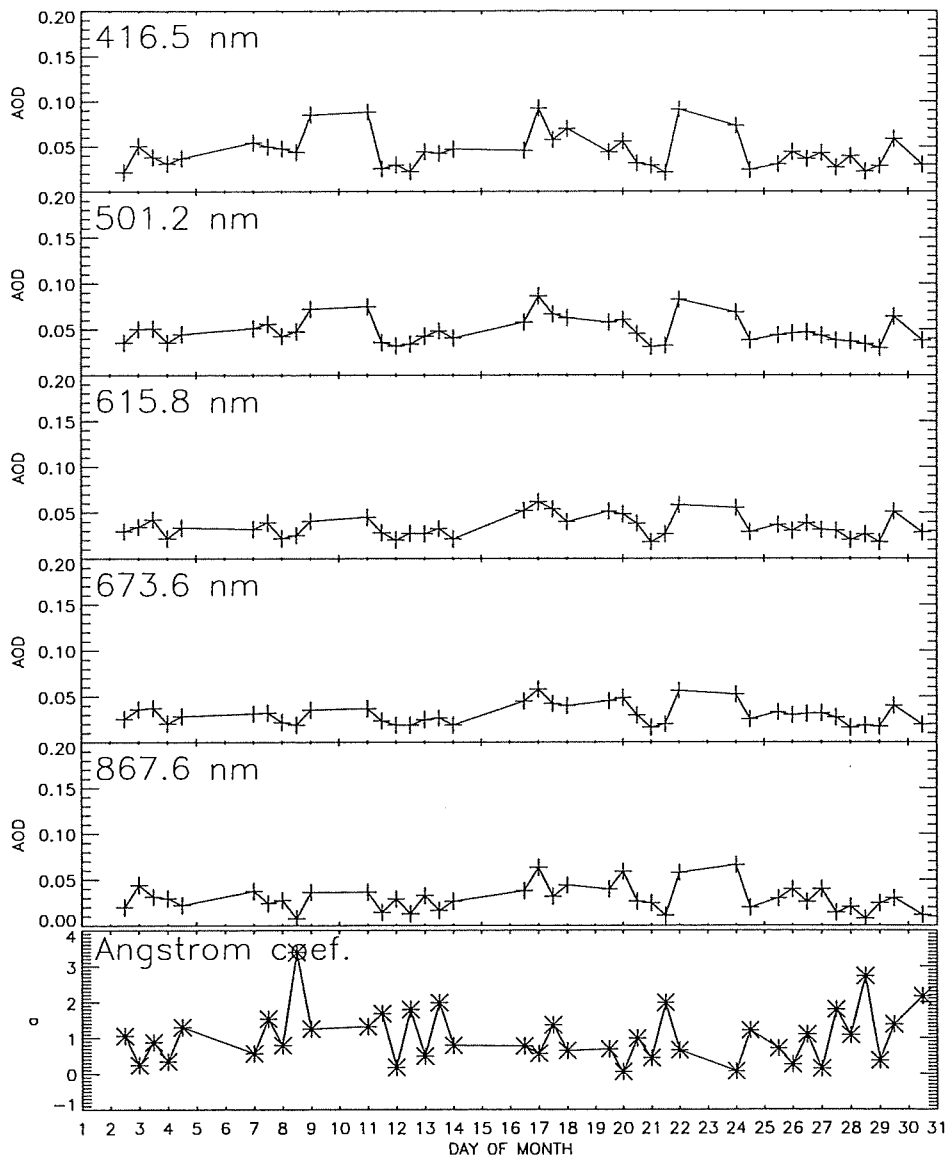


Figure 12.3: MFR7 aerosol optical depths and Angstrom coefficients for December, 1998.

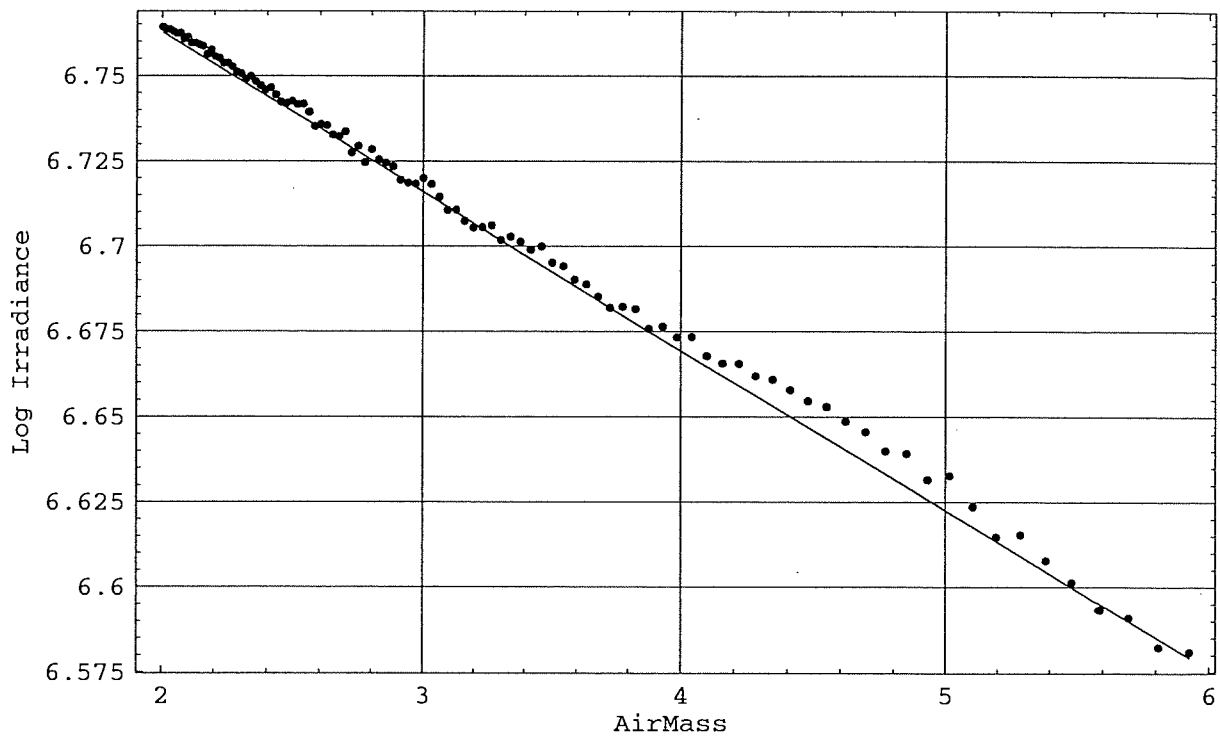


Figure 12.4: Langley regression using MFR7 865 nm channel data from the morning of November 10, 1998.

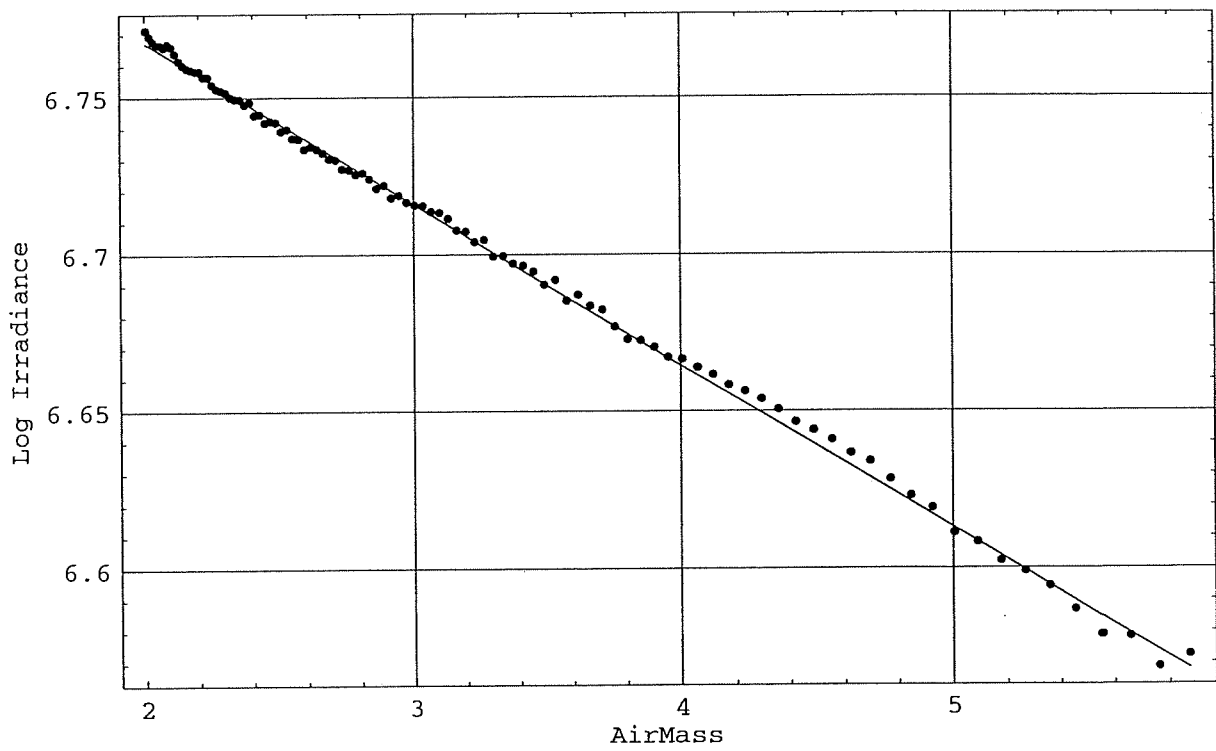


Figure 12.5: Langley regression using MFR7 865 nm channel data from the morning of December 9, 1998.

Section 13: Overall conclusions and future work (Alan Pearce and Mervyn Lynch)

The field surveys off Hillarys have provided the first comprehensive, integrated dataset for remote sensing validation in Western Australia, comprising both sea-surface temperature and ocean colour measurements, as well as showing the seasonal variability of the cross-shelf water and biological properties. Although budgetary constraints limited the quality of some of the results, we have been able to assess the reliability/accuracy of satellite estimates of these quantities in southwestern Australian continental shelf waters. Only selected aspects of the results have been presented in this report. Further analysis of the data is being undertaken, particularly regarding vertical structure in the water column and integration of the various quantities measured (temperature, salinity, chlorophyll, nutrients and light), so that the *processes* influencing the variability can be examined.

Established SST algorithms produce surface temperatures generally within 0.5° of the *in situ* measurements, but on occasion they can differ from the surface data by over 2°C (probably due to cloud which was not readily detected in the imagery). Further work is required to establish appropriate cloud-screening methods based on the AVHRR multi-channel statistics, and on the relationship between bulk and skin temperatures.

Allowing for the specified $\pm 35\%$ accuracy of chlorophyll estimates derived from SeaWiFS, agreement with *in situ* chlorophyll concentrations is often good, particularly in the open offshore (Case 1) waters where the ocean colour is dominated by phytoplankton. In the more turbid (Case 2) waters near the coast, however, where bottom reflectance also contributes to the upwelling signal, agreement is not as good, and further algorithm development is required to separate the different components in the water column and the seabed. The advent of coming satellite sensors with more bands in visible wavelengths and higher spectral resolution will also assist in discriminating the various upwelling components.

With the large expanse of the Western Australian continental shelf and the present paucity of temperature and chlorophyll data, coupled with the expense of making *in situ* measurements, satellite remote sensing offers the only feasible means of monitoring surface water temperatures and ocean productivity in the near-surface layer on a regular basis. As the algorithms are improved by field comparisons such as the Hillarys transects, it should become possible to provide sufficiently reliable temperature and chlorophyll maps to the Western Australian fishing industry, to help explain seasonal and inter-annual fluctuations in recruitment and catch to the important commercial fisheries.

Acknowledgements

- * Fisheries Research and Development Corporation (FRDC) for funding support
- * Perth Diving Academy (PDA) for leasing us the vessel at very reasonable rates, fitting in whenever possible with our time schedule, and for much-appreciated assistance from the skippers and deck-hands with the meteorological measurements during the trips.
- * Bob Griffiths, David Terhell & Neale Johnston (CSIRO Marine Research, Marmion and Hobart) for salinity and nutrient analyses.
- * Lesley Clementson and John Parslow (CSIRO Marine Research, Hobart) for cross-testing chlorophyll samples and analysing phytoplankton pigment composition and concentration from selected samples.
- * NASA/Orbimage for SeaWiFS data access and encryption.
- * WASTAC for AVHRR and SeaWiFS imagery.
- * Tenshi Ayukai (Australian Institute of Marine Science, AIMS), for the loan of the Biospherical INF300.
- * Peter Minnett (RSMAS, University of Miami, Florida) for the loan of the Hard-Hat thermistor.
- * Simon Braine (CSIRO Marine Research, Marmion) constructed some of the equipment and also undertook the early onboard sampling and laboratory analyses.
- * Peter Thompson (University of Tasmania) provided valuable advice during the planning stages of the surveys and some comments on the chlorophyll and phytoplankton results.
- * To the students from the School of Physical Sciences at Curtin University who very ably assisted on the transect days, despite the occasional bouts of sea-sickness: Nick Bower, Geoff Carter, Geoff Cureton, Marc Marinelli, Jackie Marsden, Glenn Newnham, Luigi Renzullo, Andrew Rodger, Jane Rosser and Crispin Wellington; also to Ken White, Graeme Baudains, Paul Lewis and Ron Mitchell (Fisheries WA) for the zooplankton sampling.

References

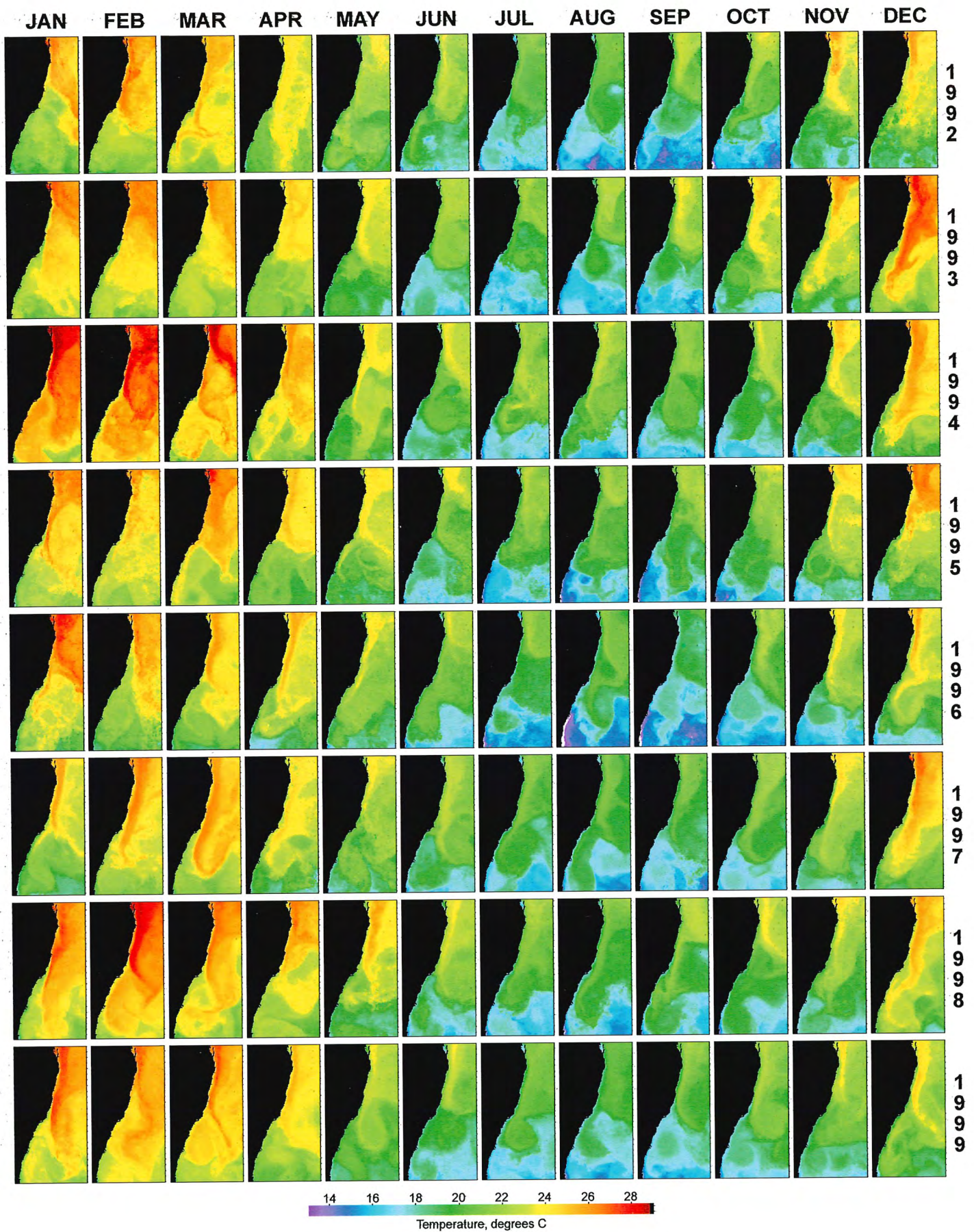
- Alaee, M.J., C. Pattiaratchi & G. Ivey (1998). A field study of the three-dimensional structure of the Rottnest Island wake. *In: Physics of Estuaries and Coastal Seas*, ed. Dronkers & Scheffers, Balkema, Rotterdam, 239-245.
- Bakun, A. (1996). *Pattern in the ocean. Ocean processes and marine population dynamics*. California Sea Grant College System. 323 pp.
- Caputi, N., W.J. Fletcher, A.F. Pearce & C.F. Chubb (1996). Effect of the Leeuwin Current on the recruitment of fish and invertebrates along the West Australian coast. *Proceedings of the International Larval Fish Conference, June 1995; Marine and Freshwater Research* 47, 147-155.
- Chamberlin, S., C.R. Booth, D.A. Kiefer, J.H. Morrow & R.C. Murphy (1990). Evidence for a simple relationship between natural fluorescence, photosynthesis and chlorophyll in the sea. *Deep-Sea Research* 37, 951-973.
- Chamberlin, S. & J. Marra (1992). Estimation of photosynthetic rate from measurements of natural fluorescence: analysis of the effects of light and temperature. *Deep-Sea Research* 39, 1695-1706.
- Chedzey, H. (1998). *SeaWiFS: spectral reflectance ratios and chlorophyll concentrations*. Curtin University of Technology School of Physical Sciences Report UG/310/1998, 87pp.
- Cole, J. & J. McGlade (1998). Clupeoid population variability, the environment and satellite imagery in coastal upwelling systems. *Reviews in Fish Biology and Fisheries* 8, 445-471.
- Colebrook, J.M. (1977). Annual fluctuations in biomass of taxonomic groups of zooplankton in the California Current, 1955-59. *U.S. Fisheries Bulletin* 75, 357-368.
- Cresswell, G.R. (1980). Satellite-tracked buoys in the eastern Indian Ocean. *Proceedings of the 4th International Symposium on Remote Sensing of Environment, San Jose, Costa Rica, April 1980*, 531-541.
- Fearn P.R.C.S. (1999). *Hillarys cross shelf transect - Optical measurements*. Unpublished internal report, Curtin University of Technology.
- Fletcher, W.J. & R.J. Tregonning (1992). The distribution and timing of spawning by the Australian pilchard (*Sardinops sagax neopilchardus*) off Albany, Western Australia. *Australian Journal of Marine and Freshwater Research* 46, 1437-1449.
- Gaughan, D.J. & W.J. Fletcher (1997). The effects of the Leeuwin Current on the distribution of carnivorous macrozooplankton in the shelf waters off southern Western Australia. *Estuarine, Coastal and Shelf Science* 45, 89-97.
- Gaughan, D.J. & I.C. Potter (1994). Relative abundance and seasonal changes in the macrozooplankton of the lower Swan Estuary in south-western Australia. *Records of the Western Australian Museum* 16, 461-474.
- Helleren, S.K.R. & J. John (1997) *Phytoplankton and zooplankton dynamics in the southern metropolitan coastal waters, Perth*. Algal Research Group, School of Environmental Biology, Curtin University of Technology, Perth, 133pp.
- Helleren, S.K.R. & A.F. Pearce (2000). *Chlorophyll-a concentration in Western Australian coastal waters: a source document*. Dalcon Environmental Technical Report 1, 167pp.

- Johannes, R.E. & C.J.Hearn (1985) The effect of submarine groundwater discharge on nutrient and salinity regimes in a coastal lagoon off Perth, Western Australia. *Estuarine, Coastal and Shelf Science* 21, 789–800.
- Johannes, R.E., A.F.Pearce, W.J.Wiebe, C.J.Crossland, D.W.Rimmer, D.F.Smith, & C.R.Manning (1994). Nutrient characteristics of well-mixed coastal waters off Perth, Western Australia. *Estuarine Coastal & Shelf Science* 39, 273-285.
- Lenanton, R.J., L.Joll, J.Penn & K.Jones (1991). The influence of the Leeuwin Current on coastal fisheries of Western Australia. *Journal of the Royal Society of Western Australia* 74, 101-114.
- McAtee, B. (1999a). Sea surface temperature measurements using TASC0 radiometer data from Hillarys cross-shelf transects. Unpublished Note 24pp.
- McAtee, B. (1999b). Calibration of TASC0 radiometer data from Hillarys cross-shelf transects. Unpublished Note 21pp.
- McMillin, L.M. & D.S.Crosby (1984). Theory and validation of the multiple window sea surface temperature technique. *Journal of Geophysical Research* 89, 3655-3661.
- Megard, R. & T.Berman (1989). Effects of algae on the secchi transparency of the southeastern Mediterranean Sea, *Limnology and Oceanography* 34, 1640-1655.
- Mueller, J.L. & R.W.Austin (1995). Ocean Optics Protocols for SeaWiFS Validation, Revision 1. NASA Technical Memorandum 104566, Vol. 25, S.B. Hooker, E.R. Firestone and J.G. Acker, Eds, NASA Goddard Space Flight Center, Greenbelt, Maryland, 67pp.
- Pearce, A.F., S.K.R.Helleren & M.Marinelli (1999). Review of productivity levels of Western Australian coastal and estuarine waters for mariculture planning purposes. Contract report prepared for the WA Aquaculture Development Council, 72pp. To be published as Fisheries WA Research Report.
- Pearce, A.F., R.E.Johannes, C.R.Manning, D.W.Rimmer, & D.F.Smith (1985). Hydrology and nutrient data off Marmion, Perth: 1979-1982. CSIRO Marine Laboratories Report 167, 46pp.
- Pearce, A.F. & C.B.Pattiaratchi (1997) Applications of satellite remote sensing to the marine environment in Western Australia. *Journal of the Royal Society of Western Australia*, 80, 1–14
- Pearce, A.F. & C.B.Pattiaratchi (1999). The Capes Current: a summer countercurrent flowing past Cape Leeuwin and Cape Naturaliste, Western Australia. *Continental Shelf Research* 19, 401-420.
- Pearce, A.F. & D.Pether (1999). Preliminary analysis of temperature logger and satellite temperature data from Marmion Lagoon: 1992 to 1998. Unpublished note.
- Pearce, A.F. & B.F.Phillips (1994). Oceanic processes, puerulus settlement and recruitment of the western rock lobster *Panulirus cygnus*. In Sammarco, P.W. & M.L.Heron (editors): *The biophysics of marine larval dispersal*. American Geophysical Union, Coastal and Estuarine Studies 45, Washington DC, 279-303.
- Pearce, A.F., A.J.Prata & C.R.Manning (1989). Comparison of NOAA/AVHRR-2 sea-surface temperatures with surface measurements in coastal waters. *International Journal of Remote Sensing* 10, 37-52.
- Smith, P.E., W.Flerx & R.P.Hewitt (1985). The CalCOFI vertical egg tow (CalVET) net. *In*: Lasker R. (ed.), *An egg production method for estimating spawning biomass of pelagic fish*:

application to the northern anchovy *Engraulis mordax*. NOAA Technical Report NMFS 36, 27-32.

Stavn,R.H. (1971). The horizontal-vertical distribution hypothesis: Langmuir circulations and Daphnia distributions. *Limnology and Oceanography* 16, 453–466.

White,K.V. & W.J.Fletcher (1997). Identifying the developmental stages for eggs of the Australian pilchard *Sardinops sagax*. Fisheries Research Report (Fisheries WA) 103. 21 pp.



East Australia Sea-surface Temperatures 1992 to 1999

Description: The poster shows monthly sea surface temperatures over the years 1992 to 1999, imaged by the AVHRR instrument aboard the series of NOAA satellites and processed at the Remote Sensing Facility of CSIRO Marine Research in Hobart, Tasmania. Each monthly image represents a composite of individual images for the middle 15 days of each month (compositing is necessary to fill in the frequent gaps caused by cloud cover). A histogram-filtering technique (Rathbone, C.E. 1998, Sea Surface Temperature Compositing by Histograms. CSIRO Marine Research, Internal Report) is used to select the appropriate temperature at each location in the image.

Acknowledgements: Chris Rathbone - Data processing and software. John Parslow - Remapping and compositing algorithms. Melanie Martin - Poster production. CSIRO Marine Research Remote Sensing - Provision of data, software and service. Data received from NOAA's series of polar orbiting satellites.



CSIRO
MARINE RESEARCH
Copyright 2000, CSIRO Marine Research.

A two boat study of the relationship between swordfish and tuna catch rates and fine- and broad-scale physical and environmental variables off eastern Australia



Jock Young, Ann Cowling, Clive Stanley and Leslie Clementson



List of contributors.....	3
Mark Ebbels, John Hinde.....	3
Abstract.....	4
Introduction.....	5
The fishery.....	6
Oceanography of the area.....	6
General movements of swordfish, yellowfin and bigeye tuna in eastern Australian waters.....	7
Aims of the study.....	8
Methods.....	8
Data collection.....	8
Oceanographic data.....	9
Data analysis.....	10
Results.....	12
Oceanography.....	12
Mooloolaba.....	12
Seasonal variation in surface waters.....	12
Vertical Structure.....	16
Bermagui.....	16
Seasonal variations in surface waters.....	16
Vertical structure.....	16
Biology.....	17
Catch composition.....	17
Catches in relation to environmental variables.....	17
Model responses.....	20
Broadbill swordfish.....	20
Yellowfin tuna.....	20
Bigeye tuna.....	23
Discussion.....	23
Oceanographic influences.....	23
Catches in relation to sea surface variables.....	26
Broadbill swordfish.....	26
Yellowfin tuna.....	27
Bigeye tuna.....	28
Summary.....	28
Limitations and future directions.....	29
Acknowledgements.....	29
References.....	31

List of contributors

Principal investigators (Ocean Colour project)	Vincent Lyne and John Parslow
Underway sampler development, installation and maintenance	Matt Sherlock , Don McKenzie, Jeff Cordell, John Parslow
Statistical support	Ann Cowling
Figures	Clive Stanley, Rosemary Bailey, Thor Carter
Longline skippers	Mark Ebbels, John Hinde
Fluorescence calibration	Leslie Clementson, John Parslow
At-sea observers	Jock Young, Don McKenzie, Clive Stanley, Geoff Dews, Rosemary Bailey
Data checking and summaries	Rosemary Bailey, Clive Stanley
Remote sensing	Chris Rathbone

Abstract

The relationship between oceanographic and environmental variables and catches of broadbill swordfish, yellowfin and bigeye tuna were examined between May 1997 and March 1999 off the east coast of Australia between 25 and 36 degrees South. The use of an underway sampler on two longliners which recorded surface temperature, salinity and fluorescence enabled the examination of the association between these variables with the point of capture of individual fish as well as more commonly used variables such as moon phase and time of year. Using a combination of generalized linear and generalized additive models we examined two separate models – one incorporating the entire study area (Model 1) and one restricted to the northern area of the fishery (Model 2) – for the three species. In Model 1, the factors area, month and fluorescence were significantly correlated to broadbill swordfish catch rates. In Model 2, salinity, nearness to front, moon and (month:year) were the main correlates of catch rate. The catch rate of yellowfin tuna in Model 1 was significantly correlated with area followed by month, fluorescence, moon, sea surface temperature and wind strength. In Model 2 salinity, month, fluorescence and year were significantly correlated with catch rate. The catch rate of bigeye tuna was significantly correlated with fluorescence followed by salinity, nearness to front and moon stage in Model 1. In Model 2 fluorescence, salinity, and nearness to front and moon stage were again significantly correlated with catch rates of bigeye tuna. Our results demonstrate that the use of the underway sampler is an effective tool in determining suitable conditions for longline fishing, particularly when used in conjunction with satellite imagery. The results particularly demonstrate the usefulness of fluorescence and salinity in determining suitable fishing water.

Introduction

Broadbill swordfish (*Xiphias gladius*), yellowfin and bigeye tunas (*Thunnus albacares* and *Thunnus obesus*) support a growing domestic longline fishery off the east coast of Australia with annual catches of swordfish alone reaching 2,000 t per annum (Australian Fisheries Management Authority data base). To catch these fish longliners commonly use a suite of environmental indicators to position their lines. These may include proximity to temperature fronts, the presence of seamounts, the colour of the water or the presence of birds. With the development of remote sensing, sea surface temperature maps are routinely used to target particular water masses by the longline industry. Other factors, including moon phase, weather conditions and the local colour of the water, all contribute to whether a particular area is fished or not. Of these, water colour is consistently used as a way of identifying “good” or “bad” fishing waters. However, it is at best a subjective interpretation relying on each fisher’s view of the water in which they work. For example, those that fish in the more productive southern waters have quite a different view of what constitutes clear, blue, green or other descriptions of a particular water mass than does someone from more tropical oligotrophic waters. As this knowledge is gained over years of experience it is difficult to quantify and even more difficult to test the relative importance of each factor in relation to the fishes’ distribution. With the increasing realization that such factors are needed for more accurate stock assessments recent studies in the northern hemisphere have begun to tease out which of these factors are important. There is growing evidence that significant correlations do exist between pelagic fish abundance and a number of environmental variables (e.g. Laurs et al 1984, Fiedler and Barnard 1987, Power and Nelson May 1991 and Swartzman et al 1995).

More recently, there have been efforts to identify the factors affecting the distribution and abundance of larger pelagic species such as swordfish. Podesta et al (1993) found that very high catch per unit effort of swordfish in the western North Atlantic occurred more frequently in the vicinity of temperature fronts than would be expected by chance. However, they noted that the high variability in catch rates they encountered could not all be explained by these fronts and suggested that other, unmeasured, factors were likely to influence catch rate. In that paper they also commented on the

lack of physical and biological data collected contemporaneously with fish captures. Bigelow et al (1999) identified a number of mesoscale factors that influenced catch rate of swordfish in the Hawaii-based swordfish fishery. These variables in order were latitude, time, longitude, lunar index, number of lightsticks, two measures of SST, wind velocity and bathymetry. Bigelow et al's study had no access to contemporaneous measures of salinity or fluorescence.

Because longlines are set over such large distances, sometimes as much as 100 km although usually ~ 50 km, environmental data can only be linked to some arbitrary position, such as the start of the set. Regional characteristics such as lunar phase or wind speed should not vary noticeably within the study area but there is little data that can be attached to individual fish at point of capture. For example, temperature, salinity and measures of ocean productivity such as fluorescence can change significantly over the course of a set. Thus, as Bigelow et al (1999) pointed out, it may be that the scale of measurements available for comparisons of catch rates with environmental variables are not appropriate to determine whether relationships exist or not. As such, valuable information, which may give us insight into a species' behaviour, may be lost.

The fishery

The east coast domestic longline fishery extends from Eden on the southern coast of NSW to as far north as Cairns in northern Queensland and although concentrated within the 200-mile Australian Fishing Zone individual boats regularly fish beyond the zone. Presently, Mooloolaba, southern Queensland, is developing as a major landing and resupply port for the broadbill swordfish and tropical tuna fishery although there are a number of ports where sizeable catches are landed. The catch ranges from a mixture of southern bluefin, yellowfin and bigeye tuna and broadbill swordfish in the south to a mixture of yellowfin and bigeye tuna and broadbill swordfish in the north (Ward in preparation).

Oceanography of the area

The fishery covers a diverse oceanography ranging from the tropical oligotrophic waters of the Coral Sea in the north to a mixture of tropical and subantarctic waters in the south. Linking much of the waters of the fishery is the East Australia Current,

which has its origin as an offshoot of the Coral Sea and extends as far south as the east coast of Tasmania. The strength of this current is determined by both seasonal and interannual factors. In the Australian summer the East Australia Current is at its strongest and pushes as far south as the southern tip of Tasmania where it finally dissipates into the waters of the subtropical convergence (Clementson et al in press). In the winter it retreats northward as the winter westerlies drive subantarctic waters northward. Interannual variations can be even more pronounced. El nino years produce relatively weak currents as the equatorial waters feeding the western Pacific are at their weakest. In contrast La nina years appear to be characterised by higher temperatures along the eastern seaboard and extend further southward.

General movements of swordfish, yellowfin and bigeye tuna in eastern Australian waters

Japanese longline catches in the southwest Pacific Ocean show that broadbill swordfish are distributed along the east coast of Australia to 45 degrees South. The developing fishery for swordfish off southern Queensland suggests that the area between 20 and 30 degrees South may be an area in which these fish concentrate. However, as fishing techniques develop the fishery has broadened its range indicating that the catches in the area may be the result of more intensive fishing. There is no tagging data from which movement patterns of these fish could be deduced. However, possible movement models include the existence of a separate stock along the east coast of Australia which is self-replenishing, although the Japanese catch data indicate this is unlikely. Alternatively, there is a wider western Pacific stock that moves in and out of eastern Australian waters in response to enhanced feeding conditions resulting from changes in the regional oceanography, or to spawn. Large spawning females are caught off Mooloolaba for an extended period over the summer months (Young 1998). The relatively warmer waters of the EAC closer to the coast may provide a suitable environment for the latter.

Yellowfin tuna are also caught along the eastern Australian coastline, and as far south as southern Tasmania in warmer years. Fishery and tag recapture data indicate that the stocks off eastern Australia are the result of overflows of the main western tropical Pacific stock down the east coast of Australia aided by the southward flow of the EAC (Hampton and Gunn 1998). There is some anecdotal evidence to suggest that the

number of yellowfin in eastern Australian waters increase in La Nina years when the EAC is at its strongest. There is no evidence to indicate that yellowfin return to tropical waters. It is more likely that they are retained in localised areas such as the eddies that form on a semipermanent basis off Eden which affords them a warm body of water close to rich feeding grounds. Catch data from both the domestic and foreign longliners indicate that bigeye tuna are caught in similar waters to swordfish off eastern Australia but are found deeper in the water column. There is little information on their movements in these waters other than they are found as far south as 43°S (Campbell 1998).

Aims of the study

As part of a larger study to calibrate remotely sensed ocean colour on the east coast of Australia we aimed in this study to examine the relationship of catch rates of broadbill swordfish, bigeye and yellowfin tuna to environmental variables. Specifically, we ask whether there is a factor, or suite of factors (physical oceanographic as well as more regional variables such as lunar phase) associated with the catch rates of broadbill swordfish, yellowfin tuna and bigeye tuna.

Methods

Data collection

As part of the SEAWIFS ocean colour satellite project (Lyne and Parslow 1994) an underway sampler was developed with the purpose of calibrating the ocean colour imagery. The sampler is described in detail elsewhere in this report. In brief, it measures three variables – temperature, salinity and fluorescence -- at the sea surface in relation to ship's position as measured by GPS and time of day. The sampler is connected to a computer that recorded the three variables at minute intervals at sea. Two of these samplers were fitted to two small longliners operating off the east coast of Australia between May 1997 and March 1999. At ~ two-monthly intervals CSIRO observers spent periods of up to a week on board these vessels. On these trips the observers recorded and identified all fish caught against the time at which they were caught. As time could be related directly to GPS position we were able to determine accurately the position of capture of individual fish. Size and biological details for all fish caught by the longlining operation were also recorded. In the laboratory observer

data were matched with the underway files to link individual fish with all contemporaneous data collected. The observers also collected samples of chlorophyll and salinity to calibrate the sampler and the SeaWifs ocean colour satellite (discussed elsewhere in this report).

Oceanographic data

The oceanographic data for this study is based largely on surface characteristics of the main water masses of the region as determined by the underway sampler. We used that data in the following ways. Off Mooloolaba we used the steaming transect out to the fishing area for each fishing trip on which there was an observer to document changes in the surface characteristics (in this case surface temperature, salinity and fluorescence) of the water. This data set was not repeated for the southern zone as fishing was generally relatively close to the coast. To provide a seasonal comparison of the surface waters in which the longliners fished during the study we used a mean of the underway data from the first set of each fishing trip regardless of whether an observer was on board or not. The underway data was supported by satellite sea surface temperature imagery provided by the NOAA AVHRR satellite although cloudy conditions limited the usefulness of satellite imagery for periods of the study (see data analysis). Ocean colour satellite imagery from the SeaWifs (Sea-viewing Wide Field of View scanner) satellite was also cloud-affected so was not used in the statistical analyses but was used in the description of the study area.

We obtained information on the vertical structure of the water column for both areas from two oceanographic cruises completed during the course of the study. The first, in May 1996 by CSIRO's research vessel MRV Southern Surveyor described the area of the southern portion of the fishery between 35 and 37 degrees South (Young et al in prep). The second cruise, in March 1999 by the Oceanographic Research Vessel Franklin under CSIRO's Dr Ken Ridgeway, examined the vertical structure of the waters covering at least part of the Mooloolaba fishery. He has made available vertical cross section data of temperature and salinity through the main fishing area off southern Queensland to a depth of 500 m. He has also provided surface current data for the region during the period of the cruise.

Data analysis

We examined the relative effect of physical and environmental factors (defined in Table 1) on the catch rate of broadbill swordfish, yellowfin tuna and bigeye tuna in the study area. Initially we produced scatter plots to visualize any potential relationships. We then applied generalised linear models (GLMs) and generalised additive models (GAMs) to investigate the relationships suggested by the plots using the S-Plus software package. We used the binomial distribution. Forward stepwise regressions were applied to the GLMs to determine the statistically significant terms in decreasing order of significance. GAMs were then fitted to the significant terms to determine the nature of the response to the variables. This procedure was followed as statistical inference from GAMs is relatively undeveloped compared with that for GLMs (Borchers et al 1997). The GAMs were necessary, however, as they allow “nonlinear effects of the covariates on the response to be estimated from the data” (Augustin et al 1998, see also Swartzman et al 1995). Once the significant main effects had been determined all two-way interactions were also tested for significance.

We assumed that each longline set was relatively stable horizontally on the basis that even if the line moved it moved in relation to the prevailing currents effectively staying with the same body of water. For this analysis we only used the underway data from the hauling period. We divided each haul into approximately equal segments composed of approximately 200 hooks. The catch data was standardised to the number of fish per 200 hooks.

The data was grouped in a number of ways before settling on two main comparisons. The first comparison used all 139 records from Areas 1 and 2 to determine which of the covariates was significantly correlated with fish abundance, the latter expressed as (the number of fish caught /number of hooks) X 100. Table 1 lists all the factors included as covariates. As the study area was effectively divided into two very different hydrographic regions – the “Mooloolaba” and “Bermagui” areas – a second analysis was run on the Mooloolaba data (Area 1) only, to examine more closely fine-scale effects in the region. The Bermagui data was not examined separately due to small sample sizes.

Table 1. Descriptions of factors used in GLM and GAM analyses

Factor	Description	Range	
		Mooloolaba	Bermagui
Area	Mooloolaba coded as 1, Bermagui as 2	Latitude 25° 05 to 27° 07 Longitude 151° 31 to 155° 18	Latitude 28° 48 to 33° 26 Longitude 150° 20 to 154° 18
Year	Years during which data were collected	1997-1999	1997 - 1998
Month	Month of the year during which data were collected	All months except May, September, October and December	February, September and November only
Moon phase	New moon coded as 1, first quarter as 2, full moon as 3, last quarter as 4	1 - 4	2 - 3
Wind speed	Average wind speed in knots recorded on vessel during the hauling of each set	1 - 20	5 - 10
Shot	Each complete hauling operation of all hooks deployed. Consecutive numbers are given for each set for each fishing trip	1 - 5	2
Subset	Consecutive 2 hour hauling period or part period during the hauling of each set	2 - 6	2 - 5
Temperature	Median value of sea surface temperature for each subset in degrees Centigrade	20.94 - 31.07	19.38 - 25.45
Salinity	Median value for sea surface salinity for each subset in parts per thousand	34.97 - 35.82	35.19 - 35.73
Fluorescence	Median values for sea surface fluorescence for each subset in standard units 9mg m-3	-0.0564 - 0.6646	0.0804 - 1.0319
Distance to temperature front	Distance from subset position to nearest sea surface temperature front (defined as a change in temperature of 1 degree within 5 kilometres). If no front was present, distance was set at 100 n.miles	3 - 40	1 - 12

Results

We made 15 trips on the two fishing boats - 5 out of Bermagui and 10 out of Mooloolaba - during the course of the study (Table 2). Surface oceanographic and environmental data was recorded on a further 37 trips when no observer was on board (Table 2). From the combined data we have provided firstly a description of the waters during the course of the study. Secondly, we have provided an analysis of the catches in terms of the physical oceanographic and environmental variables to determine the relationship, if any, between the two.

Oceanography

Mooloolaba

Seasonal variation in surface waters

In August 1997 satellite and ocean colour imagery for the waters off southern Queensland show the beginnings of the southward-flowing East Australia Current as a relatively thin wedge of warmer, nutrient-poor water close to the shelf edge and extending out to approximately Longitude 155° East (Fig. 1a). The current developed over the following months with the influx of South Equatorial waters from the east and by February 1998 the EAC had extended further to the east past Longitude 157° E (Fig. 1c). The extensive area of warm, clear water was consistent with a La nina episode at this time (Figs. 1 and 2). As winter approached the EAC subsided again before reforming the following spring, although not to the extent of the previous summer (Fig. 1 d - h). The rapid southward flow of the current next to the coast was observed in March 1999 at >1 m per second (Fig. 3).

Satellite imagery (both sea surface temperature and ocean colour) was not available for many months during the project because of cloudy conditions. However, as underway surface variables (temperature, salinity and fluorescence) were recorded at minute intervals on all trips made during the project we were able to further develop our understanding of the surface water characteristics of the region. Figure 4(a - i) shows steaming transects to the fishing grounds for all the cruises completed off Mooloolaba. They show generally colder, more saline water with higher fluorescence

Table 2a. Sampling period and effort (expressed as number of hooks set and number of longlines deployed) off Bermagui and Mooloolaba when a CSIRO observer was present

Start Date	End Date	Cruise Number	Total Hooks	Number of shots	
				Bermagui	Mooloolaba
15/05/97	16/05/97	1	700	1	0
07/10/97	13/07/97	2	2600	0	3
08/20/97	23/08/97	3	2600	0	3
13/09/97	14/09/97	4	1800	2	0
13/10/97	17/10/97	5	3900	0	4
04/11/97	08/11/97	6	1300	2	0
17/11/97	19/11/97	7	2000	0	2
09/02/98	12/02/98	8	1900	2	0
12/02/98	18/02/98	9	4000	0	4
25/04/98	29/04/98	10	720	1	0
07/06/98	13/06/98	11	3100	0	4
09/08/98	12/08/98	12	2700	0	3
04/11/98	9/11/98	13	4750	0	5
28/11/98	30/11/98	14	1950	0	2
25/03/99	29/03/99	15	3100	0	3
Total			37120	8	33

Table 2b. Sampling period and effort (expressed as number of hooks set and number of longlines deployed) off Bermagui and Mooloolaba when no CSIRO observer was present

Start Date	End Date	Cruise Number	Total Hooks	Number of shots	
				Bermagui	Mooloolaba
15/07/97	17/07/97	1	2000	0	2
24/07/97	26/07/97	2	2000	0	2
10/08/97	12/08/97	3	2000	0	2
15/08/97	17/08/97	4	2000	0	2
21/08/97	23/08/97	5	2000	0	2
26/08/97	27/08/97	6	1000	0	1
10/09/97	13/09/97	7	3000	0	3
16/09/97	20/09/97	8	4000	0	4
13/10/97	18/10/97	9	2800	0	4
06/11/97	21/11/97	10	2000	0	2
12/11/97	14/11/97	11	2000	0	2
19/11/97	21/11/97	12	2000	0	2
14/12/97	15/12/97	13	1000	0	1
16/12/97	19/12/97	14	3000	0	3
05/11/97	07/11/97	15	1300	2	0
17/11/97	18/11/97	16	1000	1	0
09/11/97	10/11/97	17	600	1	0
13/11/97	13/11/97	18	700	1	0
18/11/97	20/11/97	19	1920	2	0
25/11/97	26/11/97	20	850	1	0
27/11/97	28/11/97	21	700	1	0
05/12/97	05/12/97	22	720	1	0
11/12/97	11/12/97	23	700	1	0
16/12/97	17/12/97	24	2200	3	0
14/01/98	17/01/98	25	3000	0	4
03/02/98	07/02/98	26	4000	0	4
08/02/98	12/02/98	27	4000	0	4
14/02/98	18/02/98	28	4000	0	4
03/03/98	06/03/98	29	3000	0	3
09/03/98	13/03/98	30	4000	0	4
15/03/98	18/03/98	31	3000	0	3
08/04/98	12/04/98	32	4000	0	4
06/05/98	10/05/98	33	4000	0	4
13/05/98	15/05/98	34	2000	0	2
02/06/98	05/06/98	35	4000	0	4
08/06/98	11/06/98	36	4000	0	4
11/07/98	15/07/98	37	4000	0	4
Total			88490	14	48

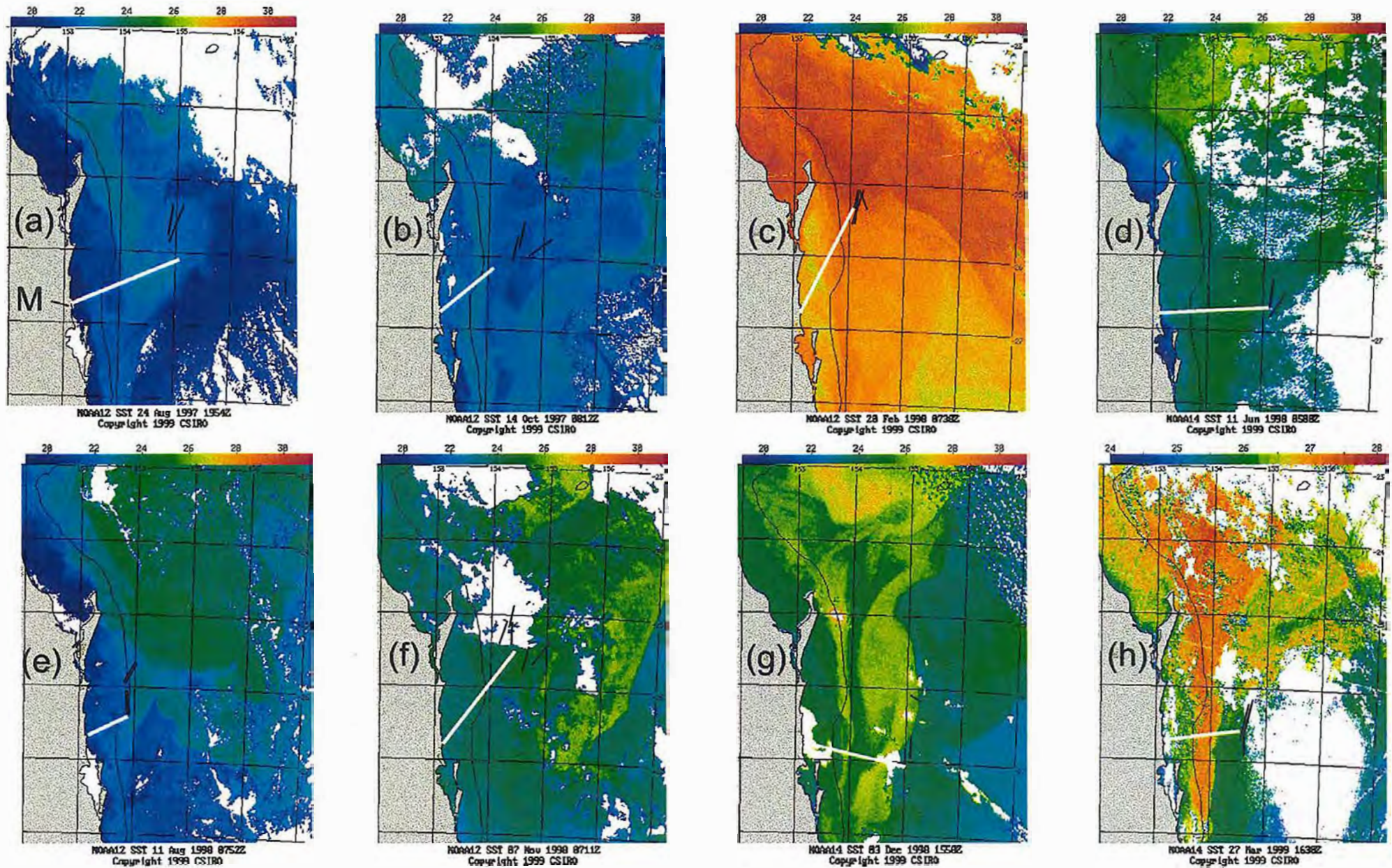


Figure 1: Seasonal changes in the sea surface temperature off southern Queensland during the study period. Black lines are individual longline sets; white line is transect to fishing ground; M=Mooloolaba)

Figure 2: Seasonal changes in ocean colour off southern Queensland during the study period (NASA Seawifs satellite).

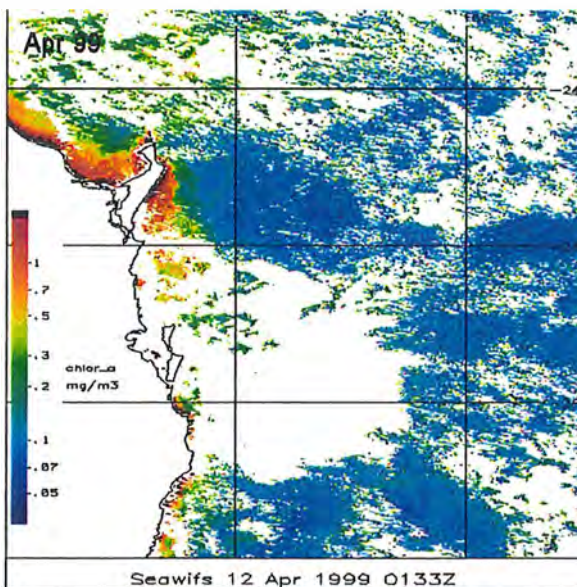
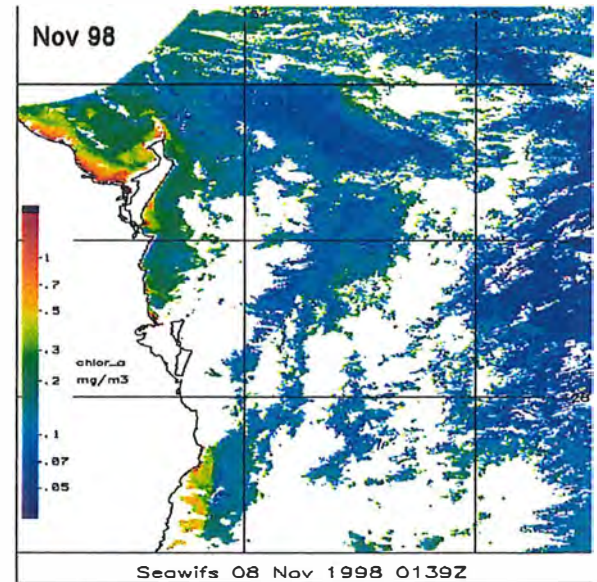
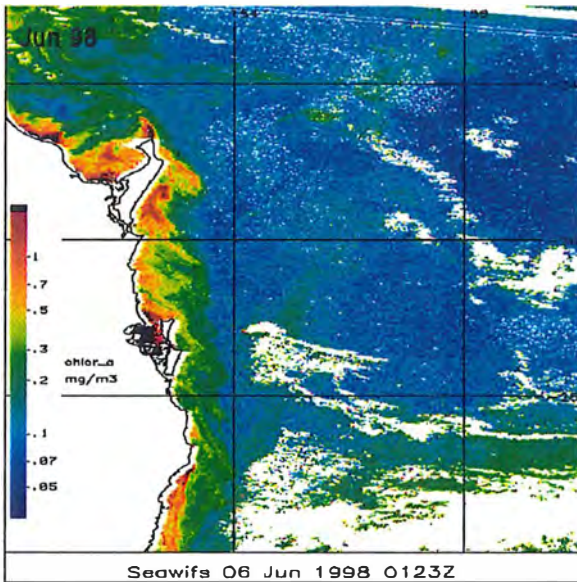
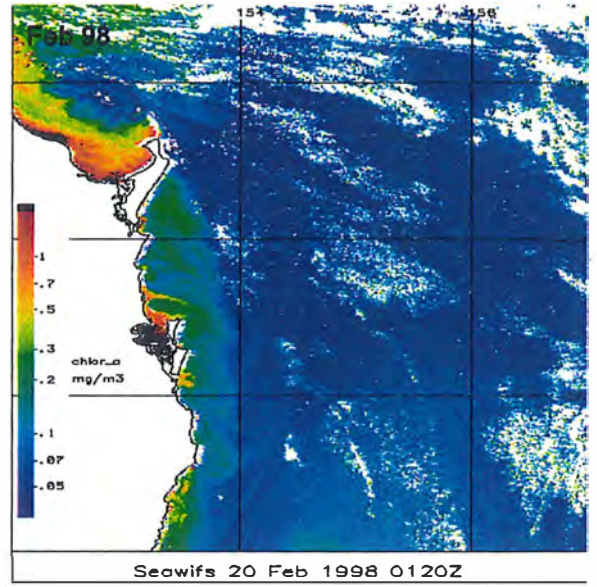
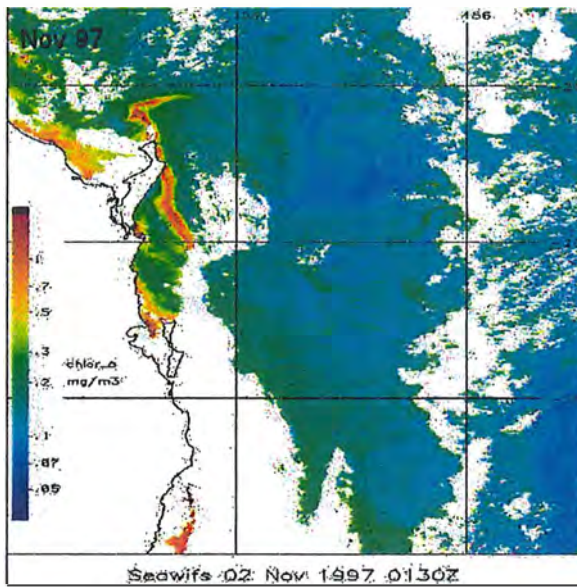


Figure 3. Current speed at 15 m depth (courtesy of K. Ridgway, CSIRO unpublished data)

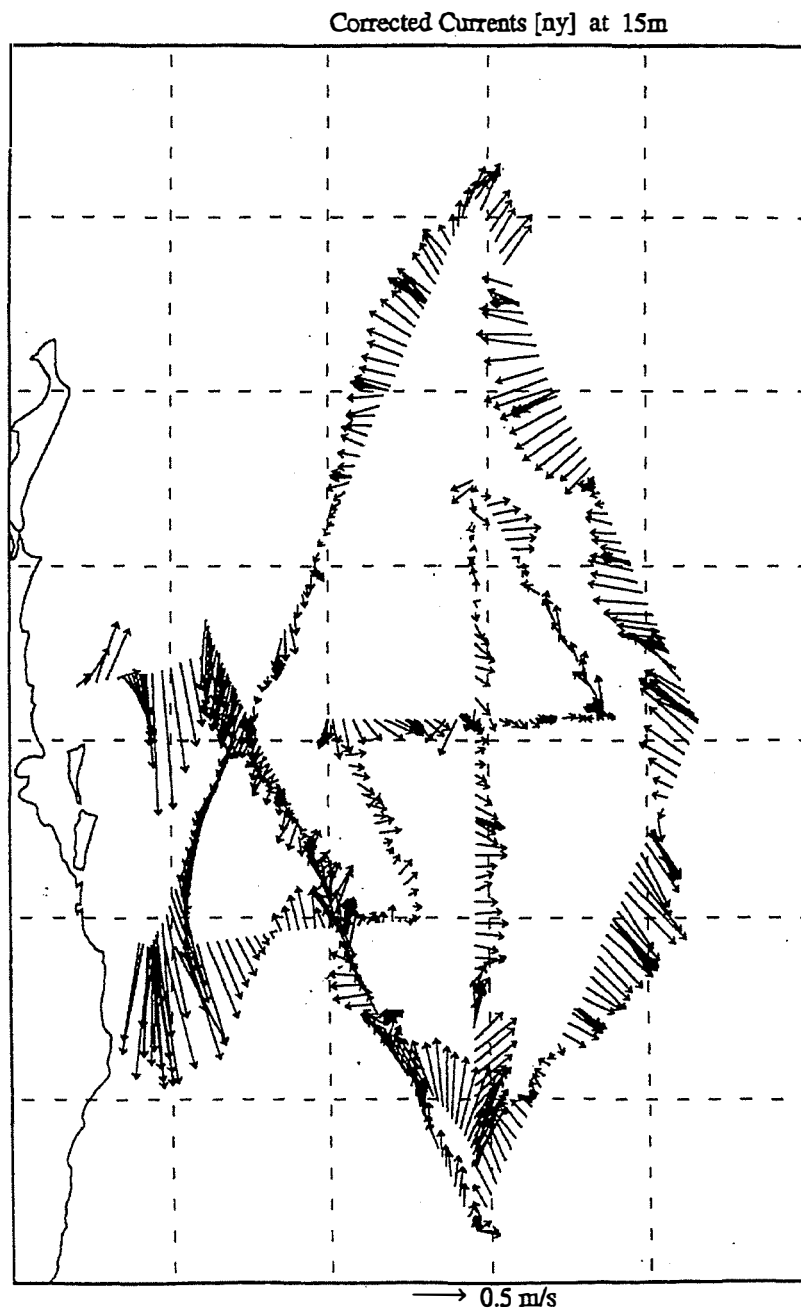
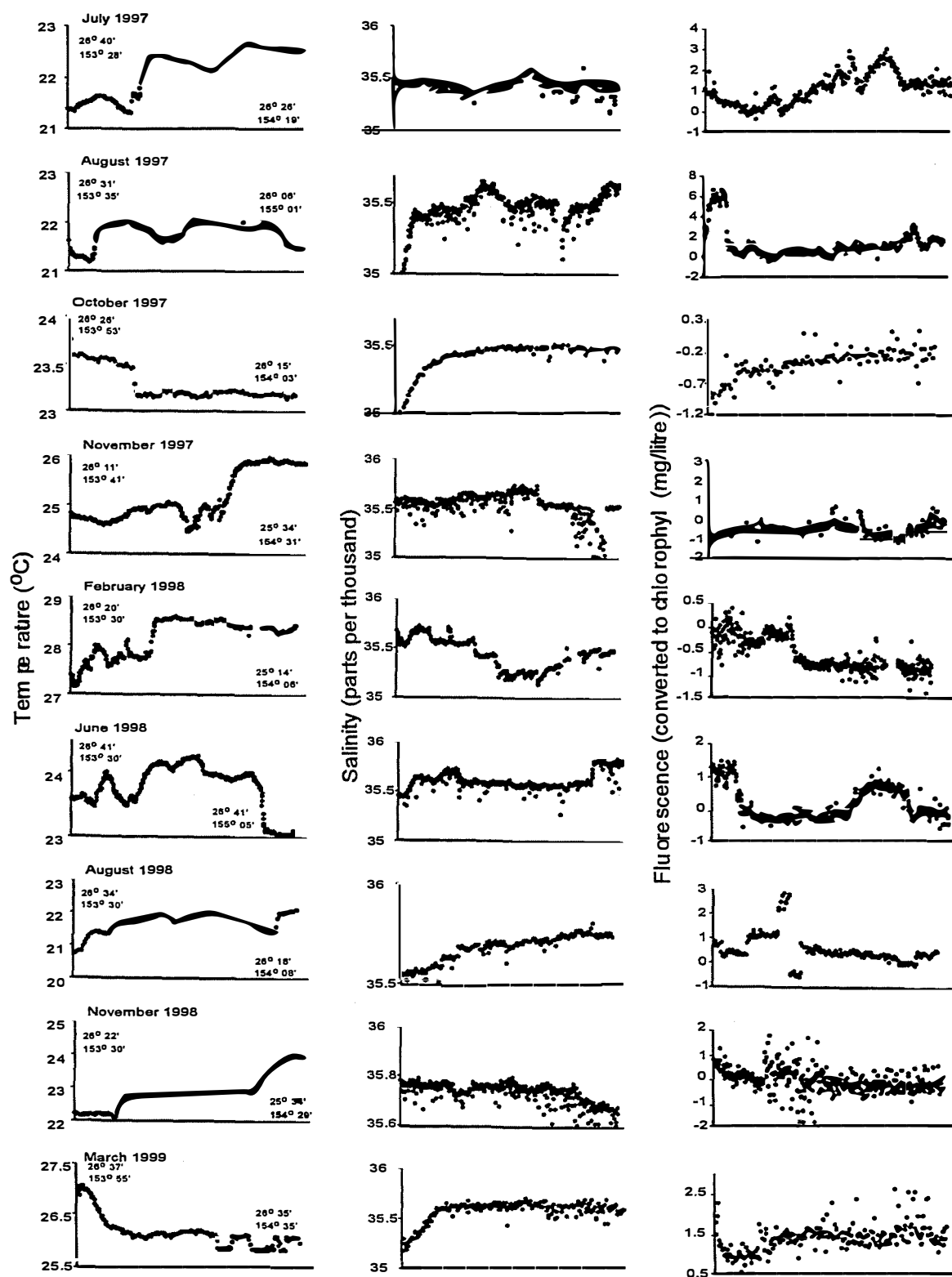


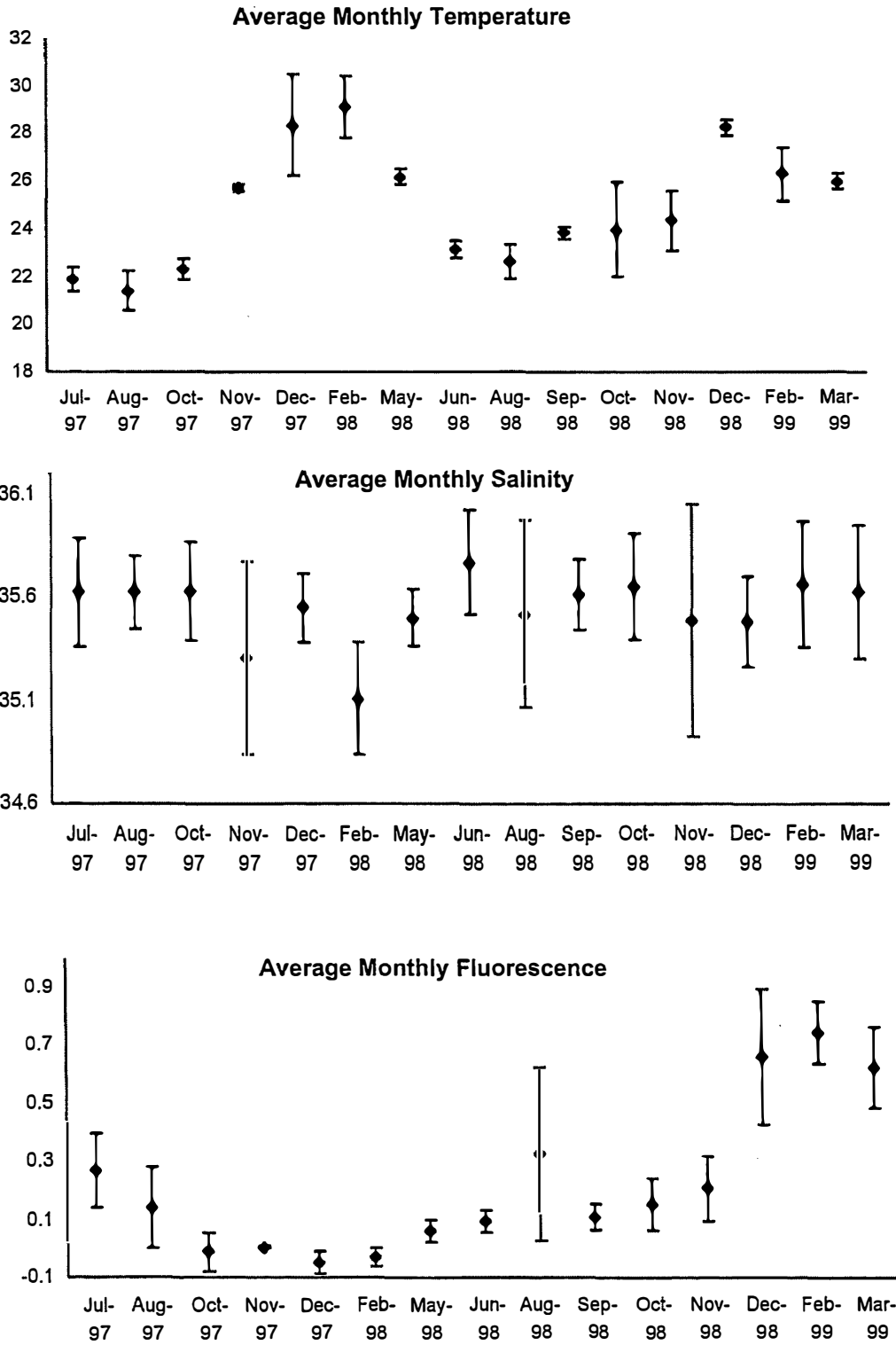
Figure 4. Surface temperature, salinity and fluorescence eastward of Mooloolaba on route to fishing grounds during the study period as determined by the underway sampler (start and end points of transects are shown here but see also Figure 1).



values inshore (eg. Fig. 4d). Progressing offshore through the main current, surface water temperature generally increased, with salinity and fluorescence decreasing, particularly over summer. A dip in temperature and fluorescence (see Fig. 4 a, b, c and e) and a rise in salinity signaled the end of the current and was generally an indication that the vessel was in suitably clear waters considered necessary for catching tuna and swordfish. This was not always the case, underlining the variable nature of surface water movements in the region. For example, in October 1997 (Fig. 4c) and March 1999 (Fig. 4i) the EAC, characterised by warm, low salinity southward flowing water was butted against the coast. In the latter, oceanographic data collected by ORV Franklin in the area estimated the southward flowing EAC at >1 m/s inside a northwesterly-flowing current coming from the east (Fig. 3, Ridgway 1999). The latter is presumably the westward inflow of South Equatorial Current water. At other times the East Australia Current extended beyond the range of the vessel (eg. February 1998).

Once on the fishing grounds underway surface temperatures ranged from a low value in August 1997 of 21.43°C peaking in February in both 1998 (29.10°C) and 1999 (slightly cooler at 28.20°C), the result of influx of South Equatorial water from the north and east (Fig. 5). The temperature sensor did not appear to be affected by conditions at sea thus the variance about the mean reflected the distance covered by the boat and the different water masses passed through during a set. Mean surface salinity ranged from 35.14 to 35.76 ppt although no clear cycle in salinity values was detected over the sampling period (Fig. 5). The variance around the mean was noticeably higher for salinity than temperature. This was attributed not only to passage through different water masses but also to weather conditions – windy weather created bubbles in the sensor which affected readings. Nevertheless, the salinities were relatively lower over the two summers, the time when the East Australia Current water, which is known to be less salty, dominated the region. For example, in February 1998 when the area was overrun by the EAC the waters were at their least saline. Generally, fluorescence values were typically low in the Mooloolaba area reflecting the oligotrophic nature of the surface waters in the region. In the first year of the study fluorescence values were highest in winter and lowest in summer. However, in the

Figure 5. Means of sea surface temperature, salinity and fluorescence on the fishing grounds off southern Queensland during the study period.



second year they increased through the summer months peaking at 0.8 μg per litre in March 1999.

Vertical Structure

The area of the fishery off southern Queensland is in an area recently thought to be important in the formation of warm core eddies within the East Australia Current. The EAC at this latitude is confined close to the coast and is most noticeable in cross section as a warm u-shaped layer butting up against the shelf (Fig. 6). Below this layer upward-sloping isotherms along the margins of the continental slope indicate upwelling. The first section (Fig. 6a) show little structure seaward apart from a relatively uninterrupted mixed layer $> 26^\circ\text{C}$ extending to approximately 60 m. However, extending the transect further seaward shows the isotherms increasingly wave-like with depth (Fig. 6b). Of note is the abrupt decrease in salinity beyond longitude 162°E to below 35.6 ppt. It is noteworthy that this change is barely reflected in the surface temperature.

Bermagui

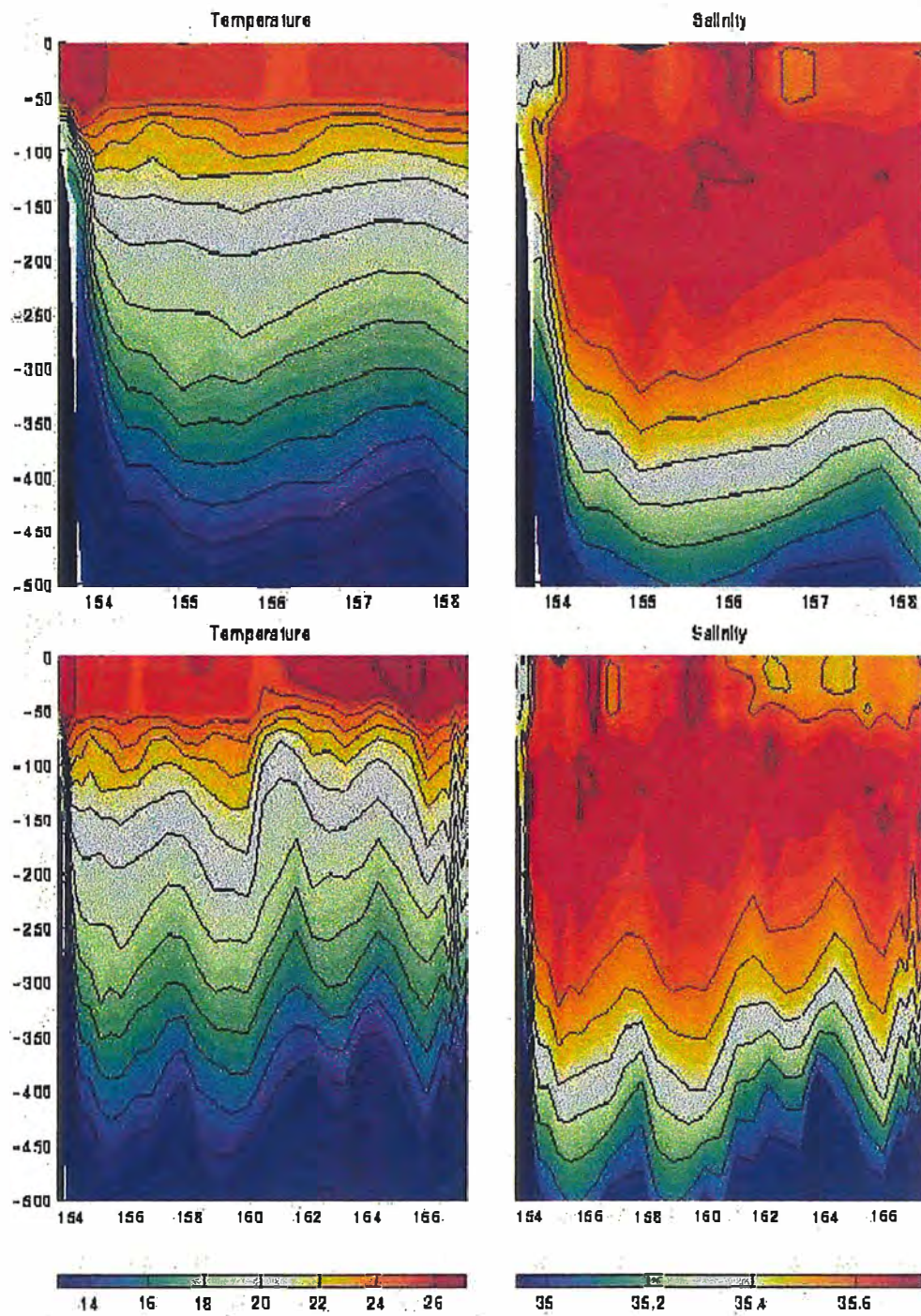
Seasonal variations in surface waters

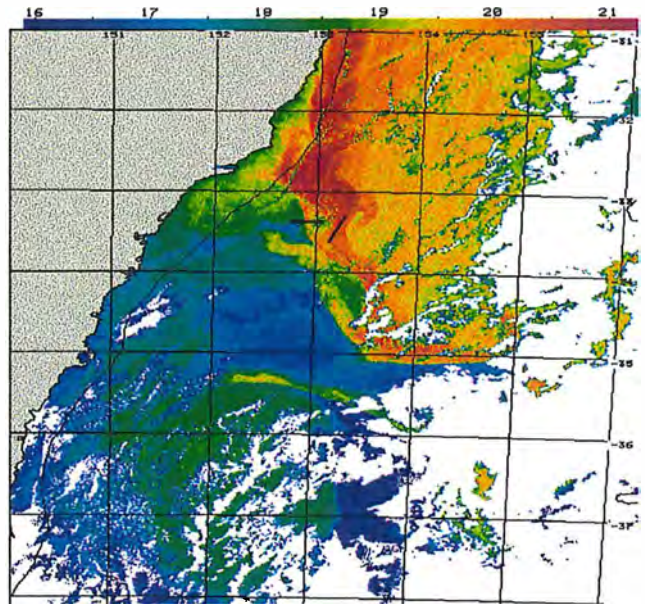
The main front of the East Australia Current was situated at approximately 35°S in September 1997 extending over summer to latitude 36°S (Fig. 7). Ocean colour imagery for the period showed relatively clear water within the main current with a rich plume of water along the shelf and in the waters below the main front (Fig. 8). Off Bermagui, temperatures in which longlines were set, ranged from 19.84 in May 1997 to 24.19 in February 1998 (Fig. 9). Salinities for the same longline sets ranged from 35.27 in May 1997 to 35.62 ppt in February 1998. Fluorescence values dipped from a high of 0.68 in May 1997 to a low of 0.12 in February 1998 before rising again in April 1998.

Vertical structure

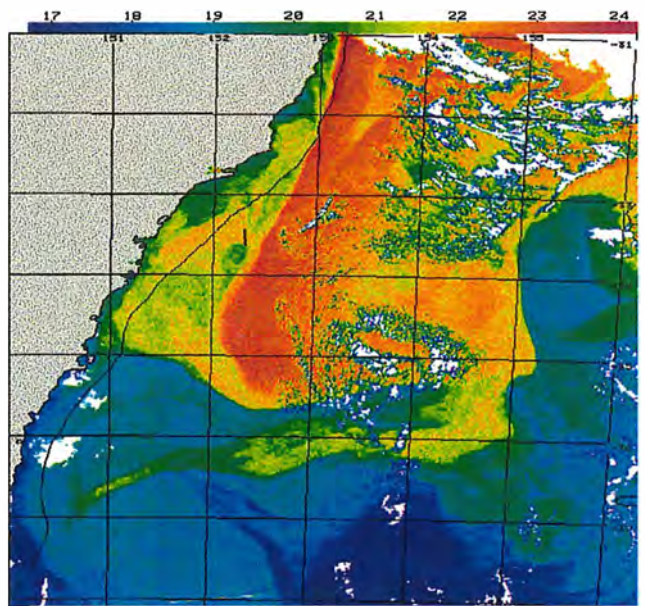
A research cruise off southeastern NSW in May 1996, originally planned to calibrate the ocean colour imagery, was completed before the underway sampling project began. Nevertheless, description of the vertical structure of the water masses prevailing at that time provides a useful understanding of the physical oceanographic

Figure 6. Vertical cross section of temperature and salinity eastward along 26 Degrees South (Courtesy of K. Ridgway, CSIRO unpublished data).

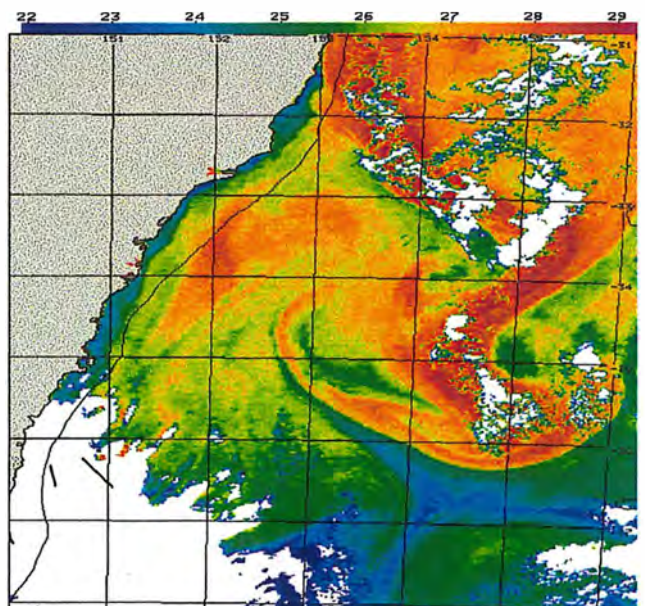




NOAA14 SST 13 Sep 1997 1555Z
Copyright 1999, CSIRO Division of Marine Research, Hobart



NOAA12 SST 06 Nov 1997 0807Z
Copyright 1999, CSIRO Division of Marine Research, Hobart



NOAA14 SST 19 Feb 1998 0400Z
Copyright 1999, CSIRO Division of Marine Research, Hobart

Figure 7: Seasonal changes in sea surface temperature off south eastern NSW during the study period. (Black lines are individual longline sets.)

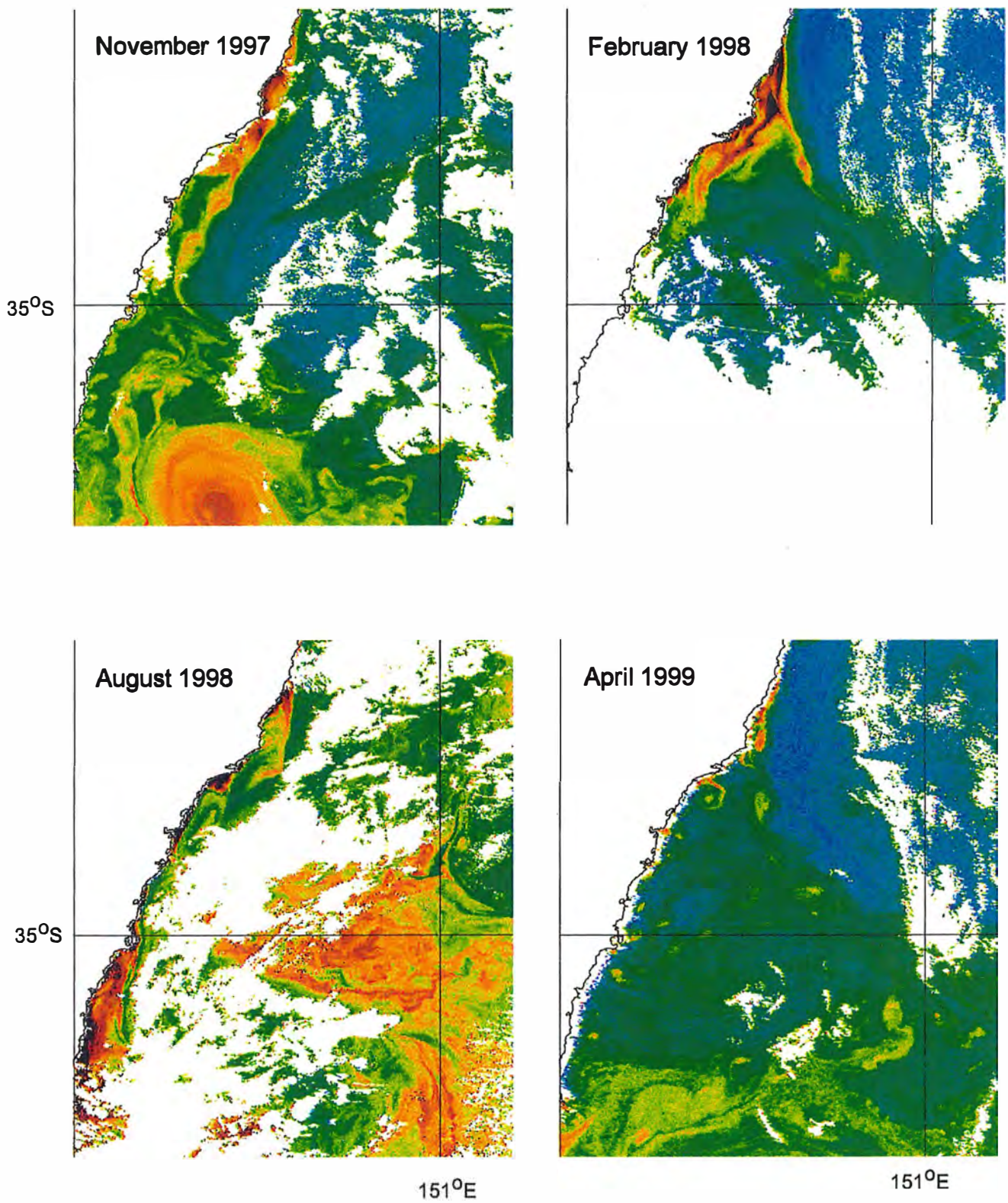
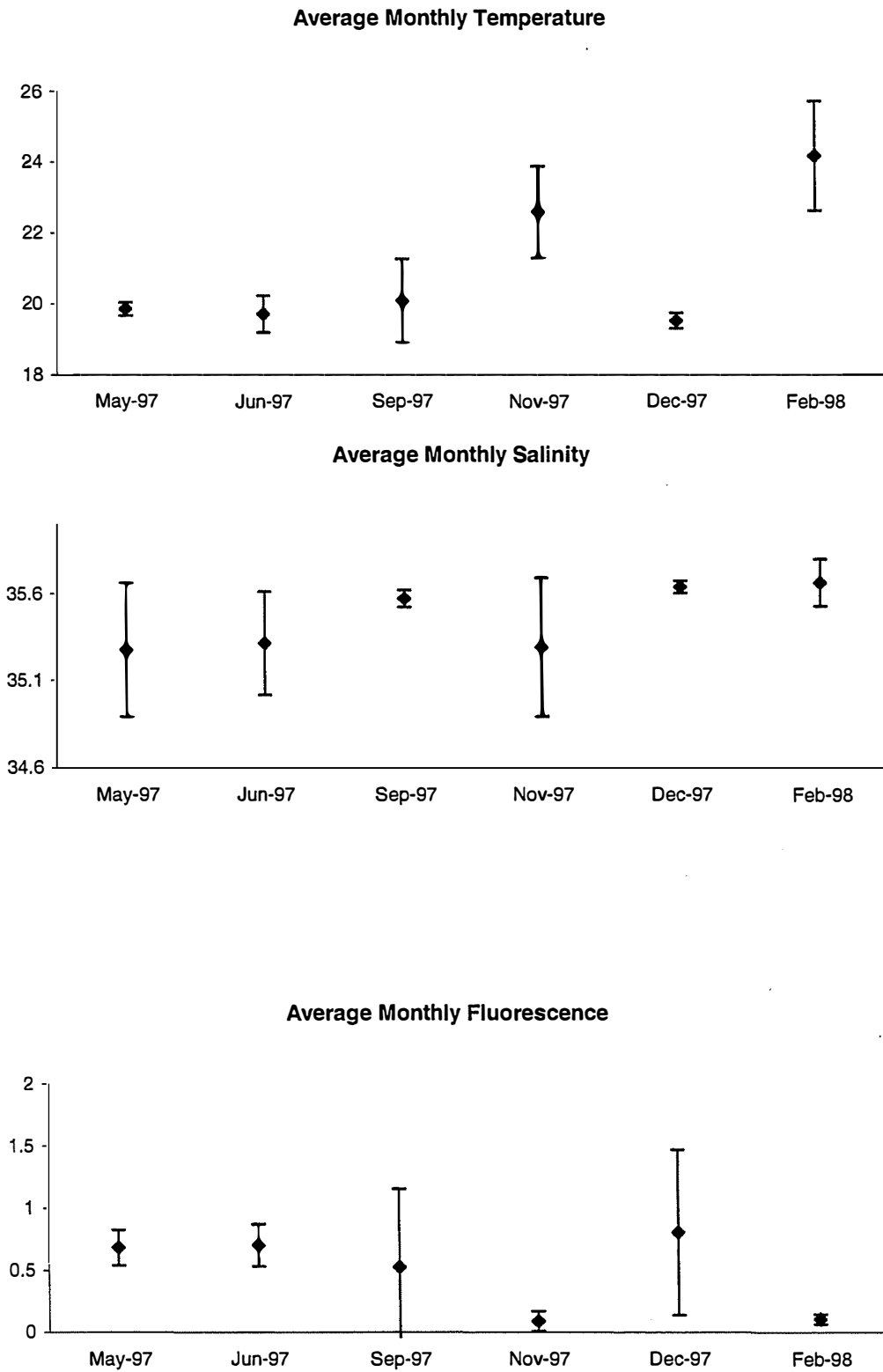


Figure 8: Seasonal changes in ocean colour off southern New South Wales during the study period (NASA Seawifs satellite).

Figure 9. . Means of sea surface temperature, salinity and fluorescence on the fishing grounds off southern New South Wales during the study period



processes affecting the area. A full description of those results is presented in Young et al (in prep) and is attached as an appendix (Appendix A). A summary is provided here. An oceanographic transect east of Bermagui in May 1996 identified a thin tongue of southward-flowing meander of the East Australia Current water to a depth of ~ 50 m. To the south, a warm-core eddy, ~ 60 n.miles in diameter was situated directly east of Green Cape, NSW between latitudes 36° 30' and 37° 30' S and within 10 n.miles of the shelf break. This eddy had recently separated from East Australia Current waters to the north as evidenced by previous satellite images of the area. It had a mixed layer of 21°C water to a depth of 100 m and at 250 m had a temperature of 15°C and a salinity of 35.4 ppt. At the western and southeastern edges of this eddy were relatively high concentrations of chlorophyll *a*. Underway sampling of fluorescence supported this observation and also that fluorescence was lowest in the centre of the eddy.

Biology

Catch composition

In all, 1,021 fish from 33 species were caught on observer-attended fishing trips out of Mooloolaba. Of these, broadbill swordfish (27.5% of total fish caught), followed by yellowfin (21.9% of total caught), bigeye (11.95%) and albacore (8.6%) made up ~70% of the catches. Nine species of shark totaled a further 9.7% of the catch (Table 4). Off Bermagui a total of 297 fish from 23 species were caught on observer-attended trips (Table 3). Of these 73% were yellowfin tuna, 7% were albacore and 1.6% were bigeye tuna. Approximately 5% of the total fish caught were sharks. Only three broadbill swordfish were caught on the trips out of Bermagui.

Catches in relation to environmental variables

Scatter plots between catch effort of the three species and the nine variables measured suggested a number of relationships. Firstly, for broadbill swordfish, highest catch rates were made in waters with a temperature range between 23 and 26 °C, salinities between 35.4 and 35.8 ppt, fluorescence values between 0 and 0.6 µg per litre. Catch rates were variable between years and months but were higher in moon phases 1 and 4. Most broadbill swordfish were caught north of 26 °S in all wind speeds but generally within 20 n.miles of the closest temperature front (Figure 10). For yellowfin tuna, the main relationships appeared to be between month (greatest in July), area

Table 3. Catch composition of longline caught fish off Bermagui

Common Name	Species Name	May 1997	Sep 1997	Nov 1997	Feb 1998	Apr 1998	Total
Family	Isuridae						
Mako shark	<i>Isurus oxyrinchus</i>		1			3	4
Long finned Mako	<i>Isurus paucus</i>						
Family	Alopiidae						
Thresher shark	<i>Alopias superciliosus</i>		1				1
Family	Carcharhinidae						
Bronze whaler shark	<i>Carcharhinus brachyurus</i>					5	5
Oceanic white-tipped shark	<i>Carcharhinus longimanus</i>						
Blue whaler shark	<i>Prionace glauca</i>		1	3			4
Tiger shark	<i>Galeocerdo cuvieri</i>		1				1
Shark	Unidentified shark			1	2	5	8
Family	Sphyrnidae						
Hammerhead shark	<i>Sphyrna spp.</i>					4	4
Family	Dasyatidae						
Pelagic ray	<i>Dasyatis spp.</i>			1			1
Sting ray	unidentified Dasyatidid						
Family	Mobulidae						
Manta ray	* <i>Manta birostris</i>			1			1
Family	Alepisauridae						
Short nosed lancetfish	<i>Alepisaurus brevirostris</i>						
Long nosed lancetfish	<i>Alepisaurus ferox</i>						
Lancetfish	<i>Alepisaurus spp.</i>			1	1		2
Family	Bramidae						
Ray's bream	<i>Brama brama</i>		1				1
Family	Trichiuridae						
Frost fish	<i>Lepidopus caudatus</i>						
Family	Gempylidae						
Black oilfish	<i>Lepidocybium flavobrunneum</i>					1	1
Oilfish	<i>Ruvettus pretiosus</i>						
Family	Scombridae						
Albacore	<i>Thunnus alalunga</i>	6	2	1	12		21
Yellowfin tuna	<i>Thunnus albacares</i>	65	108	8	22	14	217
Bigeye tuna	<i>Thunnus obesus</i>		1		4		5
Skipjack tuna	<i>Katsuwonus pelamis</i>		1	1			2
Wahoo	<i>Acanthocybium solandri</i>						
Tuna sp.	Unidentified tuna spp.						
Family	Xiphiidae						
Broadbill swordfish	<i>Xiphias gladius</i>	2				1	3
Family	Istiophoridae						
Black marlin	* <i>Makaira indica</i>					1	1
Blue marlin	* <i>Makaira mazara</i>						
Striped marlin	<i>Tetrapturus audax</i>		1	2		8	11
Shortbill spearfish	<i>Tetrapturus angustirostris</i>						
Marlin	Unidentified marlin				1		1
Family	Centrolophidae						
Rudderfish	<i>Centrolophus niger</i>				1		1
Family	Coryphaenidae						
Dolphinfish	<i>Coryphaena hippurus</i>				1		1
Family	Molidae						
Sunfish	<i>Mola ramsayi</i>				1		1
	Total number of fishes	73	118	19	45	42	297
	Number of species	3	10	9	9	9	23

* These species released, not used for commercial purposes

Table 4. Catch composition of longline caught fishes off Mooloolaba

Species Name	Jul 1997	Aug 1997	Oct 1997	Nov 1997	Feb 1998	Jun 1998	Aug 1998	Nov 1998	Dec 1998	Mar 1999	Total
<i>Isuridae</i>											
<i>Isurus oxyrinchus</i>		4	7			3	2	1	1	1	19
<i>Isurus paucus</i>	2										2
<i>Alopiidae</i>											
<i>Atopias superciliosus</i>				1		1	3				5
<i>Carcharhinidae</i>											
<i>Carcharhinus brachyurus</i>			1	1	2		2	2		1	9
<i>Carcharhinus longimanus</i>		2	3	3		2	3	3	2	1	19
<i>Prionace glauca</i>	6				1	1	8	3	1	12	32
Unidentified shark	2		4	1	2	8	1	1		1	20
<i>Sphymidae</i>											
<i>Sphyrna spp.</i>								3			3
<i>Dasyatidae</i>											
<i>Dasyatis spp.</i>					1	1		1		2	5
unidentified Dasyatidid		2					1			2	5
<i>Mobulidae</i>											
* <i>Manta birostris</i>		2	1				1			1	5
<i>Alepisauridae</i>											
<i>Alepisaurus brevirostris</i>			1								1
<i>Alepisaurus ferrox</i>	6		6			3		7			22
<i>Alepisaurus spp.</i>		2	11	3	2		10		3	3	34
<i>Trichiuridae</i>											
<i>Lepidopus caudatus</i>							2				2
<i>Gempylidae</i>											
<i>Ruvettus pretiosus</i>							1				1
<i>Scomberidae</i>											
<i>Thunnus alalunga</i>	5	55	2		3	11	3	1		8	88
<i>Thunnus albacares</i>	1	15	6	5	26	7	101	20	11	32	224
<i>Thunnus obesus</i>	13	34	7	7	37	7	6	6	1	4	122
<i>Katsuwonus pelamis</i>	1	1						1			3
<i>Acanthocybium solandri</i>					1						1
Unidentified tuna spp.					3	7					10
<i>Scomberomorous commerson</i>										1	1
<i>Xiphiidae</i>											
<i>Xiphias gladius</i>	11	64	44	17	24	27	14	32	19	29	281
<i>Istiophoridae</i>											
* <i>Makaira indica</i>	1		1		1					1	4
* <i>Makaira mazara</i>			1	2	2	1	1		3		10
<i>Tetrapturus audax</i>	2	1			1	1	2	8	5		20
<i>Tetrapturus angustirostris</i>		1									1
<i>Centrolophidae</i>											
<i>Centrolophus niger</i>	9	9	1					1		6	26
<i>Coryphaenidae</i>											
<i>Coryphaena hippurus</i>				2	1	3	1	10	1	6	24
<i>Molidae</i>											
<i>Mola ramsayi</i>	3	2	4			3	4	1		1	18
Unidentified species	3		1								4
*Hawkesbill turtle				1							1
Total number of fishes	65	194	101	42	107	86	166	101	47	112	1021
Number of species	14	14	17	11	15	16	19	17	10	18	151

* These species released, not used for commercial purposes

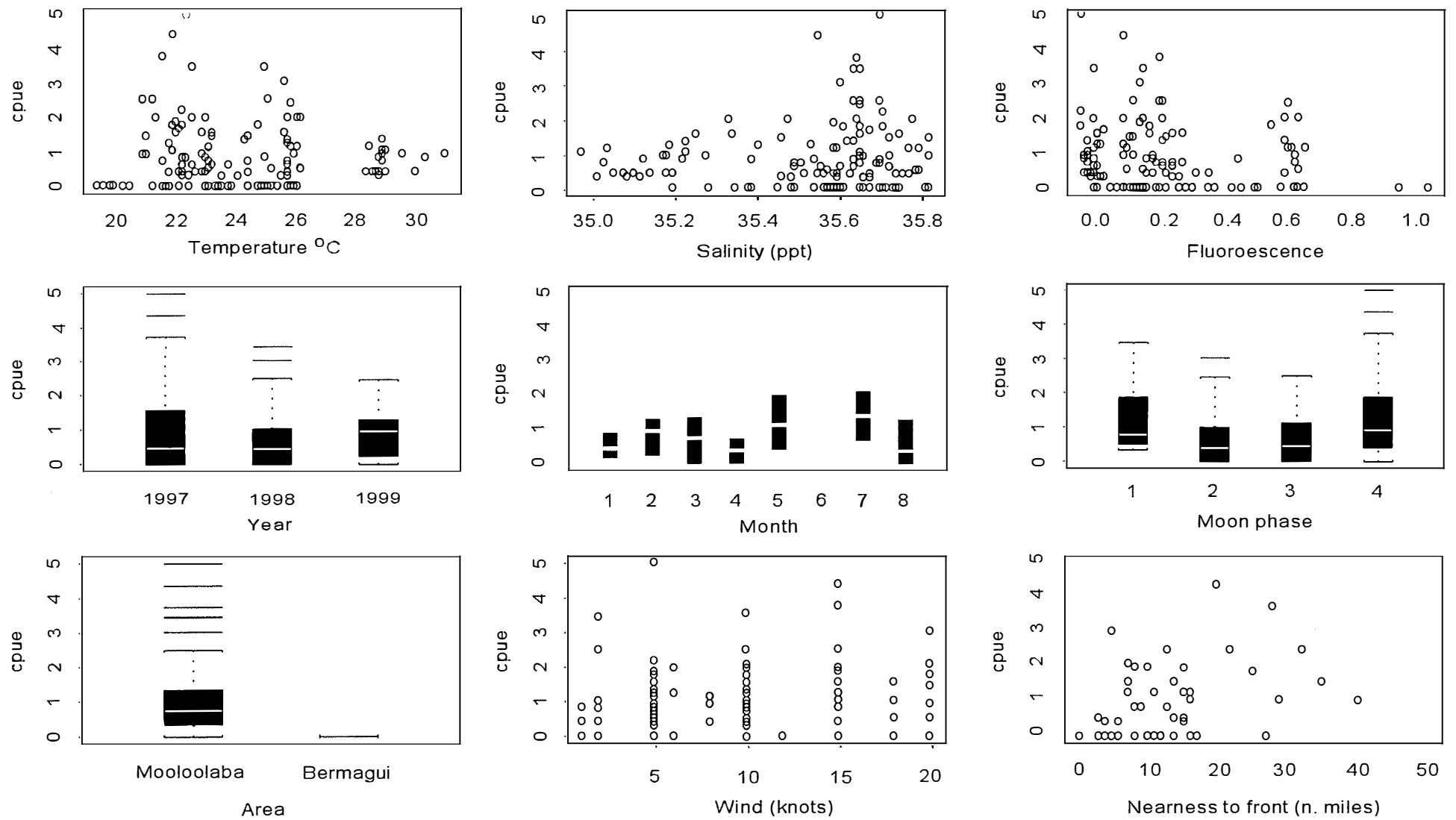


Figure 10: Scatter plots of broadbill swordfish catch per unit effort [(number of fish caught/number of hooks) x 100] in relation to the nine environmental variables measured.

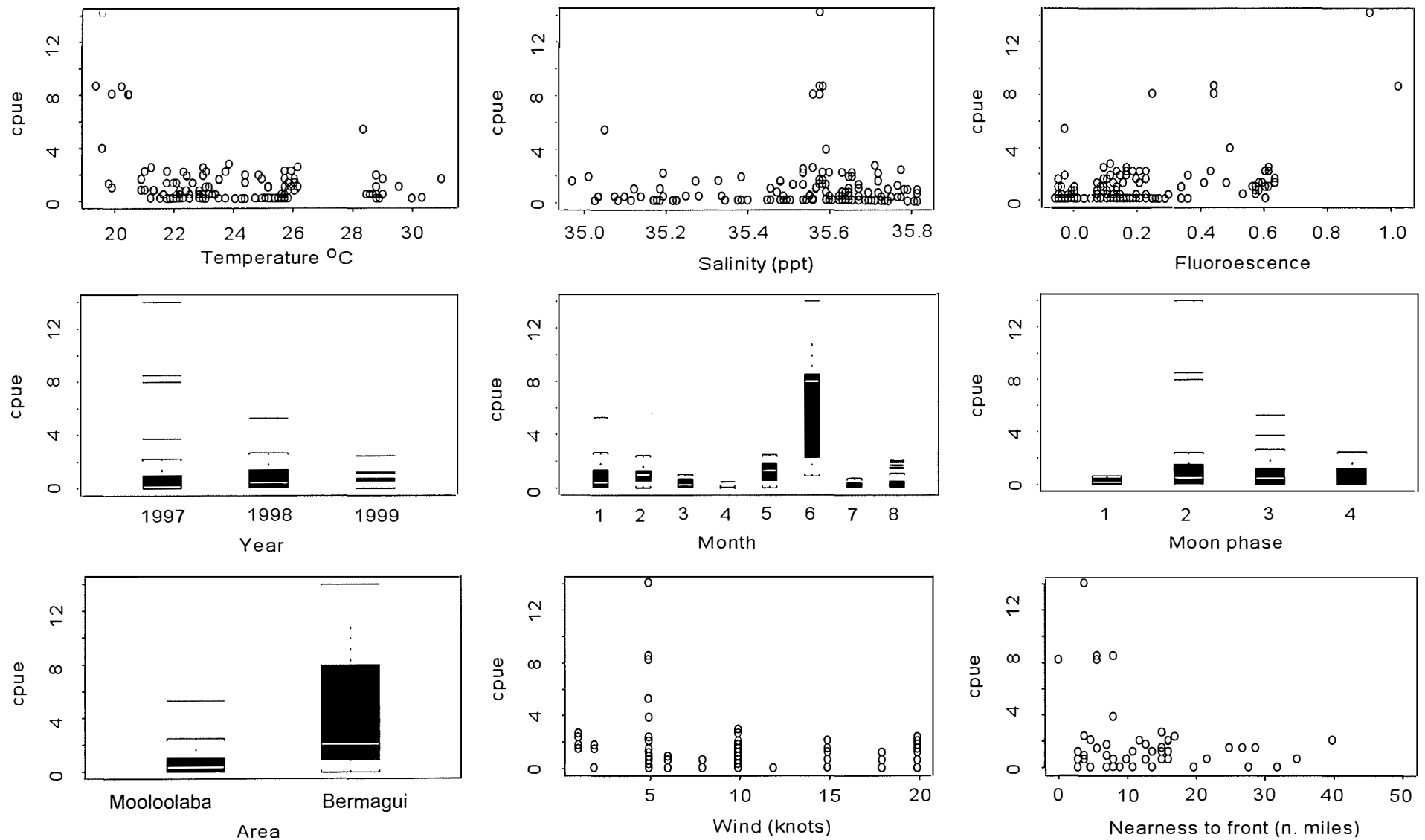


Figure 11: Scatter plots of yellowfin tuna catch per unit effort [(number of fish caught/number of hooks) x 100] in relation to the nine environmental variables measured.

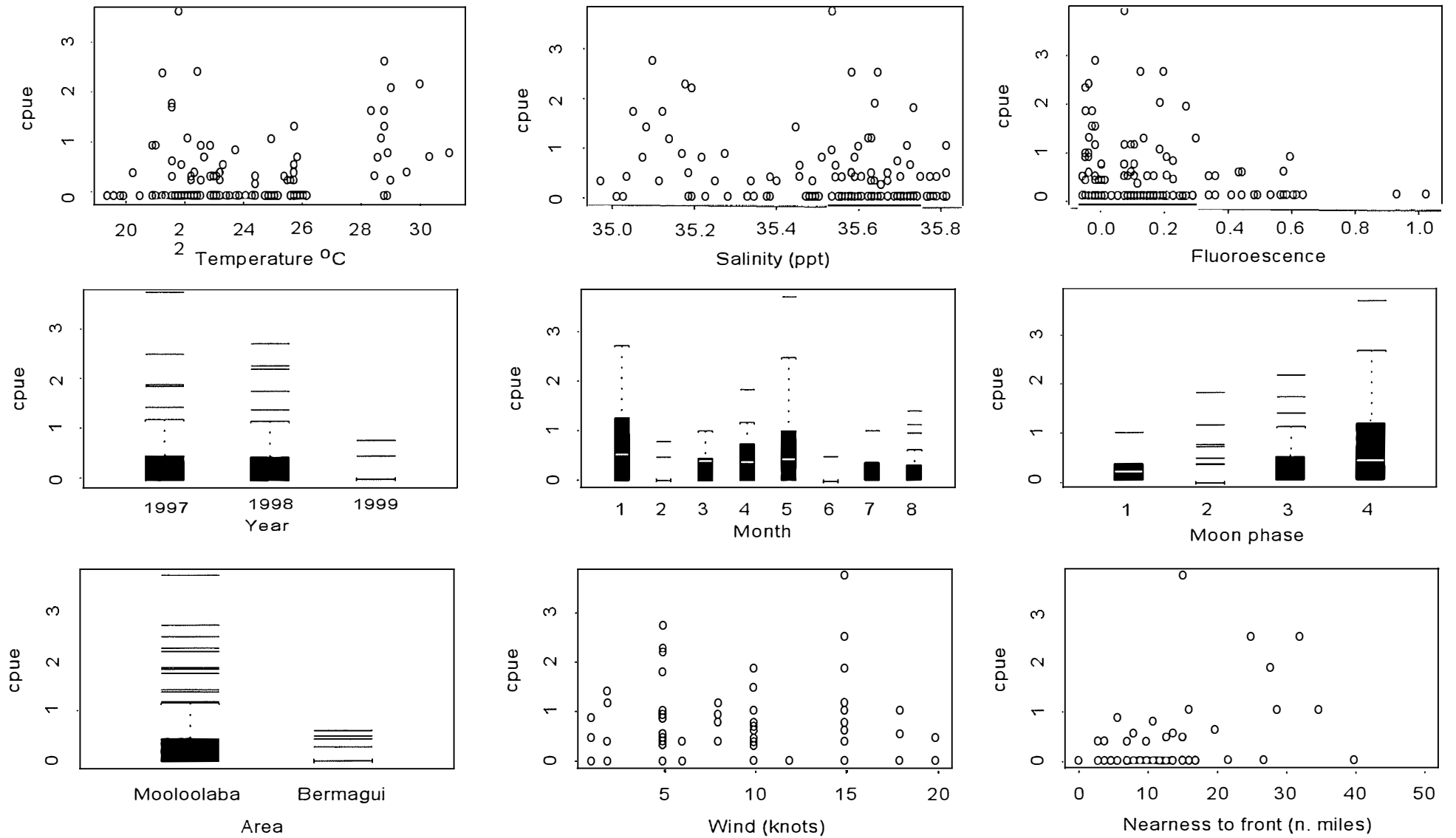


Figure 12: Scatter plots of big eye tuna catch per unit effort [(number of fish caught/number of hooks) x 100] in relation to the nine environmental variables measured.

(greatest off Bermagui), and closeness to the nearest front (within 10 n.miles)(Fig. 11). Bigeye tuna catch rates appeared to be highest in waters of low fluorescence, in moon phase 4, north of 26 °S and closer to the nearest temperature front (Fig.12).

Model responses

Broadbill swordfish

Model 1. Area followed by month and fluorescence were significantly correlated with catch rate of swordfish (Table 5). As few swordfish were caught in the study off Bermagui the significance of area in this case is not surprising. Time of year was the next most significant factor to correlate with catch rates, which were higher in the autumn and spring than at other times of the year. Finally, lower catch rates were correlated with increasing fluorescence.

Model 2. When the model was restricted to Mooloolaba we found that salinity followed by nearness to front, moon phase and year were significantly correlated with catch rate (Table 5). The smoothing splines as determined by GAM showed that catches were initially correlated with lower salinities then increased again in waters with salinities greater than 35.6 ppt (Figure 13). Catches rose steadily to approximately 10 n.miles from the nearest front after which they declined. Catches were highest in the first quarter of the moon and in the first year of the study. Neither fluorescence nor temperature was significantly correlated with catch rate.

Yellowfin tuna

Model 1. Area followed by month, fluorescence, moon, and sea surface temperature and wind all affected catch of yellowfin tuna significantly (Table 6). In contrast to broadbill swordfish Area 2 had the highest catch rates and these were variable between months. The probability of catching yellowfin was highest in waters of higher fluorescence and in the week of the new moon. The model indicated that the probability of catching yellowfin increased from 20 to 24 °C but was fairly stable in temperatures above that. The model also indicated that the probability of catching yellowfin was highest at the lowest wind speeds, declining to ~ 10 knots and then increasing as the wind strength increased.

Table 5. Broadbill Swordfish. Factors significantly correlated with swordfish catch rates as determined by GLM

Entire study area

Model	d.f.	Deviance	Residual	Deviance	Chi squared
Null model			138	278.90	
Area	1	72.01	137	206.89	0.00
Month	7	26.54	130	180.35	0.00
Fluorescence	1	4.83	129	175.52	0.03

Mooloolaba area only

	d.f	Deviance	Residual	Deviance	Pr(Chi)
NULL			99	162.38	
Salinity	1	6.698	97	155.14	0.009
Nearness to front	5	14.82	91	137.89	0.011
Moon phase	3	10.80	88	127.08	0.012
Year	1	13.70	82	106.98	0.000

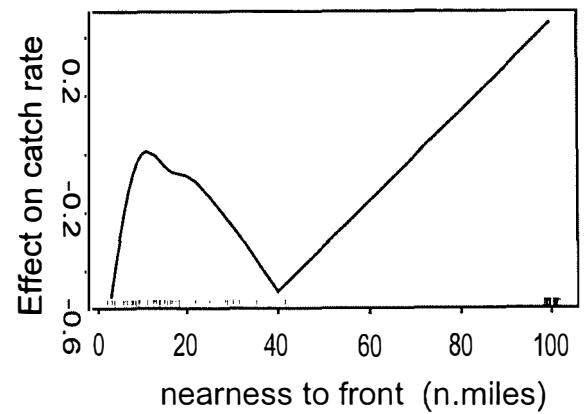
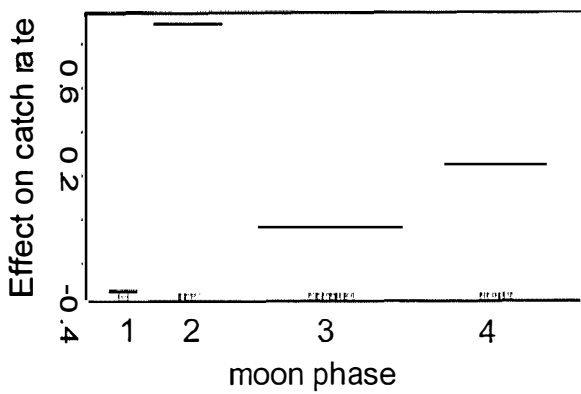
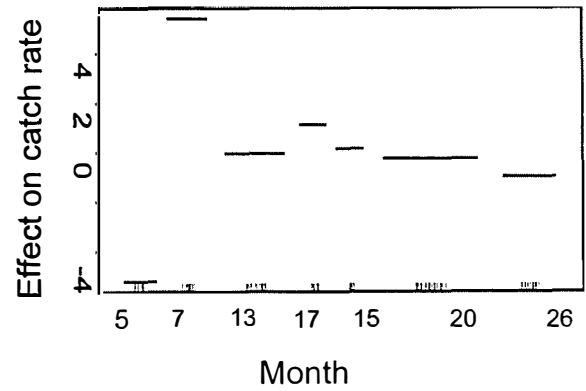
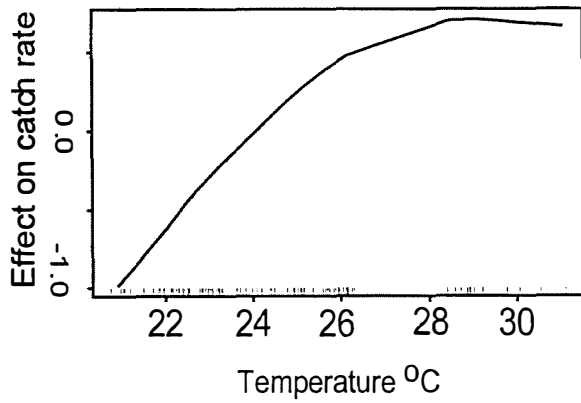
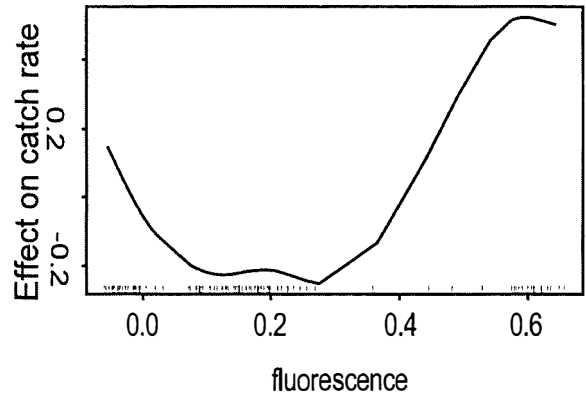
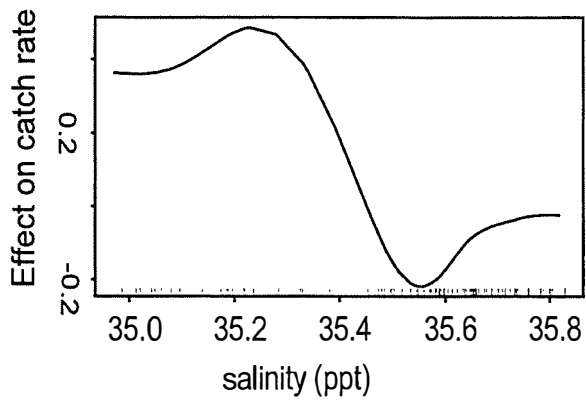


Figure 13: GAM-derived effects of salinity, fluorescence, temperature, month:year, moon and nearness to front in relation to broadbill swordfish catch rate

Table 6. Yellowfin Tuna. Factors significantly correlated with catch rates as determined by GLM

Entire study area

Model	d.f.	Deviance	Residual	Deviance	Chi squared
Null			138	609.12	
Area	1	189.89	137	419.23	0.00
Month	7	144.68	130	274.55	0.00
Fluorescence	1	24.25	129	250.30	0.00
Moon	3	25.75	126	224.55	0.00
Sea surface temperature	1	7.49	125	217.06	0.01
wind	1	5.94	124	211.12	0.01

Mooloolaba area only

Model	d.f.	Deviance	Residual	Deviance	Chi squared
Null			99	205.74	
Salinity	1	12.45	97	182.67	0.00
Month	5	17.53	83	146.94	0.00
Fluorescence	1	10.61	98	195.13	0.00
Year	1	5.37	82	141.57	0.02

Model 2. When the model run was restricted to the Mooloolaba area we found that salinity followed by month, fluorescence and year were significantly correlated with catch rate. Highest catch rates were found in the waters with the lowest salinity (Fig. 14). Similarly, the clearest water (lowest fluorescence) had the highest catch rates of yellowfin tuna, the catch rates increasing away from the main front (up to 40 n.miles).

Bigeye tuna

Model 1. The variables significantly associated with the catch rates of bigeye tuna were in order fluorescence, salinity, nearness to front and moon stage (Table 7).

Model 2. When the data was restricted to the Mooloolaba area there was no difference in the variables associated with catch rate. Fluorescence, salinity, nearness to front and moon stage were all significantly correlated with catch rate (Table 7). The gam plots showed that higher catches were associated with lower values of salinity, fluorescence and temperature, although the latter was not significant (Fig. 15). Highest catches were associated with the period before the full moon. Finally, the plot for nearness to front showed that catches initially declined with distance from the main front but then began to rise approximately 20 n.miles from the front (Fig. 15).

Discussion

Oceanographic influences

The east coast tuna and broadbill fishery operates over a wide latitudinal range – from 10 to 40° S and, as the fishery has developed, as far east as longitude 165° E. As such the fishery operates in water masses that have inputs from both the tropics and the subantarctic. In the north the South Equatorial Current feeds into the Australian zone between latitudes 14 and 18 °S. This current is the primary inflow into the Coral and Tasman Seas. The South Equatorial Current feeds the East Australia Current which continues down the coast to 30°S. At this latitude the main current separates from the coast as an eastward meander known as the Tasman front. A series of meanders and eddies generated by the EAC continue on down the coast to southern Tasmania.

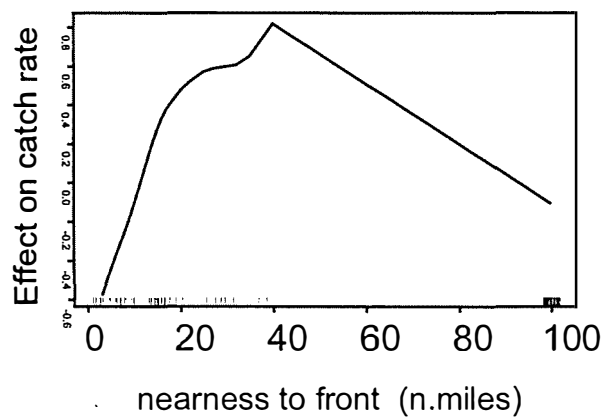
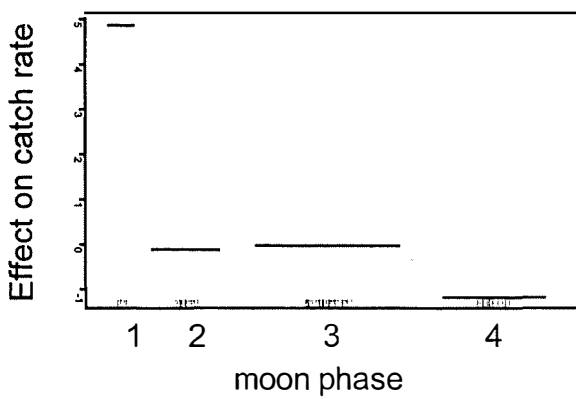
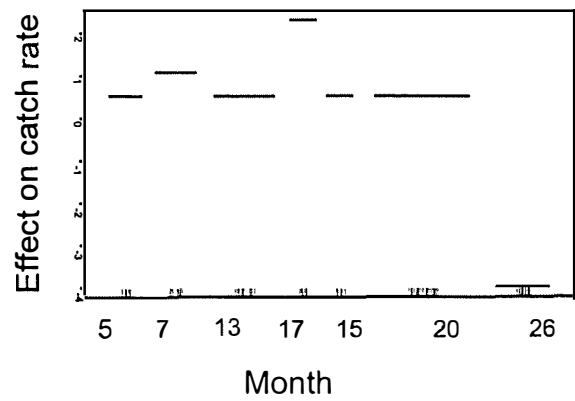
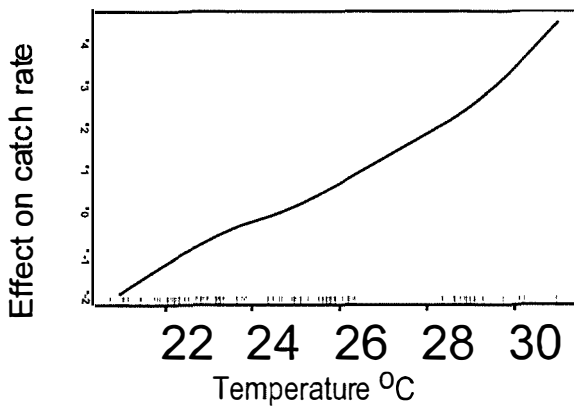
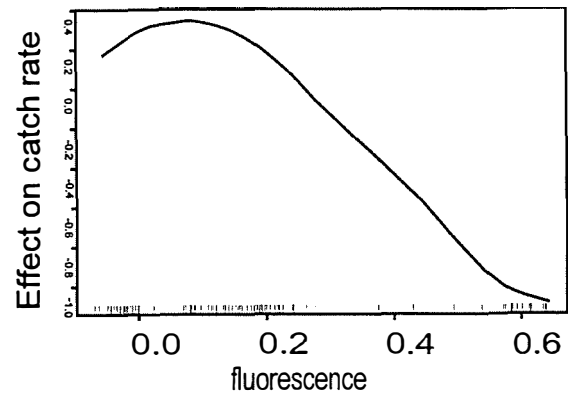
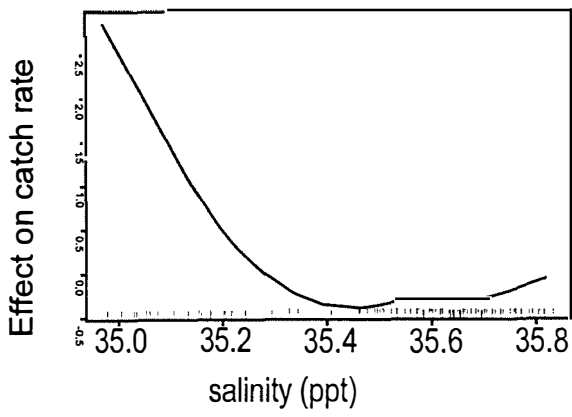


Figure 14: GAM-derived effects of salinity, fluorescence, temperature, month:year, moon and nearness to front in relation to yellowfin tuna catch rate

Table 7. Bigeye tuna. Factors significantly correlated with catch rates as determined by GLM

Entire study area

Model	d.f	Deviance	Residual	Deviance	Chi squared
Null			116	214.88	
Fluorescence	1	3310.36	115	181.51	0.000
Salinity	1	5.85	114	172.65	0.003
Nearness to front	5	12.52	108	135.51	0.000
Moon	3	8.13	105	124.38	0.011

Mooloolaba area only

Model	d.f	Deviance	Residual	Deviance	Chi squared
Null			99	188.69	
Fluorescence	1	27.56	98	161.13	0.00(*)
Salinity	1	8.86	97	152.56	0.003(*)
Nearness to front	5	30.50	91	119.25	0.00(*)
Moon	3	10.0	88	109.24	0.019(*)

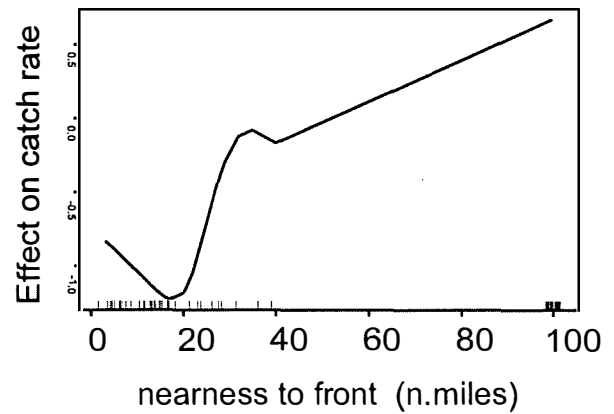
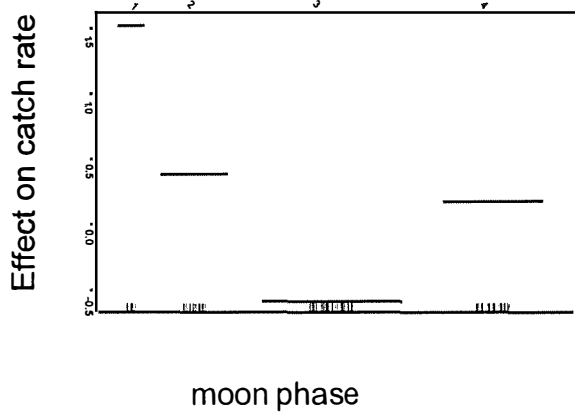
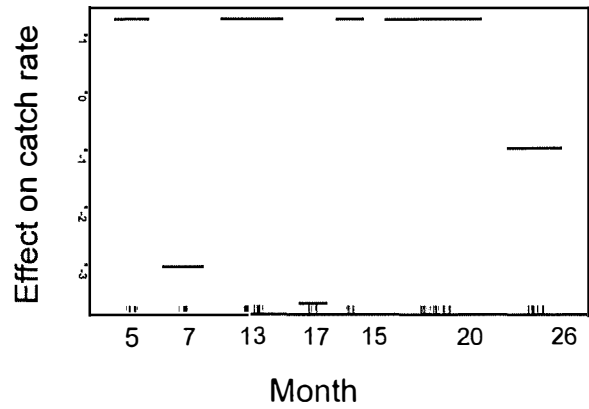
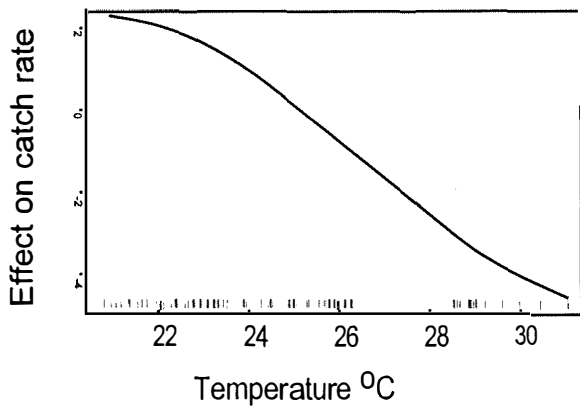
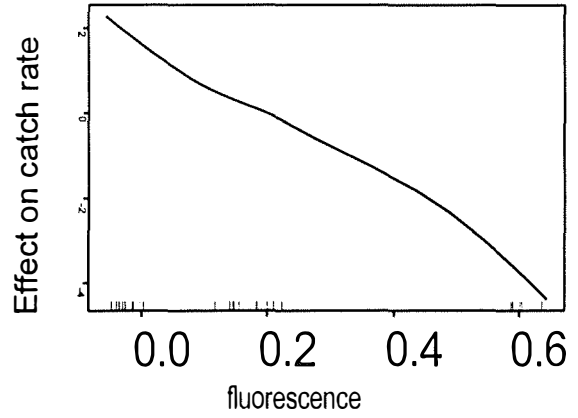
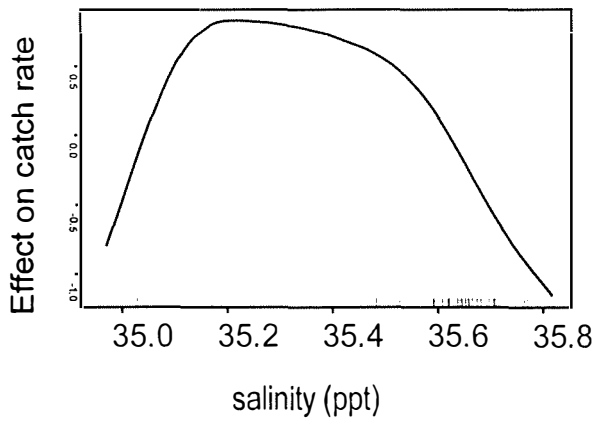


Figure 15: GAM-derived effects of salinity, fluorescence, temperature, month:year, moon and nearness to front in relation to bigeye tuna catch rate

Off southern Queensland we detected both seasonal and interannual differences in the strength and extent of the southward flow of the southward component of the EAC. In this respect, although the waters in this study are significantly warmer, it is similar to the fluctuations we reported off southeastern Australia (eg. Young et al 1996). We know that these interseasonal and interannual changes can have impacts on the distribution and abundance of pelagic fauna in more southern waters of east coast Australia (Young et al 1993). This may also be the case in oceanic waters off southern Queensland. For example, there was a massive influx of South Equatorial Current water into the northern area of the fishery in the summer of 1998. This coincided with reduced catch per unit effort for at least broadbill swordfish and bigeye tuna in the study. Although the small sample size limits any conclusions, AFMA data for the period also showed a decline in catches relative to 1997. There are a number of factors, which could have led to this result (e.g. changes in fishing practice, increased fishing competition), but the significant change in the regional oceanography cannot be discounted. We have little idea of the changes the altered oceanographic conditions made on the food webs leading to pelagic fishes in the area. It is likely, however, the absence of any significant frontal structure in the area in which the boat worked would not have provided conditions suitable for the fish.

Off southern New South Wales, where the other longliner concentrated its efforts, the main front of the EAC extended to approximately 36 degrees South over summer, retreating further north in the winter. Thus, all the fishing reported here from the Bermagui area was carried out in waters of tropical origin. The net result was water of suitable temperature for yellowfin tuna, which accounted for the majority of the catches when observers were on board. In an earlier study of the region we reported similar concentrations of yellowfin being caught in the region (Young et al Appendix A). In that study we concluded that the presence of a warm core eddy produced conditions suitable for aggregations of these tuna. That is, the eddy provided a thermal refuge close to an area where prey concentrations were elevated. Although no eddy was found in the same area in this study the presence of the front close to the shelf indicated similar conditions to those present in the earlier study. Such a relationship has been reported from the California Current as well as elsewhere (Lauritsen et al 1984, Fiedler and Barnard 1987, Power and Nelson May 1991).

Catches in relation to sea surface variables

Broadbill swordfish

In the first two models we identified six variables (Model 1 – area, month and fluorescence; Model 2 – salinity, fluorescence nearness to front, year and moon phase) that were correlated with catch rates of broadbill swordfish during the study period. Dealing with these in turn, relatively few swordfish were landed in Bermagui, thus area was, not surprisingly, the first variable to be distinguished. Whether this is a true indication of the distribution of the swordfish in the southern fishery is yet to be tested as lines were set relatively close to shore and not through the night. Japanese catches for the same latitude offshore show significant catches to 34 degrees South (Ward 1996). More interesting was the importance of time of year for catch rates. Catches peaked in autumn and spring, mirroring the pattern of catches by Japanese longliners in the same area (Ward 1996), and indicating the swordfish may be responding to peaks in productivity typical of these periods. Catches in February in both years of the study were significantly lower than other times of year; also mirroring the Japanese catches (Ward 1996). This appears to be due, particularly in 1998, to the flood of warm nutrient-poor water down the coast at that time. One explanation for the low catches was that there was little in the way of attractive feed in the area at that time. Ocean colour imagery for the period shows the clearest water extending beyond the distance of the vessel with little evidence of frontal structure. In an apparent contradiction, however, the model also found that catches were highest when fluorescence was lowest but also those catches were higher near temperature fronts. This suggests that although the broadbill prefer clearer waters, proximity to fronts (source of concentrations of feed), as indicated previously (Sakagawa 1989, Podesta et al 1993), is more important. Year was also a significant factor. However, as only two years of data were analysed this result was probably related more to seasonal factors than anything longer term. Nevertheless, this is likely to be a major factor as the fishery develops given the interannual variability of the major water mass movements off eastern Australia. Moon phase affected catch rates significantly. In contrast to Japanese catches in the same area that found highest catches around the full moon (Ward 1996), our study showed highest catches just before the full moon. However, this is more than likely related to the concentration of fishing effort as the longliner tended to make two trips each month, one either side of the moon, thus missing at least

part of the full moon period. Finally, salinity, previously inferred by Sakagawa (1989) as an important factor in the distribution of swordfish was correlated with swordfish catch rates.

Yellowfin tuna

We identified five variables (area, followed by month, fluorescence, moon and sea surface temperature) that affected catch rates of yellowfin tuna in the study area. Catches of yellowfin tuna were relatively higher in the Bermagui area than off Mooloolaba. The area off the coast of southern NSW is the site for a semi-permanent eddy which at times can provide the right conditions for aggregations of yellowfin tuna (Young et al in prep see Appendix). The semi-permanent nature of these warm-core eddies sets up an upwelling environment stable enough to establish the kind of food chain necessary for a rich food web to develop. Yellowfin tuna, although present throughout the year, appear to arrive in more southern waters with flushes of warm water from the north usually at the end of the summer. This pattern is similar to that of the Japanese longline fishery operating in the same waters (Ward 1996).

We found a positive relationship between yellowfin catches and fluorescence in the broad scale comparison but a negative one when the analysis was restricted to the waters off Mooloolaba. There are two interpretations for this result. The first is that because fluorescence was generally higher in more southerly waters - where the catch rate was highest - more subtle relationships between the yellowfin and fluorescence further north could have been masked. The other is that fluorescence generally increases in the vicinity of fronts at which yellowfin are known to concentrate (e.g. Fiedler and Barnard 1987). Yellowfin catches were greatest on the dark of the moon and were the next significant factor in the model, a result also shown for the species by the Japanese longline fishery (Ward 1996). Catch rates were positively correlated with temperature; again following the pattern demonstrated by the Japanese catches (Ward 1996). Finally, wind strength was a significant factor in the number of yellowfin caught. There is little information on local weather conditions and their impact on catch rates. However, yellowfin are regularly seen in surface waters in calm weather and it may be that they are simply more available to the longlines in these conditions.

Bigeye tuna

Previously, the prime oceanographic factors thought to influence the distribution of bigeye tuna were temperature and oxygen concentration (eg. Hanamoto 1987). However, the temperature ranges given were between 9 and 28 degrees C and oxygen concentrations above 1 ml/L, ranges which encompass a vast geographic distance. More subtle local scale data were missing. Further, Hanamoto (1987) conceded that longline catches were not a good reflection of bigeye tuna distribution as the fishing depth of the longline hooks may have missed the optimum depth for these fish.

Our model showed that fluorescence (followed by salinity, nearness to front and moon phase) was the main factor associated with catch rates of bigeye tuna in the study area. That is, higher catches were associated with the clearest water. This is not surprising, as, like most tunas, they require clear water in which to feed (Hunter et al 1986). However, our results show the opposite relationship to that found between yellowfin tuna and fluorescence providing further evidence that bigeye and yellowfin occupy separate niches within open ocean waters (Holland et al 1990). In fact, the distribution of bigeye tuna appears to favour waters with similar characteristics to that inhabited by broadbill swordfish. This conclusion is supported by Ward (1996) who found, like us, that both broadbill swordfish and bigeye tuna were caught in highest numbers in waters of similar surface temperature (and latitude), around the full moon and at similar times of the year.

Summary

The variables correlated with catch rate for the three species are summarized in Table 8. Significant relationships were found between these variables and catch rates on both fine and broad scales for all three species. Because of the novel approach taken by this study there is no equivalent study with which we can compare our results. However, oceanic fronts, which have gradients in the concentration of temperature, salinity and Chlorophyll *a*, are known to be associated with concentrations of swordfish and tunas (eg. Laurs et al 1984, Podesta et al 1993, Bigelow et al 1999). Although various measures of sea surface temperature have been linked to concentrations of these fish (dealt with elsewhere in the main report), associations with salinity have only been inferred (Sakagawa 1989, Bigelow et al 1999). Our study indicates that salinity can be related to catch rates. Although the mechanism by which

salinity is associated with these catch rates is unclear a possible interpretation is that higher salinities are indicative of greater (vertical) mixing of the water column. This mixing draws nutrients into the photic zone favouring biological production (eg. Sutcliffe et al 1983). Although associations between tuna and ocean colour have been reported (eg. Fiedler and Barnard 1987), in situ measurements have not. Our data indicate therefore that direct measurement of fluorescence and salinity, together with an awareness of the position of the major fronts, have the potential to increase our understanding of the distribution of these fish in oceanic waters off eastern Australia.

Limitations and future directions

As the sampling was restricted to only two boats spread over a distance of more than 10,000 square kilometers in at times a widely differing hydrography further effort is needed to clarify the relationships detected. Nevertheless, that significant values were computed for the same variables across the species examined indicates that the results do reflect actual patterns of distribution. We are presently continuing the field component of this work as a part of a recently funded project on the reproduction of broadbill swordfish (FRDC grant 1999/108). We aim to widen the hydrographic conditions to which we can attach catch rates for these species.

Acknowledgements

We thank the skippers and crews of the fishing vessels Tonka, Elena Rose and Laurinna P who provided extraordinary support throughout this project. In particular we would like to thank Mark Ebbels, Jim Uttley, John Hynde and Joan Puglisi. John Gunn, Alistair Hobday, Vincent Lyne and Ann Cowling made constructive comments on various drafts of this appendix. This project was funded by FRDC research grant 94/045.

Table 8. Summary of significant variables correlated with catch rates of broadbill swordfish, yellowfin and bigeye tuna

Fish species	Broadbill swordfish Model		Yellowfin tuna Model		Bigeye tuna Model	
	1	2	1	2	1	2
Temperature	-	-	+	-	-	-
Salinity	-	+	-	+	+	+
Fluorescence	+	+	+	+	+	+
Nearness to Front	-	+	-	-	+	+
Moon	-	+	+	-	+	+
Area	+	NT	+	NT	-	NT
Month	+	-	+	+	-	-
Year	-	+	-	+	-	-
Wind	-	-	+	-	-	-

(Model 1, data from entire study area; Model 2, data from "Mooloolaba" area; NT, not tested; +, $p < 0.05$)

References

- Augustin, N. H., Borchers, D. L., Clarke, E. D., Buckland, S. T. and Walsh, M. (1998) Spatiotemporal modeling for the annual egg production method of stock assessment using generalized additive models. *Can. J. Fish. Aquat. Sci.* 55, 2608 – 2621
- Bigelow, K. A., Boggs, C. H. and Hi, X. (1999) Environmental effects on swordfish and blue shark catch rates in the US North Pacific longline fishery. *Fisheries Oceanography* 8, 178 – 198
- Borchers, D. L., Buckland, S. T., Priede, I. G. and Ahmadi, S. (1997) Improving the precision of the daily egg production method using generalized additive models. *Can. J. Fish. Aquat. Sci.* 54, 2727 – 2742
- Campbell, R. and Miller, R. J. (eds.) (1998) Fishery assessment report 1997: Eastern Tuna and billfish fishery. Australian Fisheries Management Authority. Canberra, 122p.
- Carey, F. G. and Robinson, B. H. (1981) Daily patterns in the activities of swordfish, *Xiphias gladius*, observed by acoustic telemetry. *Fish. Bull.* 79, 277 – 292
- Clementson, L.A., J.S. Parslow, F.B. Griffiths, V.D. Lyne, D.J. Mackey, G.P. Harris, D.C. McKenzie, P.I. Bonham, C.A. Rathbone and S. Rintoul (1998). Controls on phytoplankton production in the Australasian sector of the Subtropical Convergence. *Deep-Sea Research* 45, 1627-1661
- Draganik, B, Cholyst, J. (1988) Temperature and moonlight as simulators for feeding activity by swordfish. International commission for the Conservation of Atlantic tunas. Collected Volume of Scientific papers. 27, 305 – 314
- Fiedler, P. C. and Bernard, H. J., (1987) Tuna aggregations and feeding near fronts observed in satellite imagery *Cont. Shelf Res.* 7, 871 – 881
- Fiedler, P. C., Smith, G. B. and Laurs, M. (1985) Fisheries applications of satellite data in the eastern north Pacific. *Marine Fisheries Review.* 46, 1 – 13
- Hampton, J. and Gunn, J. (1998) Exploitation and movements of yellowfin tuna (*Thunnus albacares*) and bigeye tuna (*T. obesus*) tagged in the north-western Coral Sea. *Mar. Freshwater Res.* 49, 475 – 489
- Hanamoto, E. (1987) Effect of oceanographic environment on bigeye tuna distribution. *Bull. Japan. Soc. Fish. Oceanogr.* 51, 203 - 216
- Herron, R. C., Leming, T. D., Li, J. (198) Satellite-detected fronts and butterfly aggregations in the northeastern Gulf of Mexico. *Continental Shelf Research.* 9, 569-588

- Holland, K.N., Brill, R. W., and Chang, R. K. C. (1990) Horizontal and vertical movements of yellowfin and bigeye tuna associated with fish aggregating devices. *Fish. Bull.* 88, 493 – 507
- Hunter, J. R., Arque, W. A., and Bayliff, W. H. (1986) The dynamics of tuna movement. Evaluation of past and future research. *FAO Fish. Tech. Pap.* 277, 23 -33
- Hynde, J. S. (1968) How sea surface temperature maps aid tuna fishermen. *Australian Fisheries Newsletter*, 23 –29
- Laurs, R. M., Fiedler, P. C. and Montgomery, D. R. (1984) Albacore tuna catch distributions relative to environmental features observed from satellites. *Deep Sea Res.* 31, 1085 – 1099
- Olson, D. B., Hitchcock, A. J., Mariano, A. J., Ashjian, C. J., Peng, G., Nero, R. W., and Podesta, G. P. (1994) Life on the edge: Marine life and fronts. *Oceanography* 7, 52 - 60
- Podesta, G. P., Browder, J. A. and Hoey, J. J. (1993) Exploring the association between swordfish catch rates and thermal fronts on U.S. longlining grounds in the western North Atlantic. *Continental Shelf Research.* 13, 253 - 277
- Power, J. H. and Nelson May, L. (1991) Satellite observed sea surface temperature and yellowfin tuna catch and effort in the Gulf of Mexico. *Fish. Bull.* 89, 429 – 439
- Ridgway, K. (1999) Tasman-Coral Sea Mass and Heat Transport/ Satellite Altimeter Verification. Cruise Summary RV *Franklin* FR 02/99. 18 pp. (Hobart: CSIRO Marine Laboratories)
- Sakagawa, G. T. (1989) Trends in fisheries for swordfish in the Pacific Ocean. In Stroud, R. H. (Ed.) (1990) Planning the future of billfishes. Research and management in the nineties and beyond. Proceedings of the Second International Billfish symposium, Kailua-Kona, Hawaii, August 1-5 1988. Part 1: Fishery and stock synopses, Data needs and management. PP 61 – 79.
- Sokolov, S. and Rintoul, S. (1999) Circulation of the Southwest Pacific: WOCE section P11, Papua New Guinea to Tasmania. *International WOCE Newsletter*, Number 36, 32 – 35
- Sutcliffe, W. H., Loucks, R. H., Drinkwater, K. F., and Coutes, A. R. (1983) Nutrient flux onto the Labrador shelf from Hudson Strait and its biological consequences. *Can. J. Fish. Aquat. Sci.* 49, 2588 – 2595
- Swartzman, G., Silverman, E. and Williamson, N. (1995) Relating trends in walleye pollock (*Theragra chalcogramma*) abundance in the Bering Sea to environmental factors. *Can. J. Fish. Aquat. Sci.* 52, 369 - 380
- Ward, P. J. (1996) Japanese longlining in eastern Australian waters 1962 – 1990. Bureau of Resource Sciences, Canberra

Young, J. W. (1998) Reproductive dynamics of broadbill swordfish (*Xiphias gladius*) in the domestic longline fishery off eastern Australia. FRDC Grant 1998/108

Young, J. W., Jordan, A. R., Bobbi, C., Johannes, R. E., Haskard, K. and Pullen, G. (1993) Seasonal and interannual variations in krill (*Nyctiphanes australis*) stocks and their relationship to the fishery for jack mackerel (*Trachurus declivis*) off eastern Tasmania, Australia. *Marine Biology*. Vol. 116, 9 - 18

Young, J. W., R. W. Bradford, T. D. Lamb and V. D. Lyne (1996) Biomass of zooplankton and micronekton in the southern bluefin tuna fishing grounds off eastern Tasmania, Australia. *Marine Ecology Progress Series*: 138, 1- 14

Young, J. W., R. Bradford, T. D. Lamb, L. Clementson, R. Kloser and H. Galea (in preparation) The biological basis for catches of yellowfin tuna (*Thunnus albacares*) off southeastern NSW, Australia in May 1996. [submitted to Marine and Freshwater Research Volume on the South East Fishery]